UNIVERSIDADE DE SÃO PAULO
Instituto de Ciências Matemáticas e de Computação

Neurocognitive Computing Platform: Prototype in Tinnitus Rehabilitation Throughout Emotion Regulation Concurrent with High Definition transcranial Direct Current Stimulation as a Neuromodulation Technique.

Iman Ghodratitoostani

Tese de Doutorado do Programa de Pós-Graduação em Ciências de Computação e Matemática Computacional (PPG-CCMC)

ICMC USP
SÃO CARLOS

Iman Ghodratitoostani

Neurocognitive Computing Platform: Prototype in Tinnitus Rehabilitation Throughout Emotion Regulation Concurrent with High Definition transcranial Direct Current Stimulation as a Neuromodulation Technique.

Doctoral dissertation submitted to the Instituto de Ciências Matemáticas e de Computação – ICMC-USP, in partial fulfillment of the requirements for the degree of the Doctorate Program in Computer Science and Computational Mathematics. *FINAL VERSION*

Concentration Area: Computer Science and Computational Mathematics

Advisor: Prof.Dr. Alexandre Cláudio Botazzo Delbem

USP – São Carlos
September 2022

Ficha catalográfica elaborada pela Biblioteca Prof. Achille Bassi
e Seção Técnica de Informática, ICMC/USP,
com os dados inseridos pelo(a) autor(a)

G427 Ghodratitoostani, Iman
/ Iman Ghodratitoostani; orientadora Alexandre Claudio Botazzo Delbem. -- São Carlos, 2022.
290 p.

Tese (Doutorado - Programa de Pós-Graduação em Ciências de Computação e Matemática Computacional) -- Instituto de Ciências Matemáticas e de Computação, Universidade de São Paulo, 2022.

1. Neurocognitive Computing. 2. Feature Optimization. 3. Artificial Cognition. 4. Clinical Study Design. 5. Cognitive Rehabilitation.. I. Delbem, Alexandre Claudio Botazzo, orient. II. Título.

Bibliotecários responsáveis pela estrutura de catalogação da publicação de acordo com a AACR2:
Gláucia Maria Saia Cristianini - CRB - 8/4938
Juliana de Souza Moraes - CRB - 8/6176

Iman Ghodratitoostani

Plataforma de Computação Neurocognitiva:Protótipo na Reabilitação do Zumbido Através da Regulação da Emoção Concomitante com a Estimulação transcraniana por Corrente Direta de Alta Definição como Técnica de Neuromodulação.

Tese apresentada ao Instituto de Ciências Matemáticas e de Computação – ICMC-USP, como parte dos requisitos para obtenção do título de Doutor em Ciências – Ciências de Computação e Matemática Computacional. *VERSÃO REVISADA*

Área de Concentração: Ciências de Computação e Matemática Computacional

Orientadora: Prof.Dr. Alexandre Cláudio Botazzo Delbem

USP – São Carlos
Setembro de 2022

Este trabalho é dedicado às crianças adultas que,
quando pequenas, sonharam em se tornar cientistas.
Em especial, ao pesquisadores do Instituto de Ciências Matemáticas e de Computação (ICMC).

ACKNOWLEDGEMENTS

First of all, I would like to express my gratitude to Almighty Allah for enabling me the strength and opportunity to propose a new research methodology successfully. Foremost, I would like to express my sincere gratitude to my advisor Prof.Dr. Alexandre C.B Delbem, for the continuous support of my Ph.D. study and research and his patience, motivation, enthusiasm, and immense knowledge.

Besides my advisor, I would like to thank the clinical advisors and colleagues Prof.Dr. Joao Pereira Leite, Tonicarlo R Velasco, Miguel Angelo Hyppolito, Camila Barros, and all clinicians and nurses in FMRP, HCRP, and CEOF for their encouragement, collaboration, support, and patience in dealing with clinical trials difficulties and requirements.

I also would like to thank CEPID-CeMEAI, Prof.Dr. Cuminato, Louzada, and CEAS, Prof.Dr. Caurin for supporting and granting my ambitious projects in founding and equipping the Neurocognitive Engineering Laboratory in Sao Carlos besides clinical centers in Ribeirao Preto.

I also would like to thank especially from Milton Miranda Netto, Zahra Vaziri, and all students who helped me in all project stages, from theoretical assignments to clinical data acquisition, analysis, and dissemination.

I also thank my family, especially my parents and two lovely sisters. Their continuous passional support has motivated me to do my best performance. I could not have imagined having a more joyful and productive Ph.D. study and research. Lastly, I would like to thank both groups who believed in our research methodology for their support and who did not believe in it, driving me to be more precise, strong, and self-driven.

“As invenções são, sobretudo,
o resultado de um trabalho de teimoso.”
(Santos Dumont)

RESUMO

GHODRATITOOSTANI, I. **Plataforma de Computação Neurocognitiva:Protótipo na Reabilitação do Zumbido Através da Regulação da Emoção Concomitante com a Estimulação transcraniana por Corrente Direta de Alta Definição como Técnica de Neuromodulação.**. 2022. 290 p. Tese (Doutorado em Ciências – Ciências de Computação e Matemática Computacional) – Instituto de Ciências Matemáticas e de Computação, Universidade de São Paulo, São Carlos – SP, 2022.

As redes cognitivas cerebrais se consolidam emergentemente de acordo com, mas não se limitando às experiências individuais ao longo da vida relacionadas à emoção, estresse, medo, atenção, aprendizado, sociedade, linguagem, religião, cultura e ambiente familiar. Portanto, o funcionamento cognitivo, questões de causalidade versus contingência, redes cerebrais, protocolo de intervenção e eficácia da reabilitação são desafios nas ciências cognitivas e das neurociências. Além disso, o conhecimento orientado a dados suporta a descoberta de padrões, a criação de estratégias de tomada de decisão e a possibilidade de análises preditivas e de perspectiva.

No entanto, a reabilitação cognitiva também é desejada pela atualização do conhecimento e aprendizagem autônoma por meio de novas condições devido à consolidação cerebral emergente individualizada. Eventualmente, a infraestrutura digital e o desempenho da computação são essenciais para tornar os modelos desenvolvidos acessíveis, acessíveis e atualizáveis para o sistema de saúde.

Uma das soluções práticas que podem enfrentar coletivamente todos os desafios é uma plataforma de computação cognitiva. A Computação Cognitiva (CC) é um nicho de conhecimento emergente baseado em ciência cognitiva, neurociência, ciência de dados e tecnologias de computador.

Arquitetonicamente, proponho uma plataforma de Computação Cognitiva construída a partir de redes de micromódulos chamada computação neurocognitiva. A Computação Neurocognitiva (NcC) é uma unidade de computação cognitiva autorregulada que pode aprender e ser treinada em tempo real para gerar mecanismos de sistemas cognitivos individualmente ou em uma rede complexa. Neste projeto de 8 anos, tentei fazer uma Plataforma de Reabilitação Cognitiva (iCRP) integrada como computação neurocognitiva para navegar no comprometimento cognitivo (desregulação emocional) e reabilitação com técnicas de estimulação elétrica transcraniana para pacientes com zumbido.

No iCRP, conceituamos e desenvolvemos parcialmente segmentos de computação neurocognitiva em paralelo, desde modelagem cognitiva teórica, ensaio clínico e mineração orientada a dados não/supervisionada até aprendizado profundo em tempo real. Tentei documentar a seção de ciências cognitivas do projeto de forma concisa e profunda, desenvolvendo caixas de ferramentas teóricas e experimentais para reconhecimento de padrões não supervisionado e explorando as metodologias orientadas por dados com avaliações de desempenho de métricas para alimentar o aprendizado de reforço profundo no futuro.

Palavras-chave: Computação Neurocognitiva, Computação Cognitiva, Plataforma de reabilitação cognitiva, Projeto de estudo clínico, Cognição artificial, Otimização de recursos, informações gananciosas.

ABSTRACT

GHODRATITOOSTANI, I. **Neurocognitive Computing Platform: Prototype in Tinnitus Rehabilitation Throughout Emotion Regulation Concurrent with High Definition transcranial Direct Current Stimulation as a Neuromodulation Technique.**. 2022. 290 p. Tese (Doutorado em Ciências – Ciências de Computação e Matemática Computacional) – Instituto de Ciências Matemáticas e de Computação, Universidade de São Paulo, São Carlos – SP, 2022.

Brain cognitive networks consolidate emergently according to but not limited to individual lifelong experiences related to emotion, stress, fear, attention, learning, society, language, religion, culture, and family environment. Therefore, cognitive functioning, causality versus contingency issues, brain networks, intervention protocol, and rehabilitation effectiveness are challenges in cognitive and neuroscience sciences. Additionally, data-driven knowledge supports discovering patterns, creating decision-making strategies, and making predictive and perspective analytics possible.

However, cognitive rehabilitation is also desired by updating knowledge and autonomous learning through new conditions due to individualized emergent brain consolidation. Eventually, digital infrastructure and computing performance are essential to make the developed models accessible, affordable, and updatable for the healthcare system.

One of the practical solutions that can collectively address all challenges is a cognitive computing platform. Cognitive Computing(CC) is an emerging knowledge niche grounded on cognitive science, neuroscience, data science, and computer technologies.

Architecturally, I propose a Cognitive Computing platform constructed from micro-module networks called neurocognitive computing. Neurocognitive Computing (NcC) is a self-regulatable cognitive computing unit that can learn and be trained in real-time to generate cognitive system mechanisms individually or in a complex network. In this 8-year project, I tried to make an integrated Cognitive Rehabilitation Platform (iCRP) as neurocognitive computing to navigate cognitive impairment (emotion dysregulation) and rehabilitation with transcranial electrical stimulation techniques for tinnitus patients.

In iCRP, we conceptualized and partially developed neurocognitive computing segments in parallel, from theoretical cognitive modeling, clinical trial, and un/supervised data-driven mining to real-time deep learning. I tried to document the cognitive science section of the project concisely and profoundly, developing theoretical and experimental toolboxes for unsupervised pattern recognition and exploring the data-driven methodologies with metric performance evaluations to fuel deep reinforcement learning in the future.

Keywords: Neurocognitive Computing, Cognitive Computing, Cognitive rehabilitation platform, Clinical study design, Artificial cognition, Feature optimization, greedy information.

LIST OF FIGURES

Figure 11 – **a)** Realistic Montage for 256-channel HydroCel Geodesic Sensor Net and The left-dlPFC as the Region Of Interest (ROI) is also mounted in the EGI-NET.

b) Co-registered 256-channel EEG, and HD-tDCS Montage on left-dlPFC based on the MR-driven head model. The stimulation electrodes located in electrode holders were placed near the EEG channels. The electrode holder for the anode is shown in red and that for the cathode is shown in blue. The electrode holders are filled with conductive gel.

c) Schemas of the protocol. Initially, the patients filled in different questionnaires- THI, TBF-12, TS, MDI, STAI-S6, and MSQ. Before and after the experiment, psychoacoustic parameters of tinnitus together with the Tinnitus Severity questionnaire were recruited. During the experiment, two sets of pictures were presented with different Valence-ratio (Vr) and arousal-ratio (Ar) rates selected from the NAPS dataset. Neutral pictures ($4 <$Vr< 6 and Ar< 6) were included in four rs blocks and the positive pictures (Vr> 6) in 2×5 consecutive visual stimulation blocks. Each visual stimulation block initiates with four pictures (Vr> 6 and Ar> 6) followed by sixteen pictures (Vr> 6) randomly selected with no replacement from a one-hundred-positive-picture set (Figure **??**a). Generally, every single block contained 20 pictures each presented for $5s$ followed by a cue (+) of $500ms$. The blocks were randomized between sessions and between patients but presented in the same order within-session. The total duration of each block presentation was two min. The TLQ "Scale your tinnitus loudness from $1-10$" was displayed 21 times, and presented in the following order: before-after each resting-state block (containing neutral pictures) and visual stimulation block (containing positive pictures), and after each Emotional Stroop task. Throughout the experiment, the responses of TLQ and EST in blue and green lines, respectively, as well as EEG signals were all recorded via Superlab software (Cedrus Corporation, San Pedro, CA, USA). The total duration of the experiment ranged between 40 and 45 min with regard to the reaction time of patients in EST and responding to TLQ.

d) Timeline of all three sessions of study including anodal stimulation-picture presentation, sham stimulation-picture presentation, only picture presentation is illustrated. In all three sessions, the sequence of presenting pictures, TLQ, and EST are the same as those described in part C. Electrical stimulation periods (sham/Active) was illustrated in movies of supplementary documents. 106

LIST OF CHARTS

LIST OF ALGORITHMS

LIST OF SOURCE CODES

LIST OF TABLES

LIST OF ABBREVIATIONS AND ACRONYMS

δ	Minimum Clinical Efficacy; *Chapter(5)*
A2C	Advantage Actor-Critic; *Chapter(10)*
A3C	Asynchronous Advantage Actor-Critic; *Chapter(10)*
ACC	anterior cingulate cortex; *Chapter(2)*
ACC	anterior cingulate cortex; *Chapter(2, 3, 3)*
AD	Average Distance; *Chapter(7, 8)*
ADM	Average Distance between Means; *Chapter(7, 8)*
API	Application Programming Interface; *Chapter(1)*
APN	Average Proportion of Non-overlap; *Chapter(7, 8)*
Ar	arousal-ratio; *Chapter(5)*
ASB	Adaptive-Seamless Bayesian; *Chapter(5)*
BA	Brodmann areas; *Chapter(5)*
BLA	basolateral amygdala; *Chapter(3)*
BN	Batch Normalization; *Chapter(10)*
BOLD	blood oxygen level-dependent; *Chapter(2)*
CAAP	Conscious Attended-Awareness Perception; *Chapter(4, 5, 9)*
CAD	computer-aided design; *Chapter(5)*
CBM	Cognitive-Behavioral Model; *Chapter(7)*
CBT	Cognitive Behavioural Therapy; *Chapter(4)*
CC	Cognitive Computing; *Chapter(1)*
CCF	Conceptual Cognitive Framework; *Chapter(4, 9)*
CGI	Clinical Global Impression; *Chapter(5, 6)*
CNN	Convolutional Neural Networks; *Chapter(10)*
CPP	conscious perception process; *Chapter(2, 3)*
CRL	Causal Reinforcement Learning; *Chapter(10)*
CS	Conditional Stimulus; *Chapter(2, 3, 4)*
CST	CausalSpace Toolbox; *Chapter(7)*
CV	Coefficient of Variance; *Chapter(5)*
DAG	Directed acyclic graph; *Chapter(10)*
DCN	dorsal cochlear nucleus; *Chapter(2, 3)*
DL	Discomfort Level; *Chapter(5)*

dlPFC Dorsolateral Prefrontal Cortex; *Chapter(5)*

DM dorsomedial; *Chapter(2, 3)*

DNN Deep Neural Network; *Chapter(1, 10)*

DQL Deep Q-learning; *Chapter(10)*

DRL Deep Reinforcement Learning; *Chapter(1, 8, 10)*

DrL Distributed Recursive Graph Layout; *Chapter(7)*

DRR Dimensionality Reduction via Regression; *Chapter(7)*

ECL Evaluative Conditional Learning; *Chapter(2, 3, 4, 5)*

EEG Electroencephalogeraphy; *Chapter(2, 3, 5)*

EF electric field; *Chapter(5)*

EGI Electronic Geodesic Incorporation; *Chapter(5)*

ER Experience Replay; *Chapter(10)*

ERP event-related potential; *Chapter(5)*

EST Emotional Stroop Task; *Chapter(4, 5)*

FastICA Independent Component Analysis; *Chapter(7)*

FC Fully Connected; *Chapter(10)*

FDA Food and Drug Administration; *Chapter(5)*

FE Finite element; *Chapter(5)*

fMRI functional Magnetic Resonance Imaging; *Chapter(1, 2, 3)*

FN Fresh noise; *Chapter(5)*

FOM Figure of Merit; *Chapter(7, 8)*

Fruchterman Reingold Fruchterman Reingold Graph Layout; *Chapter(7)*

FS Feature Selection; *Chapter(1, 7, 8)*

FT Feature Transformation; *Chapter(1, 7,8)*

GABA Gamma-aminobutyric acid; *Chapter(2, 3)*

HAV high-arousal-valence pictures; *Chapter(5)*

HD High Definition; *Chapter(2, 4, 5)*

HL Hearing Level; *Chapter(5)*

HTL Hearing Threshold Level; *Chapter(5)*

HV high-valence Pictures; *Chapter(5)*

IC inferior colliculus; *Chapter(2, 3)*

ICA Independent Component Analysis; *Chapter(7)*

iCRP integrated Cognitive Rehabilitation Platform; *Chapter(2, 5, 6)*

ITC intercalated cells; *Chapter(2, 3)*

kPCA Kernel Principal Component Analysis; *Chapter(7)*

LDL loudness discomfort level; *Chapter(5)*

LLE Locally Linear Embedding; *Chapter(7)*

LMC Loudness Misperception Correction; *Chapter(5)*

LMT Loudness Match Test; *Chapter(5)*

lPFC Lateral PFC; *Chapter(2, 3, 5)*

LPP Late Positive Potential; *Chapter(5)*

LSTM Long Short-Term Memory; *Chapter(10)*

mA Mili Amper; *Chapter(5)*

MBCT Mindfulness-Based Cognitive Therapy; *Chapter(4)*

MBI Mindfulness-based interventions; *Chapter(4)*

MCC Mathews Correlation Coefficient; *Chapter(10)*

MDI Major Depression Inventory; *Chapter(5, 6)*

MDN mediodorsal nucleus; *Chapter(2, 3)*

MDP Markov Decision Processes; *Chapter(10)*

MEG magnetoencephalography; *Chapter(2, 3)*

MGB medial geniculate body; *Chapter(2, 3)*

MGN medial geniculate nucleus; *Chapter(2,3)*

MI Mutual Information; *Chapter(7)*

MI mutual information; *Chapter(7)*

Min Minutes; *Chapter(5)*

MML Minimal Masking Level; *Chapter(5)*

MSE Minimum Squared Error; *Chapter(7)*

MSQ Mini Sleep Questionnaire; *Chapter(5, 6)*

NAc nucleus accumbens; *Chapter(2, 3)*

NAPS Nencki Affective Picture System; *Chapter(5)*

NBN narrow-band noise; *Chapter(5)*

NcC Neurocognitive Computing; *Chapter(1, 7, 8, 9, 10)*

NfTM Neurofunctional Tinnitus Model; *Chapter(3, 5)*

NfTM Neurofunctional Tinnitus Model; *Chapter(5)*

NIBS Non-invasive Brain Stimulation; *Chapter(5)*

nMDS Non-Metric Dimensional Scaling; *Chapter(7)*

NMI Normalized MI; *Chapter(7)*

NNMF Non-Negative Matrix Factorization; *Chapter(7)*

OLS Ordinary Least Square; *Chapter(5)*

PCA Principal Components Analysis; *Chapter(7)*

PCA principal component analysis; *Chapter(7)*

PEI positive emotion induction; *Chapter(5, 6)*

PET Positron emission tomography; *Chapter(3)*

PFC pre-frontal cortex; *Chapter(2, 3)*

PMT	Pitch Matching test; *Chapter(5)*
pOFC	posterior orbitofrontal cortex; *Chapter(2,3)*
POMDP	Partially- Observable Markov Decision Process; *Chapter(10)*
PTA	Pure-tone audiometry; *Chapter(5)*
q	quanta; *Chapter(7)*
RL	Reinforcement Learning; *Chapter(1, 10)*
RNN	Recurrent Neural Network; *Chapter(10)*
ROI	Region Of Interest; *Chapter(5)*
rs	resting-state; *Chapter(5)*
SARSA	State-Action-Reward-State-Action; *Chapter(10)*
SOC	superior olivary complex; *Chapter(2,3)*
SOTA	Self-Organized Tree Algorithm; *Chapter(7, 8)*
SPECT	Single-photon emission computed tomography; *Chapter(3)*
STAI-S6	State Trait Anxiety Inventory Small Questions; *Chapter(5, 6)*
t-SNE	t-Distributed Stochastic Neighbor Embedding; *Chapter(7)*
TBF-12	Tinnitus Impairment Questionnaire; *Chapter(5, 6)*
tDCS	transcranial Direct Current Stimulation; *Chapter(2, 4, 5)*
tES	transcranial Electrical Stimulation; *Chapter(5)*
THI	Tinnitus Handicap Inventory; *Chapter(5, 6, 9)*
TLQ	Tinnitus Loudness Questionnaire; *Chapter(5, 6)*
TRN	Thalamic reticular nucleus; *Chapter(2, 3)*
TS	Tinnitus Severity; *Chapter(6)*
TSCHQ	Tinnitus Sample Case History Questionnaire; *Chapter(6)*
TT	Testing Tone; *Chapter(5)*
US	Unconditional Stimulus; *Chapter(2, 3, 4)*
vm	ventromedial; *Chapter(2, 3)*
VP	ventral pallidum; *Chapter(2,3)*
Vr	Valence-ratio; *Chapter(5)*

LIST OF SYMBOLS

$\Re^d$ — $d-$Dimensional Euclidean space; *Chapter(7 and 8)*

$\mathscr{H}$ — Feature space; *Chapter(7)*

$\Phi(\cdot)$ — Feature map from $\Re^d$ to $\mathscr{H}$; *Chapter(7)*

$N_{\mathscr{H}}$ — Dimension of Feature space $\mathscr{H}$; *Chapter(7)*

$d_{ij}^{\mathscr{X}}, d^{\mathscr{X}}(\mathbf{x}_i, \mathbf{x}_j)$ — Distance in a Feature space; *Chapter(7)*

N_i^k — set with k nearest neighbors of $\mathbf{x}_i$; *Chapter(7)*

N_i^{ε} — set with neighbors include in the ball centered in $\mathbf{x}_i$ and radius ε; *Chapter(7)*

$\mathfrak{Y}$ — $t-$dimensional Feature space; *Chapter(7)*

$\mathscr{M}$ — Manifold in a Feature space; *Chapter(7)*

$\mathscr{N} - pdf$ — Normal probability density function; *Chapter(7)*

$q_{k,l}$ — Individual quanta of normal density function; *Chapter(7)*

$TPQ_{[X,Y]}$ — Total path quanta probability of path $X \longrightarrow Y$; *Chapter(7)*

$TPQ_{[X_1,X_2,\ldots,X_n]}$ — Total path quanta probability of path $X_1 \longrightarrow X_2 \longrightarrow \ldots \longrightarrow X_n$; *Chapter(7)*

$H(X)$ — Entropy of variable X; *Chapter(7)*

$H(X,Y)$ — Entropy of variable X and Y; *Chapter(7)*

$MI(X,Y)$ — Mutual information between X and Y; *Chapter(7)*

$\Pi_j^{(n)}, \Pi_j(X_1,\ldots,X_n)$ — Class with all subset of $(X_1,\ldots,X_n)$; *Chapter(7)*

$N_{n,j}, |\Pi_j^{(n)}|$ — Cardinal number of $\Pi_j^{(n)}$; *Chapter(7)*

$x_{\pi_j^{(n)}}(i)$ — A member of $\Pi_j^{(n)}$; *Chapter(7)*

$\mathfrak{X}$ — D-dimensional Euclidean space, original Feature space; *Chapter(7)*. d-dimensional Observation space; *Chapter(8)*.

$\mathscr{Y}$ — d-dimensional Euclidean space, reduced Feature space; *Chapter(7)*

$\mathscr{U}$ — Unordered variables; *Chapter(7)*. Unclustered observations; *Chapter(8)*.

$\mathscr{M}^{(k)}$ — Medoid variable from k-th interaction; *Chapter(7)*. Local medoid from the neighbors; *Chapter(8)*.

$X_{S_i^{(k)}}$ — i-th sorted variable from medoid $\mathscr{M}^{(k)}$; *Chapter(7)*

$\mathscr{P}^{(k)}$ — Sorted variable at k-th interaction; *Chapter(7)*

$\mathscr{U}^{(k)}$ — Unsorted variable at k-th interaction; *Chapter(7)*

N_{Opt} — Optimal number of medoid's neighbors; *Chapter(7)*

$\mathscr{N}^{(k)}$ — Set with neighbors of medoid $\mathscr{M}^{(k)}$; *Chapter(7)*. Neighboring of global medoid; *Chapter(8)*.

$\mathscr{F}$ — Variable collection in greedy algorithm; *Chapter(7)*. Set observation in greedy algorithm; *Chapter(8)*.

$a_i^{(k)}$ — Mutual information between $TPQ_{[\mathscr{M}^{(k)},X_1,\ldots,X_j]}$ and $X_{S_i^{(k)}}$; *Chapter(7)*

$b_i^{(k)}$ — Mutual information from the path $\mathscr{M}^{(k)};X_1;\ldots;X_{j-1};X_j$; *Chapter(7)*

$c_i^{(k)}$ — The product of $a_i^{(k)}$ and $b_i^{(k)}$; *Chapter(7)*

$a_{-i}^{(k)}$ — Mutual information between $TPQ_{[\mathscr{M}^{(k)},X_1,\ldots,X_{j-1}]}$ and X_j without $X_{S_i^{(k)}}$; *Chapter(7)*

$b_{-i}^{(k)}$ — Mutual information from the path $\mathscr{M}^{(k)};X_1;\ldots;X_{j-1};X_j$ without $X_{S_i^{(k)}}$; *Chapter(7)*

$c_{-i}^{(k)}$ — The product of $a_{-i}^{(k)}$ and $b_{-i}^{(k)}$; *Chapter(7)*

$\mathscr{C}_k$ — Grouped variable at k-th interaction; *Chapter(7)*

$\mathscr{P}(\hat{X}_k)$ — A subset of $\mathscr{F}$ without X_k; *Chapter(7)*

$d_j^{(k)}$ — Mutual information between $TPQ_{[\mathscr{P}(\hat{X}_k)]}$ and $\mathscr{M}^{(k)}$; *Chapter(7)*

$e_j^{(k)}$ — Mutual information from the path $\mathscr{P}(\hat{X}_k);\mathscr{M}^{(k)}$; *Chapter(7)*

$f_j^{(k)}$ — The product of $d_j^{(k)}$ and $e_j^{(k)}$; *Chapter(7)*

$u_j^{(k)}$ — Mutual information between $TPQ_{[\mathscr{M}^{(k)},X_1,\ldots,X_{k-2}]}$ and X_{k-1} without X_k; *Chapter(7)*

$v_j^{(k)}$ — Mutual information from the path $\mathscr{M}^{(k)};X_1;\ldots;X_{k-2};X_{k-1}$; *Chapter(7)*

$w_j^{(k)}$ — The product of $u_j^{(k)}$ and $v_j^{(k)}$; *Chapter(7)*

α — Parameter to control the accept new member in forward step; *Chapter(7 and 8)*

β — Parameter to control the accept new member in backward step; *Chapter(7 and 8)*

f_M — Maximum of $f_1^{(k)},\ldots,f_K^{(k)}$; *Chapter(7)*

ρ_{Total} — Total Correlation; *Chapter(7)*

$dCorr(X,Y)$ — Distance correlation; *Chapter(7)*

$dCov(X,Y)$ — Distance covariance; *Chapter(7)*

$dVar(X)$ — Distance variance; *Chapter(7)*

Q_{local} — Preserved local distance between original and optimized spaces; *Chapter(7)*

Q_{glocal} — Preserved glocal distance between original and optimized spaces; *Chapter(7)*

$R_{NX}(k)$ — Compute the AUC_lnK_R_NX; *Chapter(7)*

$r^2(D,\hat{D})$ — Square of Pearson correlation between D and $\hat{D}$ distances matrix; *Chapter(7)*

$d_{Eu}(x,y)$ — Euclidean distance between x and y; *Chapter(8)*

$d_1(O_i,O_j)$ — Sum of mutual information distance between O_i and O_j; *Chapter(8)*

$H(O_{i_f},O_{j_f})$ — Entropy between observations O_{i_f} and O_{j_f}; *Chapter(8)*

$MI(O_{i_f},O_{j_f})$ — Mutual Information between observations O_{i_f} and O_{j_f}; *Chapter(8)*

$F(O_{i_f}^{-})$ — CDF lower bound; *Chapter(8)*

$p_H(O_{i_f})$ — Hierarchical pdf of O_{i_f}; *Chapter(8)*

$d_2(O_i,O_j)$ — Quanta distance between O_i and O_j; *Chapter(8)*

$\mathscr{O}$ — Observation space; *Chapter(8)*

$d(O_i,O_j)$ — NcC_distance between O_i and O_j; *Chapter(8)*

$\mathscr{C}$ — Cluster pattern; *Chapter(8)*

$O(m)$ — Cluster member of $\mathscr{C}$; *Chapter(8)*

$D_1(O_i,\mathscr{C})$ — Distance Mutual Information from O_i to $\mathscr{C}$; *Chapter(8)*

$D_2(O_i,\mathscr{C})$ — Distance Quanta from O_i to $\mathscr{C}$; *Chapter(8)*

$D(O_i,\mathscr{C})$ — NcC_distance from O_i to $\mathscr{C}$; *Chapter(8)*

$\mathfrak{M}^{(k)}$ — Global medoid at k-th interaction; *Chapter(8)*

C_k — k-th cluster; *Chapter(8)*

n_k — Cardinal of unclustered data at k-th interaction; *Chapter(8)*

$O_{S_i^{(k)}}$ — i-th sorted observation from global medoid; *Chapter(8)*

$\mathscr{S}$ — Sorted data up to i-th observation at k-th interaction; *Chapter(8)*

$p_{Optimal}$ — Optimal probability that maximized the entropy; *Chapter(8)*

$n^{(k)}$ — Optimal number of neighbors of medoid $\mathfrak{M}^{(k)}$; *Chapter(8)*

$O_i^{(k)}$ — i-th sorted observation from local medoid at k-th interaction; *Chapter(8)*

$\mathscr{S}^{(k)}$ — Set with sorted observations at k-th interaction; *Chapter(8)*

$\mathscr{S}^{(k)}$ — Set with sorted observations at k-th interaction; *Chapter(8)*

C_{-l} — Cluster without $O_l^{(k)}$ observation at interaction k; *Chapter(8)*

$x_{i,nn(j)}$ — j-th nearest neighbor of observation i; *Chapter(8)*

$n(C(i))$ — Number of members in cluster $C(i)$; *Chapter(8)*

$S(i)$ — Silhouette width; *Chapter(8)*

$D(\mathscr{C})$ — Dunn index; *Chapter(8)*

$C^{i,l}$ — Cluster containing observation i where the clustering process is based on left out l feature; *Chapter(8)*

$C^{i,0}$ — Cluster with observation i based on all available data; *Chapter(8)*

$APN(\mathscr{C})$ — Average Proportion of Non-overlap; *Chapter(8)*

$AD(\mathscr{C})$ — Average Distance; *Chapter(8)*

$\bar{x}_{C^{i,0}}$ — Mean of observation $C^{i,0}$; *Chapter(8)*

$\bar{x}_{C^{i,l}}$ — Mean of observation $C^{i,l}$; *Chapter(8)*

CONTENTS

CHAPTER

1

INTRODUCTION

The decade from *1990* until *2000*, known as "the Decade of the Brain, produced the first wave of empirical studies on the neural bases of psychopathology. This research was made possible by technical advances in methodology and tools such as functional Magnetic Resonance Imaging (fMRI), tractography methods, and behavioral paradigms that correct cognitive deficits or protect against further decline. Anatomical and functional brain knowledge emerged in emotional disorder diagnosis and treatment and termed the neurocognitive perspective. The neurocognitive approach has opened new avenues for research and innovation in clinical practice. Clinical utilities were revealed in recent studies about neurocognitive evaluation in the differential diagnosis (HALE *et al.*, 2011; WEISSMAN *et al.*, 2012), the cognitive-behavioral efficacy (KUELZ *et al.*, 2006; LEGERSTEE *et al.*, 2010; MATHEWS *et al.*, 1995; MOHLMAN; GORMAN, 2005; SIEGLE; CARTER; THASE, 2006), pharmacological (HALE; FIORELLO; BROWN, 2005; HALE *et al.*, 2011), and neurocognitive rehabilitation (KERNS; ESO; THOMSON, 1999; KOSTER; FOX; MACLEOD, 2009; VASSILOPOULOS; BANERJEE; PRANTZALOU, 2009)in affective disorders and cognitive impairments(GHODRATITOOSTANI *et al.*, 2016; GHODRATITOOSTANI *et al.*, 2016a; TOOSTANI *et al.*, 2017; VAZIRI *et al.*, 2021). Another compelling reason for adopting a neurocognitive perspective is recognizing and measuring the severity of symptoms, syndromes, and disorders. Neurocognitive rehabilitation can determine nonresponders to treatment even before the beginning of interventions (MAYBERG, 2006; SIEGLE *et al.*, 2011). An autonomous system is an independent and self-regulated entity. The system continually reconfigures itself in real-time in response to novelties in its environment (VERNON, 2014). The self-reorganization aspect integrates learning, development, and evolution. "Cognition is the process that autonomous system acquires its knowledge and improves its behavior through senses, thoughts, and experiences" (ANDERSON, 1996). Cognitive processes are crucial to autonomous systems for recognition and permanence (FRANKLIN *et al.*, 2013; NEWELL, 1994). Human cognition enables humans to perform multiple tasks (CHIPMAN, 2016). Machine cognition is introduced as a combination of processes that allow computers to

fulfill human cognition levels. Human cognition relies on the brain and mind for awareness; analogously, machine cognition depends on computation and uses cognitive computing techniques. Cognitive computing is an emerging field grounded on the convergence of cognitive sciences, neuroscience, data science, and various computing technologies (HURWITZ *et al.*, 2015). Cognitive science is an interdisciplinary concept to study the mind, hypothesize, theorize and model human cognition. Neuroscience is the quantitative and qualitative study of brain structures and how the brain regulates behavior and cognitive processes. Data science is a multidisciplinary domain to build data-driven knowledge from structured and unstructured data using machine learning algorithms and statistical methods. Data science's ultimate goal is to discover patterns, create decision-making strategies, and analyze them predictively. Computer technologies are needed to deploy models that make them accessible, affordable, and autonomous, including cloud computing, high-performance computing, the internet of things, and infrastructure in software. Cognitive Computing applications can drastically reduce the public health burden incorporated with emotional disorders and lead to data-driven treatment approaches as below.

1. Gain new insights into cognitive processes, corresponding brain pathways, and possible impairments. Cognitive computing can provide new information and relationships between cognitive impairments and specific patient characteristics. The progression of the cognitive deficit and rehabilitation effects can be predicted for various rehabilitation. This inclination can provide a unique choice of treatments for patients by authorizing their data analysis to elucidate existing questions, project the course of cognitive impairment, create new insights, and make new questions to investigate.

2. Discover new knowledge and insights in real-life learning and autonomous updating of cognitive models. Real-time learning is one thing, and predicting from data-driven cognitive models of known burdens is another. We may always confront inexperienced cognitive complexity in real-life that needs to decide based on uncertainty. This new knowledge can help discover complex cognitive comorbidities problems and support individualized treatment plans, not only pattern recognition.

3. Accelerate the pace of cognitive computing. New computing technologies and algorithms increase the rate at which new information can be discovered, learned, and update in models without remodeling. The faster we can learn new cognitive tasks and disorder complexity, the quicker and more effectively we can cure cognitive disorders and decide intelligently.

4. Develop a new platform of individualized cognitive assessment and rehabilitation. We must change our approach from cognitive treatment to patient rehabilitation. Focusing on the patient's particular characteristics and the individual expression of the cognitive deficit will lead to optimized rehabilitation matched with the patient, not just population averages.

1.1 Neurocognitive Computing Architecture

Cognitive Computing (CC) is an emerging niche knowledge grounded on cognitive science, neuroscience, data science, and computer technologies. We defined Neurocognitive Computing (NcC) as the minor component of CC that can learn intelligent causality tasks and develop artificial cognition. Artificial intelligent goals (Mission) are essential to initiate designing CC.
NcC components, either individually or in a network, create artificial cognition based on the obtained knowledge from Neurocognitive *NcC_Neurocognitive*(Ch: 2, 3, 4, and 5), causality data-driven *NcC_Data-Driven* (Ch: 6, 7, 8, and 9), and Deep reinforcement learning *NcC_DRL* (Ch:10) sections collaborating with the data center.
Structurally, the NcC_Neurocognitive section projects several cognitive and neurofunctional frameworks in line with the mission. NcC_Data-Driven section demonstrates unsupervised methods on data from descriptive analytics to causality feature optimization and clustering. Eventually, the NcC_DRL section establishes Reinforcement learning algorithms for un/supervised deep learning, to develop and deploy prospective models, and deep learning to achieve artificial intelligence goals relying on the most closely related available (Observed) data.

However, further well-controlled clinical or experimental studies suggest when supporting data is not sufficient to test the desired theoretical hypotheses. Deep reinforcement Learning models individually or in combinations with other NcC components can deploy autonomous neurocognitive models in line with the chosen mission of the NcC.
Deployed models employ Application Programming Interface (API) and cloud computing to support decisions in applications. Autonomous models can decide in an inexperienced situation (untrained/unseen conditions) based on uncertainty and learn from the consequences. Similar to a human mind, NcC develops real-time deep reinforcement learning loops with the back projection of the cognitive models' accomplishment to the data center for updating patterns and models. Architecture is illustrated in Figure. 1.
Real-time autonomous learning with different types of information demands high-performance computational algorithms that generally are not supported by the available open-source or commercial toolboxes.

1.1.1 NcC_Neurocognitive section contributions and roadmap

Cognitive theories provide testable frameworks to describe various human cognition models, including how the brain represents and processes information. The brain's mental processes range from visual and auditory perception, attention, memory, imagery, and problem-solving to natural language understanding, decision making, and more complex cognitive tasks. Neuroscientists use measuring instrumentations and scientific methods to monitor brain neuronal responses to external stimuli (MCCLELLAND; RALPH, 2015). NcC demonstration begins with defining a specific cognitive mission (task, system, or disorder). Based on the complexity

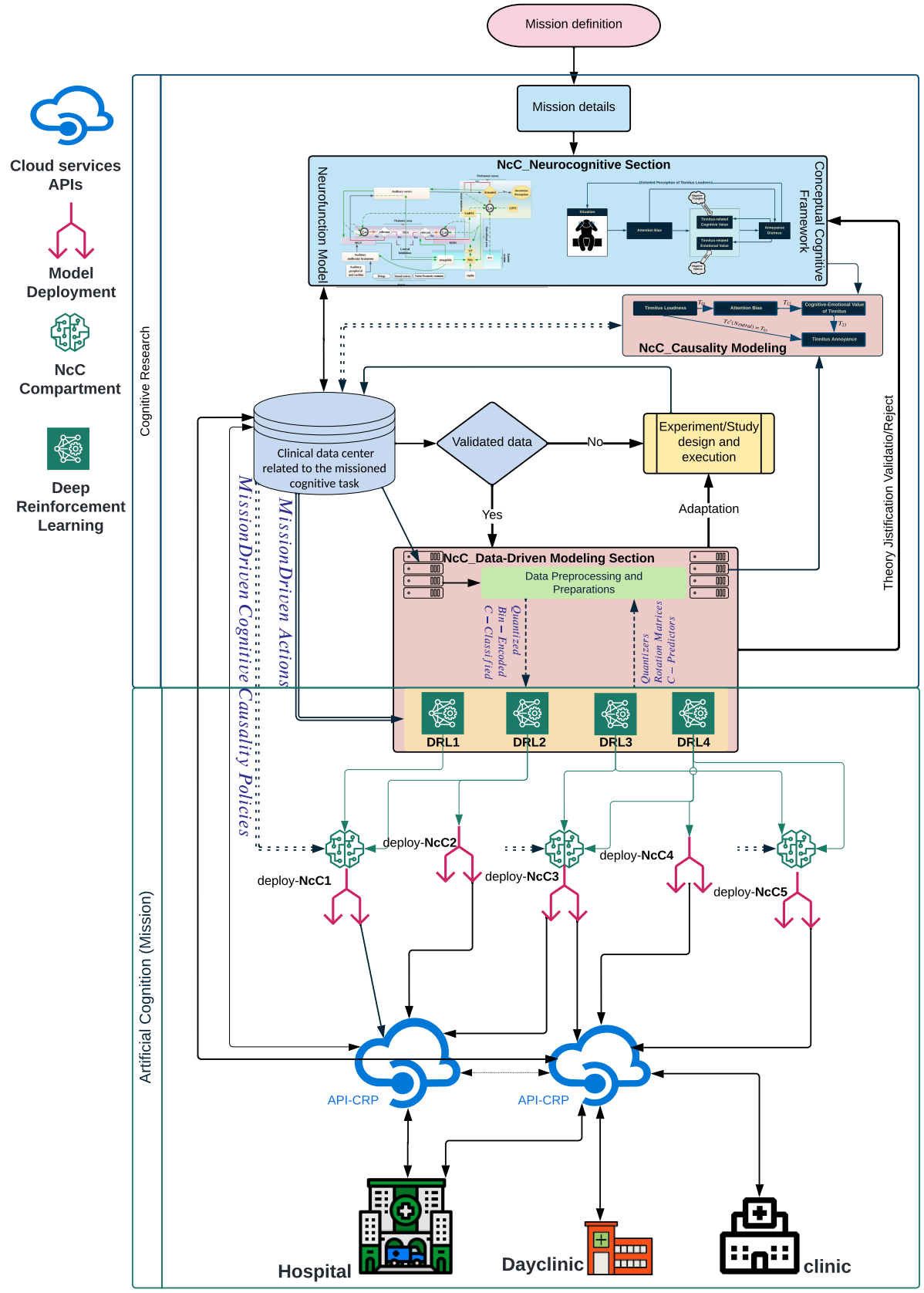

Figure 1 – Neurocognitive Computing (NcC) architecture

of the cognitive mission and available computing infrastructures, NcC-network architecture will be designed. Considering cognitive mission, the NcC_Neurocognitive section demands the following concrete objectives.

- **NcC- Mission Definition**, Network Architecture design
- **NcC-Objective I:** To develop a theoretical neurofunctional model.
- **NcC-Objective II:** To develop a Cognitive Conceptual Framework.
- **NcC-Objective III:** To design a well-control clinical study.

1.1.2 NcC_Data-Driven section contributions and roadmap

Using Big data in cognitive computing has allowed us to carry out myriad prediction tasks in conjunction with machine learning, such as identifying high-risk patients suffering from a particular disease and taking preventable measures. However, healthcare practitioners are not satisfied with mere predictions - they are also interested in the cause-effect relation between input features and clinical outcomes. Understanding such connections will help clinicians treat patients and reduce the risk effectively. Medical literature often expresses causality in probabilistic terms (MORABIA, 2005; PARASCANDOLA, 2011). The logical description of causality in medical research is considered too rigorous and occasionally not applicable. One main reason for probabilistic thinking is that we can easily quantify our beliefs in numeric values and build probabilistic models to explain the cause, given our observation.

In clinical diagnosis, the clinicians often seek the most plausible hypothesis (disease) that defines the evidence (symptom). Assume that a clinician observes a particular symptom S, and they have two explanations for this symptom, disease A or disease B. Suppose this clinician can quantify their belief into conditional probabilities. In that case, Prob(disease A|Symptom S) and Prob(disease B|Symptom S) (the likelihood of disease A or B may occur given that symptom S is observed). Then the clinician can choose the explanation with a more credible conditional probability value. However, selection and confounding biases may also affect observational studies, resulting in wrong causal conclusions.

Robust artificial intelligence aims to generate artificial agents with the same level of intelligence as human beings. The capability of causal thinking is integral to achieving this goal (FORD, 2018). Despite the rising popularity of causal inference research, the route from data preparation to machine learning and artificial general intelligence remains uncharted.

A causal diagram encodes assumptions about the causal story behind a dataset. Therefore, the dataset should exhibit certain statistical properties that agree with the causal graph. These causal assumptions govern the data generation process.

Consequently, we projected cognitive hypothesis in line with NcC mission through study/experiment design supported by acquired data. To prepare data for supervised modeling and deep

learning, we developed unsupervised causality and pattern discovery for feature optimization within NcC_Data-Driven. Literature shows that causal inferences are adoptable in deep learning modeling to reduce selection bias (ZHANG *et al.*, 2020; SCHNABEL *et al.*, 2016). The model interpretability enhances by identifying cause-effect relations between the model input and outcome. We can observe how the model outcome responds to interventions upon inputs.
The first MATLAB toolbox was developed for a new quantization algorithm independent of data type and distributions to cover NcC architecture requirements, which was explained shortly in the feature optimization chapter. Based on mutual information and the Markov chain, we developed a hybrid greedy algorithm for causal Feature Selection (FS) and Feature Transformation (FT) emerged in the second MATLAB toolbox of Feature optimization.
Model fairness aims to protect the benefit of people in minority groups or historically disadvantageous groups from the discriminative decisions produced by AI. Causal inference can also ensure model fairness against such social discriminations (KUSNER *et al.*, 2017). In addition to the attempts and progress made in this field, there are many low-hanging fruits in combining causal inference with machine learning methods. To put it in practice, We proposed a new distance matrix based on Mutual information and fuzzy dissimilarity to measure the distance between either one observation to another or a group of observations (cluster). NcC_Clustering algorithms and proposed NcC_Distance matrix guarantee the proper consideration of the minorities in NcC_Deep reinforcement learning and the future deploying models for precise deciding unseen or partially-seen observations in the dataset.
We developed the third MATLAB toolbox for clustering based on the distance matrix mentioned above through a greedy algorithm for optimizing the clustering processes. Several metric measures were tested in R-platform to benchmark the performance and cross-validation of the feature space and clusters with the routine methods. They were presented at the end of corresponding chapters. In the supervised approach, we employed the causality approach of mediatory modeling to discover causality in cognitive mission, which we developed in the IBM SPSS platform.

- **NcC- Data Preparation:** to quantized acquired data.
- **NcC-Objective IV:** To develop Feature Optimization.
- **NcC-Objective V:** To develop Clustering.
- **NcC-Objective VI:** To develop causality Modeling.

Experimental results demonstrate the proposed method's performance cross-validations based on state-of-the-art metric measurements. Comparisons are illustrated independently at the end of each chapter.

1.1.3 NcC_Deep Reinforcement Learning section contributions and roadmap

Fundamental elements of the human learning process are experimentation and observation. We already acknowledged that observing behaviors alone is insufficient to judge phenomena and their interactions with the environment to predict the outcome. Predictions' precision depends on unseen information. Therefore, the main questions are "how we integrate observation and experiment about one phenomenon to consolidate a piece of knowledge" and "how to generalize this knowledge to make the wisest decision in unexperienced situations."
The most used machine learning methodology for cognitive computing is Reinforcement Learning (RL) due to its simplistic algorithm using real-time *"trial and error"* experiments. RL uses errors to compute trials' estimations quality and store them in the table-like data structures per the trials defined as state-action pairs. Therefore, RL with minimum historical data supports online learning, essential for self-adapting to the perpetual spatiotemporal fluctuation in cognitive demand.
When Deep Neural Network models are employed to eliminate table-like structures in the RL framework by developing efficient quality-function approximators, consequently, Deep Reinforcement Learning (DRL) is created at niche(ANDRYCHOWICZ *et al.*, 2017; IIDA; LASCHI, 2011).
Consequently, we developed a conceptual Model Deep Reinforcement Learning (DRL) for the future trend of the Neurocognitive Computing platform.

- **NcC- DRL Background:** to integrate the theory and literature on that.

- **NcC-Objective VII:** To develop Conceptual Model for Deep Reinforcement Learning (DRL) in un/supervised learning strategies.

1.2 Contributions and Dissemination

We explored the main contributions and dissemination of the Neurocognitive Computing (NcC) in chapter-oriented here :

- Chapter 1 focused on the architecture of Neurocognitive Computing (NcC) which is the requirement of neurocognitive rehabilitation platforms and ecosystems disseminated as *The Substrates of Integrated Neurocognitive Rehabilitation Platforms (INCRPs)"* (GHODRATITOOSTANI *et al.*, 2019), and *"Sustainable development of cognitive science and technology ecosystem; an overview to the "human brain project" as a functioning sample"*(FARROKHI *et al.*, 2014), respectively.

- Chapter 2 focused on state-of-the-art and reviewed the literature. We published a review paper entitled, *"Theoretical Tinnitus Multimodality Framework: A Neurofunctional Model"* (GHODRATITOOSTANI *et al.*, 2016a).

- Chapter 3 illustrated the Neurofunctional modeling. We developed a testable tinnitus framework, and a method paper was published entitled *"Theoretical Tinnitus framework: Neurofunctional Model"* (GHODRATITOOSTANI *et al.*, 2016b). We also investigated the comorbidity of insomnia with tinnitus, which resulted in another review paper entitled *"The Sleep Toll in Tinnitus: A Brief Review Based on the Neurofunctional Tinnitus Model"*(TOOSTANI *et al.*, 2017).

- Chapter 4 demonstrated the conceptual methodology of the cognitive causal modeling. Based on the suggested technique, we developed conceptual cognitive frameworks for insomnia and tinnitus. We published the cognitive framework of insomnia entitled *"Conceptual Framework for Insomnia: A Cognitive Model in Practice"* (VAZIRI *et al.*, 2021). The cognitive framework of insomnia is presented here, and the manuscript is *ready to submit soon*.

- Chapter 5 provides a guideline to design a well-controlled and adequate study in dose-response noninvasive transcranial electrical stimulation in emotion regulation in line with the mission of NcC in the current prototype. Study design and methodology recently published entitled *"Dose-Response Transcranial Electrical Stimulation Study Design: A Well-Controlled Adaptive Seamless Bayesian Method to Illuminate Negative Valence Role in Tinnitus Perception"* (GHODRATITOOSTANI *et al.*, 2022). Furthermore, we investigated on gender effect on electrical distribution within brian and disseminated as *"Influence of gender-related differences in transcranial direct current stimulation: A Computational Study*"*, (THOMAS *et al.*, 2019). Eventually, within an international collaboration, we created a checklist for error minimization in the field of electrical stimulation and fMRI entitled *"A checklist for assessing the methodological quality of concurrent tES-fMRI studies (ContES checklist): a consensus study and statement"*(EKHTIARI *et al.*, 2022).

- Chapter 6 presents descriptive statistics and analysis of datasets we used for this prototype. We open-sourced anonymously all acquired and used datasets in all types of dissemination in the knowledge management platform of the Neurocognitive engineering laboratory for future scholars, with simple consent, is possible to download.

- Chapter 7 represents the entire feature optimization and validation process. We developed and evaluated several theories, algorithms, and toolboxes, including

    1. We proposed a novel Gaussian-kernel hierarchical nonuniform quantization mechanism with compensated fitting and developed the NcC-HQuantization MATLAB toolbox to implement corresponding architecture and algorithms.

2. We postulated and provided theoretical proof for a new FT method based on the joint probability and Markov chain approaches.

3. We proposed a new unsupervised hybrid FS optimization based on mutual information. To the best of our knowledge, the developed method is the first to recognize the optimized FS dependency pattern.

4. We developed regulatory parameters with an automatic optimization mechanism for dimension reduction. We also implemented related architecture and algorithms in the NcC-Feature Optimization MATLAB Toolbox. In addition, we projected Metric assessments and benchmarks in R. *"Manuscripts are in progress for dissemination."*.

- Chapter 8 introduces new clustering algorithms and NcC_Distance matrix. We provided theoretical proof and developed NcC_Clustering MATLAB toolbox. We tested Conclusion through two experiments in R, first to find out NcC_Distanc how to alter the performance of well-established clustering methods. Second to compare the performance of NcC_-Clustering with standard methods.

- Chapter 9 illustrates Supervised Causality learning based on Mediator inference modeling.*"Manuscripts are in progress for dissemination."*.

- Chapter 10 presented Deep Reinforcement Learning background and proposed a conceptual design for DRL in Neurocognitive Computing. We suggested Pseudocode for NcC_DRL as well for future applications of unsupervised learning. *"Manuscripts are in progress for dissemination."*. Further development and integration of DRL with previous toolboxes are out of the scope of the current thesis.

However, we believe the concept of Neurocognitive Computing (NcC) sheds light on causal artificial intelligence. It proposes a roadmap and landscape of the crucial infrastructure for the next generation of AIs.

CHAPTER

2

BEYOND THE-STATE-OF-THE-ART IN NCC_NEUROCOGNITVE SECTION

The ***Mission*** of this Ph.D. project was to conceptualize and prototype architecture toward an integrated Cognitive Rehabilitation Platform (iCRP) for Multidisciplinary tinnitus rehabilitation (iCRP-Tinnitus). iCRP-Tinnitus relies on Neurocognitive Computing (CC) to create dynamic and autonomous artificial cognition (GHODRATITOOSTANI *et al.*, 2019).

2.1 Cognitive Modeling Method

Cognitive models are emerging in all fields of cognition at a fast increasing rate, varying from perception to memory to problem-solving and decision making. Moreover, cognitive model applications are occurring to scatter into other fields, including human factors, clinical psychology, cognitive neuroscience, agent-based modeling in economics, and much more. Thus, cognitive modeling enhances an essential tool for cognitive science in distinct and the social sciences in general (BUSEMEYER; DIEDERICH, 2010).

Six-Steps In Cognitive Modeling

- **Step. I:** Theoretical Framework To create a conceptual, theoretical framework and reformulate its postulates into a more accurate rational context.
- **Step. II:** Ad-Hoc Assumptions To address further detailed assumptions to enhance the model. This is usually required for forming well-defined quantitative predictions. Regularly, the conceptual theory is insufficient or excessively weak to specify a model or misses relevant details effectively. Theorists try to reduce the number of ad-hoc assumptions, but this step is usually unavoidable.
- **Step. III:** Parameters Initialization To estimate model parameters with limited acquired

data. Models generally contain parameters or coefficients that are initially unknown. Assigning an initial weight to each independent feature estimated from the training data is essential. Theorists always try to reduce the number of model parameters to simplify predictions.

- **Step. IV:** Model Comparison Via Experimental Design To compare the predictions of competing models concerning their potential to describe the empirical outcomes. It is trivial to ask if a model fits on data or not (ROBERTS *et al.*, 2010). Indeed, all models are carefully demonstrated to provide simple representations of the only essential cognitive processes. Hence, a priori, we know that all models are not correct in some details, and a sufficient amount of data will always prove that a model is not valid.

- **Step. V:** Model Evaluation Answering the question of "Which model provides a better description of the cognitive system that we are trying to embody?" and test competing models to evaluate competing models empirically. Investigators try to design experimental circumstances leading to opposite qualitative or ordinal predictions from the two competing models. These qualitative experiments are intended to be parameter-free because they are applied to make these predictions for any values of free parameters. However, it is not always possible to build qualitative experiments for comparing models. We regularly need to reorganize quantitative tests to analyze models' precision, accuracy, and sensitivity by feedback on the prediction errors in model optimization. Even if it is possible to construct qualitative experiments, it helps to consider quantitative efficiency.

- **Step. VI:** Model Optimization Often it is needed to begin all over and reformulate the theoretical framework and design novel models in light of the feedback obtained from new experimental results. Model development and testing is a never-ending process. New empirical conclusions are constantly created, posturing new challenges to previous models. Previous models must be adjusted or spread to account for these new results, or in some cases, we need to discard the old models and start all over. Thus, the modeling process produces an evolution of models that improve and become more potent over time as the science in a field progresses (BUSEMEYER; DIEDERICH, 2010).

To conceptualize the Mission for iCRP-Tinnitus, we explored including brain structural compartments into more accurate anatomical connectivity associated with the known cognitive processes.

2.2 Literature review in cognitive Mission (Tinnitus)

Conscious perception of sounds without an external source is defined as tinnitus. It noticeably decreases the quality of life and can be a significant annoyance. Tinnitus affects the 30% of the general population, but 6% report debilitating symptoms(COELHO; SANCHEZ;

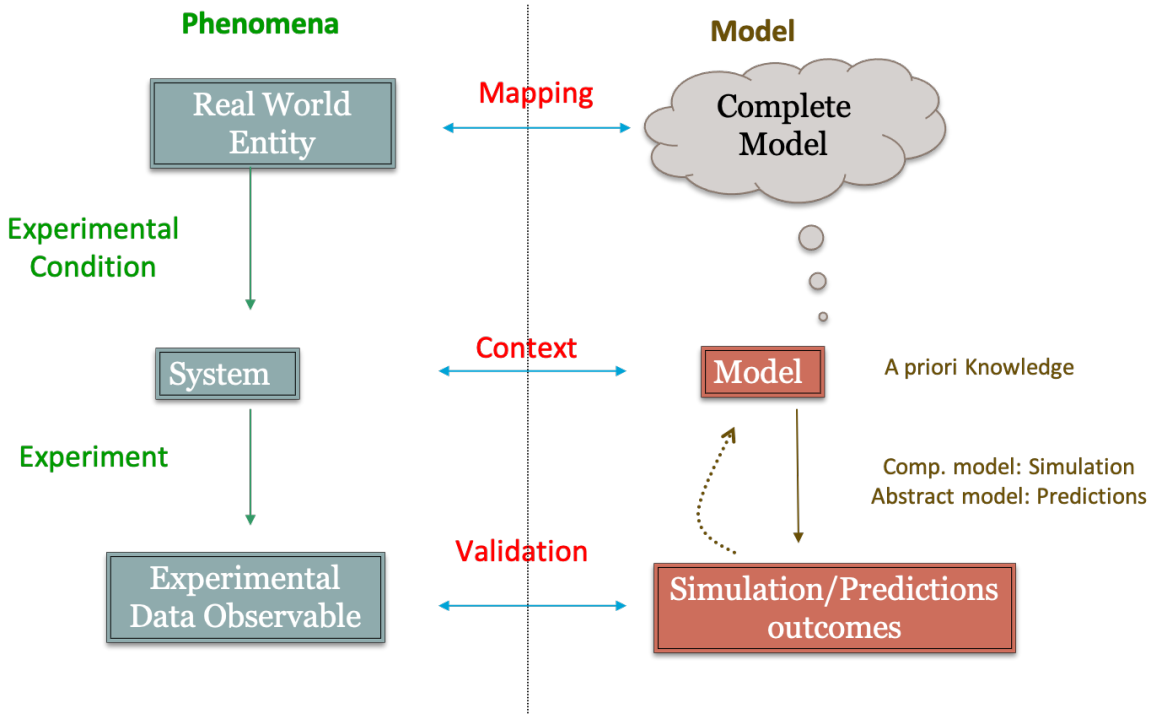

Figure 2 – Concept of Model versus Phenomena

TYLER, 2007; MILLS; ALBERT; BRAIN, 1986; SAVASTANO, 2007). Tinnitus is a severe condition in many cases that become chronic and is regularly described as "severely affecting the quality of life" and "annoying." Over the last couple of decades, several hypotheses have sought to explain tinnitus. A few of them have reached animal and human trials, successfully accepted by the academic and clinical communities, and earned a diagnosis and/or rehabilitation product stage. Considering prior functional and structural neuroimaging techniques, quantitative electroencephalography (qEEG), magnetoencephalography (MEG), and animal lesion studies, the following brain regions are documented that involved in tinnitus: the peripheral auditory system, the thalamus (reticular, medial geniculate, and dorsal nuclei), auditory cortex, the limbic system (anterior cingulate cortex, amygdala), brainstem (raphe nucleus), subcallosal and paralimbic areas which include basal ganglia (ventral pallidum), striatum (nucleus accumbens) and ventromedial prefrontal cortex (SEYDELL-GREENWALD *et al.*, 2012; RAUSCHECKER; LEAVER; MUHLAU, 2010). The current literature review addresses tinnitus structural brain network connectivity, which may gain insight into testable tinnitus framework and signal information flows.

2.3 Structural Brain Network Connectivity in Neurofunctional Tinnitus Model- [Step. I (Theoretical Framework)]

2.3.1 Thalamic Regions

The Thalamic reticular nucleus (TRN) is located between the thalamus and cerebral cortex. It receives excitatory inputs from all cerebral cortex regions and their associated thalamic nuclei and sends inhibitory projections to the thalamus (PINAULT, 2004). It is connected with a dorsal thalamic nucleus (PINAULT, 2004) and is divided into seven sectors that are independently involved in specific sensory processing (PINAULT, 2004); five of these are sensory (auditory, gustatory, somatosensory, visceral, and visual), one is motor, and one is limbic (PINAULT, 2004). The TRN is also associated with the visual brain area, and lesions in this area alter attention orientation(WEESE; PHILLIPS; BROWN, 1999; BALDAUF, 2010). Further, it receives excitatory inputs from the pre-frontal cortex (PFC) and sends inhibitory projections to the dorsal thalamus (ZIKOPOULOS; BARBAS, 2007). A mapping study of the sensory responses of the TRN has shown that some of its cells are associated with multi-modal sensory neurons (SHOSAKU; SUMITOMO, 1983). Moreover, it has been shown that the TRN mediates cross-modal effects of visual stimulation on auditory response in the medial geniculate body (MGB) and that some auditory cells in the TRN project to the somatosensory(YU *et al.*, 2009), not auditory, thalamic nuclei (KIMURA *et al.*, 2007). These findings suggest the TRN's participation in cross-modal sensory processing in the loop connectivity between the cortex and thalamus.
The TRN is involved in sensory gating (KRAUSE; HOFFMANN; HAJOS, 2003), attentional modulation (MAYO, 2009; ZIKOPOULOS; BARBAS, 2006), and generation of sleep spindles (TORRES-GARCIA *et al.*, 2012). It affects the activity in the dorsomedial (DM) thalamus. TRN lesions may influence the activity of the DM thalamus neurons via two pathways: (i) the loss of inhibitory input from the TRN due to excitatory neurons of the DM thalamus and (ii) an increase in the inhibitory action of the PFC–nucleus accumbens (NAc)–ventral pallidum (VP) pathway on the DM thalamus by the decrease in the excitatory pathway of the PFC to the NAc neurons. This action reduces the inhibitory action of the NAc on the excitatory neurons of the VP, resulting in the inhibition of the DM thalamus (CHURCHILL *et al.*, 1996; CHURCHILL; ZAHM; KALIVAS, 1996; ZAHM; WILLIAMS; WOHLTMANN, 1996; O'DONNELL *et al.*, 1997) Therefore, TRN lesions result in a dysfunctional control of the DM thalamus (ZIKOPOULOS; BARBAS, 2006), wherein the TRN receives projections from the PFC (ZIKOPOULOS; BARBAS, 2006) and has bidirectional connectivity with the dorsal thalamus (ZIKOPOULOS; BARBAS, 2007). The PFC–TRN coupling can enhance the motivation of dominant stimuli, establish pathways to the cortex, and enhance the motivation of reticular neurons to suppress distractors (ZIKOPOULOS; BARBAS, 2007) forcefully. The PFC–DM thalamus pathway, which maps via the same TRN prefrontal pathways, strengthens the transmission of relevant signals and weakens those of

distractors, a process called" lateral inhibition action" (ZIKOPOULOS; BARBAS, 2007). The auditory component of the TRN plays a gating role in the control of auditory stimuli that are relayed from the thalamus to the cortex (KIMURA *et al.*, 2012). The gating TRN involvement in cross-modal sensory processing for attention has been demonstrated. Cortical afferents from the temporal cortex, which enclose the primary and anterior auditory regions, topographically coincide with thalamic afferents from the ventromedial division of the medial geniculate nucleus (MGN) at the auditory TRN (KIMURA *et al.*, 2012).

A robust pathway from the amygdala to the TRN has recently been discovered, which is present only in humans (ZIKOPOULOS; BARBAS, 2012). In this pathway, one network originates in the basal nucleus and another in the amygdala's cortical nuclei, each following different paths within the thalamus but having coincidental terminal distributions in the TRN. Most fibers of both networks stimulate the amygdala anteriorly, are localized dorsally toward the inferior thalamic peduncle or the external capsule, and mainly enter the thalamus anteriorly (ZIKOPOULOS; BARBAS, 2012). The sensory systems transform external stimuli with emotional value to the cortex. The posterior orbitofrontal cortex (pOFC) and amygdala receive inputs from all regions of the higher-order association cortex (BARBAS; ZIKOPOULOS; TIMBIE, 2011), both of which project to the TRN via sensory cortices and their thalamic nuclei (ZIKOPOULOS; BARBAS, 2007). Thus, the pOFC and amygdala are situated in an optimal position to direct attention to external affective stimuli through the posterior TRN.

2.3.2 Auditory Cortex

Despite previous empirical evidence, it has been shown that abnormal activity in the auditory system can cause tinnitus (ROBERTS *et al.*, 2010). Animal studies have demonstrated increased spontaneous and sound-evoked neuronal activity at several auditory pathway regions. However, whether the observed abnormal activity is related to tinnitus or hyperacusis (which accompanies tinnitus in most cases) remains debatable (GU *et al.*, 2010). The detection of absolute blood oxygenation is not feasible using the intrinsic technique of fMRI, but relative blood oxygenation between conditions can be compared (LOGOTHETIS, 2008; GUSNARD; RAICHLE, 2001). Further, the influence of the top-down attention modulation on related neural activity has been detected as approximated tinnitus effect in auditory cortex hyperactivity (SEYDELL-GREENWALD *et al.*, 2012).

2.3.3 Limbic System

The limbic system's involvement in tinnitus pathology has been demonstrated in several studies, but its specific role remains uncertain (BAR, 2009; BLOOD *et al.*, 1999; BREITER *et al.*, 2001; KABLE; GLIMCHER, 2009; RESSLER; MAYBERG, 2007; SOTRES-BAYON; QUIRK, 2010; LANGGUTH, 2011; HALFORD; ANDERSON, 1991b; HALFORD; ANDERSON, 1991a; ROBINSON, 2007; MUHLAU *et al.*, 2006; LANGGUTH; KLEINJUNG; LAND-

GREBE, 2011; MOLLER, 2003; MOLLER, 2006; MAHLKE; WALLHAUSSER-FRANKE, 2004; LANDGREBE *et al.*, 2009; LANTING; KLEINE; DIJK, 2009; KALTENBACH; GODFREY, 2008; SHULMAN, 1995; RIDDER; VANNESTE; CONGEDO, 2011; RAUSCHECKER; LEAVER; MUHLAU, 2010). Rauschecker (2010) proposed that disturbance in the corticostriatal circuit can lead to permanent disruption of the gain control of the phantom sound perception, resulting in chronic tinnitus (MUHLAU *et al.*, 2006; RAUSCHECKER; LEAVER; MUHLAU, 2010). Furthermore, this disruption has been illustrated in the evaluation of other domains, such as reward, emotion, cognition, and aversiveness (BAR, 2009; BLOOD *et al.*, 1999; BREITER *et al.*, 2001; KABLE; GLIMCHER, 2009; RESSLER; MAYBERG, 2007; SOTRES-BAYON; QUIRK, 2010).

The ventromedial PFC (vmPFC) and NAc are components of the corticostriatal thalamic circuit, in which the vmPFC sends excitatory projections to the NAc (DIVAC *et al.*, 1987; FERRY *et al.*, 2000; JAYARAMAN, 1980). Studies have demonstrated a reduction in the vmPFC gray matter in tinnitus patients compared with that in the control group, indicating reduced neural activity output in tinnitus (SCHLEE *et al.*, 2009). The NAc activity increases due to diminished inhibition of the NAc by reduced input from the vmPFC to local inhibitory interneurons (SCHLEE *et al.*, 2009).

2.3.4 Amygdala

The amygdala can be divided into lateral, basal, central, and medial nuclei and intercalated cell masses. The lateral amygdala functions as a sensory gateway and receives neuronal inputs associated with sensory functions (auditory, visual, somatosensory, gustatory, and olfactory) from thalamic and cortical areas (LEDOUX, 2007). The basal amygdala receives inputs from polymodal memory and the higher-order association cortex. Internally, information flows from the lateral and basal nuclei directly to the central nucleus and indirectly via the inhibitory of the central nucleus. The lateral nucleus receives direct neuronal input from the auditory thalamus (MGB) and auditory cortex (LEDOUX, 2007; SAH; ARMENTIA, 2003). It has also been revealed that projections from the basal amygdala are related to memory (hippocampus) and high-level cognition (PFC and associative cortex) (KRAUS; CANLON, 2012).

Output from the central nucleus is associated with numerous autonomous functions. Excitatory projections from the thalamus to the hypothalamus stimulate the sympathetic nervous system to release corticosteroid hormone via the hypothalamic-pituitary gland–adrenal gland axis, thereby modulating the arousal and stress states. In addition, the amygdala processes emotions (RASIA-FILHO; LONDERO; ACHAVAL, 2000; PHELPS; LEDOUX, 2005), such as fear and anger (DAVIS; WHALEN, 2001; BAXTER; MURRAY, 2002), and drives behavioral and autonomic responses to external sensory stimuli. The amygdala detects the relevant stimuli (SANDER; GRAFMAN; ZALLA, 2003; ZALD, 2003) via bottom-up attention processing (PESSOA, 2011; COMPTON, 2003; COMPTON *et al.*, 2003) and mediates anticipatory and arousal reactions (MURRAY; WISE, 2010; MURRAY, 2007), thereby playing a vital role in motivation and deci-

sion making (BECHARA; DAMASIO; DAMASIO, 2003; PESSOA, 2011). Stimuli evaluation and motivation processing are mostly associated with the basolateral and central nuclei, respectively (BALLEINE; KILLCROSS, 2006). Their association with cognition (PHELPS; LEDOUX, 2005; PESSOA, 2010; SALZMAN; FUSI, 2010)also influences decision-making and behavior. Furthermore, the amygdala plays a role in classical fear conditioning (MAREN, 2003; MAREN, 2005). Anatomical evidence has shown lateral convergence of the auditory thalamus, auditory cortex, somatosensory thalamus, and associative cortex (WEINBERGER, 2011). Studies on the amygdala lesions have demonstrated that the MGB and the adjacent posterior intralaminar nucleus are involved in the long-term potentiation of auditory stimuli (WEINBERGER, 2011). Besides, the rat amygdala lesions have shown impaired responses to auditory stimuli (ARMONY; QUIRK; LEDOUX, 1998).

The amygdala's responses to sensory stimuli do not always occur in the conscious or awake state (PEDEMONTE; PENA; VELLUTI, 1996). Sensory evaluation during sleep is a useful feature for surviving dangerous conditions (ISING; KRUPPA, 2004), and EEG and fMRI studies have shown that sound presented during the non-rapid eye movement sleep phase can decrease the sensitivity of the amygdala to other stimuli, possibly because of a sleep protective mechanism (CZISCH *et al.*, 2009). In addition to several other brain areas involved in emotional processing, the amygdala is also involved in responses to music (BOSO *et al.*, 2006; LIMB, 2006), as shown using neuroimaging techniques in human studies (BOSO *et al.*, 2006). It responds to pleasant and unpleasant music, and unexpected musical events (JENTSCHKE; KOELSCH; FRIEDERICI, 2005). Translational studies have demonstrated that fear conditioning can activate the amygdala and improve tonotopic map plasticity in the auditory cortex. The receptive fields for frequencies of unconditioned stimuli are enhanced by co-activity of the basal forebrain, and auditory cortex (MORRIS; FRISTON; DOLAN, 1998; HARIRI *et al.*, 2003; WEINBERGER, 2007; FROEMKE; MARTINS, 2011).

Further, stimulation of the lateral amygdala can inhibit the primary auditory cortex response to sound via GABA receptors (HE; CHEN; ZHOU, 2004). In addition, neurons of the amygdala project directly to the inferior colliculus, which modulates emotion processing, thus functioning as thalamocortical feedback at a low level of the ascending auditory pathway (MARSH *et al.*, 2002). Figure.3 presents the schematic illustration of the amygdala.

2.3.5 Hippocampus

The hippocampus receives auditory sensory input directly or indirectly from the auditory association cortex via the parahippocampal cortex, the perirhinal cortex, and other forebrain areas, including the medial frontal cortex, insula, and amygdala (MOHEDANO-MORIANO *et al.*, 2007; MUNOZ-LOPEZ; MOHEDANO-MORIANO; INSAUSTI, 2010). The auditory association cortex receives inputs from the parahippocampal, and perirhinal cortices of the hippocampus (O'MARA, 2005).

The hippocampus is associated with explicit or declarative memory (EICHENBAUM, 2004;

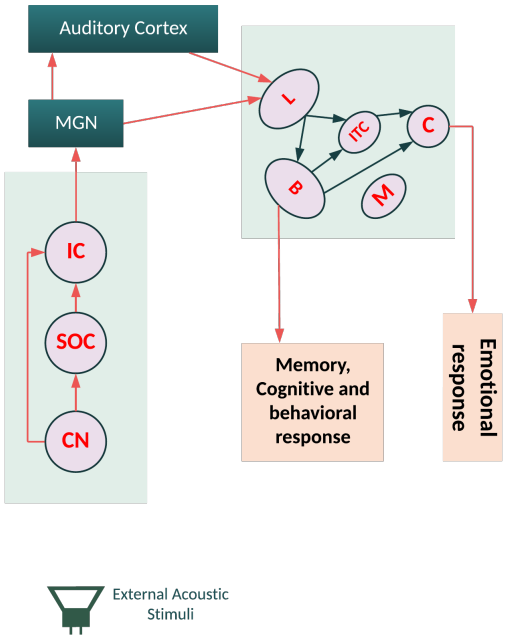

Figure 3 – Auditory pathway, modified from(GHODRATITOOSTANI *et al.*, 2016a)
Auditory midbrain/brainstem, amygdala divisions, and connections in the auditory system. The lateral amygdala receives neuronal input from the auditory thalamus (medial geniculate nucleus) and auditory cortex (primarily association areas). The basal amygdala projects to the inferior colliculus to generate an amygdalar-auditory feedback loop; B, basal amygdala; C, central amygdala; CN, cochlear nucleus; IC, inferior colliculus; L, lateral amygdala; M, medial nucleus; ITC, intercalated cells; MGN, medial geniculate nucleus; SOC, superior olivary complex.

DEVITO; EICHENBAUM, 2010). The left hippocampus is more associated with episodic memory, whereas the right hippocampus is associated explicitly with spatial memory (BURGESS; MAGUIRE; O'KEEFE, 2002). The dorsal hippocampus participates in primary cognitive information processes, whereas the ventral hippocampus is involved in emotional memory and learning tasks. The amygdala can modulate hippocampal memory; the memory formed by the hippocampus can modulate the amygdala's response to emotional stimuli (PHELPS, 2004; RICHTER-LEVIN, 2004). The projections from the amygdala to the hippocampus increase the emotional value of stimuli, facilitating hippocampal memory consolidation (ABE, 2001). The collaboration of the amygdala and hippocampus can contribute to the long-term consolidation of emotional events (RICHTER-LEVIN; AKIRAV, 2000). The primary function of the hippocampal auditory component is the formation of long-term memories. Music memory retrieval activates mainly the right hippocampal hemisphere (WATANABE; YAGISHITA; KIKYO, 2008). The hippocampus is also involved in emotional music processing. fMRI studies have shown that the right hippocampus and amygdala activity is enhanced while listening to sad music, but not neutral or pleasant music (MITTERSCHIFFTHALER *et al.*, 2007). Moreover, evidence has

shown that hearing loss is linked with hippocampal degeneration (ANGELUCCI *et al.*, 2007). The hippocampus seems to play a specific role in tinnitus, which involves emotional processing, such as sound blasts, which we did not cover in Neurofunctional Tinnitus Model.

2.3.6 Prefrontal Cortex

The PFC is thought to participate in high-level control of behavior generation (WARDEN *et al.*, 2012). It is highly interconnected with the brain, including extensive connections with cortical, subcortical, and brainstem regions (ALVAREZ; EMORY, 2006). In particular, the dorsal PFC is interconnected with brain regions involved in attention, cognition, and action, whereas the ventral PFC is interconnected with brain regions involved in emotions (PRICE, 1999). The PFC receives excitatory inputs (SESACK; PICKEL, 1992; VERTES, 2006) from the hippocampus, basolateral amygdala(BLA), NAc, and other limbic cortices via intracortical projections (JAY; WITTER, 1991; LEWIS; ANDERSON, 1995). The BLA and hippocampus exert control over the PFC cells(O'DONNELL; GRACE, 1995; GOTO; O'DONNELL, 2001). Synapses from the hippocampus to the PFC can change and articulate several types of plasticity in cognitive processes (SILVA-GOMEZ *et al.*, 2003; KOLB *et al.*, 1998).

One of the most recent fMRI studies that used voxel-based morphometry analysis has shown gray matter reduction in subcallosal regions (MUHLAU *et al.*, 2006), particularly in the vmPFC, in tinnitus patients (LEAVER *et al.*, 2011; LEAVER *et al.*, 2012). Furthermore, in a magnetoencephalography (MEG) study, vmPFC activity was positively correlated with resting-state cortical networks in tinnitus patients but not in control subjects (SCHLEE *et al.*, 2009). In another study on tinnitus subjects, the medial PFC activity was strongly altered by activity in some brain regions and weakly influenced by activity in other brain regions (SEYDELL-GREENWALD *et al.*, 2012), demonstrating functional differences in the vmPFC between tinnitus patients and controls. A positive correlation was observed between blood oxygen level-dependent (BOLD) responses in the vmPFC and psychoacoustic tinnitus parameters, such as loudness and duration. Other variables related to tinnitus, including tinnitus handicap inventory scores, hearing loss, noise sensitivity, anxiety, and depression, showed weak or no correlations with the BOLD signal (SEYDELL-GREENWALD *et al.*, 2012). The observed activity in the vmPFC is an effort to suppress the perceived sound to perform the required experimental task. The positive correlation of the vmPFC activity with psychoacoustic parameters indicates that this neural activity is associated explicitly with conscious awareness (SEYDELL-GREENWALD *et al.*, 2012).

The projections observed in the Dorsolateral Prefrontal Cortex (dlPFC), pOFC, vmPFC as part of the pOFC, and the associated thalamic mediodorsal nucleus (MDN) play crucial roles in cognition, emotion, and memory (ZIKOPOULOS; BARBAS, 2012). In addition, task difficulty and distractor saliency increase fMRI and BOLD activities in the lateral PFC(lPFC) (TOMASI *et al.*, 2005). The lPFC also plays a crucial role in suppressing internal distractions, such as intrusive thoughts and emotions (LEVESQUE *et al.*, 2003). Thus, these findings suggest that the lPFC performs an important role in cognitive evaluation, consistent with the top-down attention

valuation process.

2.3.7 Subcallosal Area and Paralimbic System

The TRN and dorsal thalamus are triggered by serotonergic neurons, which receive projections from the dorsal raphe nucleus, NAc, and paralimbic area (BROWN; MOLLIVER, 2000; O'DONNELL *et al.*, 1997). GABAergic neurons of the TRN are stimulated by serotonin (MCCORMICK; WANG, 1991; PAPE; MCCORMICK, 1989), resulting in the inhibition of the thalamic relay in sensory sectors (GUILLERY; SHERMAN, 2002). The TRN inhibition may shift between tonic and burst to fire modes of the thalamocortical relay (LLINAS; JAHNSEN, 1982; SHERMAN, 2001).

Leaver et al. (2011) proposed that NAc hyperactivity enhances the phantom sound perception appraisal. The vmPFC also projects to the TRN, manifesting its auditory distribution (ZIKOPOULOS; BARBAS, 2006), which inhibits communication between the auditory cortex and MGN. Therefore, reduced vmPFC output can further inhibit the phantom sound at the MGN (LEAVER *et al.*, 2011). Evidence has shown that patients with better preserved gray matter in the vmPFC have less hyperactivity in the NAc and medial Hexsch's gyrus, suggesting that the vmPFC can impart an inhibitory effect on the auditory system (LEAVER *et al.*, 2011). Dysregulation of the limbic and auditory networks may be at the heart of chronic tinnitus (LEAVER *et al.*, 2011). Rauschecker et al.(2010) proposed the involvement of a noise cancellation mechanism based on studies that found notable subcallosal volume loss in tinnitus patients (MUHLAU *et al.*, 2006; LANDGREBE *et al.*, 2009). Subcallosal activation correlates, at varying degrees, with the unpleasant effects of dissonant music (BLOOD *et al.*, 1999) and is altered by the perception and expectation of pain (PLOGHAUS *et al.*, 2003). Moreover, abnormal activity levels in the subcallosal area are observed in patients with certain depressive disorders (DREVETS *et al.*, 1997; MAYBERG *et al.*, 2005). The posterior portion of the subcallosal area is projected to the NAc, an essential component of the ventral striatum (BLOOD; ZATORRE, 2001; GRUBER; HUSSAIN; O'DONNELL, 2009). The ventral striatum is strongly interconnected with the subcallosal area (JOHANSEN-BERG *et al.*, 2008; ONGUR; PRICE, 2000). The NAc plays a critical role in reward behavior and avoidance learning via dopaminergic pathways (MCCULLOUGH; SOKOLOWSKI; SALAMONE, 1993). A regulatory role in sleep and several emotion-related systems via serotonergic neurons (AMBROGGI *et al.*, 2008). Almost *20%–40%* of patients with noise-induced hearing loss also develop chronic tinnitus (HOFFMAN; REED, 2004). Moreover, patients with somatic tinnitus can modulate the loudness and pitch of the phantom sound by movements of the eyes, neck, or jaw (LEVINE; ABEL; CHENG, 2003). Indicative alteration in tinnitus can occur because of sleep deprivation, or stress (ALSTER *et al.*, 1993; FOLMER; GRIEST, 2000; HALLAM, 1996). The phantom sound may completely disappear for a day or more and then return as loud as before. This intermittent perception reflects the perception suppression actions of inhibitory gating mechanisms (RAUSCHECKER; LEAVER; MUHLAU, 2010).

2.3.8 Aberrant Tinnitus-Related Plasticity in The Auditory and Limbic Systems

Three types of experimental brain plasticity are observed in tinnitus. First is alterations in the level of spontaneous neural activity in the central auditory system (KALTENBACH, 2000; EGGERMONT, 2007), such as modulation due to noise exposure and ototoxic drugs (EGGERMONT; ROBERTS, 2004), which could lead to changes in the spontaneous activity in different auditory areas of the brain. Noise exposure of any type reduces the spontaneous firing rate of the eighth cranial nerve, which results in the increase in spontaneous firing rate at several levels of the auditory brain cortex(NORENA; EGGERMONT, 2003; KALTENBACH *et al.*, 2004).

Changes in the temporal pattern of spontaneous neural activity can further modulate the synchronization of activities across auditory neurons (SEKI; EGGERMONT, 2003; EGGERMONT, 2007). Changes can occur via external auditory stimulation, so differences in neural synchrony may also be perceived as tinnitus. Burst firing and neural synchrony can occur in tinnitus patients (NORENA; EGGERMONT, 2003; SEKI; EGGERMONT, 2003). Peripheral hearing loss reduces afferent inputs to the brainstem, which contributes to changes in the neural activity of the central auditory system, thereby causing tinnitus.

Reorganization of tonotopic maps can also cause tinnitus (MUHLNICKEL *et al.*, 1998; SEKI; EGGERMONT, 2003; EGGERMONT, 2006); these readjustments may not be directly associated with tinnitus, but they can cause abnormal neural activity, such as cortical reorganization, leading to over-description of frequencies at the edge of peripheral hearing loss (RAJAN; IRVINE, 1998; EGGERMONT, 2006).

Studies on tinnitus have demonstrated that the projection of the auditory thalamus to the amygdala may generate an emotional reflex to the phantom sound (KRAUS; CANLON, 2012). Experimentally induced tinnitus has revealed the correlation between the auditory cortex and amygdala activation (MAHLKE; WALLHAUSSER-FRANKE, 2004). Tinnitus is associated with gray matter reduction in the auditory system (inferior colliculus); hippocampus, which regulates tinnitus pathophysiology (LANDGREBE *et al.*, 2009; LANTING; KLEINE; DIJK, 2009); and subcallosal region, including the NAc, which is connected with the amygdala and emotional processing (MUHLAU *et al.*, 2006).

The DCN hyperactivity in tinnitus (KALTENBACH; GODFREY, 2008). Tinnitus may alter attention and emotional responses by affecting the locus coeruleus, reticular formation, and raphe nuclei (LANGGUTH, 2011; LANGGUTH *et al.*, 2011). Neural activities observed in many types of tinnitus indicate significant roles of the amygdala and hippocampus (SHULMAN, 1995) and the parabrachial nucleus insula (LENHARDT; SHULMAN; GOLDSTEIN, 2008). The development of a learning mechanism that creates awareness of the phantom sound and involves the role of a distress network comprising the anterior insula and amygdala has been proposed (RIDDER; VANNESTE; CONGEDO, 2011). Like externally induced noises, internally generated tinnitus can cause emotional distress, resulting in mood disorders like depression.

Stress or depression may further aggravate tinnitus (ROBINSON; VIIRRE; STEIN, 2007).
In addition, evidence has shown that pathways, including the limbic system, may be involved in the noise cancellation mechanism. A feedback network from the amygdala to the auditory system can suppress the tinnitus signal at a subcortical level before it reaches the auditory cortex. This leads to conscious perception (RAUSCHECKER; LEAVER; MUHLAU, 2010). Neurons of the amygdala project to the NAc and further connect with inhibitory neurons in the TRN, which synapses with the ascending neurons in the MGB via the lateral inhibition mechanism and prevents the signal from reaching the auditory cortex. The limbic system and associated areas play an important role in tinnitus generation and suppression and can be vital targets for future tinnitus treatments. Treatment at the cognitive level may require shifting the attention away from the undesired phantom sound (ZENNER; PFISTER; BIRBAUMER, 2006).

2.4 Cognitive Processes and Functional Brain Connectivity in Neurofunctional Tinnitus Model-[Step. I (Theoretical Framework)] & [Step. II (Ad-Hoc Assumptions)]

2.4.1 Noise Cancellation Mechanism and Lateral Inhibition Circuitry

The bottom-up selective attention processes support the suppression of irrelevant stimuli, which may occur at the early stages by the TRN along with the *"lateral inhibition mechanism"* (ZIKOPOULOS; BARBAS, 2012; KIANG; MOXON; LEVINE, 1970; TYLER, 2006). The thalamocortical neurons carrying the relevant stimuli up from the thalamus to the cortex via the TRN excite the adjacent TRN neurons, inhibiting irrelevant thalamocortical neuron carriers. These adjacent TRN neurons inhibit the TRN neurons connected to the relevant thalamocortical carriers leading to decreased inhibition of the relevant signal carriers. (PINAULT; DESCHENES, 1998). This lateral inhibition mechanism ideally suppresses the noise originating from distracters and facilitates important stimuli processing. The amygdala, pOFC, and DM thalamus ending at the TRN may suppress the signal of distracting stimuli at the sensory cortex (ZIKOPOULOS; BARBAS, 2007). The TRN can perform the gain control function of the thalamocortical transmission in a highly localized manner. Because of the serotonergic neurons in the subcallosal area, the TRN inputs strongly inhibit the MGN neurons in the conscious state and anesthetic trials in a high-frequency manner (YU *et al.*, 2009). Thalamic projections to the TRN can modulate transmission from the peripheral sensory system, and brainstem to the cerebral cortex (YU *et al.*, 2009).

Furthermore, a voxel-based morphometric study on tinnitus patients has revealed that the reduction in gray matter in the vmPFC results in the decline of the vmPFC inhibitory output, leading to increased NAc activity (SCHLEE *et al.*, 2009). Although auditory cortical activity is essential for conscious perception of the phantom sound, the NAc–TRN coupling in the Neurofunctional Tinnitus Model is postulated as a noise cancellation mechanism for preventing the unpleasant permanent sound reaching the auditory cortex. This mechanism is partly consistent with the tinnitus tuning out model (RAUSCHECKER; LEAVER; MUHLAU, 2010).

The amygdala is a crucial component of the noise cancellation circuitry for processing sensory inputs with the emotional value associated with the thalamic MDN and the orbitofrontal cortex (GHASHGHAEI; HILGETAG; BARBAS, 2007).

2.4.2 Valuation Process

Selective attention prioritizes the processing of behaviorally relevant stimuli at the expense of processing irrelevant stimuli (TSOTSOS, 2011). The stimulus's relevance is determined based on an active associated neuronal network that indicates its related value or its reward

outcome in a particular context (KAPING *et al.*, 2011). Recent evidence has suggested that the brain network regularly determines and processes the values of stimuli that effectively bias the attentional stimulus selection against the more valuable stimuli in the peripherals (SEITZ; KIM; WATANABE, 2009; SHULER; BEAR, 2006; ANDERSON; LAURENT; YANTIS, 2011). Neural clusters in the vmPFC involved in valuations are disassociated from the top-down network in spatial attention. Behavioral analysis has suggested that shifting attention to less important stimuli requires a specific mechanism to overcome a motivational bias of attending to the more important stimuli (ANDERSON; LAURENT; YANTIS, 2011).

In a recent study, the visual valuation hub has demonstrated that the value selection response is correlated with the activity of neurons located across the medial-to-lateral extent of the PFC (vmPFC), ACC, and PFC (KAPING *et al.*, 2011). The highly valued stimuli suppression in humans and macaques has been conceptualized as a "self-control" process (KAPING *et al.*, 2011), which is associated with alterations in the neural activity level of the dlPFC and rostral ACC in humans (HARE; CAMERER; RANGEL, 2009). Together, these findings suggest that the valuation hub plays a similar role across different sensory modalities. The same auditory stimuli processing can drive attentional resources to hear the phantom sound in the Neurofunctional Tinnitus Model(GHODRATITOOSTANI *et al.*, 2016; GHODRATITOOSTANI *et al.*, 2016a).

2.4.3 Conscious Awareness Perception Processes and Attention

The ability to consciously perceive sensory inputs is theorized as the perception process. We propose to add more details to the model of distinction between awareness and attention (LAMME, 2003; WATANABE *et al.*, 2011). Conscious inputs originate from triggers in the sensory pathways or can be retrieved from the cortex and memory. The proposed conscious perception process (CPP) conceptual model provides logical solutions, as depicted in Figure 4. It discriminates the inputs in conscious and unconscious states in the initial stages. This approach alters the consciousness level from deep sleep to wakefulness. The wakefulness levels dynamically fluctuate during awakeness (GHODRATITOOSTANI *et al.*, 2016). The triggered inputs coming through the sensory pathways are evaluated via automated bottom-up valuation processes. The relevant and novel signals and pulled memory signals reach the top-down valuation process stage. The top-down relevant signal (one with cognitive-emotional value) is permitted to reach the attentive processes whereby the signal can be consciously perceived or remain unperceived (GRAZIANO; WEBB, 2015).

According to the CPP conceptual framework, conscious perception can be characterized as unattended, attended, and attended awareness. Attention represents a cognitive mechanism that allows certain information to be processed more intensively. Attention facilitates the transmission of the selected information across the cortex instead of the non-attended information (COHEN *et al.*, 2012). Conscious awareness requires attention because it permits information to remain online long enough to be processed entirely by an expanded network of cortical associations (COHEN *et al.*, 2012). Structurally, the lPFC is associated with attention, and inhibitory control

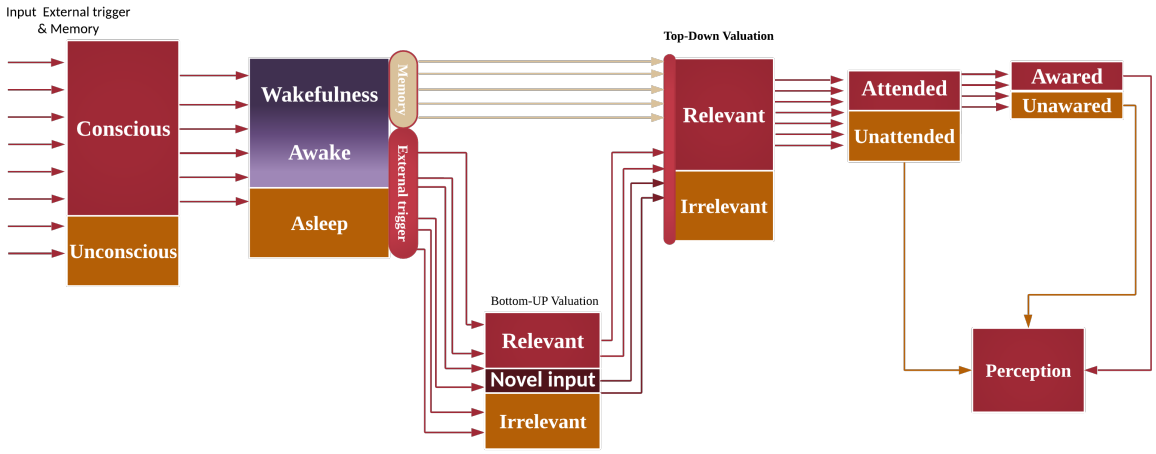

Figure 4 – Conscious perception process model modified from(GHODRATITOOSTANI *et al.*, 2016) The bottom-up valuation process performs unconscious, but Top-down valuation needs to be conscious attended awareness.

(SASAKI; GEMBA; TSUJIMOTO, 1989; MACDONALD A. W. *et al.*, 2000; PLONER *et al.*, 2005), particularly in auditory gating (KNIGHT; SCABINI; WOODS, 1989; WOODS; KNIGHT, 1986). Based on the Neurofunctional Tinnitus Model and the conscious perception process, we propose that the clinical distress in tinnitus can only be developed and maintained during conscious (attended) awareness perception of neutral tinnitus. Several studies have reported no tinnitus-related neural activity in patients during coma, anesthetics, vegetative states, restless eye movement, sleep, and dreams (GHODRATITOOSTANI *et al.*, 2016; RIDDER *et al.*, 2014). Furthermore, the top-down attention and conscious awareness processes suggest that the triggered inputs and phantom sounds cannot be perceived without attended awareness. This finding is consistent with the unconditional sensitization model, which proposes that the highly complex auditory stimulus pattern in tinnitus is controlled by attention (ZENNER; PFISTER; BIRBAUMER, 2006; GHODRATITOOSTANI *et al.*, 2016).

2.4.4 Acoustical Memory for Repeated Items

It has recently been suggested that the memory systems should not be classified in association with the conscious states because the conscious states do not influence the encoding or retrieval of information (HENKE, 2010). The critical factors are the number of elements required to encode the number and duration of information presentations. Rapidly encoded novel associations are suggested to be related to interactions between the hippocampus and certain neocortical processing areas. In a temporally extended learning state, the hippocampus might temporarily improve learning performance, but this is not essential for successful information retention, consolidation, or retrieval. The memory system relies heavily on the interactions between neocortical structures, the basal ganglia, the cerebellum, and the parahippocampal gyrus (HENKE, 2010; HANNULA; GREENE, 2012).

Considering the Henke model (2010), abnormal neural activity or sound perception best fits the temporally extended learning system related to tinnitus characteristics. The paralimbic structure, but not the hippocampus structure, is involved in tinnitus generation. This hypothesis is supported by a recent fMRI study (MAUDOUX *et al.*, 2012), which found no correlation between the hippocampus and resting-state network activity. However, it found a significant correlation between typical tinnitus connectivity networks and the parahippocampal, cerebellar, basal ganglia, subcallosal, thalamic, and amygdala regions. It also revealed a significant correlation between the ACC, auditory cortex, and PFC (MAUDOUX *et al.*, 2012). These two studies suggest that tinnitus's clinical distress is more prone to develop from a gradual learning process rather than a single exposure to an external stimulus (GHODRATITOOSTANI *et al.*, 2016).

2.4.5 Cognitive-Emotional Appraisal

The cognitive-emotional appraisal occurs as a reaction to differences between the information stored in memory and the actual information. Patients generally have no intuitive understanding of tinnitus signals; thus, the risk of negative appraisal increases. One of the crucial causes of negative appraisal is the patient's hypochondriac impression of neutral phenomena (MADDALENA; PFRANG, 1993a; MADDALENA; PFRANG, 1993b; MARCIANO *et al.*, 2003). Because their understanding of the illness mainly shapes an individual's response to illness, the personal disorder concept becomes a vital factor (ZENNER; PFISTER; BIRBAUMER, 2006). Examples of such personality disorders include the potential triggers of tinnitus and available tinnitus managements and treatments leading to appraisals, such as *"tinnitus is detrimental to my health"* or *"now, I am becoming deaf"* (ZENNER; PFISTER; BIRBAUMER, 2006).

2.4.6 Evaluative Conditional Learning(ECL)

The Neurofunctional Tinnitus Model hypothesizes that negative symptoms related to tinnitus develop in the neutral tinnitus stage together with the ECL process. When presented in association with a negative or positive Unconditional Stimulus (US), ECL indicates the change in the valence of the cognitively and emotionally neutral Conditional Stimulus (CS). This change in the valence is the retained response to the previously neutral stimulus (HOUWER; THOMAS; BAEYENS, 2001b; BAR-ANAN; HOUWER; NOSEK, 2010). Recently, studies have demonstrated that attention as the stimulus focus does not cause ECL; instead, to promote the acquisition of contingency awareness, the attention to contingencies between stimuli is crucial in ECL (KATTNER, 2012; STAHL; UNKELBACH; CORNEILLE, 2009; HUTTER; SWELDENS, 2013). Furthermore, the event-related potential–EEG source localization indicates that the medial-frontal brain regions are the likely origin of early valence discrimination signals (KUCHINKE; FRITSCH; MULLER, 2015). The prevailing tinnitus models emphasize learning by classical conditioning via pairing external events with causal physical events. We project that the clinical distress stage of tinnitus is developed and maintained through the EC learning only

in conscious (attended) awareness perception of CS (neutral tinnitus) and US (comorbidities reaction) contingencies. ECL encodes the memory through the learning pathway. Encoding memory initiates plasticity in the vmPFC and lPFC areas of the frontal cortex, resulting in plasticity in several regions of the limbic and auditory systems from the subcallosal area to the corticothalamic auditory pathway (GHODRATITOOSTANI *et al.*, 2016).
The ECL encoded memory consolidates in the MDN to bias tinnitus valence of the automated bottom-up valuation process in the subcallosal area pathway. Intermittent occurrences of ECL reinforce the tinnitus valence. In the corticothalamic auditory pathway, the ECL encoded memory leads to the plasticity of the MGN and lateral nucleus of the amygdala (LA). LA directly connects to the amygdala's central nucleus (CE) and via other amygdala regions. The output of the CE creates plasticity in the ACC. It controls the expression of the distress responses (such as fear), the related autonomic nervous system (e.g., blood pressure and heart rate), and endocrine (pituitary-adrenal hormones) responses (WEINBERGER, 2011).
Pavlovian conditioning (PC) learning needs adequate frequency of the pairing of CS and US to encode the memory. Violation in the synchrony of CS and US weakens the encoded memory. In return, ECL (valence) occurs when contingency awareness accompanies US and CS pairing. Furthermore, unpaired occurrences of CS or US have no effects on valence. Therefore, we argue that ECL is the only well-known mechanism to explain clinical distress development and maintenance in tinnitus (GHODRATITOOSTANI *et al.*, 2016).

2.5 NcC- Mission Definition, Network Architecture design

Background research and structural information about brain networks and connectivity in tinnitus demand the theoretical Neurofunctional model and cognitive framework to map Tinnitus rehabilitation hypotheses. Therefore, we defined the Mission of iCRP-Tinnitus on using High Definition- transcranial Direct Current Stimulation (HD-tDCS) neuromodulation technique for rehabilitation.

Based on the defined mission to support the proposed rehabilitation strategy, we need to consider the following issues to make the treatment effective:

- Anatomical targeting
- Functional specificity
- Causality versus Contingency parameters can affect bothersome or rehabilitation efficacy.
- Dose-response relationship The optimum dose.

CHAPTER

3

THEORETICAL NEUROFUNCTIONAL MODEL DEVELOPMENT

3.1 Neurofunctional Tinnitus Model Visualization- [Step. II (Ad-Hoc Assumptions)]

Previous functional and structural neuroimaging, quantitative EEG, MEG, and animal lesion studies, have implicated distinct brain areas in tinnitus. These areas are as follows: the peripheral auditory system, thalamus (reticular, medial geniculate, and dorsal nuclei), auditory cortex, limbic system (ACC and amygdala), brainstem (raphe nucleus), and subcallosal and paralimbic areas, including basal ganglia (VP), striatum (NAc), and vmPFC (GHODRATI-TOOSTANI *et al.*, 2016a). Figure 5 provides an overview of a schematic tinnitus network of different brain areas constructed by integrating data from SPECT, PET, fMRI, and MEG studies (GHODRATITOOSTANI *et al.*, 2016).

Authors agree that the continuous or intermittent abnormal neuronal activity at the peripheral (KALTENBACH *et al.*, 1998; BROZOSKI; BAUER; CASPARY, 2002; CHANG *et al.*, 2002) and midbrain(JASTREBOFF; SASAKI, 1986; CHEN; JASTREBOFF, 1995) auditory pathways (NORENA; EGGERMONT, 2003; ZHANG; KALTENBACH, 1998; KALTENBACH; MC-CASLIN, 1996; ZHANG *et al.*, 2011; SEKI; EGGERMONT, 2003; EGGERMONT; KOMIYA, 2000)or associative cortices, such as the limbic area (KUCHINKE; FRITSCH; MULLER, 2015; WEINBERGER, 2011; YU *et al.*, 2009; ZIKOPOULOS; BARBAS, 2007; KAPING *et al.*, 2011), can cause phantom sound generation. This abnormal neural activity can be generated by acoustic trauma, aging, brain lesions, and medicine. The Neurofunctional Tinnitus Model hypothesizes that sound perception fundamentally depends on the allocation of attentional resources via the frontal cortex, which depends on the cognitive-emotional value and the relevance of the phantom stimulus to the context. The small value of stimuli has less probability of allocating attentional resources. Noise cancellation mechanisms at the thalamic MGN level, which are governed by

TRN inhibitory projections, maintain the upward irrelevant signal's weakness. However, the high cognitive-emotional value of sensory stimuli may allocate adequate attentional resources and trigger a top-down suppression process that acts on the thalamus noise cancellation mechanism, leading to the conscious perception of the tinnitus phantom sound. Initially, the phantom sound is considered neutral, which has been defined as the "Neutral Stage" in the Neurofunctional Tinnitus Model, as illustrated in Figure 5(A) (GHODRATITOOSTANI *et al.*, 2016). Authors hypothesize that the noise cancellation mechanism's malfunction reinforces higher rates of phantom sound that reaches the auditory cortex, thus facilitating the abnormal neural plasticity in the auditory cortex and tonotopic reorganization termed "Central Tinnitus." Centralization can develop during both neutral and clinical stages of the Neurofunctional Tinnitus Model (GHODRATITOOSTANI *et al.*, 2016).

The patient's general suspicion can result in negative cognitive interpretation. This negative appraisal and Evaluative Conditional Learning (ECL) mechanism jointly enhance the associated cognitive-emotional value and the persistence of the conscious (attended) sound perception. Therefore, the probability of limbic system involvement and the appearance of negative cognitive-emotional reactions increase (such as attention deficit, anxiousness, insomnia, and phobias). If the cognitive-emotional value remains low, tinnitus will cease or be perceived as the failure of the noise cancellation mechanism and suppression at the thalamic level. This condition is identified as the "Clinical Distress Stage" of the Neurofunctional Tinnitus Model, as exhibited in Figure 5(B)(GHODRATITOOSTANI *et al.*, 2016).

3.2 Model Compartments

Auditory peripheral and cochlear system: This includes external and middle ear organs and cochlea, which receive acoustic pressure and sound as input and propagate electrical signals via auditory nerves (GHODRATITOOSTANI *et al.*, 2016).

Auditory midbrain/brainstem: This includes the cochlear nucleus, superior olivary complex (SOC), inferior colliculus auditory pathway, and raphe nucleus. The cochlear nucleus sends projection to the SOC and inferior colliculus and receives input from the auditory nerve surrounding the cochlea (KRAUS; CANLON, 2012; GHODRATITOOSTANI *et al.*, 2016a). The SOC receives inputs from the cochlear nucleus and relays the signal to the inferior colliculus (KRAUS; CANLON, 2012; GHODRATITOOSTANI *et al.*, 2016a). We ignored the internal parts of the auditory midbrain/ brainstem compartment to decrease the model's complexity.

Raphe nucleus: Serotonin is produced in the raphe nucleus of the cerebellum. Low serotonin levels can disturb normal sleep (GHODRATITOOSTANI *et al.*, 2016a).

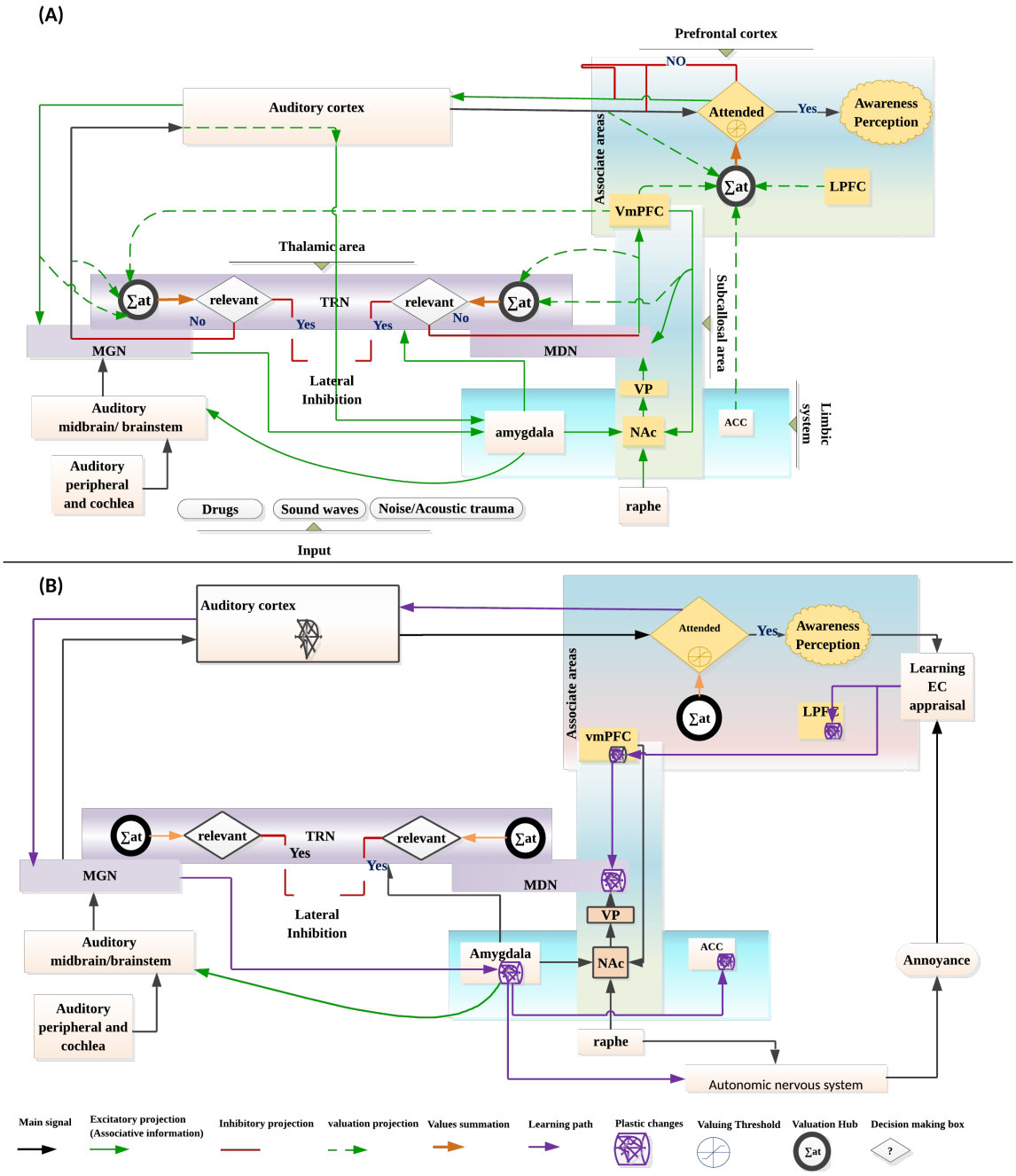

Figure 5 – The anatomical structure of the proposed Neurofunctional Tinnitus Model;
LPFC: Lateral prefrontal cortex; vmPFC: ventromedial prefrontal cortex; NAc: nucleus accumbens; ACC: anterior cingulate cortex; MGN: medial geniculate nucleus; TRN: thalamic reticular nucleus; VP: ventral pallidum; MDN: mediodorsal nucleus; Basal ganglia include VP and NAc; EC: evaluation conditioning; (A) phantom sound perception without negative reaction is defined as the "Neutral Stage" in the Neurofunctional Tinnitus Model; (B) the evaluation conditioning, appraisal learning procedure, and anatomical part of plastic changes in tinnitus brain network are identified as the "Clinical Distress Stage" in the Neurofunctional Tinnitus Model.

Thalamic area: It is located between the cerebral cortex and midbrain. We proposed that among the several regions of the thalamic area, the MGN, MDN, and TRN play crucial roles in tinnitus development. The MGN acts as a thalamic relay in the auditory system that receives excitatory inputs from the auditory midbrain (IC) and auditory cortex and inhibitory inputs from the TRN. In turn, it sends excitatory projections to the TRN, auditory cortex, and amygdala. The MDN sends excitatory output to the TRN and vmPFC and receives excitatory projections from the vmPFC and VP of the subcallosal area. The TRN receives excitatory inputs from the MGN, auditory cortex, MDN, vmPFC, and amygdala and sends inhibitory projections to the thalamus, MGN, and MDN (GHODRATITOOSTANI *et al.*, 2016a).

Auditory cortex: Includes primary, secondary, and associative auditory cortices, which receive excitatory inputs from the MGN and send excitatory projections to the MGN, TRN, PFC, and amygdala (GHODRATITOOSTANI *et al.*, 2016a).

Subcallosal area: It includes the NAc, VP, and vmPFC. The NAc receives excitatory inputs from the amygdala. The vmPFC receives serotonergic inputs from the raphe nucleus, which triggers the VP via unidirectional excitatory projection. The VP receives excitatory input from the NAc and sends excitatory projection to the MDN (GHODRATITOOSTANI *et al.*, 2016a).
PFC: It includes the lPFC, vmPFC, and associative cortex. The lPFC and vmPFC send excitatory outputs into the valuation hub of attentional allocation in the associative cortex as a cognitive-emotional value. The vmPFC sends excitatory projections to the TRN, MGN, MDN, and NAc (GHODRATITOOSTANI *et al.*, 2016a).

Limbic system: It includes the amygdala and ACC. The ACC sends output to the valuation hub as a purely emotional value of familiar audio signals. The amygdala sends excitatory projections to the TRN, midbrain (IC), and NAc. The NAc projection may trigger the vmPFC via the VP of the subcallosal area. The amygdala receives excitatory projections from the MGN and auditory cortex(GHODRATITOOSTANI *et al.*, 2016a).

3.3 Neurofunctional Tinnitus Model Information Flow [Step. III (Parameters initialization)]

In the Neurofunctional Tinnitus Model, we propose that phantom sound can lead to clinical symptoms during the two stages of tinnitus consistent with centralization. Initially,

continuous or intermittent abnormal neuronal activities develop in the peripheral or midbrain auditory pathways or associative cortices (such as the limbic area). Several other factors, such as different types of lesions, acoustic trauma, and drugs, can also cause temporary abnormal activity in the auditory cortices. Depending on the availability of attentional resources, the phantom sound may be suppressed or perceived. The weaker cognitive-emotional value of this potential phantom sound decreases the chances of its conscious (attended) awareness perception.

Irrelevance of the cognitive-emotional evaluations biases low valuation scores. This biasing of cognitive-emotional valuation strengthens the suppressive effects of both the lateral inhibition of the bottom-up selective attention and the noise cancellation mechanisms at the thalamic MGN. The noise cancellation mechanism, governed by TRN inhibitory projections, reduces the phantom sound's number of reaching the auditory cortex and maintains the signal evaluation's irrelevancy. Based on the ECL process and cognitive appraisal, phantom sound perception during the tinnitus's neutral stage gradually strengthens the negative valence of perceived tinnitus. It interprets it as suspicious and/or indicative of a disease. The cortical top-down processes weaken the noise-canceling effects (RAUSCHECKER; LEAVER; MUHLAU, 2010). The phantom sound is considered a relevant stimulus that results in the gradual formation of a vigilant auditory expectation of neutral tinnitus perception. The consequences generate a sense of cognitive and emotional reactions, which usually lead to negative reactions, such as stress and depression (HALFORD; ANDERSON, 1991a; ROBINSON; VIIRRE; STEIN, 2007; ROBINSON, 2007), anxiousness(LANGGUTH, 2011; HALFORD; ANDERSON, 1991a), hypochondriasis (MARCIANO *et al.*, 2003), phobias (ZENNER; PFISTER; BIRBAUMER, 2006; ADJAMIAN; SEREDA; HALL, 2009), and insomnia. These cognitive and emotional reactions and related comorbidities may cause tinnitus, or tinnitus may cause these conditions. Ultimately, due to the ECL process, clinical distress in tinnitus can be caused by the contingent relationship between the perceived relevant sound and negative valance of cognitive and emotional reactions (GHODRATITOOSTANI *et al.*, 2016).

Failure of lateral inhibition caused by drugs, somatosensory modulation, or other external negative events creates neuronal disturbances within the GABAergic pathways. These disturbances can cause abnormal activity due to which sourceless sounds may frequently reach the auditory cortex. However, regardless of the clinical distress stage's development from the conscious (attended) awareness perception of the neutral phantom sound, neuroplasticity, and long-term associative memory consolidation occur in the auditory cortices. Depending on the availability of attentional resources, the phantom sound may be perceived. From this point on, we name the conscious perception of phantom sound as the neutral/clinical distress tinnitus (GHODRATITOOSTANI *et al.*, 2016). Memory consolidation during centralization can bypass the noise cancellation process, strengthening the irrelevant cognitive-emotional value of the bottom-up attention. This leads to hyperactivity of the noise cancellation process, consistent with the reduction in subcallosal gray matter volume. Similarly, the failure of the noise cancellation process is recognized in the amygdala evaluation process. The basolateral part of the amygdala

receives excitatory projections from both the MGN and the auditory cortex, which can trigger the TRN to generate more inhibitory projections for irrelevant stimuli. The persistence of abnormal activity in the auditory peripheral system is not necessary for tinnitus perception; however, it can reinforce neuroplasticity and associative memory (GHODRATITOOSTANI *et al.*, 2016).

3.4 Introduction of tinnitus cognitive models [Step. IV (Model comparison via experimental design)]

Several animal models have been used to explain tinnitus by revealing its physiological characteristics in different auditory system processing centers. In the DCN, enhanced firing rates have been identified after intense acoustic exposure (KALTENBACH *et al.*, 1998; BROZOSKI; BAUER; CASPARY, 2002; CHANG *et al.*, 2002). In the inferior colliculus, elevated firing rates have been identified after large doses of salicylate induction (JASTREBOFF; SASAKI, 1986; CHEN; JASTREBOFF, 1995). It has also been established that noise trauma generates hyperactivity in the auditory cortex (ZHANG *et al.*, 2011; SEKI; EGGERMONT, 2003; EGGERMONT; KOMIYA, 2000). Other tinnitus-related animal studies have revealed tonotopic reorganization in the auditory cortex (STOLZBERG *et al.*, 2011; EGGERMONT, 2006; EGGERMONT; ROBERTS, 2004; EGGERMONT, 2007), increase in spontaneous activity in the DCN and inferior colliculus (NORENA; EGGERMONT, 2003; ZHANG; KALTENBACH, 1998; KALTENBACH; MCCASLIN, 1996), magnification in the auditory central gain (SUN *et al.*, 2009; AUERBACH; RODRIGUES; SALVI, 2014; ZENG, 2013; SUN *et al.*, 2009), and synchronization of neuronal activities (DOMINGUEZ *et al.*, 2006; STRAUSS *et al.*, 2008; LORENZ *et al.*, 2009). Moreover, a recent imaging study has demonstrated that different inhibitory and excitatory neurotransmitters modulate tinnitus-dependent hyperactivity (MIDDLETON *et al.*, 2011). Studies using MRI (CRONLEIN *et al.*, 2007; LANGGUTH *et al.*, 2007; LANDGREBE *et al.*, 2009; SCHNEIDER *et al.*, 2009; HUSAIN *et al.*, 2011; BOYEN *et al.*, 2012), fMRI (SMITS *et al.*, 2007; LANTING *et al.*, 2008), positron emission tomography (PET) (ARNOLD *et al.*, 1996; LOCKWOOD *et al.*, 1998; ANDERSSON *et al.*, 2000; LANGGUTH *et al.*, 2006; PLEWNIA *et al.*, 2007), single-photon emission computerized tomography (SPECT)(GARDNER *et al.*, 2002; MARCONDES; FREGNI; PASCUAL-LEONE, 2006), and MEG (MUHLNICKEL *et al.*, 1998) have revealed that neuroanatomical and activation alterations of the auditory pathways are correlated with abnormal activities in the non-auditory areas of the brain in tinnitus patients. Integration of information about tinnitus from different studies can provide general tinnitus models (JASTREBOFF *et al.*, 1988; JASTREBOFF; HAZELL, 2004; RAUSCHECKER; LEAVER; MUHLAU, 2010; TYLER *et al.*, 2008). Jastreboff (1988) proposed the neurophysiological model NM of tinnitus, which introduced a tinnitus management procedure known as tinnitus retraining therapy. The NM differs radically from previous models because of the following postulations:

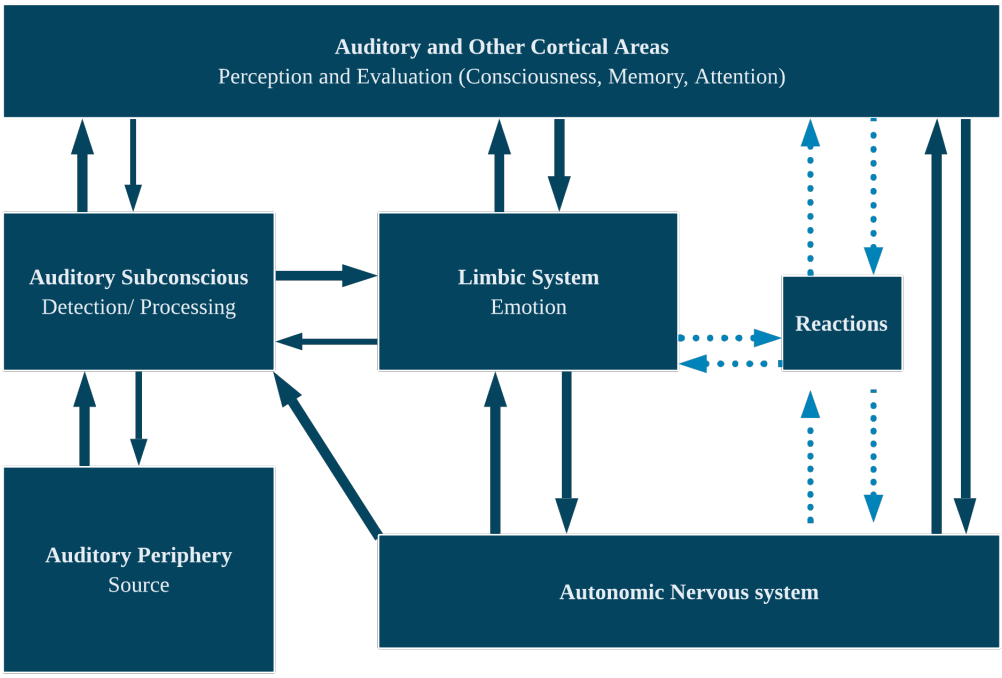

Figure 6 – Neurophysiological model of tinnitus; Modified from (JASTREBOFF, 1990)

a) tinnitus is a phantom auditory perception (JASTREBOFF, 1990);

b) tinnitus occurs due to the interaction of different brain networks with auditory pathways that result in the conscious perception of the phantom sound (principally, the limbic system is responsible for the development of tinnitus annoyance (JASTREBOFF, 1990));

c) tinnitus perception is not necessarily the key element that causes tinnitus to be problematic, and reactions to the tinnitus signal are possible without perceiving it (JASTREBOFF; JASTREBOFF, 2006);

d) sustained over-activation of the sympathetic autonomic nervous system is largely responsible for the behavioral manifestation of tinnitus-induced problems (JASTREBOFF; JASTREBOFF, 2006);

e) after a sufficient level of habituation to the reaction is reached and the tinnitus signal becomes neutral and unimportant, habituation of perception occurs (JASTREBOFF; JASTREBOFF, 2006).

The NM considers the involvement of several areas of the central and autonomic nervous systems. The flow of information commonly starts with sound wave stimulation of the peripheral auditory system, followed by a two-way connection to the "Auditory Subconscious" regions. This is followed by a two-way connection to the "Auditory and Other Cortical Areas" process of perception and evaluation of sound; it includes functions such as consciousness, memory, and

attention. The last neuroanatomical and functional component in the NM is the "Limbic System," illustrated in Figure 6. The "Limbic System" is connected via a two-way link to the components of "Auditory Subconscious" and "Auditory and Other Cortical Areas." It is also connected to the "Autonomic Nervous System," thus influencing neuroendocrine and autonomic reactions, such as respiratory, circulatory, digestive, and hormonal systems. The "Autonomic Nervous System" sends inputs to the "Auditory Subconscious" component and sends and receives inputs from the "Auditory and Other Cortical Areas." The sixth and last components are termed "Reactions," which refer to observations of clinical symptoms, such as annoyance, anxiety, panic, sleep, and concentration disturbances. These "Reactions" are connected in a two-way link to the "Limbic System," "Autonomic Nervous System," and the "Auditory and Other Cortical Areas."

The NM hypothesizes the prediction of tinnitus perception in subjects without any clinical symptoms, in whom the limbic and autonomic nervous systems are not activated, and no reactions can be observed; abnormal neuronal activities are processed as sourceless sound waves by the peripheral auditory system, which originates in the auditory periphery and move through the auditory pathways to the primary auditory cortex and other cortical areas. Conscious perception of the sound wave occurs only during the final cortical stages.

Tinnitus develops due to abnormal neural activities in the auditory pathways. When detected by the upper-stream components of the auditory pathways, it is processed at the subconscious levels. When auditory and other cortical areas are activated, the sound is consciously perceived. This conscious perception, evoked by abnormal neural activity, does not elicit emotional or behavioral reactions other than the mere perception of sound.

The abnormal neural activities are evaluated subconsciously and consciously. If they are evaluated as representing a neutral event, they will not be perceived consciously. However, suppose the neural activities are evaluated negatively or as unknown. In that case, they will be classified as potentially unpleasant and/or dangerous, thus activating the limbic and autonomic nervous systems and generating negative reactions, such as annoyance. Future perceptions of similar neural activities receive more attention than usual and are evaluated consciously. To create a condition of "reflex arc," experiencing tinnitus when at a high level of negative emotional/autonomic state is sufficient. The initial reflex arc will be created automatically. This reflex has a strong tendency to become stronger as both the signal (tinnitus) and reinforcement (reactions of the limbic and autonomic nervous systems) are contiguously present, corresponding to continuous learning that enhances the reflex's strength.

Rauschecker et al. (2010) proposed another tinnitus model based on a noise cancellation mechanism in which efferent projections from the subcallosal area are involved in suppressing the tinnitus signal as a sensory input to the thalamic level of brain processes. Functionally, the NAc and its correlated paralimbic circuitry are considered in the vmPFC, exhibiting a pivotal role in long-term habituation to continuous unpleasant sounds.

This model revealed that sound-evoked neural activity is passed from the peripheral auditory system through the brainstem and thalamus (MGN) to the auditory cortex for conscious percep-

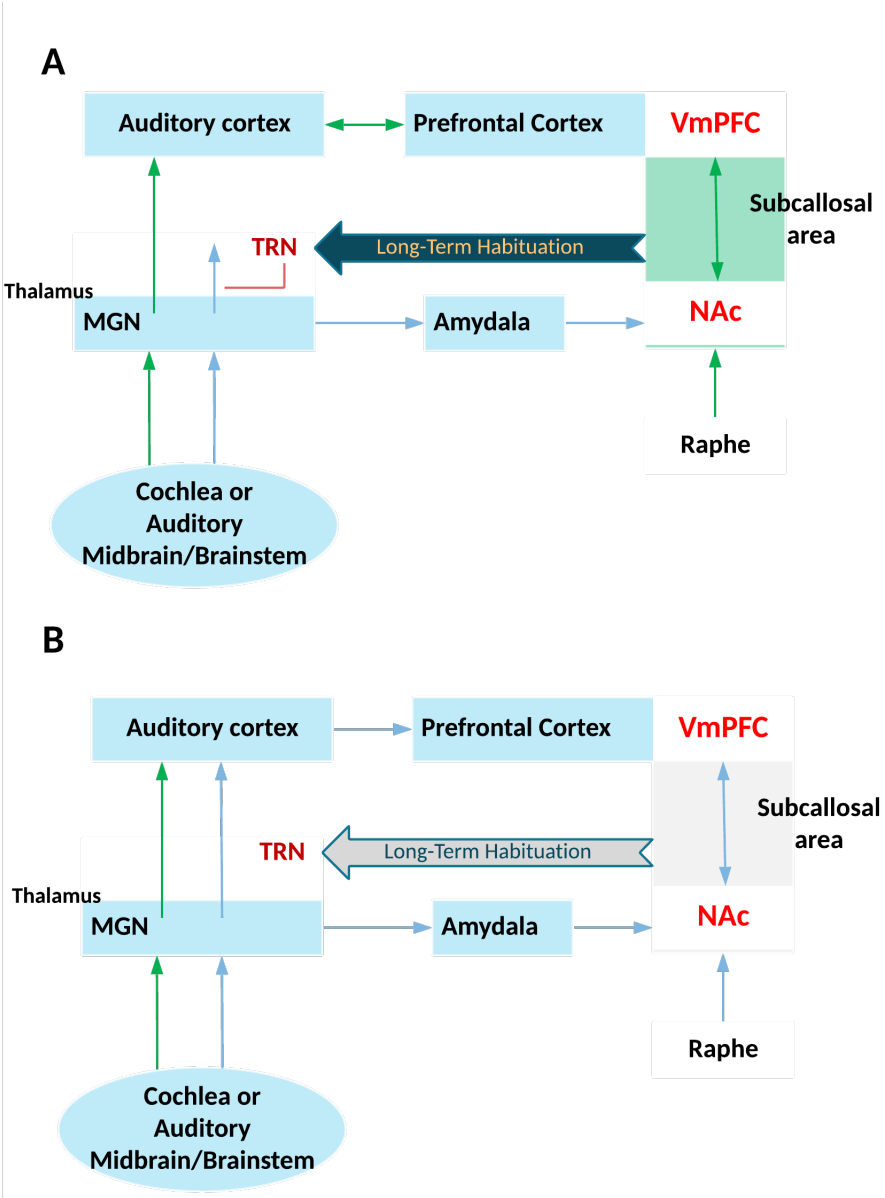

Figure 7 – Tuning out model of tinnitus, A)Normal Pathway and B)Tinnitus Pathway; Modified from (RAUSCHECKER; LEAVER; MUHLAU, 2010)

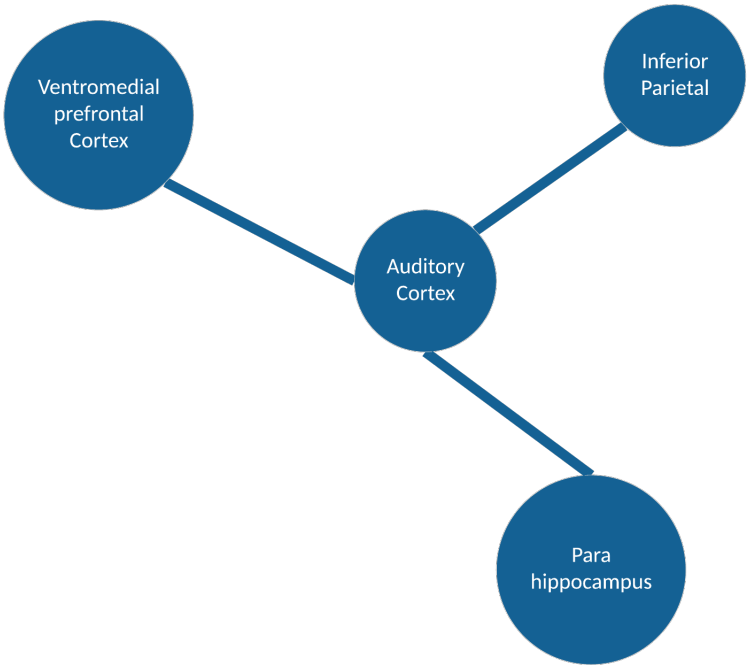

Figure 8 – Integrative tinnitus model modified from(RIDDER *et al.*, 2014)

tion. The same signal is conducted in parallel over the amygdala to the subcallosal area (which includes the NAc region of the ventral limbic striatum and the vmPFC) for emotional content evaluation of the sound. The TRN receives excitatory feedback projections from the subcallosal area and confers selective inhibition at the regions of the MGN corresponding to the unpleasant sound frequencies.

The model suggested that this gain control mechanism results in precise filtering (*"tuning out"*) of repetitive, unwanted noises, which do not reach conscious perception in the auditory cortex, as exhibited in Figure 7. It is further recommended that if the abnormal neural activity in the peripheral system generates the sourceless tinnitus, the sound signal is being filtered out at the thalamic MGN and will not be relayed to the auditory cortex in the normal tuning-out process. The NAc system weakening may no longer cause tinnitus signal cancellation at the thalamic level, leading to tinnitus perception and long-term reorganization of the auditory cortex and resulting in chronic tinnitus. Intermittent tinnitus may develop during the development of damage to the subcallosal area; this explains the fluctuating activity (and corresponding neurotransmitter) levels and transient filtering of the tinnitus signal.

An integrative model of the auditory phantom perception has been proposed based on the concept that "tinnitus core" subnetworks incorporate both the neurophysiological model and the noise cancellation mechanism. It theorizes that minimal brain areas (the auditory cortex, inferior parietal area, and vmPFC/frontopolar cortex) jointly activate to achieve tinnitus's conscious perception. The hypothesis assumes that separable tinnitus characteristics can be extracted by evaluating resting-state magnetic and electrical studies involving evaluating specific characteris-

tics and control of other parameters. Furthermore, studies using functional neuroimaging with neuromodulation could illuminate some causal relationship between the acquired correlated networks. This model proposes that tinnitus can be perceived as an emergent aspect of several dynamic overlapping subnetworks with different spontaneous oscillatory patterns and functional connectivity arrangement and that communications within different subnetworks take place in hubs, which are defined as brain regions that simultaneously participate in various brain networks and can be involved in distinct subnetworks at discrete oscillatory frequencies (RIDDER *et al.*, 2014). This model further conceptualizes that the tinnitus core comprises the neural correlates of auditory pitch awareness and memory. The tinnitus core connects to other subnetworks via hubs and leads to bothersome effects, such as mood disorders, distress, and lateralization. The integrative tinnitus model is illustrated in Figure 8.

It is important to note that all the aforementioned studies are limited in their scope as they have focused only on functional tinnitus-related activities of isolated regions. These studies have concentrated their efforts on the structural dimension, solo behavioral, and absolute clinical investigations. They are abstract in their descriptions and are only supported by minimal empirical evidence.

Therefore, this study's objective was to describe a Neurofunctional Tinnitus Model capable of predicting future results while considering a testable framework of the structural, functional, behavioral, and clinical empirical evidence.

3.5 Neurofunctional Tinnitus model predictions – [Step. IV (Model comparison via experimental design)]

We hypothesize that conscious (attended) awareness perception is necessary for neutral tinnitus to develop into clinical distress tinnitus. This concept has not been disclosed in previous tinnitus models. In our opinion, unattended phantom sound or neutral tinnitus cannot cause bothersome or distress symptoms. The attended awareness of sourceless sound allows information to remain on-line long enough to be thoroughly processed by a distributed network of cortical circuits, the limbic and autonomic nervous systems (GHODRATITOOSTANI *et al.*, 2016).

Zenner et al. (2006) proposed a role of auditory attention in establishing the neural changes underlying tinnitus. However, a specific mechanism for attention and the circumstances leading to its engagement were not described (ZENNER; PFISTER; BIRBAUMER, 2006). The Neurofunctional Tinnitus Model asserts that to perceive tinnitus, the valuation process in the frontal cortex plays a crucial role in the prioritization of sensory inputs in attention resource allocation and leads to the development of clinical distress tinnitus. The following three stages are involved: tinnitus generation, maintenance, and clinical distress development (GHODRATITOOSTANI *et al.*, 2016).

- ***Tinnitus generation:*** Our hypotheses regarding the failure of the noise cancellation mech-

anism is consistent with the model proposed by Winkler et al. (2009), which argues that attention is a factor in modulating the detection of prediction failure (detection of deviance) and in promoting the stimulus-driven binding of sensory attributes to create new auditory objects in dynamic auditory environments. We further propose that such failure results in the perception of neutral phantom sound, which is not mentioned in Rauschecker's tuning out model of tinnitus (WINKLER; DENHAM; NELKEN, 2009; RAUSCHECKER; LEAVER; MUHLAU, 2010; ROBERTS; HUSAIN; EGGERMONT, 2013; GHODRATITOOSTANI *et al.*, 2016).

- ***Tinnitus maintenance:***We argue that the auditory attention involvement (ROBERTS; HUSAIN; EGGERMONT, 2013) and the discrepancy between top-down and bottom-up attentional processes can bias the cognitive-emotional value of the neutral phantom sound. We also hypothesize that the PFC valuation hub continuously regulates the persistence of tinnitus perception and compares the value of intermittent attended awareness perceived tinnitus (phantom sound) with all sensory and auditory inputs. According to the patient's emotional stability, during conscious (attended) awareness of tinnitus, appraisal magnifies the cognitive-emotional value of tinnitus and results in increased duration of the perception. Furthermore, independent of patient perception, the continuous and repetitive abnormal neural activities reaching the auditory cortex form plasticity in auditory pathways and generate the auditory memory of tinnitus termed as "centralized tinnitus." This is consistent with the Henke memory model (HENKE, 2010; ROBERTS; HUSAIN; EGGERMONT, 2013; RAUSCHECKER; LEAVER; MUHLAU, 2010; GHODRATITOOSTANI *et al.*, 2016).

- ***Tinnitus clinical distress:***We propose that tinnitus's cognitive-emotional value increases via negative appraisal and EC learning mechanisms during conscious (attended) awareness perception of tinnitus. The tinnitus signal links with the limbic system and actuates annoyance, leading to clinical distress. We also agree that tinnitus's conscious awareness can be suppressed and substantially modulated when the patients engage in cognitively demanding tasks (SEARCHFIELD; MORRISON-LOW; WISE, 2007; SEARCHFIELD K. WISE, 2012; GHODRATITOOSTANI *et al.*, 2016).

Due to the lack of contingency and pairing of CS and US, the learning by EC versus conventional PC can strongly legitimize the development of various tinnitus symptoms in patients. However, to develop learning, both PC and EC are needed to perceive CS (tinnitus) and US simultaneously. This violates assumptions of the neurophysiological tinnitus model (JASTREBOFF, 1990). We propose that conscious perception of tinnitus and conscious (attended) awareness perception of tinnitus contingency and US (distress symptom causes) are needed to develop, maintain, and rehabilitate tinnitus.

According to the Neurofunctional Tinnitus Model, the patients can be categorized into two general groups of neutral and clinical distress tinnitus, summarized in Table1. In the neutral stage,

the patients are divided into those who only perceive tinnitus (Type NT-I), those who perceive tinnitus with auditory cortex plasticity (Type NT-II), and those who do not perceive tinnitus and have no auditory cortex plasticity (Type NT-X). Because biasing of their negative valence via EC may support future prevention programs, type X patients, who no longer perceive tinnitus, can become potential future tinnitus patients. The patients in the clinical stage can be further divided into two groups: those who perceive tinnitus and only have limbic system plasticity (Type CL-I) and Type CL-I symptoms and auditory cortex plasticity (Type CL-2). This novel view may help us investigate corresponding diagnostic assessment results under correct classifications and lead to selecting the most appropriate rehabilitative methodologies.

Tinnitus Stage	Type	Phantom sound perception	Negative reaction	Plasticity in Auditory cortex	Plasticity in Limbic system
Neutral	NT-I	Y	N	N	N
	NT-II	Y	N	Y	N
	NT-X	N	N	N	N
Clinical Distress	CL-I	Y	Y	N	Y
	CL-II	Y	Y	Y	Y

Table 1 – Required sample sizes to identify significant difference between treatment effects.

Further experimental and clinical studies on tinnitus brain mapping, brain imaging, neuromodulation, cognitive behavioral therapy, and head modeling are warranted to evaluate and validate the following Neurofunctional Tinnitus Model predictions and suggested validation methodologies:

- In cognitive rehabilitation approaches, rehabilitation cannot occur without conscious (attended) awareness perception of tinnitus (GHODRATITOOSTANI *et al.*, 2016).
  ∗ Examine changes in clinical distress symptoms during unconscious versus conscious (attended) cognitive intervention. Recently, Probst et al. (2016) described a model examining emotional states, perceived loudness of tinnitus, and tinnitus distress in patients in the clinical distress stage and not in the developing stage (PROBST *et al.*, 2016). However, let's consider the clinical distress a dynamic spectrum to maintain tinnitus bothersome. The results support our hypothesis that consciousness is necessary for neutral tinnitus to develop into clinical distress tinnitus. Besides, the tinnitus bothersome (distress) fluctuations occur during conscious (attended) awareness perception (ability to report the level of his/her tinnitus cognitively). Furthermore, in the study by Probst et al. (2016), the patients scaled their stress levels (awareness of contingency with unconditional stimulus). We agree that the awareness of contingency and conditional stimuli is necessary for the EC learning process but not in the PC learning process (GHODRATITOOSTANI *et al.*, 2016).

- Tinnitus psychoacoustic specifications encode to memory in the auditory cortex during tinnitus centralization.
  * Use resting-state fMRI–EEG analysis to investigate the brain network activity and connectivity in correlation with loudness and pitch before and after electrical neuromodulation stimulation trials in the auditory cortex (GHODRATITOOSTANI *et al.*, 2016).

- Continuous evaluation of tinnitus valence is performed in the PFC.
  * Use electrical neuromodulation stimulation on the dlPFC to indicate the decrease in bothersome and negative valence (GHODRATITOOSTANI *et al.*, 2016).

- Changes in tinnitus valence lead to changes in attentional allocation and duration of conscious perception.
  * Perform cognitive behavioral therapy to prove that decreasing the tinnitus negative valence can decrease tinnitus perception frequency and make it less bothersome (GHODRATITOOSTANI *et al.*, 2016).
  * Perform cognitive counseling trials to improve patient knowledge of tinnitus, which can decrease cognitive-emotional appraisal, negative valence, and frequency of tinnitus perception and make tinnitus less bothersome (GHODRATITOOSTANI *et al.*, 2016).

- Cognitive disorders (such as insomnia and stress) cannot cause tinnitus but can develop tinnitus negative valence and make it bothersome.
  * Perform clinical trials and meta-analysis on patients with cognitive disorders (GHODRATITOOSTANI *et al.*, 2016).

- The conscious pairing of adequate pleasant audio-visual stimulus with tinnitus can decrease tinnitus negative valence.
  * Perform pleasant multi-modality virtual reality application in future trials (GHODRATITOOSTANI *et al.*, 2016).

CHAPTER

4

CONCEPTUAL COGNITIVE MODEL OF TINNITUS AND CASUALTY

4.1 Concepts of Cognitive Model

Several cognitive and behavioral theoretical models have endeavored to unravel the influence of psychological factors and related mechanisms in emerging or relieving tinnitus distress (HALLAM; MCKENNA; SHURLOCK, 2004; JASTREBOFF, 1990; ZENNER; ZALAMAN, 2004; ZENNER; PFISTER; BIRBAUMER, 2006; ANDERSSON; MCKENNA, 2006; MCKENNA *et al.*, 2014a; GHODRATITOOSTANI *et al.*, 2016; GHODRATITOOSTANI *et al.*, 2016a). Hallam et al.(2004) suggested that incapability in habituation to tinnitus induces awareness because of negative appraisal and emotional significance. Consequently, classical conditioning was introduced as the principal mechanism promoting aversive emotional states of tinnitus (JASTREBOFF, 1990). Afterward, Zenner et al. (2006) hypothesized that tinnitus sensitization occurs when perceiving sound is classified as harmful, fear-inducing, unpredictable, and might prompt a sense of deficiency in coping and helplessness (ZENNER; ZALAMAN, 2004; ZENNER; PFISTER; BIRBAUMER, 2006). Mckenna et al.(2014a), in their study, documented that cognitive misinterpretation of the tinnitus leads to distress and physiological arousal ends in a distorted perception of sensory input (MCKENNA *et al.*, 2014a).

Different attentional paradigms have revealed significant deficiencies in selective attention within tinnitus patients (MCKENNA *et al.*, 2014a; JASTREBOFF, 1990; BAGULEY; MCFERRAN; HALL, 2013; ADJAMIAN; SEREDA; HALL, 2009; ROBERTS; HUSAIN; EGGERMONT, 2013; LI *et al.*, 2015). Trevis et al. (2016) asserted that patients with chronic tinnitus had poorer performance in cognitive tasks in a silent room with repetitive background noise than the healthy controls(TREVIS; MCLACHLAN; WILSON, 2016). Emotional Stroop Task(EST) is one of the Premier methods developed for evaluating attention bias to emotional or concern-relevant information. (GROSS, 2013; DAVIDSON; PUTNAM; LARSON, 2000).

Recently, Ghodratitoostani et al. (2016) postulated the Neurofunctional Tinnitus Model(NfTM) and emphasised that the CAAP of tinnitus is crucial for causing suffer. NfTM characterized tinnitus patients into two stages:

- "Neutral stage": perceiving tinnitus without distress reaction and
- "Clinical distress stage": experiencing distress reaction due to the corresponding negative valence when the tinnitus is perceived (GHODRATITOOSTANI *et al.*, 2016; GHODRATITOOSTANI *et al.*, 2016a).

Valence denotes emotional states ranging along a continuum from positive to negative feelings with a neutral midpoint (BRADLEY; LANG, 1994a). Tinnitus-related valence progressively shifts to negative through the Evaluative Conditional Learning (ECL) mechanism wherein repeated pairing of neutral tinnitus conditioned with similar or different negative stimuli unconditioned promotes negative valence (GHODRATITOOSTANI *et al.*, 2016; HOUWER; THOMAS; BAEYENS, 2001b).
On the other hand, negative appraisals such as *"The noise makes my life unbearable", "it will drive me crazy" or "it will overwhelm me"* (HANDSCOMB *et al.*, 2017) intermittently strengthen the cognitive value of tinnitus. Appraisal and ECL mechanisms stimulate tinnitus-related cognitive-emotional value and drive preferential attention allocation to the sound and prolonged tinnitus perception. Contrarily, NfTM has posited that the CAAP of tinnitus concurrently presenting positively-valenced stimuli might change negative valence and might begin to perceive tinnitus less frequent with a lower level of distress, (GHODRATITOOSTANI *et al.*, 2016). Cognitive functions proposed in NfTM can also be embodied in the emotion regulation process model (GROSS, 2013; GROSS, 1998a) of tinnitus, which prognosticates that the tinnitus loudness misperception may link to negative valence and selective attention. NfTM also posits that perpetual evaluation of tinnitus valence, comparing this valence with those of other sensory and auditory inputs, and monitoring persistent perception occurs in the prefrontal cortex (GHODRATITOOSTANI *et al.*, 2016).
The studies above have limited mention of causality relationships to the best of our knowledge, which can easily mislead interpretations of the findings. Thus, the design of an approach to conceptualizing these causal hypotheses is essential. A novel tinnitus theoretical-conceptual framework would enable the drawing of data models for testing causality relationships between independent variables and outcomes within retrospective studies. Besides, it also navigates research strategies in prospective studies on tinnitus cognitive rehabilitation.
The present chapter aims to fill this void in the concept of neurocognitive computing by proposing and validating a novel Conceptual Cognitive Framework (CCF) for tinnitus in light of the models mentioned above. The model draws heavily from cognitive processes proposed by NfTM (GHODRATITOOSTANI *et al.*, 2016) and is in line with the modal model of emotion (GROSS, 1998b). CCF illustrates cognitive processes and their interactions, contributing to developing and

maintaining tinnitus annoyance-distress reactions.
Initially, we developed a conceptual framework for developing clinical distress based on tinnitus stages (Neutral vs. Clinical). Forthcoming, the framework was articulated and visualized. We also developed a numerical causal model for tinnitus through the multi-mediatory (causality) methodology underlying the data-drive part of the thesis, chapter 9.

4.2 Fundamental Ideas and Postulations of Conceptual Cognitive Framework

- CCF aims to illustrate cooperation between cognitive processes causing distress in tinnitus.

- CCF mainly rests on Evaluative Conditioning to assume that CAAP into both US-CS and their contingencies is essential for attitude formation (GHODRATITOOSTANI *et al.*, 2016; HOUWER; THOMAS; BAEYENS, 2001b).

- Either or both cognitive-value and emotional-value can cause annoyance, but they can affect each other merely through annoyance. Instead, the annoyance affects cognitive-value, emotional-value and meanwhile distorts the perception of tinnitus.

- In the Neutral stage, the negative cognitive-emotional values could generate annoyance but are not sufficient to trigger distress reactions. Accordingly, annoyance and distress are considered two different concepts.

Proposed Conceptual Cognitive Framework In abstract, CCF compartments include situation, attention bias, cognitive value (arousal), emotional value (valence), annoyance-distress reaction, and distorted perception. Broadly speaking, CCF illustrates how the interaction between cognitive processes contributes to distress reactions. In this chapter, we concentrated on tinnitus experienced in silence and before sleep. CCF proposes when stimuli related to tinnitus preferentially capture attention, then, either directly or through corresponding cognitive and emotional values, triggers distress and results in distorted perception. Distress, in turn, feeds back to and influences the situation. Likewise, distress reaction fuels back corresponding cognitive and emotional values. The proposed CCF is illustrated in Figure 9.

To provide proof of concept for the proposed CCF, we primarily present supporting studies from Tinnitus literature. We then go through Mediation models to test proposed causal relationships between cognitive and emotional factors in the CCF.

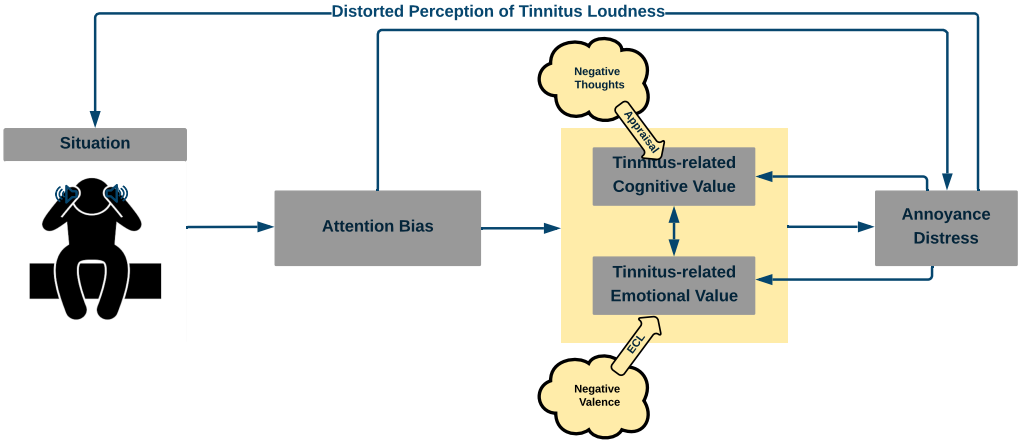

Figure 9 – Conceptual Cognitive Framework of Tinnitus; Tinnitus CCF speculates that in the pre-sleep situation when tinnitus-related cues (emotionally-laden or relevant to individuals' concerns) capture attention. Then, either directly or through tinnitus-related cognitive and emotional values, triggers an annoyance-distress mechanism leading to a distorted perception of tinnitus loudness exacerbating the tinnitus experience. Likewise, tinnitus distress reinforces the negative cognitive-emotional value of tinnitus.

4.3 Model compartments and cognitive processes

4.3.1 Situation

Nighttime silence during the pre-sleep period could facilitate CAAP of internal [tinnitus sound, body sensation or thoughts] and external [environmental sounds, light, heat] stimuli. Asnis et al. (2018) also reported that in the absence of environmental noises, the perception of tinnitus sound facilitates and interferes with the process of falling asleep or getting back to sleep (WALLHAUSSER-FRANKE; SCHREDL; DELB, 2013; ASNIS *et al.*, 2018).
Using a mobile application, Probst et al. (2017) performed an investigation on tinnitus patients' daily life and revealed that the environmental sound-level differs based on the day's time. Most severe tinnitus loudness and tinnitus distress were experienced at night and early morning hours (from 12 a.m. to 8 a.m.) because of lower environmental sound-level, which cannot attenuate tinnitus perception in these interims (PROBST *et al.*, 2017).

4.3.2 Attention Bias

Conscious attended awareness perception of internal and external stimuli shape individuals' expectations and predictions from the pre-sleep situation. Thus, any novelty or changes in the above-mentioned stimuli' features can bias attention (HORSTMANN; HERWIG, 2016). Supporting this comes from (ROBERTS; HUSAIN; EGGERMONT, 2013) and (WINKLER; DENHAM; NELKEN, 2009) studies suggesting that "discrepancy between an expectation and upcoming stimuli can bias attention" (HORSTMANN; HERWIG, 2016). Furthermore, emotionally-laden or threat-related stimuli can also receive priority over other stimuli and lead to attentional bias,

similar to what cognitive theories of anxiety disorders proposed (BECK; CLARK, 1997). According to this view, prioritized attention allocation to threat cues, Dalgleish et al. (1990) may lead to the development and maintenance of anxiety (DALGLEISH; WATTS, 1990). The threat cues for patients with tinnitus could be related to tinnitus characteristics [CAAP of tinnitus sound or changes in the tinnitus loudness or pitch] which impair the process of falling asleep as the active goal of pre-sleep time.

One of the most-used paradigms to experimentally assess attentional bias is the Emotional Stroop task (EST). In EST, a set of emotional words (relevant to the subjects' clinical condition) and neutral words (irrelevant) written in different colors are presented to the patients. The participants are supposed to respond to the color of the words as quickly as possible by pressing the corresponding key on the keyboard while ignoring the words' meaning. Prolonged responding to the color of emotionally-laden words compared with neutral words indicates biasing of attentional resources towards the emotionally-laden information (WILLIAMS *et al.*, 1988).

The number of studies assessing attentional bias in the tinnitus population through the Stroop task is limited, and the findings are inconsistent. While Andersson et al. (2005) reported a faster reaction time to tinnitus-related words, other studies could not find a Stroop effect in tinnitus patients' reaction time to tinnitus-related words (ANDERSSON *et al.*, 2000; GOLM *et al.*, 2016).

However, inconsistent results in tinnitus studies may emerge from confounding factors and possible biases effects on imperfect methodologies that are applied in the study design like in Andersson et.al ((ANDERSSON *et al.*, 2005)) study with a significant difference in the sample size of the tinnitus group $(n = 104)$ and healthy group $(n = 21)$. Furthermore, the salience of the applied emotional words is not high enough to interfere with the task. Therefore, utilizing more personalized tinnitus words to guarantee high individualized importance of the patients' stimuli might provide better results. Paradigms that examine auditory selective attention or dichotic listening tasks could be more proper to find differences on a behavioral level (GOLM *et al.*, 2016).

4.3.3 Emotional Value

The Emotional value builds up through the Evaluative Conditional Learning mechanism, which plays a crucial role in liking and disliking stimuli (GHODRATITOOSTANI *et al.*, 2016). Based on ECL, neutral stimuli (CS) can obtain positive or negative valence after frequently being paired with emotionally-laden stimuli (US) (HOUWER; THOMAS; BAEYENS, 2001b). Valence describes the emotional states varying along a continuum from positive to negative feelings with a neutral midpoint (BRADLEY; LANG, 1994b). Based on CCF, the CAAP of both CS and US and their contingencies are essential for ECL formation. In addition, Evaluative Conditioning is an accumulative procedure so that different valenced USs can aggregate to CS valence over intermittently being paired (STAHL; UNKELBACH; CORNEILLE, 2009). Accordingly, EC learning is resistant to extinction, so neither CS/US-only presence nor pairing

CS with the different USs would extinguish formerly-shaped EC learning memory (HOUWER; THOMAS; BAEYENS, 2001b). Based on CCF, the negative valence of other USs, through the ECL mechanism, fuel the negative tinnitus-related emotional value leading to annoyance or distress reaction. The frequent co-occurrence of tinnitus sound and negative USs enhance negative tinnitus-related emotional value. Thereafter, tinnitus perception alone could trigger distress reactions due to the shaped learning memory of the US's valence (GHODRATITOOSTANI *et al.*, 2016).

4.3.4 Cognitive Value

The Cognitive value of perceiving internal and external stimuli develops through the appraisal process. When the meaning of an object or event is judged in a particular situation based on beliefs, desires, and intentions, the appraisal process engages (SCHERER; SCHORR; JOHNSTONE, 2001). However, not all information demands the appraisal mechanism, but those relevant to the individuals' concern (FRIJDA, 1987) can trigger a cognitively-aroused state followed by appraisal. Accordingly, attention bias to tinnitus sound cues, as a concern-relevant stimulus, can provoke a cognitively-aroused state and subsequent appraisals about tinnitus, *"If only the noise would go away," "Why me? Why do I have to suffer this horrible noise?"* (WILSON; HENRY, 1998). Negative thoughts through appraisal mechanisms fuel the negative tinnitus-related cognitive value leading to annoyance or distress reaction.

Self-report questionnaires are widely employed to collect patients' thoughts and beliefs about events, situations, or objects, depicting the role of CAAP in appraisals to judge conditions and their respective consequences. Tinnitus Cognitions Questionnaire (WILSON; HENRY, 1998) assesses the content and the frequency of positive and negative thoughts associated with tinnitus. Wilson et al. (1998)asked two-hundred tinnitus subjects to specify how frequently they experience thoughts in Tinnitus Cognitions Questionnaire. The highest endorsement rates were for the following negative statements: *"If only the noise would go away," "Why me? Why do I have to suffer this horrible noise?" "I cannot enjoy what I am doing because of the noise," "The noise will drive me crazy."* (WILSON; HENRY, 1998). It was also reported that negative thoughts were independent of positive thoughts suggesting that the absence of positive thoughts does not indicate negative thoughts. Furthermore, high positive correlations were observed between negative Tinnitus Cognitions Questionnaire and depression, emotional distress, insomnia, and tinnitus handicap (WILSON; HENRY, 1998).

Other cognition aspects like catastrophizing and a tendency to exaggerate the negative aspects of a problem are evaluated with Tinnitus-Related Self-Statements Scale (FLOR; SCHWARTZ, 2003) and Tinnitus Catastrophizing Scale (CIMA; CROMBEZ; VLAEYEN, 2011). Using Tinnitus Catastrophizing Scale, Cima et al. (2011) revealed that a catastrophic misinterpretation of tinnitus is highly associated with enhanced fear and attention toward tinnitus and lower ratings of life quality. Similarly, (ANDERSSON *et al.*, 2006) accomplished the experimental research on the effects of suppressing tinnitus-related thoughts (as an attentional control strategy) to evaluate the

immediate consequences of suppressing versus not suppressing thought (attending to tinnitus). It was exhibited that tinnitus-related thoughts were reduced by suppressive instructions while increased by attending to tinnitus. However, similar outcomes were not observed in tinnitus patients of the control group who neither suppressed nor attended to their tinnitus.

4.3.5 Annoyance-Distress Reaction

In line with many Cognitive-Behavioral studies, CCF suggested that negative appraisal of tinnitus sound triggers the annoyance-distress reaction. Cognitive-Behavioral Model of tinnitus (MCKENNA *et al.*, 2014b) projected that the process of distress begins with intrusive, overly negative thoughts about perceived tinnitus sound. These negative thoughts provoke arousal and emotional distress and drive maintaining selective attention, monitoring, and counterproductive safety behaviors. Further studies corroborated that negative evaluations of tinnitus sound (ANDERSSON; WESTIN, 2008; CONRAD *et al.*, 2015) or catastrophic appraisals about it (WEISE *et al.*, 2013) were associated with tinnitus distress severity. However, the study of (HEINECKE *et al.*, 2008) revealed that negative appraisal does not necessarily lead to physiological arousal. (HEINECKE *et al.*, 2008) designed a crossover experiment that presented stress-inducing conditions to a group of tinnitus patients (HEINECKE *et al.*, 2008). The results showed that tinnitus groups compared with controls reported higher subjective strain while no differences were detected in physiological stress measures. The investigators attributed the mismatch between subjective self-reports and objective measurements to negative appraisal processes and catastrophizing thoughts in tinnitus patients (HEINECKE *et al.*, 2008).

4.3.6 Distorted perception

CCF proposed that valence and cognitive-arousal as two components of emotion can affect the patients' judgment about tinnitus pitch and loudness. The following findings lend support to this proposal; (YOO; LEE, 2015) explored the effect of modulating arousal and valence on time-perception in subjects with social anxiety, comparing the time duration of presented stimuli with the standard duration in training sessions. It was exhibited that the duration of negative-stimuli against positive-stimuli was estimated longer with high arousal but shorter with low arousal levels. This finding suggests that modification in the tendency and magnitude of valence and arousal modulates time-perception (YOO; LEE, 2015); it can also be analogous with the tinnitus loudness perception versus annoyance. In (DURAI; O'KEEFFE; SEARCHFIELD, 2017) study, it was revealed that emotional stimuli with weighted valence and arousal could affect tinnitus patients' judgment in the rating of tinnitus annoyance and loudness but not in loudness match (DURAI; O'KEEFFE; SEARCHFIELD, 2017). Likewise, psychological and Cognitive-Behavioral therapy studies on tinnitus expressed a significant improvement in tinnitus distress or tinnitus-related quality of life, while tinnitus loudness match did not change (ANDERSSON; LYTTKENS, 1999; MARTINEZ-DEVESA *et al.*, 2007).

4.4 Conceptual Cognitive Model Hypotheses

We hypothesized that in the Neutral stage, failure in ignorance and negative cognitive-emotional valuation is essential for CAAP of phantom sound to generate annoyance but not sufficient to cause distress (Continuous-Learning-Path). Moreover, in the Clinical stage, we postulated that CAAP of tinnitus sound directly or through "Continuous-Learning-Path" enhances annoyance, ending with distress.
Secondarily, we are proposing that in the Clinical stages, intermittent distress experience leads to a misperception about tinnitus loudness.

4.5 Clinical implications

The Conceptual Cognitive Framework highlights the contribution of cognitive and emotional processes to the development and maintenance of tinnitus clinical distress and promotes the following clinical implications and predictions but are not limited to:

CCF predicts that interventions comprising "attention-shifting" techniques or Attention Bias Modification training can decrease attentional bias to tinnitus sound

Several studies trained patients to shift their attention away from tinnitus toward music (EYSEL-GOSEPATH *et al.*, 2004; PAPE *et al.*, 2014), bodily sensation (ANDERSSON; KALDO, 2006), positive images (HENRY; WILSON, 1998) to reduce tinnitus distress. Similarly, relaxation training instructs patients to associate tinnitus with pleasant and relaxing mental images (LINDBERG *et al.*, 1989). In tinnitus retraining therapy (JASTREBOFF; HAZELL, 1993), noise generators assist attention-shifting from an inner sound to an outside sound to help the patients cope with tinnitus. Eysel et al. (2004) investigated the effectiveness of a different attention diversion form in tinnitus therapy. Forty chronic tinnitus patients, who received proper counseling and relaxation training, were instructed to direct their attention away from tinnitus through a)Sound or music; and b) Imagination with light and warmth stimuli. Patients of both groups reported less annoyance and disability by tinnitus instantly after therapy and after six months (EYSEL-GOSEPATH *et al.*, 2004).
These findings suggest that tinnitus patients could use auditory and visual-thermal sensations for attention distraction. However, Henry et al.(1998) reported that attention-switching and mental imagery exercises combined with cognitive reconstruction techniques provided a greater reduction in tinnitus distress than two single treatments or waiting list control (HENRY; WILSON, 1998).

CCF predicts that therapies aiming to influence/manipulate ECL and appraisal processes could reduce annoyance and distress reactions

4.5.1 Cognitive Behavioural Therapy (CBT) Mechanism to Diminish the negative cognitive value related to tinnitus

CBT rests on the notion that our thoughts or beliefs influence our emotional and behavioral responses giving rise to cognitive, behavioral, or somatic symptoms. CBT therapists help patients see the link between thoughts and feelings arising from an event (tinnitus) and modify their negative thoughts while using education, attentional manipulations, cognitive restructuring, relaxation techniques, and exposure to fearful situations (JUN; PARK, 2013). Several systematic reviews and meta-analyses support the effectiveness of CBT for tinnitus. In a Cochrane approach review, (MARTINEZ-DEVESA *et al.*, 2007), it was found that CBT significantly improved quality of life and decreased global tinnitus severity compared with other interventions or waiting list control conditions. Similarly, (HESSER *et al.*, 2011) conducted a meta-analysis of randomized controlled trials of CBT for tinnitus distress and reported that CBT was significantly more effective on tinnitus-related distress than active and passive control conditions. Results also showed that improvements remained over a follow-up period (HESSER *et al.*, 2011). The results of a more newly published systematic review (LANDRY *et al.*, 2020) are consistent with previous studies confirming that CBT is an effective tinnitus therapy.

4.5.2 Mindfulness-Based Cognitive Therapy (MBCT) to reduce the negative cognitive and emotional value related to tinnitus

The third wave of CBT mostly centered on acceptance and mindfulness, has recently attracted much attention. In Mindfulness-based interventions (MBI), rather than changing the negative thoughts, patients learn to take a non-judgmental viewpoint toward their thoughts and emotions, openly attending to present-moment experiences and maintain this attention over time (LUDWIG; KABAT-ZINN, 2008). In 2019, RADEMAKER *et al.* conducted a systematic review of the MBI effect on tinnitus distress and reported that MBI could decrease the tinnitus distress score while not affecting depression or anxiety in tinnitus patients. Using a qualitative approach focused on the individuals' experiences, Marks et al. (2020) investigated how and why MBCT could reduce tinnitus-related distress. They revealed that multiple processes, including mindful awareness, attitudes of equanimity, kindness, and compassion, helped patients change their relationship with tinnitus, from fighting with it to allowing it to be (MARKS; SMITH; MCKENNA, 2020). Moreover, improvement of tinnitus severity was supported by decreased amygdala-parietal resting-state functional connectivity (HUSAIN *et al.*, 2019). In HUSAIN *et al.* study, improvement of tinnitus handicap was associated with increased grey matter volume in superior frontal gyrus (HUSAIN *et al.*, 2019).

4.5.3 Using Positive emotion induction techniques paired with CAAP of tinnitus could modify tinnitus-related negative valence into neutral

Based on the ECL mechanism, pairing CAAP of tinnitus sound with positive emotion-inducing stimuli such as pictures, films (UHRIG *et al.*, 2016b), audio (BERGMAN *et al.*, 2016), music, and video clips (LAZAR; PEARLMAN-AVNION, 2014; SIEDLECKA; DENSON, 2019)might reduce the negative valence of tinnitus resulting in less distress and minor appearance of negative distress-reactions. Accordingly, we designed an adaptive seamless observational crossover, randomized, single-blind study in three sessions:

1. The Active Control, positive emotion induction via presenting a set of validated positively-valenced pictures.
2. The Anodal(20 min, two mA with 30 s RAM Up/Down) with the pictures presented.
3. The Placebo effect, Sham stimulation with the Picture presentation.

We expect to weaken the negative valence of tinnitus in the Clinical-Distress stage by pairing its conscious perception with positively valenced pictures (current running study, unpublished data). At the moment, due to the advancement of technology, the presentation of emotion-inducing stimuli could be through a Game-like design, app-based format, goggles of virtual reality, or a screen to provide affordable home-care individualized treatments.

CCF predicts that technology-based devices could help for the correction of distorted perception in tinnitus quality.

Recently, Probst et al. (2016) utilized a mobile application to track changes in rating tinnitus loudness in daily life to indicate what can distress patients. He reported that emotional state partially mediates the relationship between tinnitus loudness and tinnitus distress. Consequently, we believe technology-based approaches to provide the online measurement of tinnitus loudness-match can render correct distorted perception in loudness judgment based on CCF suggesting strategies.

Furthermore, CCF predicts clinical interventions aiming to modulate or regulate emotions -like those mentioned above, CBT, MBCT- could decrease the experience of tinnitus distress and prevent the distorted perception of tinnitus loudness. Additionally, neuromodulation techniques such as transcranial direct current stimulation over the dorsolateral prefrontal cortex have provided promising results in tinnitus-distress reduction as measured with a visual analog scale, and numerical rating scale (VANNESTE *et al.*, 2010; RIDDER; VANNESTE, 2012; FRANK *et al.*, 2012). On the other hand, Shakhawat et al.(2018) used HD-tDCS with the anode as the central electrode placed on the right dorsolateral prefrontal cortex and reported a significant

reduction in tinnitus loudness but not annoyance. Inconsistent findings raise the need for further research and studies to explore more precisely the above-mentioned predictions.

4.6 Future Trends

The proposed connections between model components remain to be validated empirically. Testing proposed scenarios and hypothesized interaction between the cognitive processes require specific considerations to provide accurate and reliable results. For instance, Evaluative Conditioning is an accumulative procedure in which other negatively-valenced USs can add to CS negative valence after repeatedly being paired. Therefore, future studies should pay careful attention to minimizing the effects of other USs by designing well-controlled experiments accurately and exclusively targeting desired CS-US relations. The studies should control for any concurrent and irrelevant physical, psychological, and environmental stimuli containing negative valence since they can add to the negative valence of CS. For instance, patients with a history of psychiatric disorders cannot be part of the study. The other confounding factor affecting the results is the personality type of the patients. Those with type-D, for instance, are more easily annoyed and generally feel distressed with less likely to experience positive mood states (PEDERSEN; DENOLLET, 2003). This information could help for future studies' inclusion and exclusion criteria for validating the model.

CHAPTER

5

DOSE-RESPONSE TRANSCRANIAL ELECTRICAL STIMULATION STUDY DESIGN

5.1 Why are new clinical studies essential?

Based on the selected mission, "iCRP-Tinnitus on using High Definition- transcranial Direct Current Stimulation (HD-tDCS) neuromodulation technique for rehabilitation." We highlighted that neuromodulation research is complicated due to cognitive processes and brain networks' involvement.

- Despite its accessibility, affordability, and flexibility, the HD-tDCS neuromodulation technique has some limitations in its methodologies and potential applications. Primarily, anatomical and functional targeting of the brain is required to boost the neuromodulation effect. For anatomical targeting, we developed an atlas-based head model for the pilot study. Head-model can be individualized in more advanced parts of Neurocognitive Computing. The positive emotion induction technique was used for functional targeting and to provoke positive emotional processing of dlPFC to reduce negative tinnitus valence.

- Extra modules of the designed study support investigations on neuro markers, biomarkers, surrogate endpoints, and objective measurement factors throughout dense-array EEG, emotional Stroop task, functional and structural MRI, as well as a battery of questionnaires.

- Dose parameters, including waveform, polarity, intensity, duration, electrode sizes, and montages, regardless of the dose design's flexibility, can induce complexities and unexplored factors.

FDA recommends statistical inferences on efficacy and safety that should be performed based

on the responses of the primary study endpoints collected from a sufficient number of subjects while employing suitable statistical methods originating from the study design and objectives to accomplish a well-controlled study. Neuromodulation studies with HD-tDCS clinical trials have similar limitations as well-controlled studies. Therefore, the Adaptive Seamless Bayesian approach plays a pivotal role in addressing the problems by employing

1. A Bayesian approach to control type I error and improve power
2. The adaptive methodology to prevent misusing of patient resources for investigating undesired doses and to finalize the trial in case of inefficient neuromodulation technique,
3. A seamless approach to lead to the confirmatory phase when the evidence in the exploratory phase infers the requirement
4. Adapting the ongoing study to the actual variability in the accumulating data for shortening or postponing study termination
5. Exploring a longitudinal surrogate endpoint in predicting final results for patients with incomplete data in the carried out pilot study based on neurofunctional tinnitus model to predict the loudness misperception.

5.2 Hypotheses

This study proposed a novel model to target tinnitus. In the proposed methodology, during the induction of the functional targeting under HD-tDCS montage and dose-finding process, simultaneously neuromodulation efficacy of the intervention was investigated. The continuous updating of prior knowledge adapts anticipated dose-response and simulated curve with the longitudinal model to define the minimum and maximum effective doses resulting in the neuromodulation approach's superiority effect.

The results were promising for a highly effective dose due to the study's transformation to develop a standard randomized confirmatory trial in which active HD-tDCS protocol is compared with a Sham trial (placebo). Establishing the HD-tDCS intervention protocol with the corresponding functional targeting as an effective methodology can achieve robust evidence for a regulatory agency in the confirmatory trial that validates the effectiveness. The suggested methodology's principal disadvantages are limited to the requirement of continuous computational analysis and a sophisticated logistic management system.

Overall, the current chapter will be beneficial and enlightening for scholars and professionals to devise better diagnoses and interventions. It would also help improve the existing methodologies, thereby reducing the severity and associated disorders of tinnitus. We also conducted two large controlled studies to investigate the clinical efficacy and outcomes variation underlying different positive emotional induction techniques. (MCKENNA *et al.*, 2014b)

5.3 Background and Hypotheses

Different attentional paradigms have revealed significant impairments in selective attention among tinnitus patients (MCKENNA *et al.*, 2014b; JASTREBOFF, 1990; BAGULEY; MCFERRAN; HALL, 2013; ROBERTS; HUSAIN; EGGERMONT, 2013; LI *et al.*, 2015). Trevis et al.(2016) reported that patients with chronic tinnitus had weaker performance in cognitive tasks in a silent room with repetitive background noise than the healthy controls(TREVIS; MCLACHLAN; WILSON, 2016). EST is one of the earliest methods developed for assessing attentional bias to emotional or concern-relevant information. (GROSS, 2013; DAVIDSON; PUTNAM; LARSON, 2000).
Recently, Ghodratitoostani et al.(2016) proposed the NfTM and highlighted that the CAAP of tinnitus is essential for causing bothersome.
NfTM classifies tinnitus patients into two stages

A) "Neutral stage": perceiving tinnitus without distress reaction and

B) "Clinical distress stage": experiencing distress reaction because of the corresponding negative valence when the tinnitus is perceived (GHODRATITOOSTANI *et al.*, 2016; GHODRATITOOSTANI *et al.*, 2016a). Valence represents emotional states varying along a continuum from positive to negative feelings with a neutral midpoint (BRADLEY; LANG, 1994a). Tinnitus-related valence progressively becomes negative through the ECL mechanism wherein repeated pairing of neutral tinnitus conditioned with similar or different negative stimuli unconditioned develops negative valence (GHODRATITOOSTANI *et al.*, 2016; HOUWER; THOMAS; BAEYENS, 2001b).

On the other hand, negative appraisals such as *"The noise makes my life unbearable," "it will drive me crazy" or "it will overwhelm me"* (HANDSCOMB *et al.*, 2017) intermittently reinforce the cognitive value of tinnitus. Appraisal and ECL mechanisms drive tinnitus-related cognitive-emotional value and lead to preferential attention allocation to the sound and prolonged tinnitus perception. Contrarily, NfTM has postulated that the CAAP of tinnitus concurrently presenting positively-valenced stimuli might improve negative valence and lead to perceiving tinnitus less frequently and with a lower level of distress (GHODRATITOOSTANI *et al.*, 2016). Cognitive functions suggested in NfTM can also be embodied in the emotion regulation process model (GROSS, 2013; GROSS, 1998a) of tinnitus, which predicts that tinnitus loudness misperception may be associated with negative valence and selective attention. NfTM also postulates that continuous evaluation of tinnitus valence, comparing this valence with those of other sensory and auditory inputs, and monitoring persistent perception occurs in the prefrontal cortex (GHODRATITOOSTANI *et al.*, 2016). More specifically, the dlPFC revealed associations between auditory attention (BREIT; SCHULZ; BENABID, 2004) and the processing of emotional information (JACOB *et al.*, 2014; STEELE; LAWRIE, 2004). Neuroimaging studies on emotion

have shown enhanced activity in dlPFC, especially in the left hemisphere. An association between positive mood orientation and positive-stimuli processing was also noticed (DAVIDSON; PUTNAM; LARSON, 2000). NfTM proposed that anodal tDCS modulatory effect at the left dlPFC reinforces the induced positive emotional stimulation and reduces tinnitus-related negative valence.

Using tDCS for relieving tinnitus-related negative valence (GHODRATITOOSTANI *et al.*, 2016) depends on the effect of electrical stimulation on the active brain networks that reinforce or decline the excitability underneath the anode or cathode, respectively (RAHMAN *et al.*, 2013). The impact of down-regulating negative emotional processing was documented with the application of anodal tDCS on dlPFC, but not with the cathodal stimulation in some studies (LANG *et al.*, 2005; FREGNI *et al.*, 2005; NITSCHE; PAULUS, 2000). tDCS specificity generally depends on functional and anatomical targeting mechanisms. Targeting refers to subthreshold modulatory-effects on particular functionally-active brain regions regarding stimulation (anodal or cathodal) montages. Functional targeting in tDCS applications may occur through preferentially modulating persistent function on an active brain network (JACKSON *et al.*, 2016). Functional targeting may also occur due to applied bias to different synaptic inputs (BIKSON; RAHMAN, 2013).

Anatomical targeting is the focal neuromodulation of specific brain regions by delivering the desired electrical dose achieved only by regulating the tDCS parameters (PETERCHEV *et al.*, 2012). The dose-response relationship can be measured after assessing the causal response of the associated functionally-active networks affected via induced current circuitry, even though the brain targeted region is involved in multiple tasks during tDCS stimulation (BIKSON; RAHMAN, 2013). HD-tDCS employs multielectrode montages to improve the anatomical targeting by enhancing the focality of current flow (BIKSON; RAHMAN, 2013; DMOCHOWSKI *et al.*, 2011). The electrical-dose of tDCS emerges from stimulation device settings that affect the electrical field generated in the targeted brain areas. Dose parameters include stimulation waveform (direct current-DC), intensity, duration, polarity, montage, number of sessions, number, type, and shape of electrodes (PETERCHEV *et al.*, 2012).

The dose can be calculated by multiplying current-intensity by time (duration of stimulation) formulated in Equation.(5.1) below

$$\text{Dose} = \text{Intensity} \times \text{Time}, \tag{5.1}$$

while electrode type, waveform, polarity, applied intensity, and montage remain constant (JAMIL *et al.*, 2017). Individual anatomical variations in head size, skull, skin thickness, and color have been shown to affect Dose to the targeted area (THOMAS *et al.*, 2019).

The mechanism of current-intensity, duration, electrode size, and montage affecting tDCS-related responses remains uninvestigated (MONTE-SILVA *et al.*, 2013). Moreover, determining sufficient stimulating sessions and intervals pose potential challenges associated with clinical treatment planning while considering the individual diversity in brain anatomy, connectivity,

and emerging functions (JAMIL *et al.*, 2017; THOMAS *et al.*, 2019; GOLDSWORTHY; HORDACRE, 2017).
In this study, we employed the self-assessment Tinnitus Loudness Questionnaire (TLQ) scale as a surrogate endpoint to verify the correction of loudness misperception in correlation with ongoing modulations of tinnitus negative-valence. TLQ was regularly collected under applying HD-tDCS concurrent with positive emotion induction (through presenting positively-valenced pictures) against only positive emotion induction. Moreover, ongoing recording variations of TLQ rating concurrent with HD-tDCS helped investigate the dose-response relationship.
We hypothesized that

- The conscious pairing of adequate pleasant visual stimuli concurrent with tinnitus perception results in correction of loudness misperception.
- Active HD-tDCS on the left dlPFC facilitates the correction of loudness misperception.
- The dose-response relationship between HD-tDCS specificity and the correction of loudness misperception is proposed.

We designed a well-controlled, two-stage, seamless, adaptive double-blind, and randomized crossover trial. We conducted a pilot study on six tinnitus patients for sample size calculation, clinical endpoint (minimally clinical efficacy) optimization, and dose selection in a single-session stimulation. We applied conventional and adaptive approaches for seamless statistical Bayesian design for analytical comparison. Meanwhile, the designed protocol promotes data-driven investigation on EEG-driven neuro markers, Stroop-driven attentional bias, and neuroimaging-driven brain network connectivity-dynamics. These are explained in the latter part of this paper.

5.4 Study Design

An adaptive seamless observational crossover, randomized, double-blind study was designed in the following three sessions:

1. Active-Control or positive emotion induction (PEI) via the presentation of a set of validated positively-valenced pictures,
2. Anodal HD-tDCS$_{4\times1}$ (20 min, 2 mA with 30 s Ramp-up/ ramp-down) concurrent with PEI, and
3. Placebo effect i.e., sham stimulation concurrent with PEI. (Figure11d).

An audiologist assisted and accompanied the patients through the experiment. The audiologist instantly before and after each session was responsible for evaluating the clinical tinnitus to measure tinnitus type, side, and pitch to specify its psychoacoustic parameters. The patients were

Figure 10 – Clinical space and setup 3-Dimensional simulation for educational approach
Exam Room; *selected rendered-picture from Panoramic View with Camera at 200 cm Attitude:* **A.** 30° degree angle **B.** The perspective of the exam room was showed from the LCD's top **C.** 90° degree angle.
Control Room; *selected rendered-picture from Panoramic View with Camera at 200 cm Attitude:* **D.** Exam room view was simulated from the clinician's perspective. **E.** The perspective of both exam and control rooms. **F.** Overview of the control room and setup.

tested to identify the best match to their tinnitus's perceived frequency, followed by assessments of tinnitus-related parameters. Such parameters included the hearing HTL, LMT, MML, and LDL, which took 5–15 min only. The patients sat on a fixed pneumatic-armchair in a dark and quiet experiment room in front of a 40-inch LCD at 185 cm. Chair height was calibrated individually to ensure that the patients' eyes were at the same altitude from the LCD center. Clinical space was depicted as a 3-Dimensional simulation in Figure10. (A to F).

5.4.1 High Definition transcranial Direct Current Stimulation (HD-tDCS)

A battery-driven current source 1×1 DC-Stimulator (Soterix Medical, NY, USA) and a 4×1 distributor (Soterix Medical, NY, USA) were administered to deliver 2 mA, HD-tDCS for 20 min with a 30 s ramp up and 30 s ramp down. High-definition gel-based electrodes were used to increase anatomical focality in comparison to conventional electrode pads (NITSCHE *et al.*, 2007). According to the head model designed for anodal stimulation of the left-dlPFC and also the international $10-10$ EEG system (JURCAK; TSUZUKI; DAN, 2007), the center electrode was placed on F3 with a 2 mA current set. The four cathode-electrodes were placed over F1, F5, AF3, and FC3, and the circuit was closed uniformly dividing the total current among the

four cathodes placed approximately 3.5 cm away from the anode (Figure11*b*). Such stimulation electrodes were mounted on a 256-channel EEG-Net(Figure11*a*).
The sham stimulation was performed for 20-min with the same electrode montage to generate the placebo effect. It started and finished with a 30s ramp-up instantly followed by a 30s ramp-down, but insignificant current delivery in between was documented. In this way, the patients experienced the same sensations as that of active HD-tDCS and were kept blind to the intervention (Placebo effect).

5.4.2 Positive Emotion Induction

Based upon the ECL mechanism, tinnitus neutral sound (conditional stimulus) can obtain negative valence after frequent pairing with negatively-valenced stimuli (unconditional stimulus)(HOUWER; THOMAS; BAEYENS, 2001a). Similarly, we hypothesized that the valence of tinnitus perception paired with positively-valenced stimuli might change to a less negative perception. In practice, specific emotional states can be induced by appropriate and controlled stimuli such as pictures, sound, film, text, and virtual reality (MARCHEWKA *et al.*, 2014; RIEGEL *et al.*, 2016). One of the most commonly applied and accepted stimuli for emotion induction is pictures (UHRIG *et al.*, 2016a). The Nencki Affective Picture System(NAPS) is a database of standardized pictures for studying emotion and attention. It provides a detailed list of normative ratings in three dimensions: valence, arousal, and dominance elicited by each picture. It enables researchers to select stimuli triggering a specific customized range of emotions for their experiments (MARCHEWKA *et al.*, 2014). In the rating of the NAPS dataset, valence points to the positive versus negative emotional state, whereas arousal points to the strength of emotional arousal or excitement (CITRON *et al.*, 2014). The pictures were rated using a modified 9-point Likert scale of Self-Assessment Manikin scale for arousal-ratio(Ar): 1 = unaroused/calm, 9 = aroused/excited; for r Valence-ratio (Vr): 1 = unhappy/annoyed, 9 = happy/satisfied (RIEGEL *et al.*, 2017).
We employed a set of validated positive emotion-inducing pictures from the NAPS dataset to induce positive emotion simultaneously with CAAP of tinnitus to reduce the tinnitus negative valence. Pictures were aligned at a fixed location at the center of the screen in 1600×1200 pixels. We presented neutral pictures ($4 <$Vr< 6 and Ar< 6) included in resting-state (rs) blocks and positive pictures (Vr> 6) included in PEI blocks developed in Superlab Software. The blocks contained 20 pictures, each presented for 5*s*, followed by a 500 ms cue (+). Every single block ended with TLQ. The total duration of each block presentation was two min.
The rs blocks were constructed with neutral pictures that were randomized between sessions and between patients but were presented in the same within-session order. Neutral pictures were selected for evaluating baseline neural activity, which is not elicited by a task. So, the rs block was displayed four times to provide a reference and cover all possible repeated measures of rs brain activity that might be affected by previous tasks (Figure11.c).

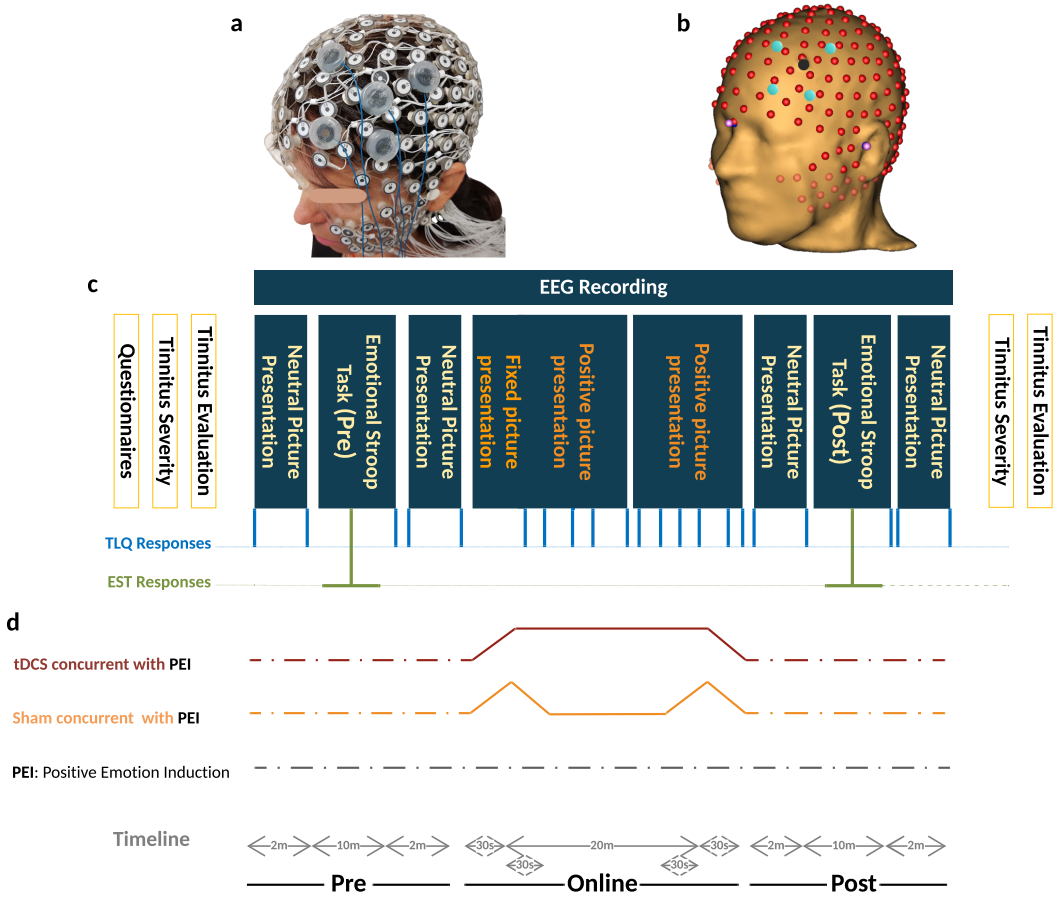

Figure 11 – **a)** Realistic Montage for 256-channel HydroCel Geodesic Sensor Net and The left-dlPFC as the Region Of Interest (ROI) is also mounted in the EGI-NET.
b) Co-registered 256-channel EEG, and HD-tDCS Montage on left-dlPFC based on the MR-driven head model. The stimulation electrodes located in electrode holders were placed near the EEG channels. The electrode holder for the anode is shown in red and that for the cathode is shown in blue. The electrode holders are filled with conductive gel.
c) Schemas of the protocol. Initially, the patients filled in different questionnaires- THI, TBF-12, TS, MDI, STAI-S6, and MSQ. Before and after the experiment, psychoacoustic parameters of tinnitus together with the Tinnitus Severity questionnaire were recruited. During the experiment, two sets of pictures were presented with different Valence-ratio (Vr) and arousal-ratio (Ar) rates selected from the NAPS dataset. Neutral pictures ($4 < Vr < 6$ and $Ar < 6$) were included in four rs blocks and the positive pictures ($Vr > 6$) in 2×5 consecutive visual stimulation blocks. Each visual stimulation block initiates with four pictures ($Vr > 6$ and $Ar > 6$) followed by sixteen pictures ($Vr > 6$) randomly selected with no replacement from a one-hundred-positive-picture set (Figure **??**a). Generally, every single block contained 20 pictures each presented for $5s$ followed by a cue (+) of $500ms$. The blocks were randomized between sessions and between patients but presented in the same order within-session. The total duration of each block presentation was two min. The TLQ "Scale your tinnitus loudness from $1-10$" was displayed 21 times, and presented in the following order: before-after each resting-state block (containing neutral pictures) and visual stimulation block (containing positive pictures), and after each Emotional Stroop task. Throughout the experiment, the responses of TLQ and EST in blue and green lines, respectively, as well as EEG signals were all recorded via Superlab software (Cedrus Corporation, San Pedro, CA, USA). The total duration of the experiment ranged between 40 and 45 min with regard to the reaction time of patients in EST and responding to TLQ.
d) Timeline of all three sessions of study including anodal stimulation-picture presentation, sham stimulation-picture presentation, only picture presentation is illustrated. In all three sessions, the sequence of presenting pictures, TLQ, and EST are the same as those described in part C. Electrical stimulation periods (sham/Active) was illustrated in movies of supplementary documents.

5.5 Statistical study design and sample size calculation

Food and Drug Administration (FDA) recommends performing statistical inferences on efficacy and safety based on the responses of the primary study endpoints collected from a sufficient number of subjects while utilizing suitable statistical methods originating from the study design and objectives to accomplish a well-controlled study.
As mentioned in the current Chapter, TLQ was collected through paper-based Tinnitus Severity Questionnaires obtained before and after the experiment and the pressing corresponding keys on the keyboard during the experiment. TLQ as the surrogate endpoint was measured to test the superiority of concurrent positive emotion induction (PEI) and HD-tDCS against only PEI as an active control. . Minimum Clinical Efficacy (δ) is indicated to test superiority. An inappropriate selection of δ can influence sample size calculation and inference validity. The FDA suggests selecting δ between 25–50% of the effect size of the active control (CHOW *et al.*, 2017). Since PEI has not yet been practiced for the tinnitus population, a Bayesian crossover adaptive *"seamless trial"* (CHOW; TU, 2008) was designed to study δ and dose selection .The Bayesian model employed the probabilistic model to represent all uncertainties within the model (GELMAN *et al.*, 2013), both the hypotheses and the prior knowledge δ. For this, we adapted the sample size for the subsequent confirmatory trial by measuring surrogate endpoints and single session HD-tDCS$_{4\times1}$ dose-response relationship (Figure 12).
The seamless design combines two independent trials inside a single study. A seamless adaptive design most often incorporates two-stages before adaptation (exploratory-stage) and after adaptation (confirmatory-stage). The exploratory stage aims at obtaining information regarding the uncertainty of the testing treatment to apply adaptation. It may be similar to opening the door for investigators to stop the trial beforehand due to single or multiple issues based on safety, futility, and accrued data efficacy. The scope of the confirmatory-stage is to verify preliminary findings from the exploratory-stage.
The major advantage of the two-stage adaptive seamless study is in its capability of merging collected data from both stages to derive a more accurate and reliable inference.
Six patients were recruited to conduct the current clinical pilot study to calculate the sample size and to investigate the following hypotheses:

- The conscious pairing of PEI simultaneously with tinnitus perception results in the correction of loudness misperception
- Active HD-tDCS on the left-DLPFC but not sham facilitates correction of the loudness misperception.
- A dose-response relationship between HD-tDCS dosage and correction of loudness misperception exists.

5.5.1 Study Roadmap

We propose an innovative Adaptive-Seamless Bayesian (ASB) method that can revolutionize improved clinical trial ethics, design, execution, and performance. ASB helps the investigators control unknown potential confounders (i.e., unforeseen issues at the beginning of the study) considering any prior knowledge. The adaptation can be individually or collectively employed for measurement factors, sample size, randomization, clinical endpoints, biomarkers, and surrogate endpoints to achieve significant credibility and reproducibility in ongoing studies. Consequently, testing hypotheses across the ASB method results in well-controlled, accurate, and time-cost efficient studies. To our knowledge, this is the first-ever crossover study with active control (PEI) applied to the tinnitus population. Conventional approaches in study design need to conduct at least three dedicated consecutive studies to investigate the hypotheses mentioned above. First, to conduct a prospective comparative research study to learn and quantize the effect of positive emotional induction (with validated images) in the tinnitus population. Subsequently, a comparative crossover or parallel study could be performed to investigate the superiority effect of "tDCS concurrent with PEI (tP)" but not "Sham concurrent with PEI (SP)" on the correction of loudness misperception and tinnitus bothersome against the PEI. Overall, to select the effective dose, a dose-response study must be run to establish the single-session response relationship to the applied doses. Understanding the minimum and maximum effective doses leads us to adequate and controllable doses for multisession treatments. ASB method enables the coverage of all hypotheses collectively within an adaptable progressive study. The sample size should be adapted to all progressive stages of the study towards maximizing the credibility margin (95%) in testing hypotheses. Our pilot study results demonstrated that the coefficient of variance showed statistically significant differences (90% power at 1% significance level) between the loudness perception of tinnitus during PEI and neutral picture presentations creating prior knowledge of the δ exploratory stage. Based on prior knowledge, interims (sample size N_3) of the confirmatory stage are computed to derive δ value within the desired credibility margin. In every single interim of δ confirmatory (N_3), the posterior delta is calculated and proceeds in one of the following states to generate the processed-δ:

1. Regardless of the difference between posterior and anterior δ (meaningful or not), when δ is not placed in the desired credibility margin, the anterior δ remains acceptable. This occurs due to the magnitude of certainty, and upcoming recruitment is performed by the next interim of the δ validation sample size in the confirmatory stage.

2. The difference between posterior and anterior δ is significant and placed in the desired credibility margin. Therefore, the anterior δ replaces the posterior, and updated δ shapes new prior knowledge for the δ exploratory stage. This stage adapts all credibility margins of other hypotheses and corresponding sample sizes. However, upcoming recruitment builds upon the adapted sample size interims of the new δ within the confirmatory stage.

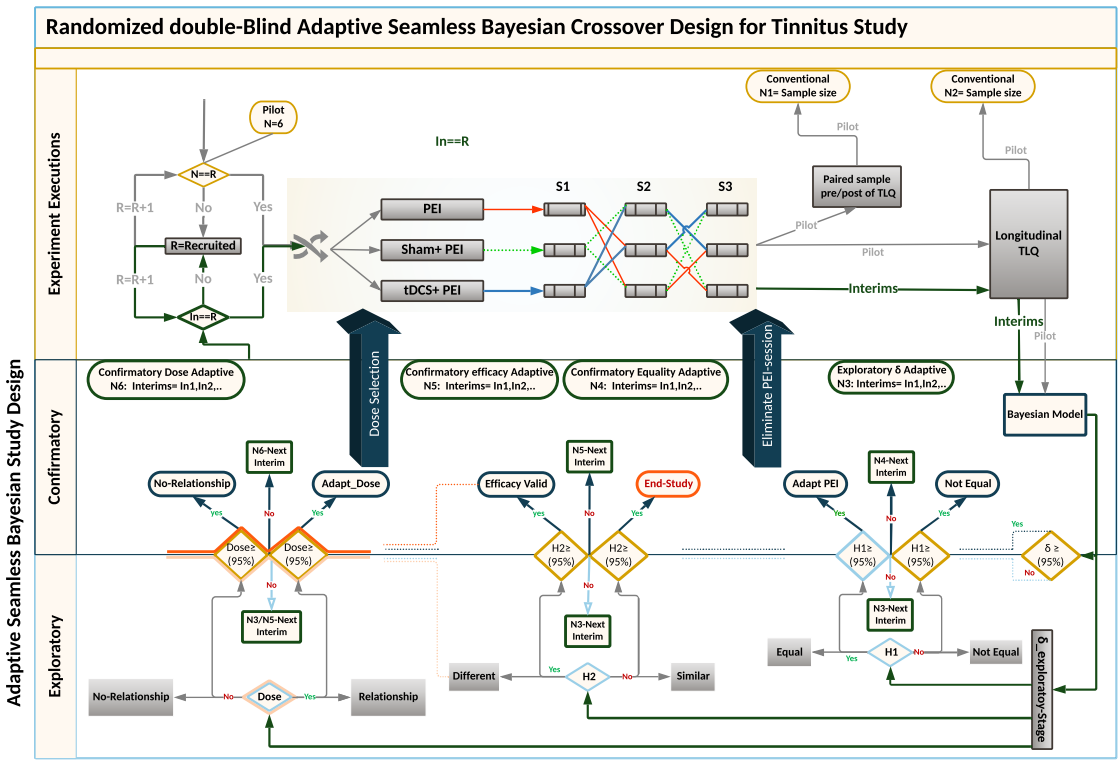

Figure 12 – Adaptive Seamless Bayesian Study Design:
Experiment execution: Study recruitment, randomization, interim applications, and three crossover interventions were illustrated. Interventions were PEI, "tDCS + PEI", and "Sham +PEI". Six patients were recruited and randomly assigned to the interventions based on the William design. Conventionally, either (paired sample analysis)TLQ difference between before and after interventions or (longitudinal analysis) repeated measures of surrogate endpoint TLQat specific time-points could be used for sample size calculation. Frequent interim analyses based on Markov-chain Monte Carlo estimate Bayesian posterior probability distributions, with multiple imputations and estimations of unknown trial parameters and patient outcomes.
Exploratory and confirmatory stages: The seamless design connects independent trials inside a single study. An Adaptive-Seamless Bayesian (ASB) design consolidates with two stages exploratory-stage and confirmatory-stage. The Minimum Clinical Efficacy (δ) is defined as 50% of the observed effectiveness for PEI treatment, which was determined after assessing the variability observed during the online period. Since PEI has not yet been practiced for the tinnitus population, the Bayesian model utilized the probabilistic model to represent all uncertainties within the model (GELMAN *et al.*, 2013), both the hypotheses and prior knowledge (Processed-δ or non-credible δ). Testing hypotheses are $\mathbf{H_1}$: The conscious pairing of PEI simultaneously with tinnitus perception results in the correction of loudness misperception. In the current ASB the following hypotheses were tested simultaneously, $\mathbf{H_2}$: Active HD-tDCS on the left-DLPFC but not sham facilitates correction of the loudness misperception, and **Dose**: A dose-response relationship between HD-tDCS dosage and correction of loudness misperception exists. Since the processed-δ is not changed, interim analyses on hypotheses in exploratory and confirmatory stages will be processed. The results of the hypotheses are partially valid within the uncertainty range of the processed-δ. When δ becoming valid decision making and adaptation on H_1 and H_2 is possible. However, as soon as Processed-δ is changed, the hypotheses needed to be reevaluated. When δ and H_2 became credible concurrently, regulating the dose and judgment about the dose-response relationship is possible. In other cases, the validity of dose-related parameters depends on processed-δ and efficacy uncertainty.

3. Though insignificant, the difference between posterior and anterior δ is placed in the desired credibility margin. Therefore, the anterior δ is valid, and the δ confirmatory stage ends. Upcoming recruitments are then used by the corresponding interims of the hypothesized sample size in the confirmatory stage. Eventually, in every interim after δ confirmation, "valid δ" applies to test hypotheses with the corresponding sample size interims.

During each interim analysis, the corresponding processed-δ applies to test the hypotheses. Possible results for testing hypotheses are enumerated below:

H_1: Reduction in tinnitus loudness perception during "Sham concurrent with PEI (SP)" is similar to only PEI. When δ is valid, evidence in favor of H_1 in a credible margin leads to the conclusion that "SP" is similar to PEI, so the study adapts with the PEI session elimination. In contrast, when the evidence is against H_1 in a credible margin, "SP" differs from the PEI. When δ is valid, and the H_1 result is partially acceptable, it supports temporary decision-making in an ongoing study. Therefore, the study recruitment proceeds with N_4 interims. When processed-δ is present, regardless of its credibility, the certainty ratio is involved in the H_1 result. Therefore, the study recruitment goes on with the N_3 interims.

H_2: Reduction in tinnitus loudness perception during tDCS concurrent with PEI "tP" differs from that in PEI. When δ is valid, evidence in favor of H_2 in a credible margin leads to the conclusion that automatic content recognition short "tP" does not differ from only PEI. However, if the evidence is against H_2 in a credible margin, it leads to the conclusion that "tP" is not different from only PEI, so the study ends. When δ is valid and H_2 is partially acceptable, temporary decision-making in an ongoing study can be corroborated. The study recruitment proceeds with N_4 interims. While processed-δ is present, regardless of its credibility, the certainty ratio is involved in the H_2 result, so the study recruitment continues with N_3 interims. The results of H_2 drive the dose-response relationship investigation with partial certainty, except for the rejecting state of H_2 within a credible margin.

Dose: A dose-response relationship between HD-tDCS dosage and correction of loudness misperception exists. Valid δ with credible H_2 leads to either of the following conclusions:

A) If Dose is accepted in a credible margin, it establishes the dose-response relationship, and the minimum and maximum dose can be defined. The study adapts to the subsequent multisession clinical study.

B) The evidence against Dose in a credible margin shows no dose-response relationship. Valid δ together with non-credible H_2 results provides partially acceptable results for Dose. This supports temporary decision-making in the ongoing study, and the study recruitment moves on with N5 interims. Valid δ, together with the credible

H_2 result, provides partially acceptable results for the Dose that supports temporary decision making in the ongoing study and the study recruitment moves on with N6 interims. When processed-δ is present, the Dose result is available with certainty ratio regardless of H_2 results credibility. Therefore, the study recruitment continues with N_3 interims.

5.6 Discussion

In a nutshell, FDA recommends that statistical inferences on efficacy and safety should be performed based on the responses of the primary study endpoints collected from a sufficient number of subjects while employing suitable statistical methods originating from the study design and objectives to accomplish a well-controlled study.
This study proposes a novel Adaptive-Seamless Bayesian (ASB) methodology for HD-tDCS Dose-Response Study Design that facilitates the long journey of neuromodulation from a research protocol to the clinical recommendation and treatment individualization. The method was prototyped for six tinnitus patients as a pilot to elucidate the tinnitus negative valence role. Here below, we discuss the advantages, challenges, and future trends of the protocol and ASB methodology.

5.6.1 Protocol Advantages and Challenges

Neuromodulation research is complicated on account of the involvement of cognitive processes and brain networks. Therefore, developing a testable framework such as a Neurofunctional Tinnitus Model (NfTM) is essential for simplifying the brain complexity and providing a roadmap to find a proper research approach, an analytical method, and procedures for the research question. In the presented prototype, the Neurofunctional Tinnitus Model's use improved our knowledge and enabled the right prediction of cognitive impairments and their rehabilitation. In light of the Neurofunctional model predictions, hypotheses are formulated to measure clinical endpoints.

- Despite its accessibility, affordability, and flexibility, the HD-tDCS neuromodulation technique has some limitations in its methodologies and potential applications. Primarily, anatomical and functional targeting of the brain is required to boost the neuromodulation effect. For anatomical targeting, we developed an atlas-based head-model for the pilot study. Head-model can be individualized in more advanced parts of the journey. The positive emotion induction(PEI) technique was used for functional targeting and to provoke positive emotional processing of Left dlPFC to reduce tinnitus negative valence.

- Extra modules of the designed study support investigations on neuro markers, biomarkers, surrogate endpoints, and objective measurement factors throughout dense-array EEG,

emotional Stroop task, functional and structural MRI, as well as a battery of questionnaires.

- Dose parameters including waveform, polarity, intensity, duration, electrode sizes, and montages, regardless of the flexibility in the dose design, can induce complexities as well as unexplored factors.

5.6.2 Advantages and Challenges of method

Food and Drug Administration (FDA) recommends the statistical inferences on efficacy and safety should be performed based on the responses of the primary study endpoints collected from a sufficient number of subjects while employing suitable statistical methods originating from the study design and objectives to accomplish a well-controlled study. Analogously, neuromodulation studies with HD-tDCS clinical trials have similar limitations as in a well-controlled study. Therefore, ASB plays a pivotal role in addressing the problems by employing the following:

1. Bayesian approach to control type I error and improve power;
2. The adaptive methodology to prevent misusing patient resources for investigating undesired doses, and
3. To finalize the trial when it is sufficiently clear that the neuromodulation technique is inefficient;
4. Seamless to lead to the confirmatory phase when the evidence in the exploratory phase infers the requirement;
5. Adapting the ongoing study to the actual variability in the accumulating data for shortening or postponing the study termination;
6. Exploring a longitudinal surrogate endpoint in predicting final results for patients with incomplete data in the carried out pilot based on neurofunctional tinnitus model to predict the loudness misperception.

5.6.3 Future Trends in protocol and clinical study methodologies

- Updating the head-model is essential to adapt the methodology for other neuromodulation techniques (transcranial Electrical Stimulation, transcranial Magnetic Stimulation, and low-intensity focused ultrasound).
- ASB can support individualized treatment planning according to the nature of the Bayesian approach.

- To improve functional targeting in needed large-scale study concurrent with neuromodulation for improving the efficacy.
- Functional targeting can adapt to each patient individually.

Further validation of the proposed methodology is suggested in future studies.

5.7 Conclusion

This study proposed a novel model to target tinnitus. In the proposed methodology, during the induction of the functional targeting under HD-tDCS montage and dose-finding process, simultaneously neuromodulation efficacy of the intervention was investigated. The continuous updating of prior knowledge adapts anticipated dose-response and simulated curve with the longitudinal model to define the minimum and maximum effective doses resulting in the neuromodulation approach's superiority effect.
The results may be promising with a highly effective dose due to transforming the study for the development of a standard randomized confirmatory trial in which active HD-tDCS protocol is compared with a Sham trial (placebo).
The establishment of the HD-tDCS intervention protocol with the corresponding functional targeting as an effective methodology can achieve powerful evidence for a regulatory agency to confirmatory trial validates the effectiveness. The principal disadvantages of the suggested methodology are limited to the requirement of continuous computational analysis and a sophisticated logistic management system.
Overall, the current paper will be beneficial and enlightening for scholars and professionals to devise better diagnoses and interventions. It would also help improve existing methodologies, thereby reducing the severity and associated disorders of tinnitus. We also highlight the need for large controlled studies for better clinical efficacy and improved outcomes.

CHAPTER

6

DATA DESCRIPTION

6.1 DSet-1: Data Description for the dataset used in NcC_Data-Driven Algorithms

In line with the mission of NcC, iCRP-Tinnitus, we organized the pilot Dataset to test the hypotheses of cognitive models as bellow.
The aggregation of THI, MSQ, STAI-S6, and TS, embedded in DSet-1.
To build a bridge between unsupervised discoveries and supervised modeling, we considered TS as the target to develop and train Nc_Data-driven predictive modelings. For an abstract presentation, we illustrate descriptive analytics for target variables and the questionnaires' scores in this chapter.
The histogram and box plot of the variable's Gender is illustrated in Figure 13.

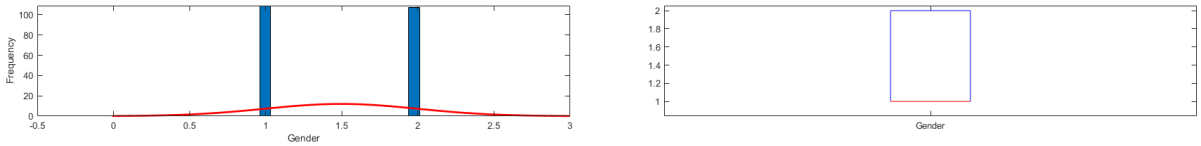

Figure 13 – Distribution and Box plot of the gender variable that aggregated in**DSet-1**

Similarly, the age variable's descriptive information was shown in Figure 14.

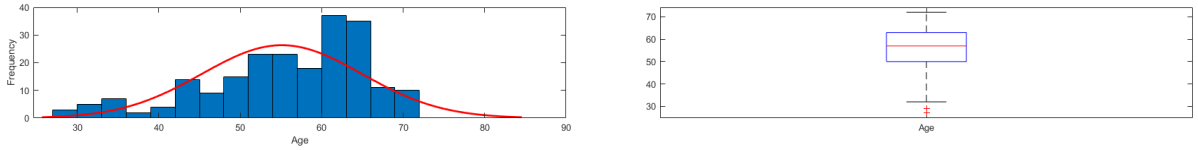

Figure 14 – Distribution and Box plot of the age variable that aggregated in**DSet-1**

6.1.1 Tinnitus Handicap Inventory questionnaire (THI)

THI questionnaire aims to identify, quantify, and evaluate the difficulties patients with tinnitus may experience. The THI is a 25-item test, and the maximum score is 100. Histograms and Box plots of THI are illustrated in Figure 15 for items from 1 to 9,

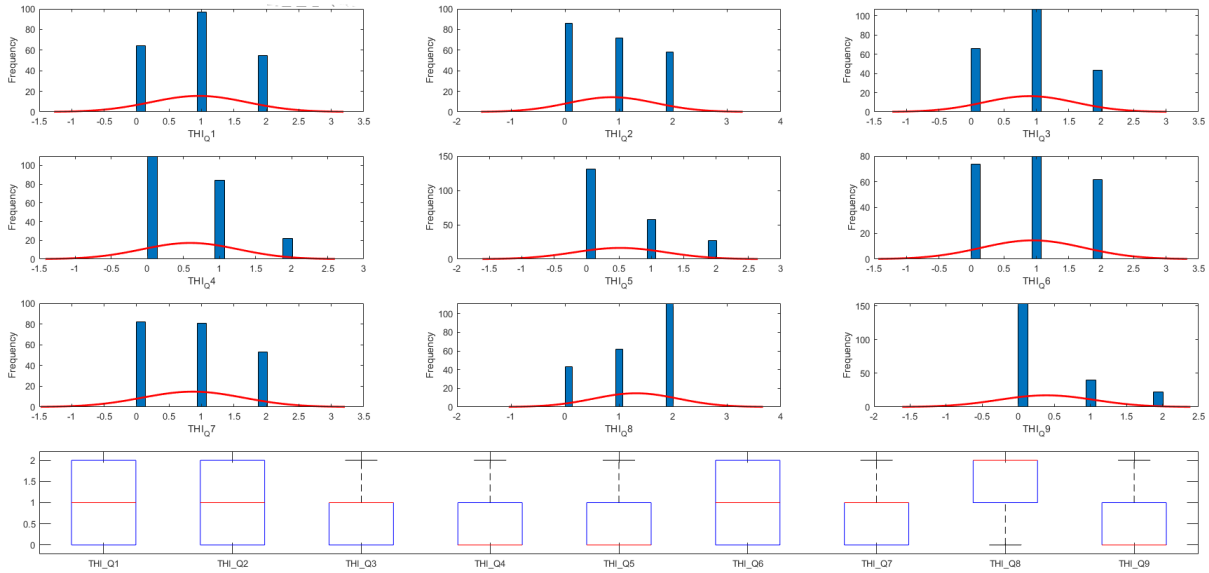

Figure 15 – Distribution and Box plot of THI items 1-9 that aggregated in the **DSet-1**

Figure 16 for items from 10 to 18,

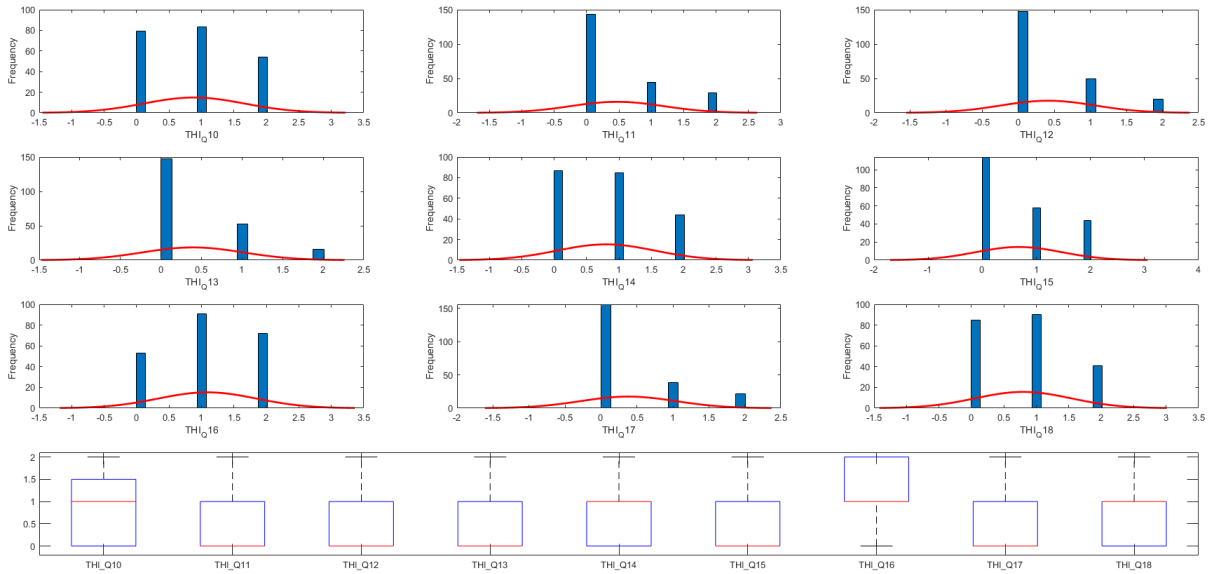

Figure 16 – Distribution and Box plot of THI items 10-18 that aggregated in the **DSet-1**

and Figure 17 for items from 19 to 25.

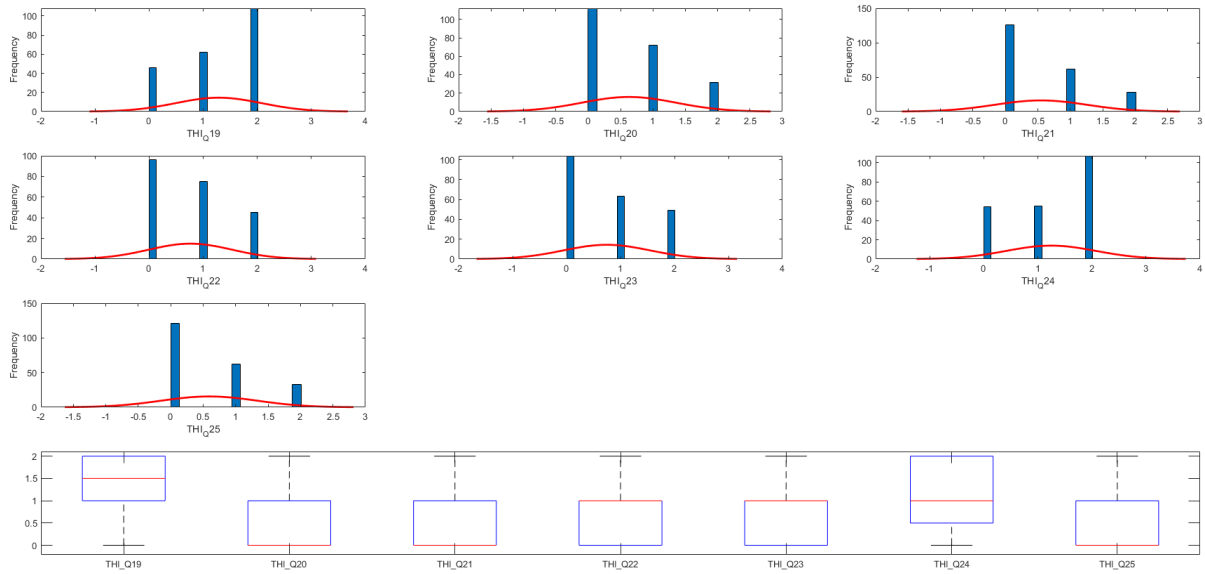

Figure 17 – Distribution and Box plot of THI items 19-25 that aggregated in the **DSet-1**

Correlation coefficients between all THI items included in **Dset-1** were shown as heat map representation that ranged between [-1 1]in the Figure 18.

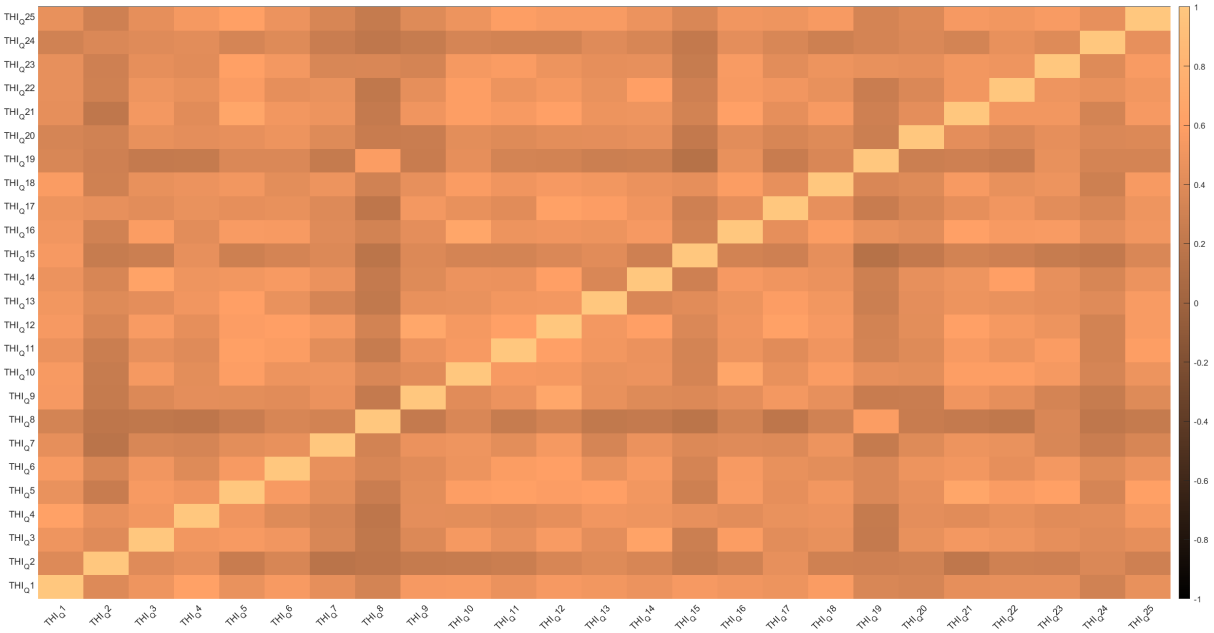

Figure 18 – Correlational relationship of all THI items that aggregated in the **DSet-1** which dark and light copper color represents negative and positive correlations, respectively

Descriptive statistics, including range, mean, Standard deviation, skewness of distribution, and standard error, are depicted in Table.2

	N	Minimum	Maximum	Mean	Std. Deviation	Skewness	
	Statistic	Statistic	Statistic	Statistic	Statistic	Statistic	Std. Error
THI_Q1	216	0	2	.96	.743	.067	.166
THI_Q2	216	0	2	.87	.808	.241	.166
THI_Q3	216	0	2	.89	.704	.152	.166
THI_Q4	216	0	2	.59	.669	.693	.166
THI_Q5	216	0	2	.52	.709	1.003	.166
THI_Q6	216	0	2	.94	.793	.100	.166
THI_Q7	216	0	2	.87	.781	.240	.166
THI_Q8	216	0	2	1.31	.785	-.620	.166
THI_Q9	216	0	2	.39	.666	1.464	.166
THI_Q10	216	0	2	.88	.778	.205	.166
THI_Q11	216	0	2	.47	.721	1.187	.166
THI_Q12	216	0	2	.41	.655	1.331	.166
THI_Q13	216	0	2	.39	.623	1.341	.166
THI_Q14	216	0	2	.80	.755	.348	.166
THI_Q15	216	0	2	.68	.793	.648	.166
THI_Q16	216	0	2	1.09	.757	-.148	.166
THI_Q17	216	0	2	.38	.664	1.508	.166
THI_Q18	216	0	2	.80	.738	.343	.166
THI_Q19	216	0	2	1.29	.796	-.562	.166
THI_Q20	216	0	2	.63	.729	.702	.166
THI_Q21	216	0	2	.55	.714	.920	.166
THI_Q22	216	0	2	.76	.774	.436	.166
THI_Q23	216	0	2	.75	.804	.494	.166
THI_Q24	216	0	2	1.25	.830	-.486	.166
THI_Q25	216	0	2	.59	.741	.818	.166

Table 2 – Descriptive statistics of the THI data aggregated in **Dset-1**

6.1.2 State-Trait Anxiety Inventory (STAI)

State Trait Anxiety Inventroy Small Questions (STAI-S6) is one of the assessment instruments for individuals' anxiety levels most widely used by psychologists worldwide and the seventh most broadly used by clinical psychologists. STAI-S6 has two separate sections to evaluate trait and state of anxiety.

6.1.2.1 Trait Anxiety Section of STAI (STAI-QI)

The Trait section of STAI-S6 measures individuals' predisposition to perceive diverse stimuli as threatening. Thus, an individual with high trait anxiety is more likely to produce an anxiety response. In the trait anxiety subscale, response options range between 1=quase nunca [almost never], 2=as vezes [sometimes], 3=muitas vezes [often] and 4=quase sempre [almost always]. Descriptive statistics are presented in Table 3.

	N	Minimum	Maximum	Mean	Std. Deviation	Skewness	
	Statistic	Statistic	Statistic	Statistic	Statistic	Statistic	Std. Error
STAI_QI_1	216	1	4	2.79	.800	-.101	.166
STAI_QI_2	216	1	4	1.66	.785	1.142	.166
STAI_QI_3	216	1	4	3.01	.894	-.491	.166
STAI_QI_4	216	1	4	1.50	.747	1.604	.166
STAI_QI_5	216	1	4	2.68	.933	-.176	.166
STAI_QI_6	216	1	4	1.79	.851	.916	.166

Table 3 – Descriptive statistics of the Trait anxiety section of STAI questionnaire that data aggregated in **Dset-1** and so-called STAI-I

Descriptive information of the Trait Anxiety section of STAI-S6 included in the **DSet-1** are shown in Figure 19.

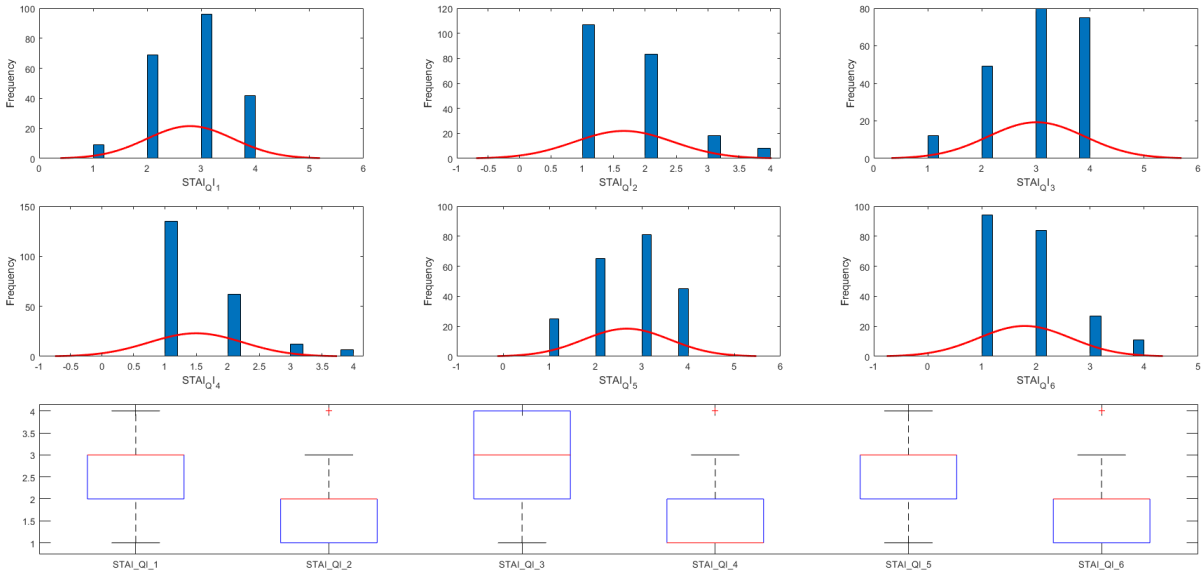

Figure 19 – Distribution and Box plot of Trait anxiety STAI-S6 that aggregated in the **DSet-1**

6.1.2.2 State Anxiety Section of STAI (STAI-QII)

The State anxiety section of STAI-S6 measures the existence of threat-related stimuli in the respondent's environment around the time of the assessment. In the state anxiety subscale, response options range between 0=nada [not at all], 1=algo [somewhat], 2=bastante [moderately] and 3=muito [very much].
Descriptive statistics are presented in Table 4.

	N	Minimum	Maximum	Mean	Std. Deviation	Skewness	
	Statistic	Statistic	Statistic	Statistic	Statistic	Statistic	Std. Error
STAI_QII_1	216	1	4	2.89	.893	-.175	.166
STAI_QII_2	216	1	4	2.10	.862	.593	.166
STAI_QII_3	216	1	4	2.94	.892	-.269	.166
STAI_QII_4	216	1	4	2.42	.916	.359	.166
STAI_QII_5	216	1	4	1.98	.815	.875	.166
STAI_QII_6	216	1	4	2.77	.983	-.123	.166

Table 4 – Descriptive statistics of the State anxiety section of STAI questionnaire that data aggregated in **Dset-1** and so-called STAI-II

Descriptive information of the State Anxiety section of STAI-S6 included in the **DSet-1** are shown in Figure 20.

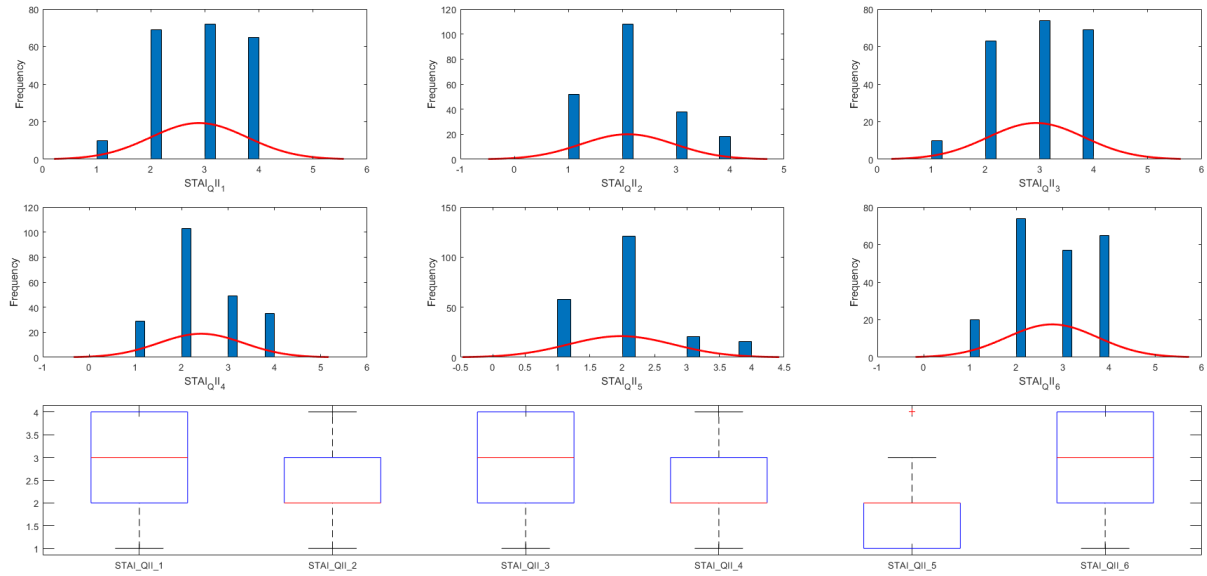

Figure 20 – Distribution and Box plot of State anxiety STAI-S6 that aggregated in the **DSet-1**

Correlation coefficients between all STAI-S6 items included in **Dset-1** were displayed as a heat map representation that ranged between [-1 1]in the Figure 21.

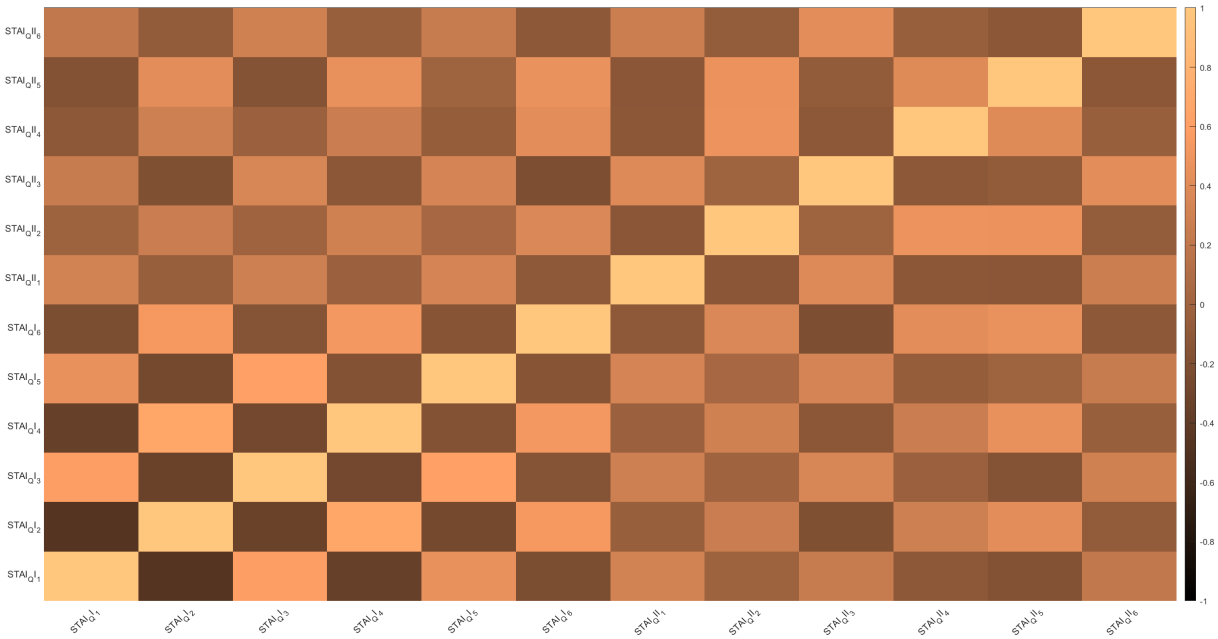

Figure 21 – Correlational relationship of all STAI items that aggregated in the **DSet-1** which dark and light copper color represents negative and positive correlations, respectively

6.1.3 Mini-Sleep Questionnaire (MSQ)

The Mini Sleep Questionnaire (MSQ) is an instrument developed to screen for sleep disturbances in clinical populations. It comprises ten items assessing both insomnia and excessive daytime sleepiness. Each item is scored on a six-point Likert scale ranging from 1 (never/Nunca) to 6 (always/sempre), and the total score for each subscale (e.g., insomnia and hypersomnia) is

defined as the arithmetic sum of the scores for its items. Descriptive statistics are presented in Table 5.

	N	Minimum	Maximum	Mean	Std. Deviation	Skewness	
	Statistic	Statistic	Statistic	Statistic	Statistic	Statistic	Std. Error
MSQ1	216	1	6	3.32	1.705	.092	.166
MSQ2	216	1	6	3.25	1.477	.043	.166
MSQ3	216	1	6	1.65	1.338	2.079	.166
MSQ4	216	1	6	2.79	1.463	.141	.166
MSQ5	216	1	6	3.43	1.454	-.232	.166
MSQ6	216	1	6	3.52	1.679	-.213	.166
MSQ7	216	1	6	4.16	1.451	-.720	.166
MSQ8	216	1	6	2.49	1.450	.513	.166
MSQ9	216	1	6	2.99	1.450	-.002	.166
MSQ10	216	1	6	2.87	1.536	.329	.166

Table 5 – Descriptive statistics of the MSQ data aggregated in **Dset-1**

Descriptive information of the MSQ included in the **DSet-1** are shown in Figure 22.

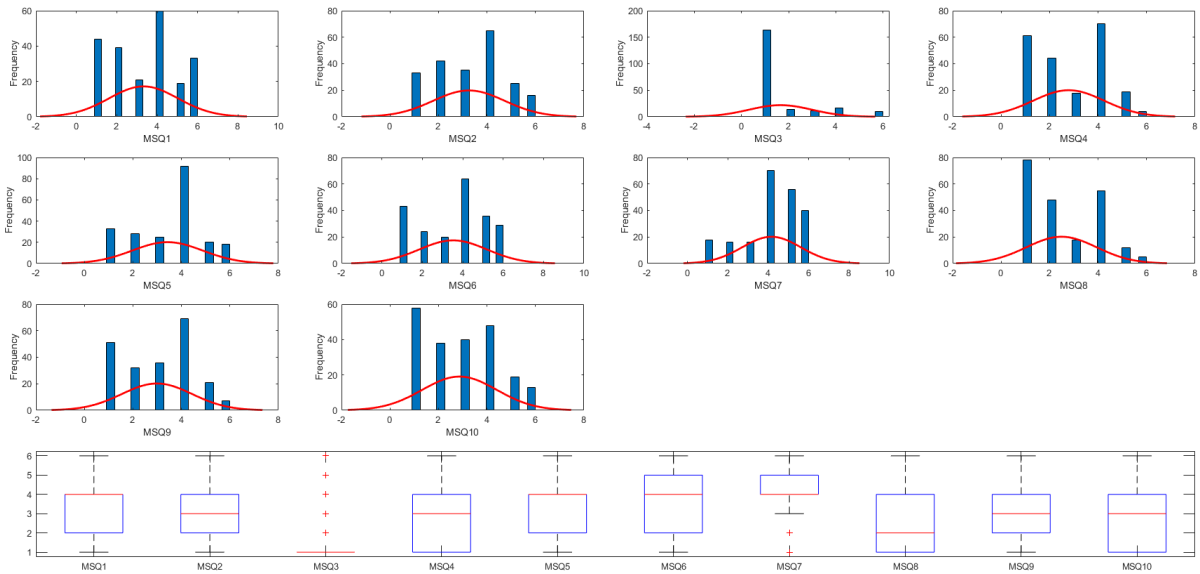

Figure 22 – Distribution and Box plot of the MSQ aggregated in the **DSet-1**

Correlation coefficients between all MSQ items included in **Dset-1** were displayed as a heat map representation that ranged between [-1 1]in the Figure 23.

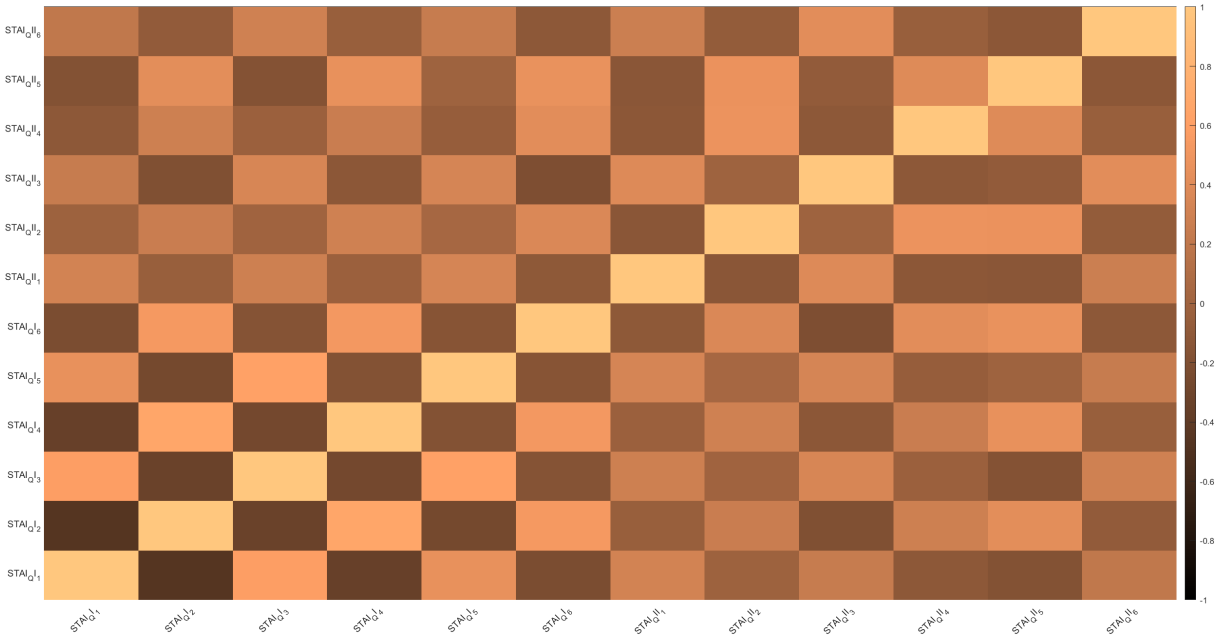

Figure 23 – Correlational relationship of all MSQ items that aggregated in the **DSet-1** which dark and light copper color represents negative and positive correlations, respectively

6.1.4 Target Variables

Tinnitus severity is a self-report 10-point Likert scale broadly used for tinnitus severity levels. Relying on the Cognitive Conceptual Model proposed in Chapter 4 of the current thesis, emotional and cognitive values are not distinctive from the patient side, so we simply summed them up to have merged information. We also presented the final score of the THI questionnaire as THIR. All items mentioned above are considered Target variables for learning and supervised modeling in future investigations. Descriptive statistics are presented in Table 6.

	N	Minimum	Maximum	Mean	Std. Deviation	Skewness	
	Statistic	Statistic	Statistic	Statistic	Statistic	Statistic	Std. Error
Ts2Pr	216	1	10	6.44	2.158	-.225	.166
Ts3Pr	216	0	10	6.34	2.708	-.341	.166
Ts4Pr	216	0	10	5.96	2.515	-.220	.166
Ts5Pr	216	0	10	5.69	2.999	.016	.166
Ts6Pr	216	0	10	5.92	2.543	-.086	.166
Ts36Pr	216	0	20	12.26	4.893	-.198	.166
THIR	216	0	100	38.20	24.683	.509	.166

Table 6 – Descriptive statistics of the MSQ data aggregated in **Dset-1**

Descriptive information of target variables included in the **DSet-1** are shown in Figure 22.

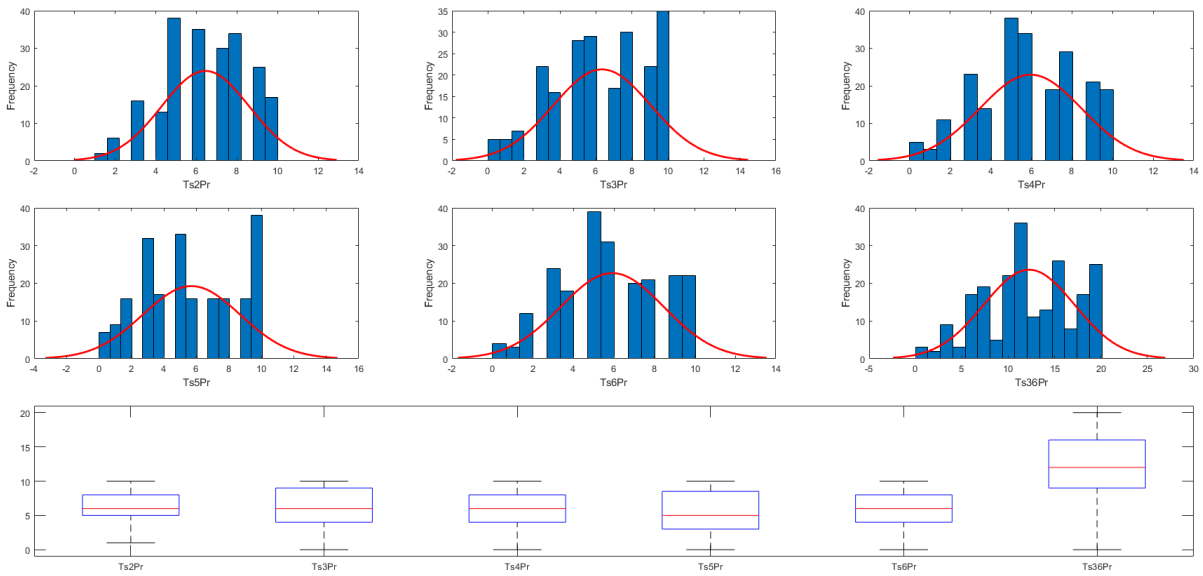

Figure 24 – Distribution and Box plot of the Target variables aggregated in the **DSet-1**

Correlation coefficients between all the target variables included in **Dset-1** were displayed as a heat map representation that ranged between [-1 1]in Figure 25.

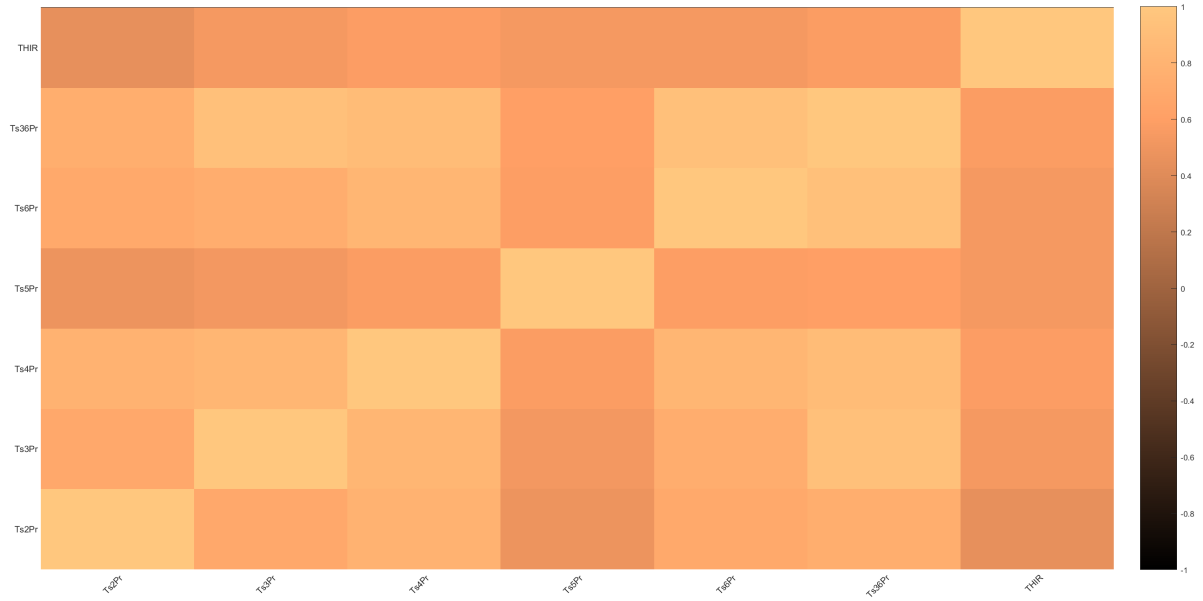

Figure 25 – Correlational relationship of all MSQ items that aggregated in the **DSet-1** which dark and light copper color represents negative and positive correlations, respectively

6.1.5 Correlational relationship in the Dset-1

Correlation coefficients between all aggregated variables per observations included in **Dset-1** explored as a heat map representation that ranged between [-1 1]in the Figure 26.

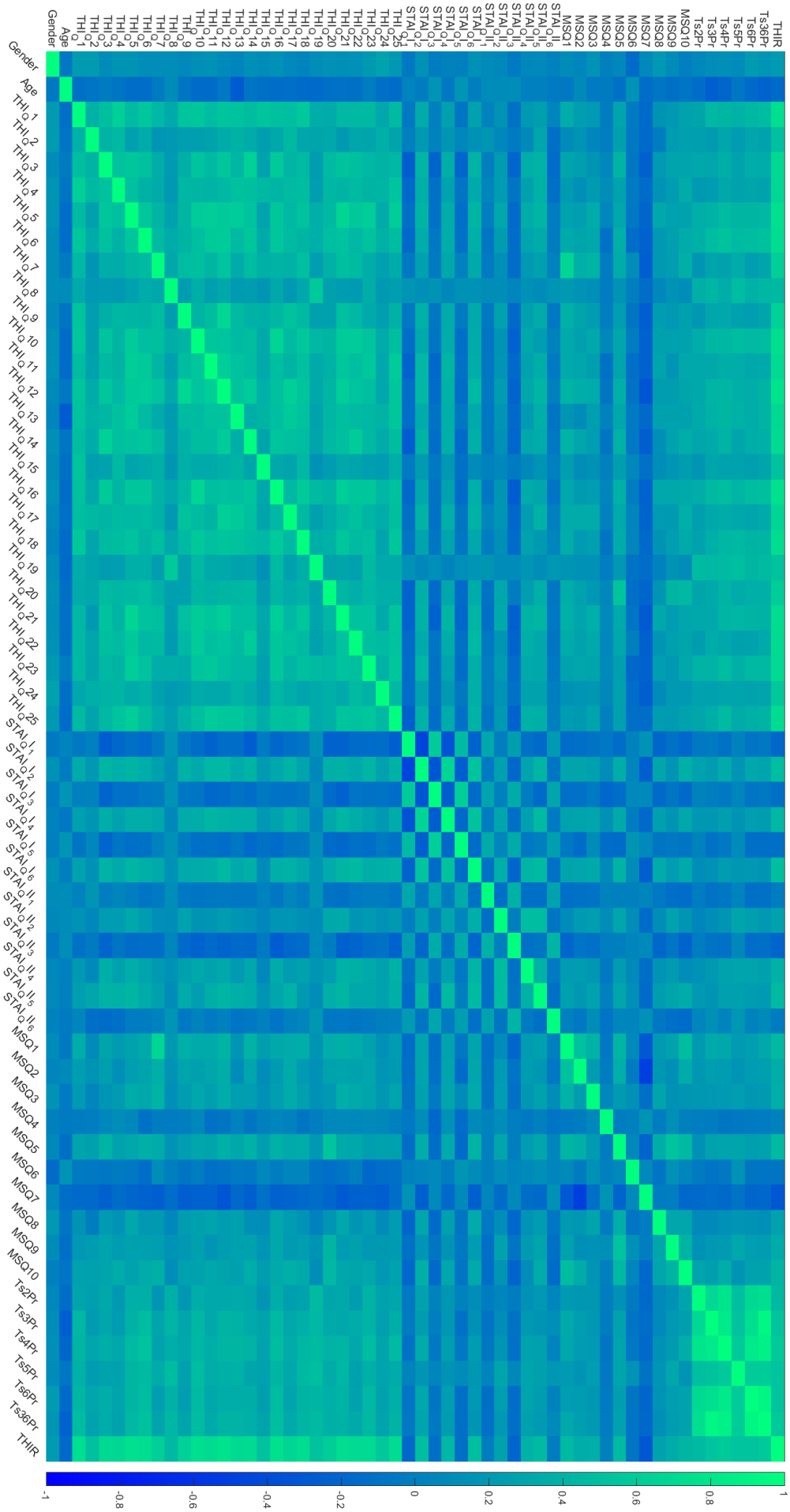

Figure 26 – Correlational relationship of all features aggregated in the **DSet-1** which dark blue and green colors represent negative and positive correlations, respectively.

6.2 DSet-2: Data Description for the dataset used in the Supervised Causality of NcC_DataDriven Modeling

The data were anonymized to ensure blinding. Initially, those with missing values were omitted, resulting in 253 session-wised questionnaires from the first and second studies. Primarily, data sets were aggregated and segmented based on different tinnitus severity stages. Scores of the THI questionnaire lower than 20 ($THIR < 20$) were labeled as neutral otherwise ($THI - R \geq 20$), the Clinical. We also made two additional sub-datasets (Tinnitus-Neutral and Tinnitus-Clinical) to conduct statistical analysis.

Descriptive statistics are presented in Table 7.

	N	Minimum	Maximum	Mean	Std. Deviation	Skewness	
	Statistic	Statistic	Statistic	Statistic	Statistic	Statistic	Std. Error
Age	253	27	72	54.43	10.308	-.751	.153
THIResult	253	0	100	38.91	24.551	.459	.153
TS_Pre.Q2	252	1	10	6.57	2.161	-.299	.153
TS_Pre.Q4	252	0	10	6.12	2.499	-.257	.153
TS_Pre.Q5	252	0	10	5.83	2.992	-.047	.153
Ts36Pr	252	.00	10.00	6.3036	2.46693	-.230	.153

Table 7 – Descriptive statistics of the all variables aggregated in the **Dset-2**

Descriptive information of all variables included in the **DSet-2** are shown in Figure 27.

Correlation coefficients between all aggregated variables per anonymous observation included in **Dset-2** explored as a heat map representation that ranged between [-1 1]in the Figure 28.

6.3 DSet-3:Data set used in the Pilot Adaptive seamless Bayesian Dose-response study for Sample size calculation

Six subjects recruited for this study underwent a 3-session crossover trial to create Bayesian inferences to calculate a sufficient sample size for efficacy, safety, and single-session dose-response relationship. The studied relationship corresponds to the behavior of a transformation performed on TLQ, “surrogate endpoint, “During the trial, TLQ was recruited longitudinally

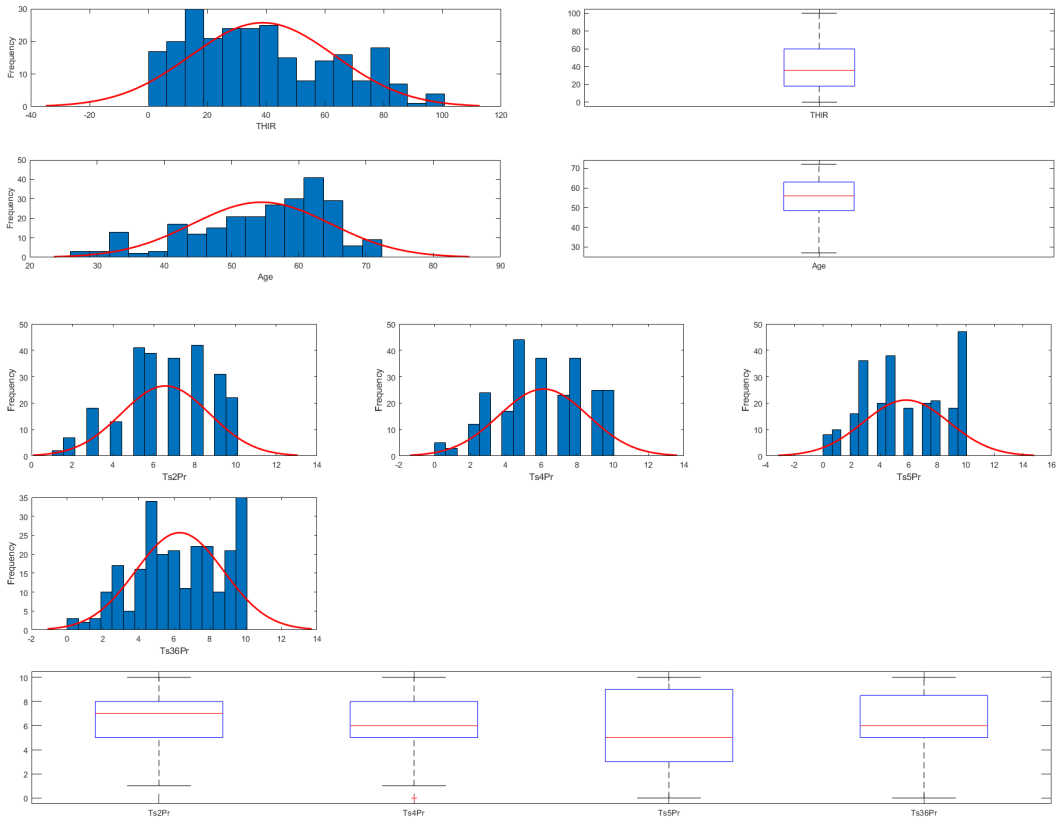

Figure 27 – Distribution and Box plot of the all variables aggregated in the **DSet-2**

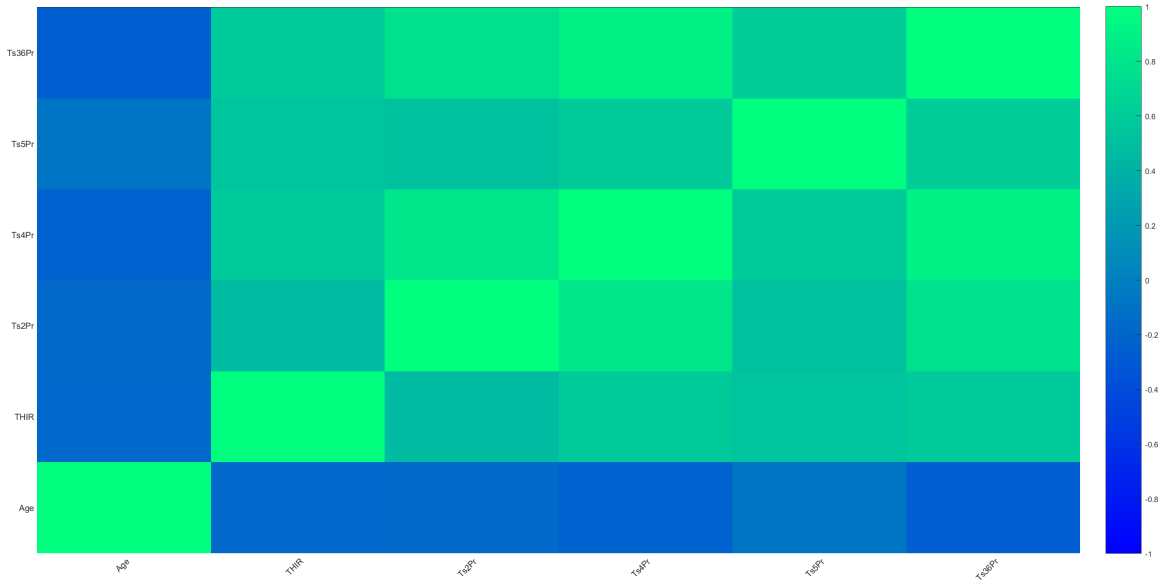

Figure 28 – Correlational relationship of all features aggregated in the **DSet-2** which dark blue and green colors represent negative and positive correlations, respectively.

at 21 different time points. It was also acquired before and after each session through questionnaires. TLQ is a 10-point Likert scale that represents patients' tinnitus loudness perception. Two

patients reported no change in their TLQ scores through all the recorded time points.
However, preprocessing and descriptive information is already published and accessible through the following DOI:$https://doi.org/10.3389/fnhum.2022.811550$. Consequently, we decided not to include descriptive analysis in the current theses to prevent repeating the already open access and published information.

6.3.1 Ethical approval and consent to participate

Data were collected from participants in a study on neurofunctional tinnitus model validation - 1) A randomized crossover three-session double-blind study approved by the Ethics Committee for Analysis of Research Projects, Specialized Center of Otorhinolaryngology and Speech Therapy, Hospital das Clínicas de Ribeirão Preto, University of São Paulo, Brazil (HCRP no 55716616.1.1001.5440). All subjects gave written informed consent.

Funding Disclosure
This research is part of a Multidisciplinary Cognitive Rehabilitation (MCR) Platform and was supported (Grant number: 2013/07375-0) by the Innovation and Diffusion of Mathematical Sciences Center Applied to Industry (CEPID-CeMEAI) of Sao Paulo Research Foundation (FAPESP), the University of Sao Paulo, and the Coordenação de Aperfeiçoamento de Pessoal de Nível Superior (CAPES) for student's scholarship.

6.3.2 Data Availability Statements

The supplementary materials and data-sets used during this study are available with the corresponding author with filling out the consent of NEL- knowledge management platform and redirecting to 'Zenodo' for access to the following:

- Datasets; **DOI: 10.528/zenodo.4554504**.
- 3D-Simulation of clinical space and environment; **DOI: 10.528/zenodo.4554510**.
- R-toolbox for dose-response sample size calculation; **DOI: 10.528/zenodo.4554516**.
- Superlab protocols; **DOI: 10.528/zenodo.4554508**.

CHAPTER

7

UNSUPERVISED DATA DISCOVERY FOR NCC-DATA-DRIVEN SECTIONS; FEATURE OPTIMIZATION

7.1 Feature optimization

High-dimensional data, particularly clinical ones, suffer from redundant information (ELHAMIFAR; VIDAL, 2013) and collinearity, which means some features might be perfect linear combinations of others and cause overfitting in the learning stage of cognitive computing. Feature space (FS) optimization is recommended to address this challenge through either feature-transformation (FT) or feature-selection to solve the collinearity and overfitting problems. Feature selection suggests choosing the important features and removing the unnecessary ones from the original feature set according to certain evaluation methods.

FT develops a set of transformed features rather than a subset of the original features like quantization. The optimized FS is expected to help machine learning tasks, increase interpretation and visualization, and reduce the curse of dimensionality, the risk of over-fitting, and computational cost (SHARMIN *et al.*, 2019). FS can be optimized with supervised, unsupervised, and semi-supervised methodologies (SHEIKHPOUR *et al.*, 2017).

The semi-supervised FS optimization evaluates features from a small number of labeled data and many unlabeled data (ZHANG *et al.*, 2018). In supervised FS optimization, discriminative features are selected or transformed using existing label information (SONG *et al.*, 2007). Unsupervised FS optimization evaluates features by maintaining particular properties of the data. Unsupervised feature-selection(YANG *et al.*, 2011; CAI; ZHANG; HE, 2010; DU *et al.*, 2017; LI *et al.*, 2012; LEE; SEO; KIM, 2018)and FT (LEVER; KRZYWINSKI; ALTMAN, 2017; JOLLIFFE, 2003; SCHÖLKOPF *et al.*, 1998; TORGERSON, 1952; TENENBAUM; SILVA; LANGFORD, 2000; ROWEIS; SAUL, 2000; LUXBURG, ; COIFMAN; LAFON, 2006; KA-

MADA; KAWAI, 1989; HINTON; ROWEIS, 2002; MAATEN; HINTON, 2008; HYVARINEN, 1999; LAPARRA; MALO; CAMPS-VALLS, 2015) methodes drew more attention due to the difficulty in labeling (WANG *et al.*, 2015).
Feature-transformation(FT) supports changing or computing new representative features from data while maintaining key patterns. FT relying on different criteria: maximizing the variation (LEVER; KRZYWINSKI; ALTMAN, 2017; JOLLIFFE, 2003; SCHÖLKOPF *et al.*, 1998), distance matrices (TORGERSON, 1952; TENENBAUM; SILVA; LANGFORD, 2000), improving the statistical independence between features (MAATEN; HINTON, 2008; HYVARINEN, 1999), Laplacian eigenmaps(LUXBURG,), diffusion maps(COIFMAN; LAFON, 2006), similarity distance between vertices (KAMADA; KAWAI, 1989), and stochastic methods(HINTON; ROWEIS, 2002). FT extensively applies to multivariate data sets for identifying the patterns despite keeping components independent (LAPARRA; MALO; CAMPS-VALLS, 2015). Furthermore, similarity information among patterns is employed with several unsupervised feature-selection methods, such as the Laplacian matrix, to preserve local behavior(YANG *et al.*, 2011; CAI; ZHANG; HE, 2010; DU *et al.*, 2017; LI *et al.*, 2012; YANG *et al.*, 2011; WANG *et al.*, 2015)
In this chapter, to support the NcC autonomous and real-time learning, we proposed a new hybrid unsupervised method for both the FT and feature selection to optimize the FS. It considers mutual information to evaluate hierarchical feature dependencies.

Experimental results demonstrate the proposed method performance and cross-validations based on the state-of-the-art of total correlation. The main contributions of this chapter are as follows:

- We proposed a novel Gaussian-kernel hierarchical nonuniform quantization mechanism with compensated fitting and developed the NcC-HQuantization MATLAB toolbox to implement corresponding architecture and algorithms.

- We postulated and provided theoretical proof for a new FT method based on the joint probability and Markov chain approaches.

- We proposed a new unsupervised hybrid FS optimization based on mutual information. To the best of our knowledge, the developed method is the first to recognize the optimized FS dependency pattern.

- We developed regulatory parameters with an automatic optimization mechanism for dimension reduction. We also implemented related architecture and algorithms in the NcC_-Feature Optimization MATLAB Toolbox. In addition, we projected Metric assessments and benchmarks in R. *"Manuscripts are in progress for dissemination."*.

This chapter is organized as follows. section 2 reviews the evolution of unsupervised FS optimization methods. Section 3 proposes the integrated FS optimization problem and an iterative

algorithm for the solution. In section 4, various experimental results are analyzed. Conclusions are drawn in section 5.

7.2 Background and Related works

7.2.1 PCA and kPCA

The principal component analysis (PCA) conceptualized the dimension reduction of a data set, including various interrelated variables, while holding the primary dataset's maximum variation. PCA computes a new set of variables that are not correlated but consists the most of the variance of the original variables despite the reduction in numbers(LEVER; KRZYWINSKI; ALTMAN, 2017; JOLLIFFE, 2003).
Kernel Principal Component Analysis (kPCA) generalizes PCA to handle nonlinear dependencies between variables. kPCA conceptualized to dimensionality reduce the mapped data into a high dimensional space using a possibly nonlinear function (SCHÖLKOPF *et al.*, 1998). Let $\mathbf{X}_i \in \Re^d$, for $i = 1,\ldots,n$, a $d-$dimensional data. The kPCA algorithm can be see as a two-step process

- **Non-linearly transform** the $i-$th data $\mathbf{X}_i \in \Re^d$ into a point $\Phi(\mathbf{X}_i)$ in an $N_{\mathscr{H}}-$dimensional *feature space* $\mathscr{H}$, where

$$\Phi(\mathbf{X}_i) = (\phi_1(\mathbf{X}_i),\ldots,\phi_{N_{\mathscr{H}}}(\mathbf{X}_i)) \in \mathscr{H}, \quad i = 1,\ldots,n.$$

  The map $\Phi : \Re^d \longrightarrow \mathscr{H}$, is called *feature map*, and each of $\{\phi_j\}$ is a nonlinear map.

- **Eigenvalue problem:** Given $\Phi(\mathbf{X}_1),\ldots,\Phi(\mathbf{X}_n) \in \mathscr{H}$, with $\sum_{i=1}^{n}\Phi(\mathbf{X}_i) = 0$, solve a linear PCA problem in feature space $\mathscr{H}$, which will have a higher dimensionality than that of output space, i.e., $N_{\mathscr{H}>d}$.

It proposes that a low-dimensional structure is more easily discovered when it becomes embedded in the larger space $\mathscr{H}$.

7.2.2 Isomap

Classical Scaling can treat arbitrarily defined distances. Tenenbaum (2000) projected to use of geodesic distances to estimate the manifold structure, $\mathscr{M}$. Geodesic distances are made by showing the distance on the graph, $\mathscr{G}$, and classical Scaling performs to find an embedding in fewer dimensions. Let $\mathbf{X}_i \in \mathfrak{X}$ for $i = 1,\ldots,n$ and $\mathfrak{X} = \Re^d$. The Isomap algorithm for dimension reduction has the following steps

- **Neighborhood graph:** For K or ε fix, where K as an integer and $\varepsilon > 0$. Calculate the distance matrix with

$$d_{ij}^{\mathfrak{X}} = d^{\mathfrak{X}}(\mathbf{x}_i,\mathbf{x}_j) = ||\mathbf{x}_i - \mathbf{x}_j||_{\mathfrak{X}},$$

for $i, j = 1, \ldots, n$. In general we use the Euclidean distance. Now we determine the neighbored of $\mathbf{x}_i$. If K is fix so

$$N_i^K = \{\mathbf{x}_{j_1}, \ldots, \mathbf{x}_{j_K} \in \mathfrak{X} \mid \mathbf{x}_{j_l} = argmin_{j; j \notin \{1,\ldots,j_{l-1}\}} \{d(\mathbf{x}_i, \mathbf{x}_j)\}, \quad l = 2, \ldots, K\}$$

or

$$N_i^\varepsilon = \{\mathbf{x}_j \in \mathfrak{X} \mid d(\mathbf{x_i}, \mathbf{x_j}) < \varepsilon\}.$$

Connecting the close data point and do a symmetrical adjacent matrix of a graph $\mathscr{G}$. Put $d_{ij}^{\mathfrak{X}}$ as a weighted w_{ij}, on edge linked $\mathbf{x}_i$ and $\mathbf{x}_j$.

- **Compute Graph Distances:** We estimate the unknown true distance $\{d_{ij}^{\mathscr{M}}\}$, between pair of points in $\mathscr{M}$ by a graph distance $\{d_{ij}^{\mathscr{G}}\}$, with respect to the graph $\mathscr{G}$. The graph distance is the shortest path distance between all pairs in the $\mathscr{G}$ graph.

- **Embedding via Multidimansional Scaling:** Let $\mathbf{D}^{\mathscr{G}} = (d_{ij}^{\mathscr{G}})$ be the symetric $(n \times n)-$matrix of graph distances. Apply the Multidimensional Scaling to $\mathbf{D}^{\mathscr{G}}$ to give the reconstructed data points in a $t-$dimensional feature space $\mathfrak{Y}$, with $t \ll d$, such that, preserved geodesic distances on $\mathscr{M}$ as much as possible.

7.2.3 Locally Linear Embedding

Points that place on a manifold in a high dimensional space can model through linear combinations of their neighborhoods if the manifold is adequately sampled and the neighborhoods settled on a locally linear patch (ROWEIS; SAUL, 2000). Like a Isomap, the LLE algorithm also consists of three steps.

- **Nearest Neighbor search:** Fix $K \ll d$ and define

$$N_i^K = \{\mathbf{x}_{j_1}, \ldots, \mathbf{x}_{j_K} \in \mathfrak{X} \mid \mathbf{x}_{j_l} = argmin_{j; j \notin \{1,\ldots,j_{l-1}\}} \{d(\mathbf{x}_i, \mathbf{x}_j)\}, \quad l = 2, \ldots, K\}.$$

- **Constrained Least Squares Fits:** Reconstruction $\mathbf{x}_i$ by pooled-sum of its K nearest neighbors,

$$\hat{\mathbf{x}}_i = \sum_{l=1}^{K} w_{ij_l} \mathbf{x}_{j_l},$$

where $w_{ij_l} \in [0,1]$ for all i, j_l, and $\sum_{l=1}^{K} w_{ij_l} = 1$. This weight is given by

$$(w_{1j_1}, \ldots, w_{1j_K}) = \mathbf{w}_i = argmin_w \left|\left| \mathbf{x}_i - \sum_{l=1}^{K} w_{ij_l} \mathbf{x}_{j_l} \right|\right|^2,$$

subject to

$$\sum_{l=1}^{K} w_{ij_l} = 1.$$

- **Eigen problem:** For the optimal fix weight $\hat{w}_i$ $i = 1,\ldots,n$ found at the step 2. We search the best vector $\mathbf{y}_i$ with $t-$dimensional and $t \ll d$, of embedding coordinates, such that

$$\hat{\mathbf{y}}_i = argmin_{\mathbf{y}} \left|\left| \mathbf{y}_i - \sum_{l=1}^{K} w_{ij_l} \mathbf{y}_{j_l} \right|\right|^2,$$

subject to

$$\sum_i \mathbf{y}_i = \mathbf{0} \quad \text{and} \quad n^{-1} \sum_i \mathbf{y}_i \mathbf{y}_i^T = \mathbf{I}_t.$$

7.2.4 Laplacian Eigenmap

spectral clustering to separate non-convex clusters in DR domains using graph embedding and so-called Laplacian Eigenmap (BELKIN; NIYOGI, 2003). according to the analogy, the concepts following modifications have been proposed, **a)**The graph can be created sparsely by retaining only the k nearest neighbors or defining a " neighborhood. **b)**The Gaussian kernel is used to compute a similarity matrix. **c)** all distances are considered equal (LUXBURG,). The Laplacian Eigenmap algorithm consists of three steps

- **Nearest-Neighbor search:** Fix an integer K or a $\varepsilon > 0$ and define the neighbors of $\mathbf{x}_i$

$$N_i^K = \{\mathbf{x}_{j_1},\ldots,\mathbf{x}_{j_K} \in \mathfrak{X} \mid \mathbf{x}_{j_l} = argmin_{j;j\notin\{1,\ldots,j_{l-1}\}}\{d(\mathbf{x}_i,\mathbf{x}_j)\}, \quad l = 2,\ldots,K\}$$

or

$$N_i^{\varepsilon} = \{\mathbf{x}_j \in \mathfrak{X} \mid d(\mathbf{x_i},\mathbf{x_j}) < \varepsilon\}.$$

- **Weighted adjacency matrix:** Let $\mathbf{W} = (w_{ij})_{n\times n}$ be a symetric $(n\times n)$ weighted adjacency matrix defined as fellows

$$w_{ij} = \begin{cases} \exp\left\{-\frac{||\mathbf{x}_i-\mathbf{x}_j||^2}{2\sigma^2}\right\}, & \mathbf{x}_j \in N_i, \\ 0, \quad otherwise. \end{cases}$$

These weights are determined by Isotropic Gaussian Kernel with scale parameter σ.

- **Eigen-problem:** Let $\mathbf{D} = (d_{ij})$ be an $(n\times n)$ diagonal matrix with diagonal elements $d_{ii} = \sum_{j\in N_i} w_{ij} = (\mathbf{W1}_n)_i$ for $i = 1,\ldots,n$. The $(n\times n)-$matrix $\mathbf{L} = \mathbf{D} - \mathbf{W}$ is known as the *graph Laplacian* for $\mathscr{G}$ graph. Let $\mathbf{y} = (y_i)$ be an $n-$vector. Then, $\mathbf{y}^T\mathbf{L}\mathbf{y} = \frac{1}{2}\sum_{i=1}^n \sum_{i=1}^n w_{ij}(y_i - y_j)^2$, so that $\mathbf{L}$ is non-negative definitive. Then the matrix Y with $(t\times t)-$dimensional where $t \ll d$, of embedding vector is given by

$$\hat{\mathbf{Y}} = argmin_{\mathbf{YDY}=\mathbf{I_t}} tr\{\mathbf{YLY}\}.$$

7.2.5 Diffusion Maps

Diffusion Maps (COIFMAN; LAFON, 2006) for the manifold's approximation receive a distance matrix and calculates the transition probability of a diffusion process among the points. Later the embedding is done by eigenvalue decomposition to determine the coordinates of the embedding.

7.2.6 Force Directed Methods

The similarity distance between vertices may be considered a graph with weighted connections. Force-directed algorithms consider the graphs' connections as enhancing or reducing force between the nodes and set out to minimize the overall energy of the graph (KAMADA; KAWAI, 1989).

7.2.7 t-SNE

Stochastic Neighbor Embedding (SNE)(HINTON; ROWEIS, 2002) is a method that minimizes the Kullback-Leibler divergence of scaled similarities of the vertices in a high dimensional space. SNE employs a Gaussian kernel to estimate similarities in multidimensional space. The t-Distributed Stochastic Neighbor Embedding (t-SNE)(MAATEN; HINTON, 2008) develops on SNE using t-Distribution as a kernel in low dimensional space.()

7.2.8 ICA

Independent Component Analysis (ICA) represents data as a mixture of independent signals. ICA is a linear rotation of the data, similar to PCA, but alternatively, it recovers statistically independent components(HYVARINEN, 1999).

7.2.9 DRR

Dimensionality Reduction via Regression (DRR) is a recent technique extending PCA. It predicts excessive information from the residual components utilizing nonlinear regression. The DRR has a distinct advantage due to rendering the definite forward and inverse function. However, mutual information (MI) approaches for nonlinear FT have not been established yet because of requiring higher-order statistics and computational complexity.
Estimating MI between two random variables is feasible through histograms or kernel-based quantizations using feature-selection rather than FT(GRASSBERGER, 1985; SOMORJAI, 1986; STÖGBAUER *et al.*, 2004) and suffers dramatically from the curse of dimensionality. However, MI greedy algorithms grounded on sequential feature selection are suboptimal and suffer dramatically from the curse of dimensionality, consequently failing to find a feature set that would concurrently maximize the MI between the features and the targets. Pedro et al. demonstrated a

supervised feature selection procedure utilized on regression problems (CARMONA; SOTOCA; PLA, 2012). Makoto et al.(2014) discovered a nonlinear causal relationship on selected features using hierarchical clustering based on squared-loss mutual information between inputs and residuals (YAMADA; SUGIYAMA; SESE, 2014). Voot et al. (2017)showed quadratic mutual information for linear-supervised FT (TANGKARATT; SASAKI; SUGIYAMA, 2017). They maximized dependency between projected input and output features. They also used mutual information to recognize outliers in the tested data set.

7.3 Background

In parallel with the conceptualization of the method, we also illustrated the results based on the selected cognitive mission in NcC prototype.

7.3.1 Quantization and discretizing

We demonstrated a novel hierarchical quantization based on the compensated non-uniform Normal pdf kernel to transform data into discrete variables with the finite quantized level. This transformation is independent of datatype such as continuous, ordinal, and categorical. Categorical features are required a fixed pattern of categories.

- features (V=variable) are normally distributed with mean (μ), standard deviation (σ), and normal probability density function ($\mathcal{N}$-pdf).
- Considering the ($\mathcal{N}$-pdf) range as $[-4\sigma, +4\sigma]$ that guarantees 99.9% of data with variance normalization $\tilde{x}$ places data between [0, 1]. Consequently, out of this range is outlier.

$$\tilde{x} = \frac{(x-\mu)/4\sigma + 1}{2} \tag{7.1}$$

- Normalized features were standardized with z-score.

$$\tilde{x} = \frac{x-\mu}{\sigma} \tag{7.2}$$

- Class orders in categorical data types are one-time defined, and change is not allowed.
- Observations with missing values are eliminated from the dataset.

7.3.2 Hierarchical Quantization

quanta (q): is a stripe on $\mathcal{N}$-pdf at each feature in linear divisions and proportional to the standard deviation. Thereby, the related probability of individual quanta can be calculated:

$$q_{k,l} = \int_{z_{min}}^{z_{max}} \frac{1}{2\pi} e^{-\frac{z^2}{2}} dz \tag{7.3}$$

We propose the uniform distribution within quanta. Therefore minimum quantization size (K_f) can be determined based on acceptable Minimum Squared Error (MSE) in each feature (f).

$$\mathbf{MSE} = \frac{1}{N}\sum_{k=1}^{K_f}\left(\frac{1}{n_k}\sum_{i=1}^{n_k}\left(Z_i - \tilde{Z}_k\right)^2\right) \tag{7.4}$$

In this equation, k is the quanta number. where N and n_k are training dataset and k^{th}quanta sample sizes, respectively. let's $\tilde{Z}_k$ represent quanta uniform value. The maximum value(K_F) of the K_f-vector considers as the fixed quantization size for the feature space. then we are applying uniform Quantization with K_F size and corresponding quanta-step on all features.

$$K_F = MAX\left\{K_1, K_2, \cdots, K_f\right\} \tag{7.5}$$

and

$$\text{Quanta Step} = q_{step} = \frac{2 \times 4\sigma}{K_F}$$

7.3.2.1 Optimizing quantization in each feature:

To not losing information and preventing noise induction to the quantized data, features are individually optimized for non-uniform quantization. Empty quantas merge with occupied adjacent quantas proportionate to their corresponding probabilities without making fractions in quanta units.

7.3.2.2 Compensated HQ

The quantized feature deviates PDF from a normal distribution, so the divergence is compensated within the non-uniform histogram context. Since the quantization process fixes the width of the quantas, the corresponding probability of the quanta can be corrected with the ratio of the expected number of samples in $\mathcal{N}$-pdf to the available ones.

$$Q = \frac{\text{Available number of samples in the quanta}}{\text{Expected sample in quanta based on } \mathcal{N}\text{-pdf strip}} \times q_k \text{and it should be equal to:} Q = \frac{n_k}{N} \tag{7.6}$$

7.3.2.3 Total Path Quantas Probability

HQ transforms any dataset to a discrete format that facilitates dimension reduction in the feature space. Since we are in a probability domain, we employ Total Path Quantas Probability (TPQ) as a Marginal-Probability to merge two consecutive variables. Consider two nonuniform quantized variables X and Y with $X = \{x_1, x_2, \cdots, x_n\}$, and $Y = \{y_1, y_2, \cdots, y_m\}$ different values or categories.

$$p_{x,y}(x,y) = P(X = x \text{ and } Y = y) = P(X \cap Y) = p\left(x_i, y_j\right)$$

It can be written in conditional distribution as bellow:

$$p\left(x_i, y_j\right) = P(Y|X).P(X) = P(X|Y).P(Y)$$

Where $P(Y|X)$ is the conditional probability of Y given X:

$$Path\ Probability\ = P(Y|X) = P[X|Y] = P_{x_i \to y_j} = \frac{\text{Count paths from } x_i \text{ to } y_j}{\text{Count Paths from } x_i \text{ to } Y} \tag{7.7}$$

and therefore, TPQ of X and Y is calculating from:

$$TPQ_{[X,Y]} = p\left(x_i, y_j\right) = P(Y|X).P(X) = \left(P_{x_i \to y_j}\right).P(x_i) \tag{7.8}$$

Consequently, In feature space, X and Y are replaced by $TPQ_{[X,Y]}$.
We generalized TPQ calculations based on the Chain rule of probability for several variables (showed in Equation.7.9).

$$\begin{aligned} TPQ_{[X_1,X_2,\cdots,X_n]} =& p(X_1,X_2,\cdots,X_n) = P(X_n \cap X_{n-1} \cap \cdots \cap X_1) \\ &= P(X_1)\prod_{i=2}^{n} P\left(X_i \middle| \bigcap_{j=1}^{j=i-1} X_j\right), \end{aligned} \tag{7.9}$$

by Markov property we get

$$\begin{aligned} TPQ_{[X_1,X_2,\cdots,X_n]} =& P(X_1)\prod_{i=2}^{n} P\left(X_i \middle| \bigcap_{j=1}^{j=i-1} X_j\right) = P(X_1)\prod_{i=2}^{n} P\left(X_i \middle| X_{i-1}\right) \\ &= P(X_1)\prod_{i=2}^{n} P_{x_{i-1} \to x_i} \end{aligned} \tag{7.10}$$

7.3.3 Information theory (Entropy)

A random variable's entropy is the average level of information or uncertainty inherent in its possible outcomes (Shannon 1984). Given a discrete random variable X, possible outcomes $x_1,\ldots,x_n$, which occur with probability $\mathrm{P}(x_1),\ldots,\mathrm{P}(x_n)$, the entropy of X is formally defined as:

$$H(X) = -\sum_{i=1}^{n} p(x_i)\log p(x_i). \tag{7.11}$$

Estimating the MI between X and Y, $I(X;Y)$ needs to evaluate the joint probability density function (X,Y).

Histogram and kernel-based pdf calculations are the most ordinarily used techniques (LEVER; KRZYWINSKI; ALTMAN, 2017). We developed a novel hierarchical compensated normal-pdf quantization that improves the estimation of joint probability and mutual information noted in . Joint Entropy is a measure of the uncertainty related to a set of variables

$$H(X,Y) = -\sum_{i=1}^{m}\sum_{j=1}^{n} P(x_i,y_j) log_2[p(x_i,y_j)] \tag{7.12}$$

7.3.3.1 Mutual Information

Mutual Information (MI) between two random variables (X and Y) can be measured using the amount of knowledge on Y presented by X or vice versa. Therefore, it can be defined as (KAMADA; KAWAI, 1989):

$$I(X;Y) = H(Y) - H(Y|X) \tag{7.13}$$

MI is also equal to the reduced uncertainty of Y when X is known. If Y is the target variable in predictive analytics, X's importance in a model for Y estimates MI (HINTON; ROWEIS, 2002). Using the properties of the entropy, MI can be revised into:

$$I(X;Y) = H(X) + H(Y) - H(X,Y) \tag{7.14}$$

Mutual Information for discrete variables Consider two discrete variables X and Y with $x_1, x_2, \ldots, x_n$, and $y_1, y_2, \ldots, y_m$ different values or categories. When $N(x_i, y_j)$ denotes the number of samples with x_i and y_j values, and N_T be the total number of samples. The joint probability mass $p(x_i, y_j)$, the marginal probability $p(x_i)$, $p(y_j)$, and mutual information $I(X;Y)$ can be accordingly calculated.

$$p(x_i, y_j) = \frac{N(x_i, y_j)}{N_T}, \qquad I(X;Y) = \sum_{i,j} p(x_i, y_j) log \frac{p(x_i, y_j)}{p(x_i)P(y_j)} \tag{7.15}$$

Teorema 1. Let be $MI(x_1;x_2)$ the mutual information of X_1 and X_2, then

$$MI(x_1;x_2) = H(x_1) + H(x_2) - H(TPQ_{[x_1,x_2]}).$$

Proof. By definition we have

$$\begin{aligned} MI(x_1;x_2) &= \sum_{x_1}\sum_{x_2} P(x_1,x_2) \log\left(\frac{P(x_1,x_2)}{P(x_1)P(x_2)}\right) \\ &= \sum_{x_1}\sum_{x_2} P(x_1,x_2) \log\left(\frac{P(x_1,x_2)}{P(x_1)P(x_2)}\right) \\ &= \sum_{x_1}\sum_{x_2} P(x_1,x_2) \left[\log(P(x_1,x_2)) - \log(P(x_1)P(x_2))\right], \\ &= \sum_{x_1}\sum_{x_2} P(x_1,x_2) \log(P(x_1,x_2)) - \sum_{x_1}\sum_{x_2} P(x_1,x_2) \left[\log P(x_1) + \log P(x_2)\right], \end{aligned}$$

Note that $\sum_{x_1}\sum_{x_2} P(x_1,x_2)\log(P(x_1,x_2)) = \sum_{x_1}\sum_{x_2} TPQ_{[x_1,x_2]}\log(TPQ_{[x_1,x_2]}) = -H(TPQ_{[x_1,x_2]})$ So we get

$$\begin{aligned} MI(x_1;x_2) &= -H(TPQ_{[x_1,x_2]}) - \sum_{x_1}\sum_{x_2} P(x_1,x_2)\log P(x_1) - \sum_{x_1}\sum_{x_2} P(x_1,x_2)\log P(x_2) \\ &= -H(TPQ_{[x_1,x_2]}) - \sum_{x_1}\log P(x_1)\sum_{x_2} P(x_1,x_2) - \sum_{x_2}\log P(x_2)\sum_{x_1} P(x_1,x_2), \end{aligned}$$

Followed by marginalization as,

$$MI(x_1;x_2) = -H(TPQ_{[x_1,x_2]}) - \sum_{x_1} P(x_1)\log P(x_1) - \sum_{x_2} P(x_2)\log P(x_2),$$

but by definition $-\sum_{x_1} P(x_1)\log P(x_1) = H(x_1)$, and $-\sum_{x_2} P(x_2)\log P(x_2) = H(x_2)$, and consequently

$$MI(x_1;x_2) = H(x_1) + H(x_2) - H(TPQ_{[x_1,x_2]}).$$

□

Teorema 2. Let be $MI(x_1;x_2;x_3)$ the mutual information of X_1, X_2 and X_3, then

$$MI(x_1;x_2;x_3) = MI((x_1,x_2);x_3) - MI(x_1;x_3) - MI(x_2;x_3).$$

Proof. By definition, we have

$$MI(x_1;x_2;x_3) = \sum_{x_1}\sum_{x_2}\sum_{x_3} P(x_1,x_2,x_3)\log\left(\frac{P(x_1,x_2,x_3)P(x_1)P(x_2)P(x_3)}{P(x_1,x_2)P(x_1,x_3)P(x_2,x_3)}\right), \tag{7.16}$$

The right side of (7.16) can be written like this

$$\begin{aligned}\sum_{x_1}\sum_{x_2}\sum_{x_3} P(x_1,x_2,x_3)[&\log P(x_1,x_2,x_3) + \log P(x_1) + \log P(x_2) + \log P(x_3) + \\ &- \log P(x_1,x_2) - \log P(x_1,x_3) - \log P(x_2,x_3)],\end{aligned} \tag{7.17}$$

expanding (7.17), we have

$$\sum_{x_1}\sum_{x_2}\sum_{x_3} P(x_1,x_2,x_3)\log P(x_1,x_2,x_3) +$$

$$+\sum_{x_1}\log P(x_1)\sum_{x_2}\sum_{x_3} P(x_1,x_2,x_3) + \sum_{x_2}\log P(x_2)\sum_{x_1}\sum_{x_3} P(x_1,x_2,x_3)$$

$$+\sum_{x_3}\log P(x_3)\sum_{x_1}\sum_{x_2} P(x_1,x_2,x_3) - \sum_{x_1}\sum_{x_2}\log P(x_1,x_2)\sum_{x_3} P(x_1,x_2,x_3)$$

$$-\sum_{x_1}\sum_{x_3}\log P(x_1,x_3)\sum_{x_2} P(x_1,x_2,x_3) - \sum_{x_2}\sum_{x_3}\log P(x_2,x_3)\sum_{x_1} P(x_1,x_2,x_3).$$

Now, note that $\sum_{x_1}\sum_{x_2}\sum_{x_3} P(x_1,x_2,x_3)\log P(x_1,x_2,x_3) = -H(TPQ_{[x_1,x_2,x_3]})$ and by marginalization we get

$$-H(TPQ_{[x_1,x_2,x_3]}) + \sum_{x_1} P(x_1)\log P(x_1) + \sum_{x_2} P(x_2)\log P(x_2) + \sum_{x_3} P(x_3)\log P(x_3) +$$

$$-\sum_{x_1}\sum_{x_2} P(x_1,x_2)\log P(x_1,x_2) - \sum_{x_1}\sum_{x_3} P(x_1,x_3)\log P(x_1,x_3) - \sum_{x_1}\sum_{x_3} P(x_1,x_3)\log P(x_1,x_3),$$

So, by considering the definition of Entropy, we have

$$\begin{aligned}
&-H(TPQ_{[x_1,x_2,x_3]})-H(x_1)-H(x_2)-H(x_3)+H(TPQ_{[x_1,x_2]})+H(TPQ_{[x_1,x_3]})+H(TPQ_{[x_2,x_3]})=\\
&\quad=-(H(x_1)+H(x_3)-H(TPQ_{[x_1,x_3]}))-(H(x_2)+H(x_3)-H(TPQ_{[x_2,x_3]}))+\\
&\quad+H(x_3)+H(TPQ_{[x_1,x_2]})-H(TPQ_{[x_1,x_2,x_3]}),
\end{aligned}$$

Therefore, by definition of Mutual Information, we have

$$MI(x_1;x_2;x_3)=MI((x_1,x_2);x_3)-MI(x_1;x_3)-MI(x_2;x_3)$$

□

Initially, before presenting the general result of Mutual Information, some notation is needed to be defined. The combination of n random variables in the sub-set of j variables is given by

$$\Pi_j^{(n)}=\Pi_j(X_1,\ldots,X_n)=\left\{(X_{p_1},\ldots,X_{p_j})|\{p_1,\ldots,p_j\}\in\binom{n}{j}\right\},$$

for $1\leq j\leq n$, and $|\Pi_j^{(n)}|=N_{n,j}=\binom{n}{j}$. We denote one member of $\Pi_j^{(n)}$ by $x_{\pi_j^{(n)}(i)}$ for $1\leq i\leq N_{n,j}$.

Teorema 3. Let be $X_1,X_2,\ldots,X_n$ random variables, then the Mutual Information of them is given by

$$MI(x_1;x_2;\ldots;x_n)=\sum_{j=1}^{n-1}(-1)^{n-j}\left(\sum_{i=1}^{N_{n-1,j}}MI(x_{\pi_j^{(n-1)}(i)};x_n)\right).$$

Proof. By induction, for $n=2$ we have

$$\begin{aligned}
MI(x_1;x_2)&=H(x_1)+H(x_2)-H(TPQ_{[x_1,x_2]})\\
&=MI(x_1)+MI(x_2)-MI(x_1;x_2).
\end{aligned}$$

Now, we suppose true for $n>2$ and proof for $n+1$. First, define $\mathbf{x}=(x_1;x_2;\ldots;x_{n-1})$, so we have

$$\begin{aligned}
MI(x_1;x_2;\ldots;x_{n-1};x_n;x_{n+1})&=MI((x_1;x_2;\ldots;x_{n-1});x_n;x_{n+1})\\
&=MI(\mathbf{x};x_n;x_{n+1}),
\end{aligned}$$

by Theorem 2 we get

$$MI(x_1;x_2;\ldots;x_{n-1};x_n;x_{n+1})=MI((\mathbf{x},x_n);x_{n+1})-MI(\mathbf{x};x_{n+1})-MI(x_n;x_{n+1}),$$

Then, by the Induction Hypothesis $MI(\mathbf{x};x_{n+1})$ we write

$$\begin{aligned}
&MI(x_1;x_2;\ldots;x_{n-1};x_n;x_{n+1}) = \\
&\quad = MI((\mathbf{x},x_n);x_{n+1}) - \sum_{j=1}^{n-1}(-1)^{n-j}\left(\sum_{i=1}^{N_{n-1,j}} MI(x_{\pi_j^{n-1}(i)};x_{n+1})\right) - MI(x_n;x_{n+1}) \\
&\quad = MI((\mathbf{x},x_n);x_{n+1}) + \sum_{j=1}^{n-1}(-1)^{n+1-j}\left(\sum_{i=1}^{N_{n-1,j}} MI(x_{\pi_j^{n-1}(i)};x_{n+1})\right) - MI(x_n;x_{n+1}), \quad (7.18)
\end{aligned}$$

Thus, rewriting the sum on right side of (7.18) we have

$$MI(x_1;x_2;\ldots;x_{n-1};x_n;x_{n+1}) = \sum_{j=1}^{n}(-1)^{n+1-j}\left(\sum_{i=1}^{N_{n,j}} MI(x_{\pi_j^n(i)};x_{n+1})\right).$$

□

Teorema 4. Let be $X_1,X_2,\ldots,X_n$ random variables, then the Mutual Information of them is given by

$$MI(x_1;x_2;\ldots;x_n) = \sum_{j=1}^{n}(-1)^{j-1}\left(\sum_{i=1}^{N_{n,j}} H(x_{\pi_j^{(n)}(i)})\right).$$

Proof. By induction, for $n=2$, we have

$$\begin{aligned}
MI(x_1;x_2) &= H(x_1)+H(x_2)-H(TPQ_{[x_1,x_2]}) \\
&= H(x_1)+H(x_2)-H(x_1,x_2) \\
&= \sum_{j=1}^{2}(-1)^{j-1}\left(\sum_{i=1}^{N_{2,j}} H(x_{\pi_j^{(2)}(i)})\right).
\end{aligned}$$

Now, we suppose true for $n>2$ and proof for $n+1$. First, define $\mathbf{x}=(x_1;x_2;\ldots;x_n)$, so we have

$$\begin{aligned}
MI(x_1;x_2;\ldots;x_{n-1};x_n;x_{n+1}) &= MI((x_1;x_2;\ldots;x_{n-1};x_n);x_{n+1}) \\
&= MI(\mathbf{x};x_{n+1}),
\end{aligned}$$

by Theorem 1 we get

$$MI(\mathbf{x};x_{n+1}) = H(\mathbf{x})+H(x_{n+1})-H(\mathbf{x},x_{n+1}),$$

apply the Induction Hypothesis on $H(\mathbf{x})$, we have

$$\begin{aligned}
MI(\mathbf{x};x_{n+1}) &= \sum_{j=1}^{n}(-1)^{j-1}\left(\sum_{i=1}^{N_{n,j}} H(x_{\pi_j^{(n)}(i)})\right) + H(x_{n+1}) - H(\mathbf{x},x_{n+1}) \\
&= \sum_{j=1}^{n}(-1)^{j-1}\left(\sum_{i=1}^{N_{n,j}} H(x_{\pi_j^{(n)}(i)})\right) + H(x_{n+1}) - H(x_1,x_2,\ldots,x_{n-1},x_n,x_{n+1}) \quad (7.19)
\end{aligned}$$

rewriting (7.19) we have

$$MI(x_1;x_2;\ldots;x_{n-1};x_n;x_{n+1}) = \sum_{j=1}^{n+1}(-1)^{j-1}\left(\sum_{i=1}^{N_{n+1,j}} H(x_{\pi_j^{(n+1)}(i)})\right). \tag{7.20}$$

□

7.3.3.2 Normalized Mutual Information

We introduced a method to Normalize MI (NMI) in which the total entropy of the X and Y is applied as the denominator adjusts the value of MI within$[0,1]$, the NMI expression is presented as (SUN *et al.*, 2019):

$$\begin{aligned}
&\textbf{Method I}: I_{\hat{N}}^{1}(X;Y) = 2\times\frac{I(X;Y)}{H(X)+H(Y)}\\
&\textbf{Method II}: I_{\hat{N}}^{2}(X;Y) = \frac{I(X;Y)}{MAX\{H(X),H(Y)\}}\\
&\textbf{Method III}: I_{\hat{N}}^{3}(X;Y) = \frac{I(X;Y)}{H(X,Y)}
\end{aligned} \tag{7.21}$$

7.4 New algorithm for Feature Space optimization

This section explores CausalSpace Toolbox and Causal feature optimization algorithms in Neurocognitive computing. CausalSpace Toolbox employ NMI distance to discover a causal relationship between variables. The most cumulative mutual information with the residual variables of the space is selected as the first member of the new feature; this variable is called ***Medoid***. After Medoid discovery, due to sorting other variables as potential members of the new feature, iteratively reordering the rest of the variables to find the variable with the most cumulative NMI to previous ones. The process continues to find the last variable in order. Followingly, the neighboring algorithm identifies the border of the feature with Maximum entropy and emerges neighbor's subset. The neighbor's subset within the greedy algorithm, through the forward and backward steps, iteratively tests the variables to find and filter the variables with the less causal relation. The unfiltered set forms the first feature, and filtered variables insert into the residual data set. This procedure repeatedly continues till shaping optimized causal features(NcC-CF1). However, if the number of the causal features in the optimized space is not satisfying, CST repeats the whole process on the optimized space to shape a more optimized space(NcC-CF2). Feature Optimization process in detail explored bellow within this section.

First, we consider the original feature space $\mathscr{X} = \Re^D$, a $D-$dimensional. So the vector of features will be represented by

$$\begin{aligned} &\mathbf{X} = (X_1, X_2, \ldots, X_D), \qquad \mathbf{X} \in \mathscr{X}, \\ &\text{with} \qquad dim(\mathscr{X}) = D. \end{aligned}$$

The reduced feature space will be denote by $\mathscr{Y} = \Re^d$ with $d \ll D$. The variable vector in this space will be denoted by

$$\mathbf{y} = (y_1, y_2, \ldots, y_d),$$

where $y_i = TPQ_{[C_i]}$, C_i is $i-$th cluster of variables. This method maintains the joint entropy of the original space as shown in the Theorem 5.

Teorema 5. TPQ-Dimension Reduction method retains joint entropy of the original feature space.

Proof. By definition, we have, correction needed in TPQ

$$\begin{aligned} H(y_1, \ldots, y_d) &= \sum p(y_1, \ldots, y_d) \log p(y_1, \ldots, y_d) \\ &= \sum p(TPQ_{[y_1, \ldots, y_d]} \log p(TPQ_{[y_1, \ldots, y_d]}) \\ &= \sum p(x_1, \ldots, x_D) \log p(x_1, \ldots, x_D) \\ &= H(x_1, \ldots, x_D). \end{aligned}$$

□

We describe each step of the NcC_Feature Optimization algorithm to explore how it holds the present primary information in the original variable space.

7.4.1 Step-I: Matrix of Normalized Mutual Information

First, compute the Normalized Mutual Information for all $x_i, x_j \in \mathscr{X}$, for $1 \leq i, j \leq D$ and construct matrix of information

$$a_{ij} = \frac{I_N^3(x_i; x_j)}{TPQ_{[x_i, x_j]}},$$

The information matrix exhibits shared information among the variable. Groups of variables with more shared information show more dependency and imply more causality. NcC_Feature optimization uses this concept to transform variables into causal feature space. Therefore, NcC causal features build from variables with more interactive information, shared information between more than two variables, to emerge causal feature space.

7.4.2 Step-II: Medoid selection

To indicate a group of variables with the maximum shared information, first, should determine the medoid given by

$$\mathscr{M}^{(k)} = arg \max_{x_j \in \mathscr{U}} \sum_{i=1}^{\mathscr{U}} I_N^3(x_i, x_j),$$

Medoid is a variable with the maximum accumulated information with all the current dataset variables and shapes the first variable of the kth sorted dataset to create the kth causal feature.

7.4.3 Step-III: Ordering variable from medoid

To create the $k-$th causal feature, reordering the current dataset for optimization is needed. The $k-$th reordering process starts with finding the second variable from unordered variables $\mathscr{U}$ with the maximum shared information with the medoid $\mathscr{M}^{(k)}$.
NcC continues the $k-$th reordering process to find the following variable in order by finding the variable with the maximum average shared information with all the previously ordered in the $k-$th process. This process continues to the last variable of the dataset, placed in the correct order based on the average of shared information.

$$\text{First: } X_{S_i^{(k)}} = arg \max_{x_i \in \mathscr{U}^{(k)}} \{I_N^3(x_i; \mathscr{M}^{(k)})\}$$

$$\text{Second: } X_{S_i^{(k)}} = arg \max_{x_i \in \mathscr{U}^{(k)}} \left\{ \sum_{x_j \in \mathscr{P}^{(k)}} I_N^3(x_i; x_j) \right\}$$

with

$\mathscr{P}^{(k)} = \{X_{S_1^{(k)}}, X_{S_2^{(k)}}, \ldots, X_{S_{i-1}^{(k)}}, \mathscr{M}^{(k)}\}$ and

$\mathscr{U}^{(k)} = \mathscr{U} / \mathscr{P}^{(k)}$.

The kth reordered dataset supports similarity ranking based on shared information.

7.4.4 Step-IV: Neighborhood

To determine the neighborhood of $\mathscr{M}^{(k)}$ NcC considers two bounding conditions sharing high versus low information between two variables. When two variables share high information, we have

$$H(V_1 \mid V_2) + H(V_2 \mid V_1) \approx 0,$$

we can see in the depicted Venn diagram

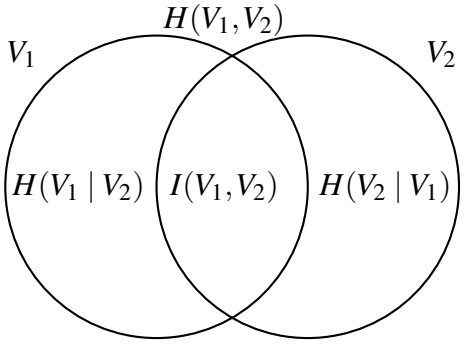

In terms of TPQ, we can write

$$\max H(V_1,V_2) = H(TPQ_{[V_1,V_2]}),$$

even when

$$H(V_1)+H(V_2) = H(\tilde{V}),$$

where $H(\tilde{V})$ is core entropy, so we get

$$H(\tilde{V}) = \frac{H(TPQ_{[V_1,V_2]})}{2},$$

and for the N variable, we have

$$H(\tilde{V}) = \frac{H(TPQ_{[V_1,\ldots,V_N]})}{N}.$$

The NcC algorithm defines the optimal numbers of variables in the $\mathscr{M}^{(k)}$ neighborhood to minimize the computation process of creating a causal feature. Now we have

$$\left| \frac{1}{N}\sum_{i=1}^{N} H(V_i) - \frac{H(TPQ_{[V_1,\ldots,V_N]})}{N} \right| = a > 0$$

We defined a target function to decide the optimal number of variables in the $\mathscr{M}^{(k)}$th neighborhood. Consider

$$\Pi = \{(\Pi_1,\Pi_2,\ldots,\Pi_j) \mid \Pi_j = \{X_{S_1^{(j)}}, X_{S_2^{(j)}}, \ldots, X_{S_{N_j}^{(j)}}\}\}.$$

Sorted feature space partitioned in j segments $\Pi_1,\Pi_2,\ldots,\Pi_j$, each one with $N_1,\ldots,N_j$ variables. Then for each segment, we define

$$\begin{aligned} G_1(\Pi) &= sd(H) \\ G_2(\Pi) &= sd(I_N^3(x_{pq})), \quad p,q \in \Pi_l, l = 1,\ldots,j, \end{aligned}$$

G_1 and G_2 Functions measure the heterogeneity levels of segments in the entropy variation between and within the segments, respectively. To segregate feature space well and maximize

the entropy of the causal feature, we expect G_1 and G_2 to be minimized. Therefore, the optimum configuration(partition) Π^* of feature-space given by:

$$minimize\ \ G_1(\Pi)\ \ \&\ \ minimize\ \ G_2(\Pi) \tag{7.22}$$

The value of N that get the optimal neighborhood conditional to Eq.7.22 which is given by

$$N_{opt} = \min\left\{ arg \max_{N\in\{1,\ldots,|\mathscr{U}|\}} \left| \frac{1}{N}\sum_{i=1}^{N} H(V_i) - \frac{H(TPQ_{[V_1,\ldots,V_N]})}{N} \right|, 6 \right\}$$

So, we denote the neighborhood of $\mathscr{M}^{(k)}$ by:

$$\mathscr{N}^{(k)} = \{X_{S_1^{(k)}}, X_{S_2^{(k)}}, \ldots, X_{S_{N_{opt}}^{(k)}}\}.$$

7.4.5 Step-V: Causal feature Greedy-Algorithm - Forward Step

In the forward step, the NcC algorithm evaluates whether to include a new variable, $X_{S_i^{(k)}}$, from the neighborhood to the final causal feature or not? $\mathscr{N}^{(k)}$ in the collection of variables with $\mathscr{M}^{(k)}$. Let be

$$\mathscr{F} = \{\mathscr{M}^{(k)}, X_1, \ldots, X_{N_j}\},$$

the variable collection after the backward step. Define

$$\begin{aligned} a_i^{(k)} &= I_N^3(TPQ_{[\mathscr{M}^{(k)},X_1,\ldots,X_j]}; X_{S_i^{(k)}}) \\ b_i^{(k)} &= I_N^3(\mathscr{M}^{(k)}; X_1; \ldots; X_j; X_{S_i^{(k)}}) \\ c_i^{(k)} &= a_i^{(k)} \times b_i^{(k)}, \end{aligned}$$

After that we define equivalent quantity for variables collection without the new variable $X_{S_i^{(k)}}$. Let be

$$\begin{aligned} a_{-i}^{(k)} &= I_N^3(TPQ_{[\mathscr{M}^{(k)},X_1,\ldots,X_{j-1}]}; X_j) \\ b_{-i}^{(k)} &= I_N^3(\mathscr{M}^{(k)}; X_1; \ldots; X_{j-1}; X_j) \\ c_{-i}^{(k)} &= a_{-i}^{(k-1)} \times b_{-i}^{(k-1)}, \end{aligned}$$

If

$$c_i^{(k)} \geq (1-\alpha) \times c_{-i}^{(k)} \tag{7.23}$$

so we add the new variable to the variables collection with $\mathscr{M}^{(k)}$ doing

$$\mathscr{F} = \mathscr{F} \cup \{X_{S_i^{(k)}}\}.$$

NcC algorithm evaluates the conditions of causal feature for the transformed variables collection from the forward step given by Section 7.4.6.

Otherwise, if the condition 7.23 was not satisfied for variable j. NcC algorithm updates the variable collections as

$$\mathscr{F} = \{\mathscr{M}^{(k)}, X_1, \ldots, X_{N_j}\} = \mathscr{C}_k$$

and remove the members from $\mathscr{C}_k$ of the unprocessed data $\mathscr{U}$, and go back to the Forward step in Step 7.4.5.

7.4.6 Step-VI: Backward-approach and stopping criteria in dimension reduction

In this step, the NcC algorithm relying upon the leave-one-out process evaluates transformed variable collection from the forward step would satisfy the causal feature conditions better or any combination with one variable less. Therefore, the NcC algorithm assigns all variables in the collection $\mathscr{F}$ given by Step 7.4.5. Let be

$$K = |\mathscr{F}|,$$

Defining leave-one-out process as bellow

$$\mathscr{P}(\hat{X}_k) = \{\mathbf{X}_{-k} \mid \mathbf{X}_{-k} = (X_1, \ldots, X_{k-1}, X_{k+1}, \ldots, X_{K-1})\},$$

for $k = 1, \ldots, K-1$, the medoid $\mathscr{M}^{(k)}$ will be present in all $\mathscr{P}(\hat{X}_k)$. to test the validity of the conditions condition of the backward step, we need to calculate

$$\begin{aligned} d_j^{(k)} &= I_N^3(TPQ_{[\mathscr{P}(\hat{X}_k)]}; \mathscr{M}^{(k)}) \\ e_j^{(k)} &= I_N^3(\mathscr{P}(\hat{X}_k); \mathscr{M}^{(k)}) \\ f_j^{(k)} &= d_j^{(k)} \times f_j^{(k)}, \end{aligned}$$

for $1 \leq k \leq K-1$. Now we define

$$u_k^{(k)} = I^3_{j\hat{N}}(TPQ_{[\mathscr{M}^{(k)},X_1,\ldots,X_{k-2}]};X_{k-1})$$
$$v_k^{(k)} = I^3_{j\hat{N}}(\mathscr{M}^{(k)};X_1;\ldots;X_{k-2};X_{k-1})$$
$$w_k^{(k)} = u_k^{(k)} \times v_k^{(k)}.$$

If

$$w_k^{(k)} \geq (1-\beta) \times \max\{f_1^{(k)},\ldots,f_{K-1}^{(k)}\},$$

then go to Step 7.4.5.

Otherwise, let be

$$f_M = \max\{f_1^{(k)},\ldots,f_{K-1}^{(k)}\},$$

and $\mathscr{P}(\hat{X}_M)$ its partition. After that, we update the $\mathscr{F}$ set doing

$$\mathscr{F} = \mathscr{P}(\hat{X}_M),$$

and go to Step 7.4.5.

7.4.7 Step-VII: Compute New Dimension

Feature-space optimization is finalized by transforming k variables collections into causal feature construction.

Based on Markov Chain and reserving the variable orders within each variable collection, the NcC algorithm emerges TPQ for each causal feature. We define

$$TPQ : \mathscr{X} \longrightarrow \mathscr{Y},$$

and for each variable collection we define

$$\mathscr{C}_k = \{\mathscr{M}^{(k)}, X_{S_1^{(k)}},\ldots,X_{S_{N_j}^{(k)}}\} \longmapsto y_k \in \mathscr{Y},$$

where

$$y_k = TPQ_{(k)}[P(\mathscr{M}^{(k)})P(\mathscr{M}^{(k)} \to X_{S_1^{(k)}})\ldots P(X_{S_{N_{j-1}}^{(k)}} \to X_{S_{N_j}^{(k)}})].$$

Then the optimized causal feature-space is

$$(TPQ_1, TPQ_2, \ldots, TPQ_d).$$

7.4.8 Step-VIII: Algorithm

Algorithm 1 TPQ-Dimension Reduction Algorithm

while $\mathscr{U} \neq \emptyset$ **do**
- Medoid Selection
- Ordering Variable from Medoid
- Determine neighborhood of Medoid $\mathscr{N}^{(k)}$
- **while** $\mathscr{N}^{(k)} / [X_{S_1^{(k)}}, X_{S_2^{(k)}}, \ldots, X_{S_j^{(k)}}] \neq \emptyset$ **do**
  - **if** $c_i^{(k)} \geq (1-\alpha) \times c_{-i}^{(k)}$ **then**
    - **if** $w_K^{(k)} \geq (1-\beta) \times \max\left\{f_1^{(K)}, \ldots, f_{S_{K-1}}^{(K)}\right\}$ **then**
      - Keep $\mathscr{F}$ and go to the next neighbor.
    - **else**
      - Do $\mathscr{F} = \mathscr{P}(\hat{X}_M)$ and go to the next neighbor
  - **else**
    - Do $\mathscr{C}_k = \{\mathscr{M}^{(k)}, X_{S_1^{(k)}}, \ldots, X_{S_{N_j}^{(k)}}\}$ and updating the unprocessed set
    - $\mathscr{U} = \mathscr{U} / \mathscr{C}_k$ and go to step Medoid Selection

for l *in* $(1, 2, \ldots, N_j)$ **do**
- Compute $y_i = TPQ[\mathscr{C}_i] = TPQ[\mathscr{M}^{(i)}, X_{S_1^{(i)}}, \ldots, X_{S_{N_j}^{(i)}}]$

7.4.9 Causal Feature Space Conclusions

We coined Causal Feature for transformed features through NcC_feature optimization algorithm due to the casual rationality of decision criteria for merging features we discussed bellow:

- NcC algorithm ensures the inflation of the mutual information between the Joint entropy of primary variables and the new one is acceptable.
- NcC algorithm ensures the inflation of the interactive information between all merging variables is acceptable.
- NcC algorithm guarantees the best combinations of causal features to optimize the feature space.

7.5 Metrics for Evaluation of Features Optimization

This section describes qualitative metrics used to evaluate the CausalSpace Toolbox (CST) performance in Feature Optimization. Metrics exhibit how posterior optimized features preserve the variance of the primary variable space.

7.5.1 Total Correlation

Let be $X_1, X_2, \ldots, X_D$ original variables and $Y_1, Y_2, \ldots, Y_d$ optimized feature. The Total Correlation is defined by

$$\rho_{Total} = \sum_{j=1}^{d} \sum_{i=1}^{D} \frac{Cor^2(X_i, Y_j)}{D}, \tag{7.24}$$

That means the better feature optimization method has a more significant sum of the mean squared correlations of the original variables with the optimized features should be maximized. Consequently, it ranks the methods from best to worst from maximum to minimum correlation.

7.5.2 Distance Correlation

Let be $\mathbf{X} = (X_1, X_2, \ldots, X_D)$ primary variables and $\mathbf{Y} = (Y_1, Y_2, \ldots, Y_d)$ posterior optimized features. The distance correlation is defined by

$$dCorr(\mathbf{X}, \mathbf{Y}) = \frac{dCov(\mathbf{X}, \mathbf{Y})}{\sqrt{dVar[\mathbf{X}] dVar[\mathbf{Y}]}}, \tag{7.25}$$

where

$$dCov(\mathbf{X}, \mathbf{Y}) = \sqrt{E[||\mathbf{X} - \mathbf{X}'||||\mathbf{Y} - \mathbf{Y}'||] + E[||\mathbf{X} - \mathbf{X}'||]E[||\mathbf{Y} - \mathbf{Y}'||] - 2E[||\mathbf{X} - \mathbf{X}'||||\mathbf{Y} - \mathbf{Y}''||]}$$
$$dVar[\mathbf{X}] = \sqrt{E[||\mathbf{X} - \mathbf{X}'||^2]E^2[||\mathbf{X} - \mathbf{X}'||] - 2E[||\mathbf{X} - \mathbf{X}'||||\mathbf{X} - \mathbf{X}''||]}$$
$$dVar[\mathbf{Y}] = \sqrt{E[||\mathbf{Y} - \mathbf{Y}'||^2]E^2[||\mathbf{Y} - \mathbf{Y}'||] - 2E[||\mathbf{Y} - \mathbf{Y}'||||\mathbf{Y} - \mathbf{Y}''||]}.$$

Where $(\mathbf{X}, \mathbf{Y})$, $(\mathbf{X}', \mathbf{Y}')$ and $(\mathbf{X}'', \mathbf{Y}'')$ are independent and identically distributed (iid) copies. The distance correlation is a square of the correlation between original and new variables (features). High distance correlation means new features recover well the old variables.

7.5.3 Q-local

Let be $d_{ij} = d(x_i, x_j)$ distance between x_i an x_j in original space and $\hat{d}_{ij} = d(y_i, y_j)$ the distance between y_i and y_j in the optimized feature space. Define

$$\hat{r}_{ij} = |\{k : \hat{d}_{ik} < \hat{d}_{ij} \text{ or } (\hat{d}_{ik} = \hat{d}_{ij} \text{ and } 1 \leq k < j \leq n)\}|, \tag{7.26}$$

as the rank of y_j with respect to y_i. For the original space, we will define an identical measure. Let be

$$r_{ij} = |\{k : d_{ik} < d_{ij} \text{ or } (d_{ik} = d_{ij} \text{ and } 1 \leq k < j \leq n)\}|, \tag{7.27}$$

the rank of x_j with respect to x_i. Now, we can define a $2-d$ histogram of ranks given by

$$q_{kl} = |\{(i, j) : \hat{r}_{ij} = k \text{ and } r_{ij} = l\}|, \tag{7.28}$$

This measure is an element of the normalized co-ranking matrix Q with a pre-identified $k-$th nearest neighbors in the original variables and optimized feature space, defined as

$$Q_{NX}(k) = \frac{1}{kn} \sum_{i=1}^{k} \sum_{i=1}^{k} q_{ij}. \tag{7.29}$$

Q-local measures the preserved local distance within observations between original and optimized spaces. This measure is defined by

$$Q_{local} = \frac{1}{k_{max}} \sum_{k=1}^{k_{max}} Q_{NX}(k), \tag{7.30}$$

Therefore, closer to 1 is more significant in feature optimization performance.

7.5.4 Q-global

Q-global measures how much the new feature space keeps the original's global distance, and it is defined as

$$Q_{global} = \frac{1}{n - k_{max}} \sum_{k=k_{max}}^{n-1} Q_{NX}(k), \tag{7.31}$$

Q-global interpretation is similar to Q-local in that being closer to 1 is more significant in feature optimization performance.

7.5.5 AUC_lnK_R_NX

To define the AUC_lnK_R_NX measure, initially, we should define the mean of $Q_{NX}(k)$ that give by

$$R_{NX}(k) = \frac{(n-1)Q_{NX}(k) - k}{n - 1 - k}, \tag{7.32}$$

Here, 0 and 1 orderly correspond to embedded values into the k-array neighborhood randomly and perfectly, respectively. Now defining a parameter-less measure is possible. Let be

$$AUC_{lnK}(R_{NX}(k)) = \frac{\sum_{k=1}^{n-2} R_{NX}(k)}{\sum_{k=1}^{n-2} \frac{1}{k}}, \tag{7.33}$$

Let be the area under the curve. Similar to the $R_{NX}(k)$ would be maximized when close to k at a log scale.

7.5.6 Cophenetic Correlation

Cophenetic correlation is a remarkable measure in comparison between two feature groups. The main idea is to compute the correlation between upper (or lower) triangles of the

distance matrices in the original and optimized feature space. The Cophenetic Correlation is given by

$$1 - r^2(D, \hat{D}) \tag{7.34}$$

where r is the Pearson correlation ,and D and $\hat{D}$ are the distance matrices consisting of elements d_{ij} and $\hat{d}_{ij}$, respectively. Less value represents better feature optimization performance.

7.6 Experiments

In this section, we presented the result of experiments that we established to metrically evaluate developed algorithms in CausalSpace Toolbox (CST) of Neurocognitive Computing (NcC). In these experiments, we used **DSet-1** as the training dataset in NcC-CST in MATLAB-version 2021 besides R-packages [***dimRed***: Framework for dimension reduction, V_0.2.5; and ***coRanKing***: Co-Ranking Matrix,V_0.2.3] in a R-Version of 4.1.3. We projected *experiment I* the optimized space with twenty-two causal features (NcC-CF1) and *experiment II* the optimized space with nine causal features (NcC-CF2) to test the performance besides the quality of the optimized feature space. We compared NcC-CFx optimized causal feature space with the eleven standards and accepted dimension reduction methods in the literature using six metrics for ranking, as depicted in Figure 29.
Dset-1 raw data, including 216 observations of 49 variables and OID, were used as the input of all the standard methods in R and NcC-CRT in MATLAB. We inserted NcC-CFx (CDF and PDF values separately for each causal feature) into the R package as an additional method for ranking with the six matrices. Therefore, we illustrated ranking graphs per matrices in each experiment for CDF and PDF side by side.

We employed linear and nonlinear methods for dimension reduction in the raw data of the *Dset-1*. We included Linear methods principal component analysis (PCA), Independent Component Analysis (FastICA), Locally Linear Embedding (LLE), and Non-Negative Matrix Factorization (NNMF). Along with Nonlinear methods, including Dimensionality Reduction via Regression (DRR),Fruchterman Reingold Graph Layout (Fruchterman Reingold), Laplacian Eigenmaps, Kernel Principal Component Analysis (kPCA), Non-Metric Dimensional Scaling (nMDS), and Distributed Recursive Graph Layout (DrL). For each method, we fitted the new space with the maximum number of features each method supports to get a reliable comparison.

Six matrices are considered for measuring and ranking the results of included methods within two metric groups. The first group is formed on the correlation between features from the original space and the embedded one, including distance correlation, total correlation, and cophenetic correlation. The second group is formed based on the distance methods that can be preserved in the embedded space from the original space, including Q-global, Q-local, and $AUC_{lnK}(R_{NX}(k))$. Experiment workflow was depicted in Figure 29 that represents the process we follow for comparison and fitting each method.

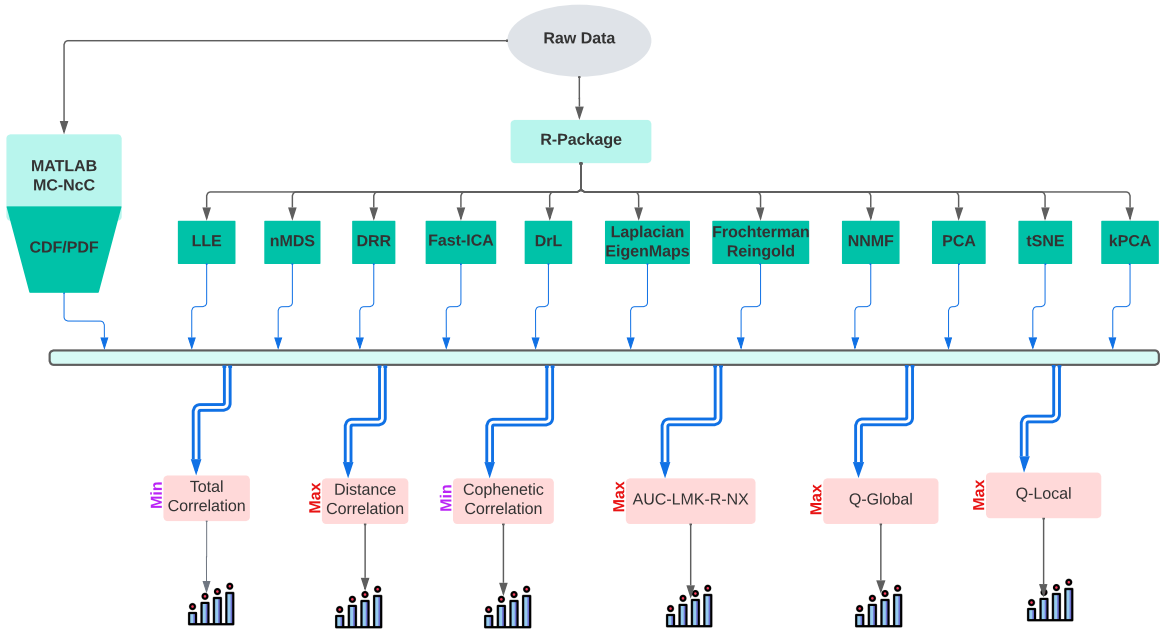

Figure 29 – Workflow of the experiment to evaluate the quality of Causal Feature Space compared to the standard Dimension Reduction methods in the literature.

7.6.0.1 Experiment I: DSet-1 Optimized with 22 Causal Features through NcC-CF

In this experiment, we used a data set called **DSet-1** which has 216 observations from 89 variables, one of them is ID. We conducted two trials; In the first one, we used the Causal Feature built by CDF values. The second is based on PDF. In both experiments, the new space has 22 optimized causal features.

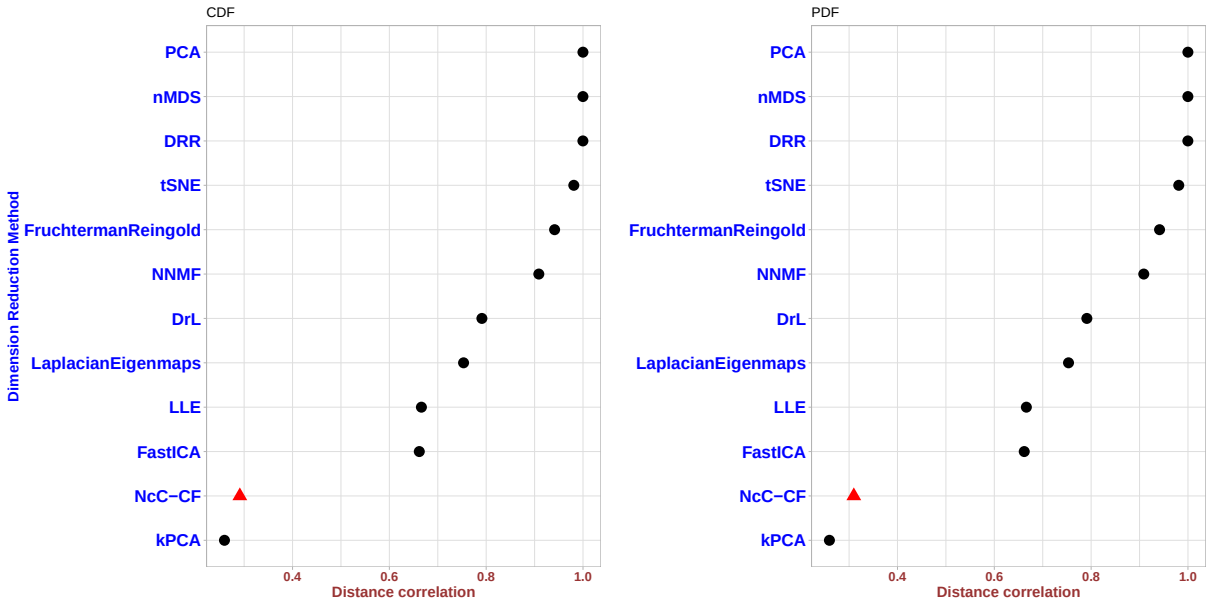

Figure 30 – Distance correlation for each Dimension reduction method used in experimental data set. NcC-CF is red point.

Distance correlation was computed for each applied method in the experiment of embedding (Feature optimization), except for NcC-CF and kPCA, all included feature optimization processes showed a distance correlation ratio greater than 0.6. The NcC-CF's distance correlation ratio was measured at nearly 0.4, as illustrated in Figure 30.
As noted in Equation 7.25, a maximized distance correlation ratio is desired to support the precise reconstruction of the original variables from the optimized features. Considering the NcC-CF algorithm, indeed, it cannot interpret as the NcC-CF's non-reliable performance in the initial variables reconstruction. In fact, NcC's causal feature optimization algorithm is grounded on the nonlinear relationship of original variables, entropy, so it does not fit well in the linear correlation comparison assessment between the original and the optimized feature spaces. Similar behavior is revealed on kPCA as another nonlinear method.

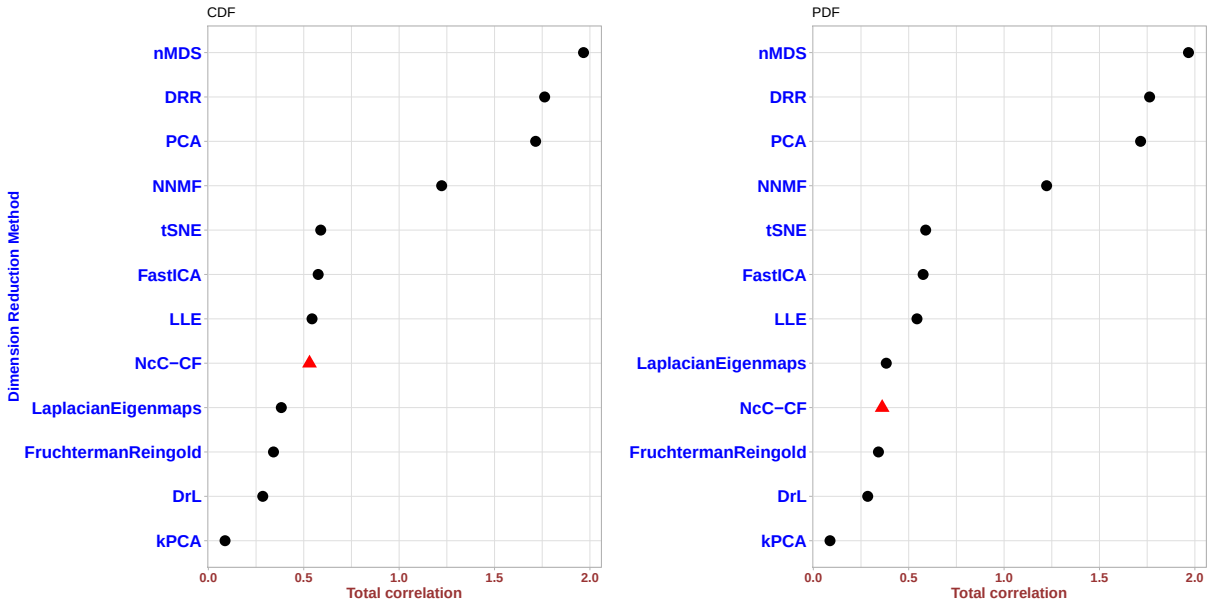

Figure 31 – Total correlation for each Dimension reduction method used in experimental data set. NcC-CF is red point.

The total correlation was computed for all applied methods in the *experiment I* of embedding (Feature optimization) and depicted in Figure 31. The NcC-CF total correlation value was 0.5, representing average performance but maximized total correlation is desired. Since the linear scale does not fit well for Nonlinear mechanisms, comparing the different methods with nonlinear approaches is impossible. We only can emphasize this measure was not designed for nonlinear algorithms.

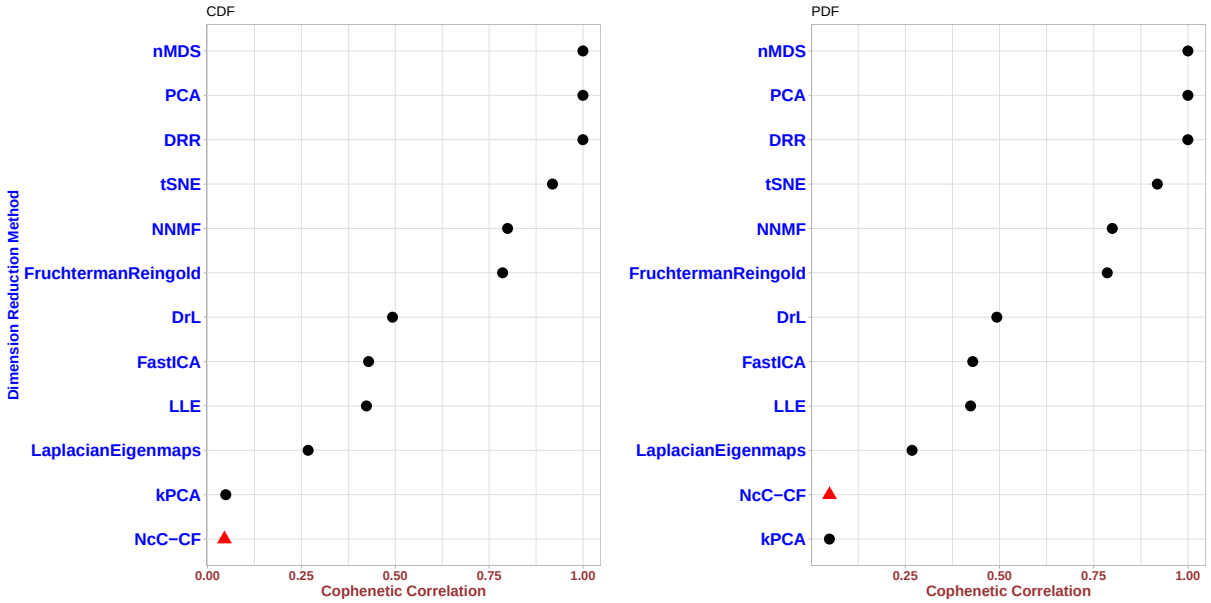

Figure 32 – Cophenetic correlation for each Dimension reduction method used in experimental data set. NcC-CF is red point.

Cophenetic correlations were computed for embedded spaces by each applied method. The Cophenetic correlation ratio assesses the correlation differences between observations in the original space and their transformed features in the new space as depicted in Figure 32. A minimum ratio is desired to support maximum similarity between original and embedded spaces. The NcC-CF displayed the maximum Cophenetic correlation ratio between all applied methods due to preserving entropy of the original space within the optimized feature space.

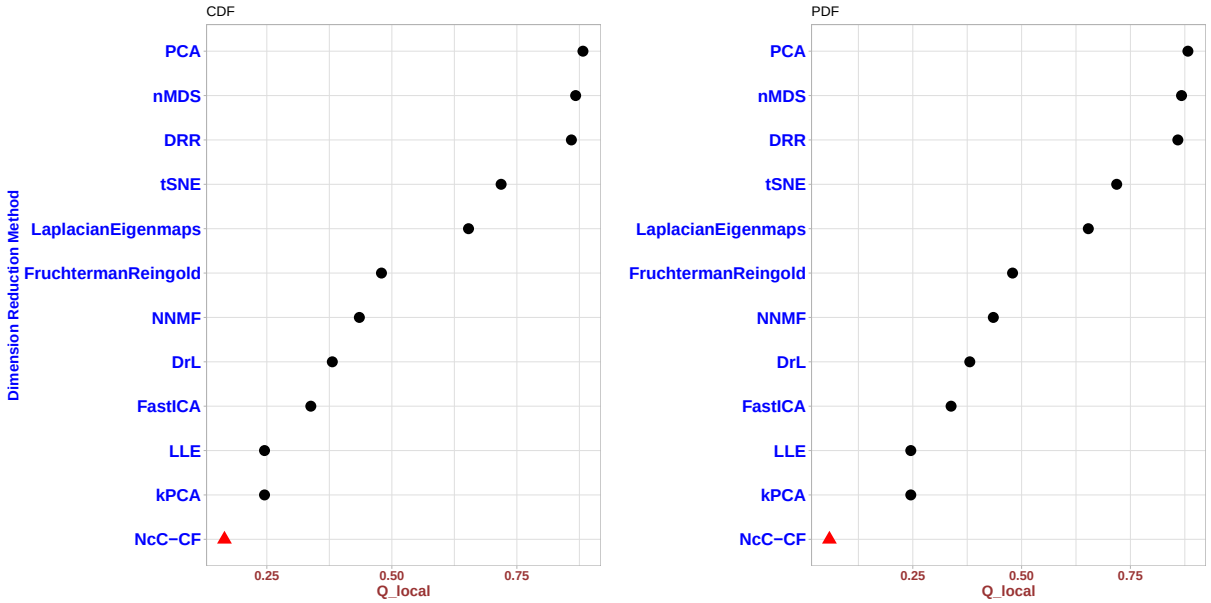

Figure 33 – Q-local for each Dimension reduction method used in experimental data set. NcC-CF is red point.

Q-local measures the linear preserved local distance from the original space compared

with the optimized one, as shown in Figure 33. Likewise, the insufficient performance of NcC-CF returns to its nonlinear characteristics.

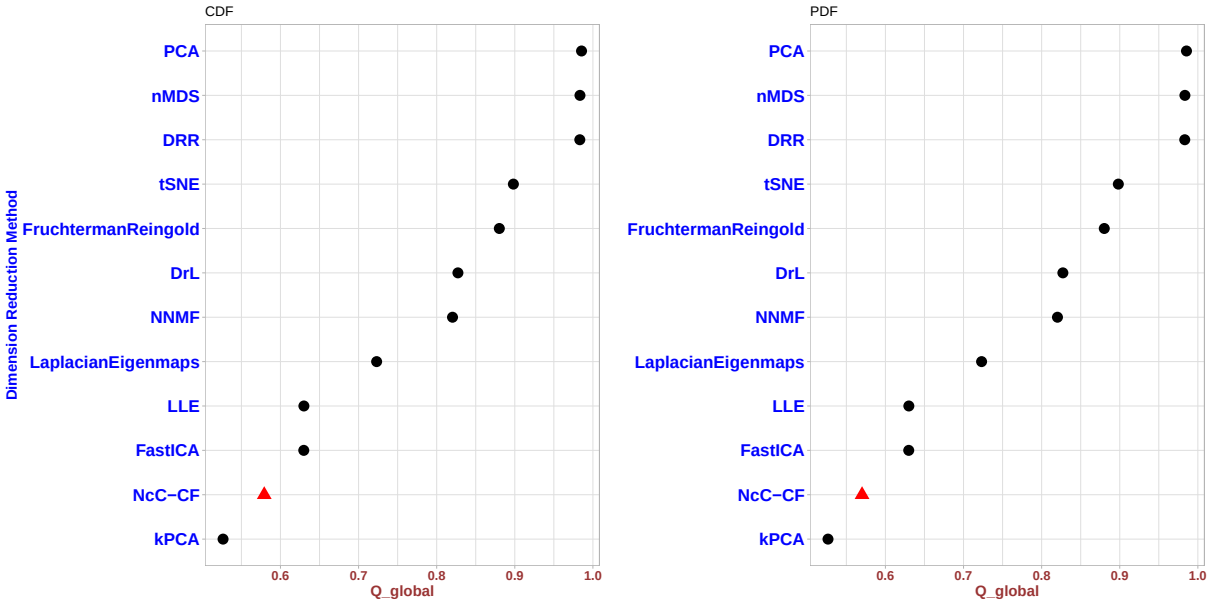

Figure 34 – Q-global for each Dimension reduction method used in experimental data set. NcC-CF is red point.

Q-global measures the linear preserved global distance from the original space compared with the optimized space. The Q-global value was calculated for each feature optimization method as shown in Figure 34. Similar to Q-local, NcC-CF showed poor performance in Q-global due to its algorithm's nonlinear characteristics.

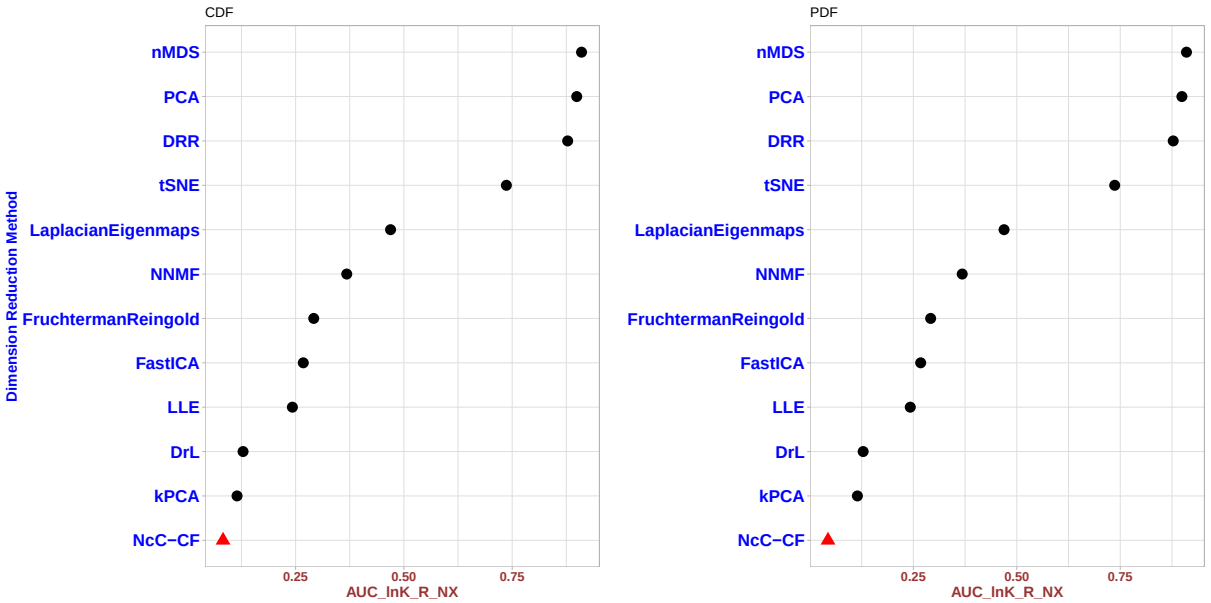

Figure 35 – AUC-lnK-R_NX for each Dimension reduction method used in experimental data set. NcC-CF is red point.

The AUC-lnK-R_NX value represents the linear relation between new features and original variables that are demonstrated for all applied methods and depicted in Figure 35. Like all linear assessments, NcC-CF showed poor performance due to its nonlinear algorithm characteristics based on entropy.

7.6.0.2 Experiment II: DSet-1 Optimized with 9 Causal Features through NcC-CF

In this experiment we used a data set called **DSet-1** which has 216 observation from 89 variables, one from them is ID. We consider two trials, the first one we used the Causal Feature built by CDF values. The second, based on PDF. In both experiments, the new space has 9 optimized causal features.

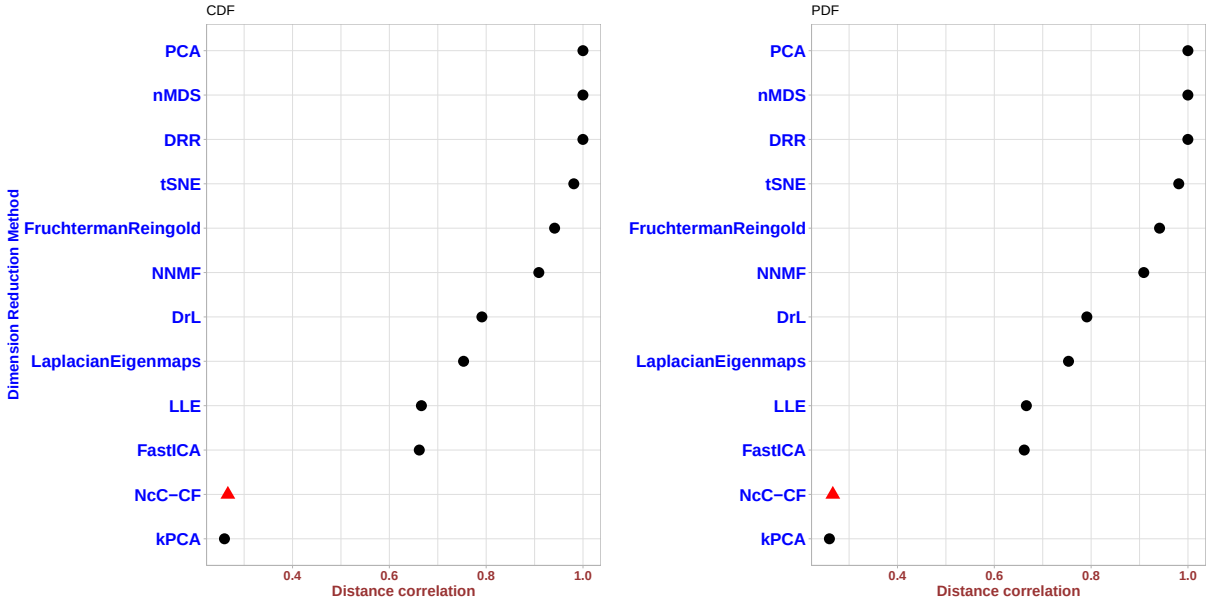

Figure 36 – Distance correlation for each Dimension reduction method used in experimental data set. NcC-CF is red point.

Distance correlation was computed for each applied method in the experiment of embedding (Feature optimization); except for NcC-CF and kPCA, all included feature optimization processes showed a distance correlation ratio greater than 0.6. The NcC-CF's distance correlation ratio was measured at nearly 0.4, as illustrated in Figure 36.

As noted in Equation 7.25, a maximized distance correlation ratio is desired to support the precise reconstruction of the original variables from the optimized features. Considering the NcC-CF algorithm, indeed, it cannot interpret as the NcC-CF's non-reliable performance in the initial variables reconstruction. In fact, NcC's causal feature optimization algorithm is grounded on the nonlinear relationship of original variables, entropy, so it does not fit well in the linear correlation comparison assessment between the original and the optimized feature spaces. In *experiment* II, compared with *experiment I*, the performance of NcC-CF was reduced due to

employing the more profound nonlinear algorithm to achieve better optimization in 9 features. Similar behavior is revealed on kPCA as another nonlinear method.

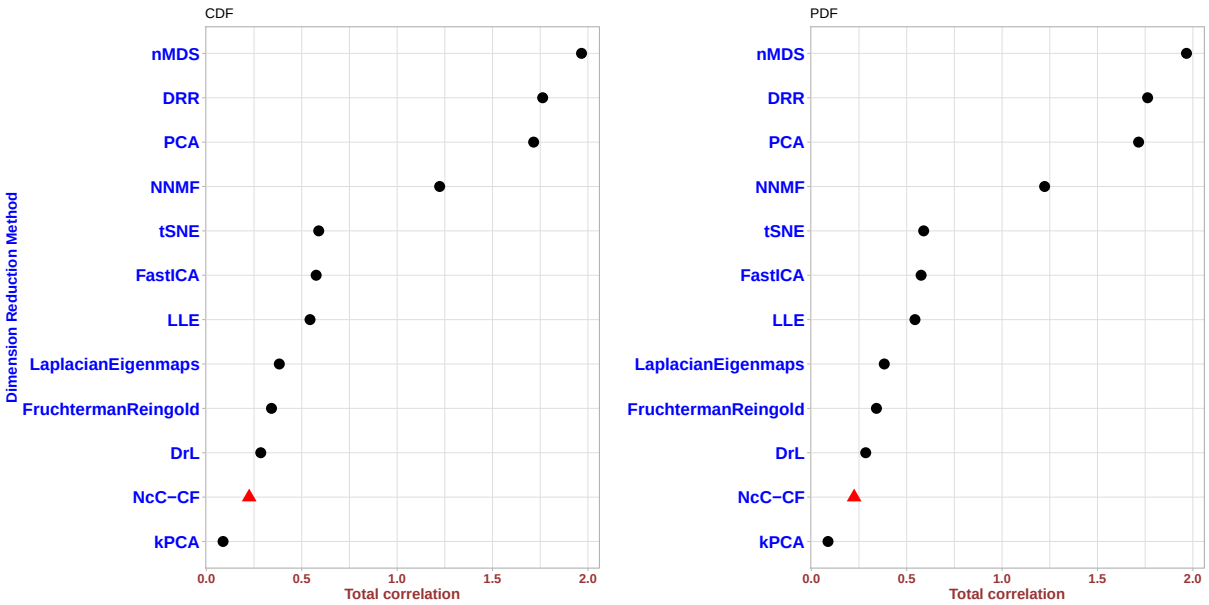

Figure 37 – Total correlation for each Dimension reduction method used in experimental data set. NcC-CF is red point.

The total correlation was computed for all applied methods in the *experiment II* of embedding (Feature optimization) and depicted in Figure 37. The NcC-CF total correlation value in *experiment II* was dramatically reduced compared with *experiment I*. In the same algorithm with different levels of non-linearity, the meaningful dropped value emphasizes that the total correlation is not a suitable measurement for nonlinear approaches. Still comparing the different methods with nonlinear approaches is impossible.

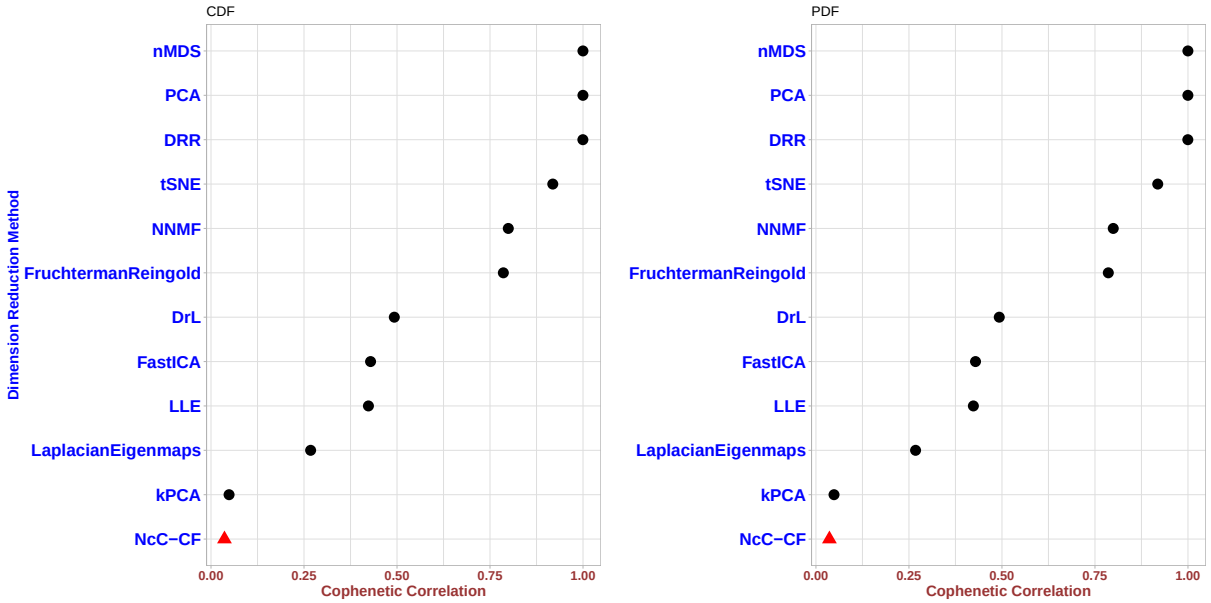

Figure 38 – Cophenetic correlation for each Dimension reduction method used in experimental data set. NcC-CF is red point.

Cophenetic correlations were computed for embedded spaces by each applied method. The Cophenetic correlation ratio assesses the correlation differences between observations in the original space and their transformed features in the new space as depicted in Figure 38. A minimum ratio is desired to support maximum similarity between original and embedded spaces. The NcC-CF displayed the maximum Cophenetic correlation ratio between all applied methods due to preserving entropy of the original space within the optimized feature space. In *experiment II*, Cophenetic correlation improved compared with *experiment I*, representing despite using a more profound non-linear algorithm, reducing Causal features improves the performance.

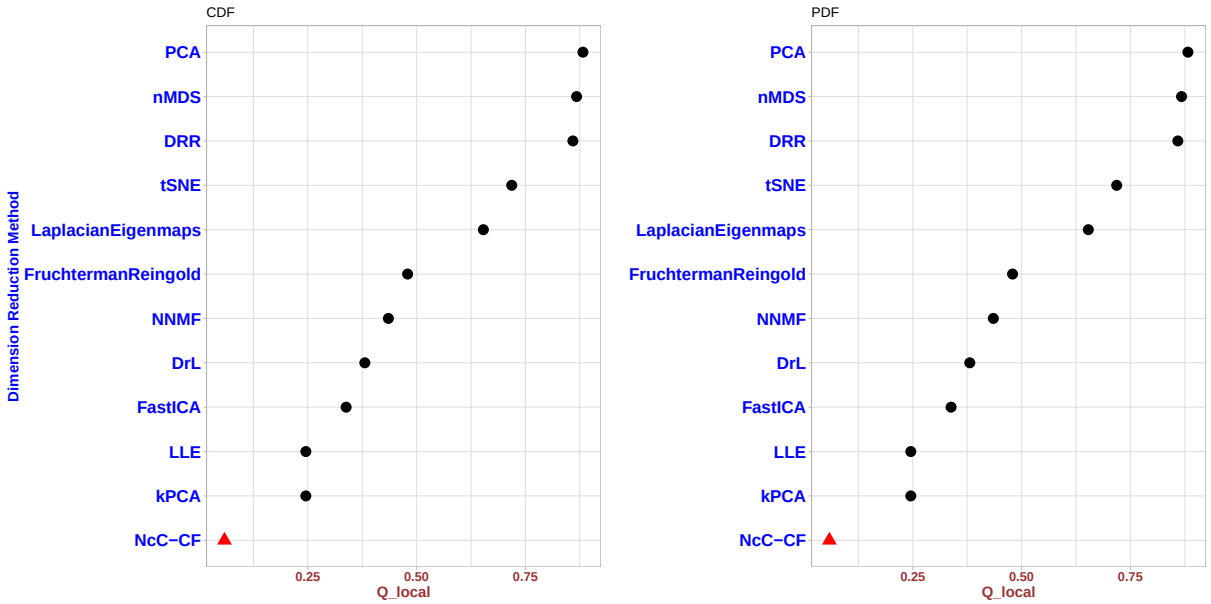

Figure 39 – Q-local for each Dimension reduction method used in experimental data set. NcC-CF is red point.

Q-local measures the linear preserved local distance from the original space compared with the optimized one, as shown in Figure 39. Likewise, the insufficient performance of NcC-CF returns to its nonlinear characteristics. In *experiment II*, Q-local does not change significantly compared with *experiment I*.

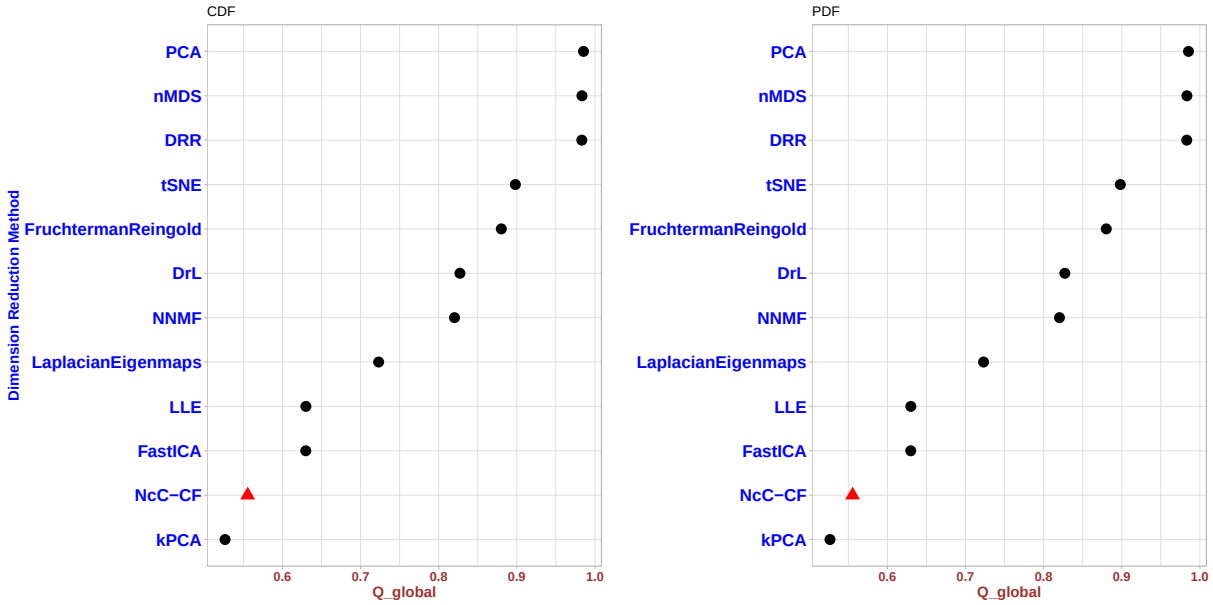

Figure 40 – Q-global for each Dimension reduction method used in the experimental data set. NcC-CF is shown with a red point.

Q-global measures the linear preserved global distance from the original space compared with the optimized space. The Q-global value was calculated for each feature optimization method as shown in Figure 40. Similar to Q-local, NcC-CF showed poor performance in Q-global due to its algorithm's nonlinear characteristics. In *experiment II*, Q-global does not change significantly compared with *experiment I*.

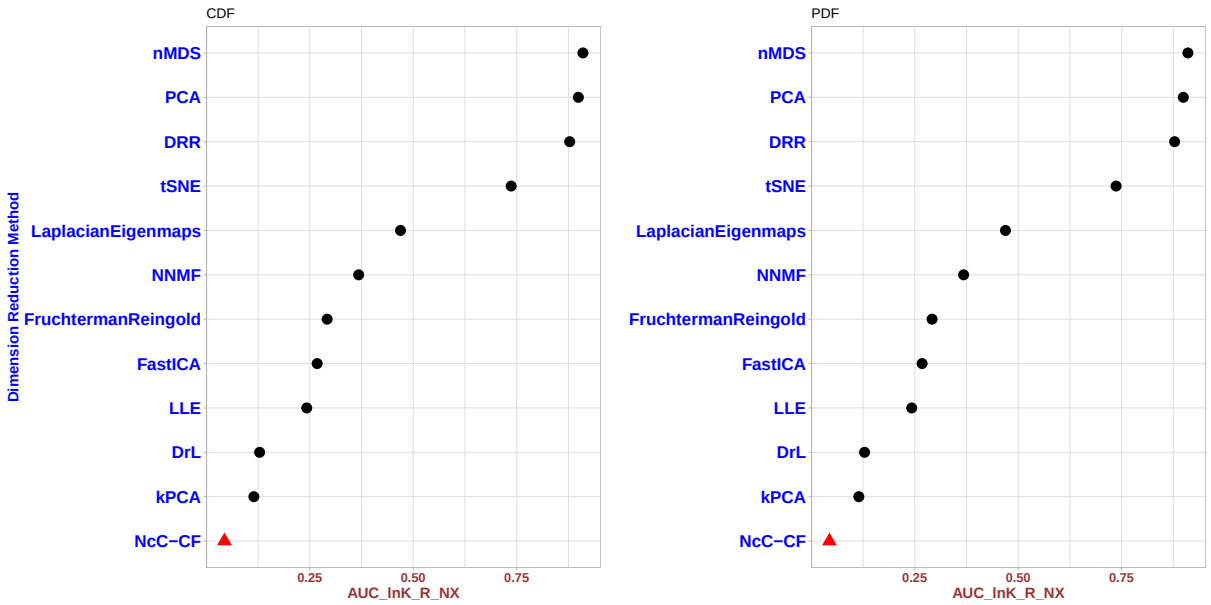

Figure 41 – AUC-lnK-R_NX for each Dimension reduction method used in the experimental data set. NcC-CF is shown with a red point.

The AUC-lnK-R_NX value represents the linear relation between new features and original variables that are demonstrated for all applied methods and depicted in Figure 41. Like all linear assessments, NcC-CF showed poor performance due to its nonlinear algorithm characteristics based on entropy. In *experiment II*, AUC-lnK-R_NX value does not change significantly compared with *experiment I*.

CHAPTER

8

CLUSTERING

8.1 Introduction

Clusters have been extensively used in machine learning applications. We re-conceptualized Clustering for Neurocognitive Computing (NcC) to support the cognitive-based decision and Deep Reinforcement Learning through data abstraction and segmentation. (JAIN, 2009; JAIN; DUBES, 1988; KAUFMAN; ROUSSEEUW, 2009). Clustering in Neurocognitive Computing supports:

- homogeneous sub-classes creation of data (or objects).
- complex features or abstract models creation for unknown features across unsupervised data discovery.
- users to recognize the natural grouping or similarities in a data set.

Therefore, cluster members are a set of similar observations but dissimilar from other clusters' members (LAROSE, 2015). NcC-Clustering incorporates method-driven, data-driven, and target-driven to establish data discovery, predictive analytics, and learning. The feature space optimization phase is a preprocessing stage to enhance the clustering performance by eliminating noisy variables, Feature Selection (FS), and reducing causal and dependent features, Feature Transformation (FT). In FS, original feature subsets are selected. In transformation, combinations of features can map to new features (JOLLIFFE, 2003)to optimize the feature space more effectively. Ghodratitoostani et al. (Chapter.7) developed hierarchical quantization and feature space optimization algorithms for the NcC platform. Based on NcC unsupervised data discovery in dimension reduction, we optimized feature space causally and made the initial point in the NcC-clustering methodology. Clustering generally has been utilized based on hierarchical distance (FRIEDMAN *et al.*, 2001), partitioning k-distance (JAIN, 2009), Similarity approaches

(GONG *et al.*, 2012). Clustering broadly performs on multivariate datasets for data segmentation and pattern discoveries. In this chapter, we demonstrated NcC-clustering method could improve conventional clustering with the new projected distance matrix. We also proposed a new unsupervised NcC-clustering methodology relying on the optimization process to minimize the average distance between the observations within the cluster. We designed and demonstrated an experiment to test and cross-validate the proposed NcC-clustering and improved methods with existing state-of-the-art clustering methods. The primary contributions of this chapter are as follows:

- We proposed a novel NcC unsupervised clustering based on the average distance approach.
- We postulated that the Normalized Mutual Information (NcC_NMI)distance matrix improves the conventional clustering.
- We developed generalized a distance matrix to evaluate the similarity between one observation and clusters.
- We developed a new method to calculate patterns of the clusters.

The remainder of this paper is organized as follows. Section 2 reviews the evolution of clustering methods. Section 3 demonstrates the NcC Clustering method. In Section 4, various experimental results are analyzed. Conclusions are drawn in Section 5.

8.2 Related works

Clustering approaches apply the dissimilarities or the distance between observations when creating the clusters. This distance can compute on a single dimension or multiple dimensions. The general way of computing distance between observations in a multidimensional space is to perform Euclidean distance. If x_i and y_i are the two points, the distance between them:

- **Euclidean distance;** It is merely the geometric distance in the multidimensional space. It computes as:

$$\text{Euclidean distance} = d_{Eu}(x,y) = \sqrt{\sum_{i=1}^{N}(x_i - y_i)^2} \tag{8.1}$$

- **Squared Euclidean distance;** To square the standard Euclidean distance to set progressively greater weight on objectives that are further apart. The distance computes as:

$$distance(x,y) = \sum_{i=1}^{N}(x_i - y_i)^2$$

- **City-block (Manhattan) distance;** The average difference across dimensions. Usually, this distance measure yield results similar to the simple Euclidean distance. The city block distance computes as:

$$distance(x,y) = \sum_{i=1}^{N} |x_i - y_i|$$

- **Chebychev distance;** distance is defined in a vector space as the greatest of their differences along with any coordinate dimension of two observations. distance computes as:

$$distance(x,y) = max(|x_i - y_i|)$$

- **Power distance;** when the progressive weight requires to decrease or increase, which is located on dimensions where the corresponding weights are different. This is achieved by power distance. The distance computes as:

$$distance(x,y) = \left(\sum_{i=1}^{N} |x_i - y_i|^p\right)^{\frac{1}{r}}$$

where r and p relation requires to define. If the values for dimensions applied in the analysis are categorical in nature, this type of measure is suitable. The significant advantage of clustering to classification is the flexibility to change and help single out valuable features that characterize different groups.

8.2.1 NcC_distance

In this section, we describe a new distance called NcC_Distance. This metric use Mutual information distance, given by:

$$d_1(O_i, O_j) = \sum_{f=1}^{d} \frac{H(O_{i_f}, O_{j_f}) - MI(O_{i_f}, O_{j_f})}{H(O_{i_f}, O_{j_f})}, \tag{8.2}$$

and a new metric that computes distance in each quanta, defined as

$$d_2(O_i, O_j) = \begin{cases} \frac{1}{d}\sum_{f=1}^{d} \left| \left(F(O_{i_f}^-) + \frac{p_H(O_{i_f})}{2}\right) - \left(F(O_{j_f}^-) + \frac{p_H(O_{j_f})}{2}\right) \right|, \text{ if } MI(O_{i_f}, O_{j_f}) = 0, \\ \qquad \text{for all } f = 1, \ldots, d. \\ 0, \text{ if } MI(O_{i_f}, O_{j_f}) \neq 0, \end{cases} \tag{8.3}$$

where d is dimension of observation space, $F(O_{i_f}^-)$ and $F(O_{j_f}^-)$ is CDF lower bound for O_{i_f} and O_{j_f}. The quantities $p_H(O_{i_f})$ and $p_H(O_{i_f})$ are heuristic PDF for O_{i_f} and O_{j_f}. NcC_Distance is computable only when mutual information between observations be zero, $MI(O_{i_f}, O_{j_f}) = 0$ implies that $d_2(O_i, O_j)$ is a psudo-distance, but total distance meets all criteria of distance. This result is present in Proposition 1.

Proposition 1. The metric $d_2(\cdot,\cdot)$ defined in (8.3) is a pseudo-distance.

Proof. Three conditions need to be checked for any new distance matrix :

- For all $O_i \in \mathscr{O}$, $d_2(O_i, O_i) = 0$
- For $O_i, O_j \in \mathscr{O}$, $d_2(O_i, O_j) = d_2(O_j, O_i)$
- For $O_i, O_j, O_k \in \mathscr{O}$, $d_2(O_i, O_j) \leq d_2(O_i, O_k) + d_2(O_k, O_j)$.

Note that $MI(O_i, O_i) \neq 0$ so

$$d_2(O_i, O_i) = 0,$$

and the first condition is verified.

For next condition, we assume that $MI(O_i, O_j) = 0$, so we have

$$\begin{aligned} d_2(O_i, O_j) &= \frac{1}{d}\sum_{f=1}^{d}\left|\left(F(O_i^-) + \frac{p_H(O_i)}{2}\right) - \left(F(O_j^-) + \frac{p_H(O_j)}{2}\right)\right| \\ &= \frac{1}{d}\sum_{f=1}^{d}\left|(-1)\left[\left(F(O_j^-) + \frac{p_H(O_j)}{2}\right) - \left(F(O_i^-) + \frac{p_H(O_i)}{2}\right)\right]\right| \\ &= \frac{1}{d}\sum_{f=1}^{d}\left|\left(F(O_j^-) + \frac{p_H(O_j)}{2}\right) - \left(F(O_i^-) + \frac{p_H(O_i)}{2}\right)\right| \\ &= d_2(O_j, O_i). \end{aligned}$$

Let be $O_i, O_j, O_k \in \mathscr{O}$ with

$$\begin{aligned} MI(O_i, O_j) &\neq 0, \\ MI(O_i, O_k) &\neq 0, \\ MI(O_k, O_j) &\neq 0. \end{aligned} \tag{8.4}$$

So, under assumptions (8.4) we have

$$\begin{aligned} d_2(O_i, O_j) &= \frac{1}{d}\sum_{f=1}^{d}\left|\left(F(O_i^-) + \frac{p_H(O_i)}{2}\right) - \left(F(O_j^-) + \frac{p_H(O_j)}{2}\right)\right| \\ &= \frac{1}{d}\sum_{f=1}^{d}\left|\left(F(O_i^-) + \frac{p_H(O_i)}{2}\right) - \left(F(O_k^-) + \frac{p_H(O_k)}{2}\right) + \right. \\ &\quad \left. + \left(F(O_k^-) + \frac{p_H(O_k)}{2}\right) - \left(F(O_j^-) + \frac{p_H(O_j)}{2}\right)\right| \\ &\leq \frac{1}{d}\sum_{f=1}^{d}\left|\left(F(O_i^-) + \frac{p_H(O_i)}{2}\right) - \left(F(O_k^-) + \frac{p_H(O_k)}{2}\right)\right| + \\ &\quad + \frac{1}{d}\sum_{f=1}^{d}\left|\left(F(O_k^-) + \frac{p_H(O_k)}{2}\right) - \left(F(O_j^-) + \frac{p_H(O_j)}{2}\right)\right| \\ &= d_2(O_i, O_k) + d_2(O_k, O_j). \end{aligned}$$

□

With the distance $d_1(\cdot,\cdot)$ and $d_2(\cdot,\cdot)$ well defined, now we present the definition of NcC_Distance.

Definition 1. Let be $O_i, O_j \in \mathscr{O}$. The NcC_Distance from O_i to O_j is given by

$$d(O_i, O_j) = d_1(O_i, O_j) + d_2(O_i, O_j). \tag{8.5}$$

As a result from Definition (1) we have the Corollary (1)

Corollary 1. NcC_distance is a pseudo-distance.

Proof. Follow from Proposition (1) that $d_2(\cdot,\cdot)$ is pseudo-metric. So $d(\cdot,\cdot)$ is pseudo-metric because it is a sum of metric with a pseudo-metric. □

8.2.1.1 NcC_distance from one observation to cluster pattern

Let be $\mathscr{C}$ a cluster pattern with M cluster-members $O(m)$. Now we define a distance from one observation O_i to cluster pattern $\mathscr{C}$. We use the definition of distance present in (8.2) to present a distance that computes the amount of Mutual Information from one observation to cluster members given by

$$D_1(O_i, \mathscr{C}) = \sum_{f=1}^{d} \sum_{m=1}^{M} \left(\frac{H(O_{i_f}, O_f(m)) - MI(O_{i_f}, O_f(m))}{H(O_{i_f}, O_f(m))} \right). \tag{8.6}$$

Now we define a distance analogous to (8.3) for an observation O_i and cluster pattern $\mathscr{C}$

$$D_2(O_i, \mathscr{C}) = \frac{1}{d} \sum_{f=1}^{d} \frac{1}{M} \sum_{m=1}^{M} \left[\left(F(O_{i_f}^{-}) + \frac{p_H(O_{i_f})}{2} \right) - \left(F(O_f^{-}(m)) + \frac{p_H(O_f(m))}{2} \right) \right], \tag{8.7}$$

as average quanta distance from observation O_i to each cluster member $O(m)$ in cluster pattern $\mathscr{C}$. Now we present a definition that combine both concept in (8.6) and (8.7) called NcC_distance from one observation to a cluster pattern

$$D(O_i, \mathscr{C}) = D_1(O_i, \mathscr{C}) + D_2(O_i, \mathscr{C}). \tag{8.8}$$

8.2.2 Partitioning methods

Partitioning is often desirable because of its simplicity of implementation and ease of understanding. Corresponding algorithms divide data into several clusters in one shot, typically using exclusive landmarks. In each iteration, observations are associated with their closest landmark, and then landmarks are readjusted based on the associated observations to the cluster. Standard methods for partitioning are PAM, K-Means [46], K-Median, and K-Medoid. K-Means

is used to make k clusters within n observations wherein each observation assigns the cluster with the closest mean. Given a set of observations $(x_1, x_2, \cdots, x_n)$, where each d-dimension place into k ($k \leq n$) sets $s_1, s_2, \cdot, s_k$ minimizing the within-cluster sum of squares:

$$\arg\min_{\mathbf{S}} \sum_{i=1}^{k} \sum_{\mathbf{x} \in S_i} \|\mathbf{x} - \mu_i\|^2 = \arg\min_{\mathbf{S}} \sum_{i=1}^{k} |S_i| \operatorname{Var} S_i \tag{8.9}$$

where μ_i is mean of observations (Centroid) in s_i. However, CLARA uses bootstrap sampling to speed up the algorithms of clustering.

8.2.3 Hierarchical Clustering

Hierarchical clustering (HC)represents the clusters hierarchically in a dendogram with varying granularity levels (FRIEDMAN *et al.*, 2001). HC representation is independent of the developing method, either agglomerative or divisive.

- Agglomerative is a bottom-up strategy that assigns cluster to individual observations at the beginning and successively merge clusters to build a tree-like structure. Merging strategies play a crucial role in forming the tree, such as all-linkage and centroid-linkage clustering (FRIEDMAN *et al.*, 2001). In all-pairs linkage, the average overall pairs are used,

  $$\textbf{Unweighted average linkage clustering} = \frac{1}{|A| \, . \, |B|} \sum_{a \in A} \sum_{b \in B} d_{Eu}(a, b)$$

  whereas, in centroid-linkage, the distance between the centroids is used.

  $$\textbf{Centroid linkage clustering} = \left\| c_i - c_j \right\|$$

  where c_i and c_j are the centroids of clusters i and j, respectively.

- Divisive is a top-down strategy that divides observations successively into a tree-like structure. Any partitioning algorithm, like DIANA, can be employed to perform subdivisions at each step. Divisive partitioning allows greater flexibility regarding the tree's hierarchical structure and the balance level in the different clusters. However, this method is out of the scope of this paper (FRIEDMAN *et al.*, 2001). Advantages of the Hierarchical clustering method are the adaptable difficulty of similarity and distance flexibility regarding granularity (highly detailed) independent from the data type. Dopazo et al.(1997) proposed the Self-Organized Tree Algorithm (SOTA) as an unsupervised network clustering with a divisive hierarchical binary tree structure. SOTA is generally used in microarray gene expression data (HERRERO; VALENCIA; DOPAZO, 2001).

8.2.4 SOM

SOM is a standard algorithm in unsupervised Machine Learning based on a neural network. It perfectly can map and visualize high-dimensional data in two dimensions.

8.2.5 FANNY

The FANNY algorithm initiates with the fuzzy membership of observations into clusters; consequently, observations place in the clusters with the maximum weighted values. FANNY stands for Fuzzy Clustering Analysis.

8.2.6 Model-Based Clustering

Model-Based clustering is a statistical algorithm that fits a finite Gaussian mixture model to the data. In this method, mixture components represent clusters that estimate group membership using the expectation-maximization algorithm.

8.3 NcC Clustering Algorithm

In this section, we explored the Neurocognitive Computing algorithms and the developed NcC_Clustering toolbox in MATLAB for unsupervised Clustering. NcC_Clustering relies on information theory to create the NcC distance matrix, neighboring algorithm, cluster pattern, and stepwise greedy optimization. We initially calculate the NcC_Distance matrix between observations to recognize the Medoid and place it on the sorted dataset. In other words, Medoid is the observation with the minimum average distance to others. After Medoid discovery, due to sorting other observations as potential members of the new cluster, iteratively reordering the rest of the observations to find the observation with the minimum cumulative distance to previous ones. The process continues to find the last observation in order. By sorting all observations, NcC_Neighboring algorithms consider the preservation of the maximum entropy in each dimension, discover the border of Neighbor (the number of potential observations in one cluster), and shape the neighbor dataset. The neighbor dataset under the greedy algorithm will inspect and optimize the combination of observations to create the cluster with maximum entropy and similarity. Consequently, cluster members (observations) were eliminated from the dataset, and the process was repeated iteratively to finalize the clustering process and all observations. Within the greedy algorithm, the cluster pattern is calculated and embedded as meta information into cluster characteristics based on the range of observed probability density in each dimension. Before describing each step of NcC-Clustering, we need to set some definitions used in the next subsections. First of all, we describe the notation used for observation and feature. Let be $\mathscr{X} = \mathfrak{R}^d$ the feature-space. Each observation in data-set $\mathbf{O}_i$, for $i = 1, \ldots, n$, will be represented as a point in feature-space, so we have $\mathbf{O}_i \in \mathfrak{R}^d$, it means

$$\mathbf{O}_i = (x_1, \ldots, x_d),$$

we denoted all observations in the dataset by

$$\mathscr{O} = \{\mathbf{O}_1, \mathbf{O}_2, \ldots, \mathbf{O}_n\},$$

All observations before being included in a cluster are so-called unprocessed datasets.

$$\mathscr{U} = \{\mathbf{O}_i \in \mathscr{O} \mid \mathscr{O}_i \notin C_k, \text{ for all } k\}.$$

8.3.1 Step1: Compute the Distance Matrix

Starting with $\mathscr{O} = \{\mathbf{O}_1, \mathbf{O}_2, \ldots, \mathbf{O}_n\}$ we compute the distance matrix between all observation

$$a_{ij} = d(\mathbf{O}_i, \mathbf{O}_j),$$

where $d(\cdot,\cdot)$ is a NcC_distance given by

$$d(\mathbf{O}_i, \mathbf{O}_j) = d_1(\mathbf{O}_i, \mathbf{O}_j) + d_2(\mathbf{O}_i, \mathbf{O}_j).$$

NcC_Distance measures the distance between observations that use in the unsupervised clustering process. Two similar observations are very close to each other with a high value of Mutual Information, which results in a small distance. On the other hand, a considerable distance between two observations means low mutual information. The NcC_Distance supports the equivalent class between observations with small distances.

8.3.2 Step 2: Medoid Recognition based on the NcC_distance

To discover potential members of a cluster C_k, first, the global Medoid in the unprocessed dataset is needed to be determined, given by

$$\mathfrak{M}^{(k)} = \arg\min_{\mathbf{O}_j \in \mathscr{O}} \sum_{\{\mathbf{O}_i \in \mathscr{U} : \mathbf{O}_i \neq \mathbf{O}_j\}} d(\mathbf{O}_i, \mathbf{O}_j),$$

where $n_k = |\mathscr{U}|$ is number of observation in the unprocessed data. The Medoid $\mathfrak{M}^{(k)}$ is a reference point of the kth cluster.

8.3.3 Step 3: Sorting data

At this step NcC_Clustering algorithm orders all observations in unprocessed data $\mathscr{U}$ based on the average distance from the medoid and previously sorted data. For $i = 1$ we have

$$\mathbf{O}_{S_1^{(k)}} = \arg\min_{\mathbf{O}_i \in \mathscr{U}/\{\mathfrak{M}^{(k)}\}} \{d(\mathfrak{M}^{(k)}, \mathbf{O}_i)\},$$

for $2 \leq i \leq n_k$ we do

$$\mathbf{O}_{S_i^{(k)}} = \arg\min_{\mathbf{O}_i \in \mathscr{U}/\mathscr{S}} \left\{ \sum_{\mathbf{O}_j \in \mathscr{S}} d(\mathbf{O}_i, \mathbf{O}_i) \right\},$$

where $\mathscr{S} = \{\mathfrak{M}^{(k)}, \mathbf{O}_{S_1^{(k)}}, \ldots, \mathbf{O}_{S_{i-1}^{(k)}}\}$ is sorted data up to $i-$th observation. The kth reordered dataset based on NcC_Distance supports the similarity of the unprocessed data.

8.3.4 Step 4: Neighborhood's size

By global medoid $\mathfrak{M}^{(k)}$ discovery, NcC_Neighboring algorithm selects the optimum number of potential members of the kth cluster. First, let be $p_{Optimal}$ the probability which maximizes the entropy

$$p_{Optimal} = \arg\max_{p} H[\log p].$$

NcC defines the optimum number of neighbors for $\mathfrak{M}^{(k)}$ as a solution to the following optimization problem

$$n^{(k)} = \arg \max_{n \in \{1,\ldots,n_k\}} \sum_{i=1}^{n} p(O_{S_i^{(k)}})$$

subject to

$$\sum_{i=1}^{n} p(O_{S_i^{(k)}}) \leq p_{Optimal}. \tag{8.10}$$

8.3.5 Step 5: Neighboring sorting

Let be $\mathscr{N}^{(k)} = \{\mathfrak{M}^{(k)}, \mathbf{O}_{S_1^{(k)}}, \mathbf{O}_{S_2^{(k)}}, \ldots, \mathbf{O}_{S_{n^{(k)}}^{(k)}}\}$ the neighboring of medoid $\mathfrak{M}^{(k)}$. Now we sort again the members of $\mathscr{N}^{(k)}$ Neighbor Dataset to define a local medoid for the neighborhood.

$$\mathscr{M}^{(k)} = \arg \min_{\mathbf{O}_j \in \mathscr{N}^{(k)}} \sum_{\{\mathbf{O}_i \in \mathscr{N}^{(k)} : \mathbf{O}_i \neq \mathbf{O}_j\}} d(\mathbf{O}_i, \mathbf{O}_j),$$

Then, similar to step. 8.3.3 neighboring members $\mathscr{N}^{(k)}$ are being reordered.

$$\mathbf{O}_1^{(k)} = \arg \min_{\mathbf{O}_i \in \mathscr{N}^{(k)} / \{\mathfrak{M}^{(k)}\}} \{d(\mathfrak{M}^{(k)}, \mathbf{O}_i)\},$$

for $2 \leq i \leq n^{(k)}$ we do

$$\mathbf{O}_i^{(k)} = \arg \min_{\mathbf{O}_i \in \mathscr{N}^{(k)} / \mathscr{S}^{(k)}} \left\{ \sum_{\mathbf{O}_j \in \mathscr{S}^{(k)}} d(\mathbf{O}_i, \mathbf{O}_i) \right\},$$

where $\mathscr{S}^{(k)} = \{\mathscr{M}^{(k)}, \mathbf{O}_1^{(k)}, \ldots, \mathbf{O}_{i-1}^{(k)}\}$ is the first i sorted observations.

8.3.6 Step 6: Forward method

Let be $\mathscr{O}$ the $d-$dimensional space of observations. We define a parameter that controls the admissibility of a new member in cluster C_k given by

$$\alpha = 0.25 \times (d+1).$$

We start the greedy algorithm, set $\mathscr{F}$ as initial cluster with $\mathscr{M}^{(k)}$ and $\mathbf{O}_1^{(k)}$. For each $i \in \{2,3,\ldots,n^{(k)}\}$, we include $\mathbf{O}_i^{(k)}$ into cluster $\mathscr{F}$, if

$$d(\mathbf{O}_i^{(k)},\mathscr{F}) \leq \alpha + \max_{\mathbf{O}_p^{(k)},\mathbf{O}_p^{(k)} \in \mathscr{F}} \{d(\mathbf{O}_p^{(k)},\mathbf{O}_p^{(k)})\},$$

And go to Backward step in 8.3.7.

Otherwise, remove $\mathbf{O}_i^{(k)}$ from neighboring set $\mathscr{N}^{(k)}$ to unprocessed data $\mathscr{U}$, and go to the next sorted neighbor set member $\mathbf{O}_{i+1}^{(k)}$.

8.3.7 Step 7: Backward method

In this step, the NcC algorithm relying upon the leave-one-out process evaluates the complete cluster quality by adding a new observation $\mathbf{O}_i^{(k)}$ with any combination of the cluster members with one observation less. Let be

$$\beta = 0.15 \times (d+1),$$

where $d = dim(\mathscr{O})$, dimension of observation space. NcC_Clustering algorithm uses a leave-one-out process

$$C_{-l} = \{\mathscr{M}^{(k)},\mathbf{O}_1^{(k)},\mathbf{O}_2^{(k)},\ldots,\mathbf{O}_{l-1}^{(k)},\mathbf{O}_{l+1}^{(k)},\ldots,\mathbf{O}_i^{(k)}\},$$

for $1 \leq l \leq i$, and $C_{-0} = \{\mathbf{O}_1^{(k)},\mathbf{O}_2^{(k)},\ldots,\mathbf{O}_i^{(k)}\}$. In this process, $\mathbf{O}_{-l}$ indicates which observation was eliminated from the cluster members.

If

$$D(\mathbf{O}_i^{(k)},C_{-i}) \geq \max_{l \in \{0,1,\ldots,i\}} \{D(\mathbf{O}_{(k)},C_{-l})\}$$

and

$$d(\mathbf{O}_{-l},\mathbf{O}_i^{(k)}) > \beta + D(\mathbf{O}_i^{(k)},C_{-i}),$$

remove O_{-l} from cluster member $\mathscr{F}$ and go back to Forward step in 8.3.6.

8.3.8 Step 8: Cluster finalization

Let be $\mathscr{F}$ a set with observations after Forward-Backward steps. Define $C_k = \mathscr{F}$ and go to Step 8.3.2 for the next cluster and repeat the process until the last observation in unprocessed data will be included in a cluster.

8.3.9 Algorithm

Algorithm 2 NcC_clustering Algorithm

while $\mathscr{U} \neq \emptyset$ **do**
- Medoid Selection: $\mathfrak{M}^{(k)} = \arg\min_{\mathbf{O}_j \in \mathscr{O}} \sum_{\{\mathbf{O}_i \in \mathscr{U}: \mathbf{O}_i \neq \mathbf{O}_j\}} d(\mathbf{O}_i, \mathbf{O}_j)$
- Sorting unclustered observations from Medoid $\mathfrak{M}^{(k)}$
- Determine neighborhood's size: $n^{(k)}$
- Sorting Neighborhood $\mathscr{N}^{(k)}$
- **while** $\mathscr{N}^{(k)} / [O_{S_1^{(k)}}, O_{S_2^{(k)}}, \ldots, O_{S_j^{(k)}}] \neq \emptyset$ **do**
  - **if** $d(\mathbf{O}_i^{(k)}, \mathscr{F}) \leq + \max_{\mathbf{O}_p^{(k)}, \mathbf{O}_p^{(k)} \in \mathscr{F}} \{d(\mathbf{O}_p^{(k)}, \mathbf{O}_p^{(k)})\}$ **then**
    - **if** $D(\mathbf{O}_i^{(k)}, C_{-i}) \geq \max_{l \in \{0,1,\ldots,i\}} \{D(\mathbf{O}_{(k)}, C_{-l})\} \wedge d(\mathbf{O}_{-l}, \mathbf{O}_i^{(k)}) > \beta + D(\mathbf{O}_i^{(k)}, C_{-i})$ **then**
      - Remove O_{-l} from cluster member $\mathscr{F}$ and go back to Forward step in 8.3.6.
    - **else**
      - Keep $\mathscr{F}$ and go to the next neighbor
  - **else**
    - move $\mathbf{O}_i^{(k)}$ from neighboring $\mathscr{N}^{(k)}$ to unclustered data $\mathscr{U}$, and go to the next sorted neighbor $\mathbf{O}_{i+1}^{(k)}$
- Define $C_k = \mathscr{F}$ and go to Step Medoid Selection for the next cluster.

8.4 Metrics for Evaluation Quality of Clustering

8.4.1 Internal Measure

8.4.1.1 Connectivity

Let be N the number of observations and D the number of causal features in a dataset. Assume that each dimension (columns) is numeric. Denote $nn_{i(j)}$ as a jth nearest neighbor of observation i, and define

$$x_{i,nn_{i(j)}} = \begin{cases} 0, & \text{if } i \text{ and } j \text{ are in the same cluster} \\ \frac{1}{j}, & \text{otherwis.} \end{cases}$$

Then, given a particular clustering partition $\mathscr{C} = \{C_1, \ldots, C_K\}$ of the N observation into K disjoint clusters, the connectivity is defined by

$$Conn(\mathscr{C}) = \sum_{i=1}^{N} \sum_{j=1}^{L} x_{i,nn_{i(j)}},$$

Where L controls the number of nearest neighbors to use, the range of connectivity is from 0 to ∞, and the minimized value is desired.

8.4.1.2 Silhouette width

Let be a_i given by

$$a_i = \frac{1}{n(C(i))} \sum_{j \in C(i)} dist(i,j),$$

The average distance between i and all other observations in the same cluster. Let be b_i defined as

$$b_i = \min_{C_k \in \mathscr{C}\ C(i)} \sum_{j \in C_k} \frac{dist(i,j)}{n(C_k)},$$

The average distance between i and the observations in the "nearest neighboring cluster". Then, the Silhouette width is defined by

$$S(i) = \frac{b_i - a_i}{\max\{b_i, a_i\}},$$

the Silhouette value ranges between $[-1,1]$, and the maximized is desired.

8.4.1.3 Dunn Index

Let be $diam(C_m)$ in the maximum distance between observations in cluster C_m. The Dunn Index is defined by

$$D(\mathscr{C}) = \frac{\min_{C_k, C_l \in \mathscr{C}, C_k \neq C_l} \left(\min_{i \in C_k, j \in C_l}\right)}{\max_{C_m \in \mathscr{C}} diam(C_m)}.$$

The Dunn Index is the ratio of the smallest distance between observations from different clusters to the most considerable intra-cluster distance. The range of value of the Dunn Index is from 0 to ∞, and the maximum value is desired.

8.4.2 Stability Measure

The stability measure compares clustering results based on the entire data to the leave-one-out process of each feature in the dataset. This measurement is suitable for highly correlated data, like genomics data. The Average Proportion of Non-overlap (APN), the Average Distance (AD), the Average Distance between Means (ADM), and the Figure of Merit (FOM) is examples of stability measure. In all cases, the average is taken over all the left-out features, minimized value is desired.

8.4.2.1 Average Proportion of Non-overlap

Let be $C^{i,0}$ the cluster containing observation i based on all available data, and $C^{i,l}$ the cluster containing observation i where the clustering processes is based on left out l feature.

Then, the Average Proportion of Non-overlap (APN) measure is defined as

$$APN(\mathscr{C}) = \frac{1}{ND}\sum_{i=1}^{N}\sum_{j=1}^{D}\left(1 - \frac{n(C^{i,l} \cap C^{i,0})}{n(C^{i,0})}\right).$$

The range of APN is $[0,1]$, and should be minimized.

8.4.2.2 Average Distance

the Average Distance (AD) measures the average distance between observations placed in the same cluster by clustered with a l left-out features and the full data. The AD measure is defined by

$$AD(\mathscr{C}) = \frac{1}{ND}\sum_{i=1}^{N}\sum_{l=1}^{D}\frac{1}{n(C^{i,0})n(C^{i,l})}\left[\sum_{i\in C^{i,0}, j\in C^{i,l}} dist(i,j)\right],$$

the range of AD measure is from 0 to ∞, and should be minimized.

8.4.2.3 Average Distance between Means

Let be $\bar{x}_{C^{i,0}}$ the mean of observations in the cluster that contains observation i, when the clustering process is based on the full data. Let be $\bar{x}_{C^{i,l}}$ the mean of observation in the cluster which contains observation i, but in this case, the clustering process is based on the l left out features. It is defined as

$$ADM(\mathscr{C}) = \frac{1}{ND}\sum_{i=1}^{N}\sum_{j=1}^{D} dist(\bar{x}_{C^{i,l}}, \bar{x}_{C^{i,0}}).$$

In general, Average Distance between Means (ADM) only uses the Euclidean distance. It also has a value between 0 and ∞, and minimized is desired.

8.4.2.4 Figure of Merit

Define $x_{i,l}$ the value of the ith observation in the lth, and $\bar{x}_{C_k(l)}$ is the average of cluster $C_k(l)$. Currently, Figure of Merit (FOM) only used the Euclidean distance. The FOM measure is defined for a particular column l, left-out as

$$FOM(l,\mathscr{C}) = \sqrt{\frac{1}{N}\sum_{k=1}^{K}\sum_{i\in C_k(l)} dist(x_{i,l}, \bar{x}_{C_k(l)})},$$

FOM measure is multiplied with an adjusted factor $\sqrt{\frac{N}{N-K}}$, to relieve the tendency to decrease when the number of clusters increases. The final value is average overall left-out features, ranges between 0 and ∞, and minimized is desired.

8.5 Experiments

In this section, we presented the result of experiments that we established to metrically evaluate developed algorithms in Clustering of Neurocognitive Computing (NcC). In these experiments, we used **DSet-1** as the data-set in NcC_Clustering in MATLAB-version 2021 besides R-packages [***clValid***: Framework for cluster evaluation, V_0.7; ***cluster***: for cluster algorithms, V_2.1.2; and ***kohonen***: for SOM algorithm, V_3.0.11] in a R-Version of 4.1.3.
We projected *Experiment I* to compare the NcC_Clustering with other ordinary clustering methods. We used the Euclidean distance in R-package and NcC distance for NcC_Clustering. To guarantee a reliable comparison, we fitted all methods with 26 clusters. Figure (42) show the workflow of *experiment I* with all methods and metrics on that.

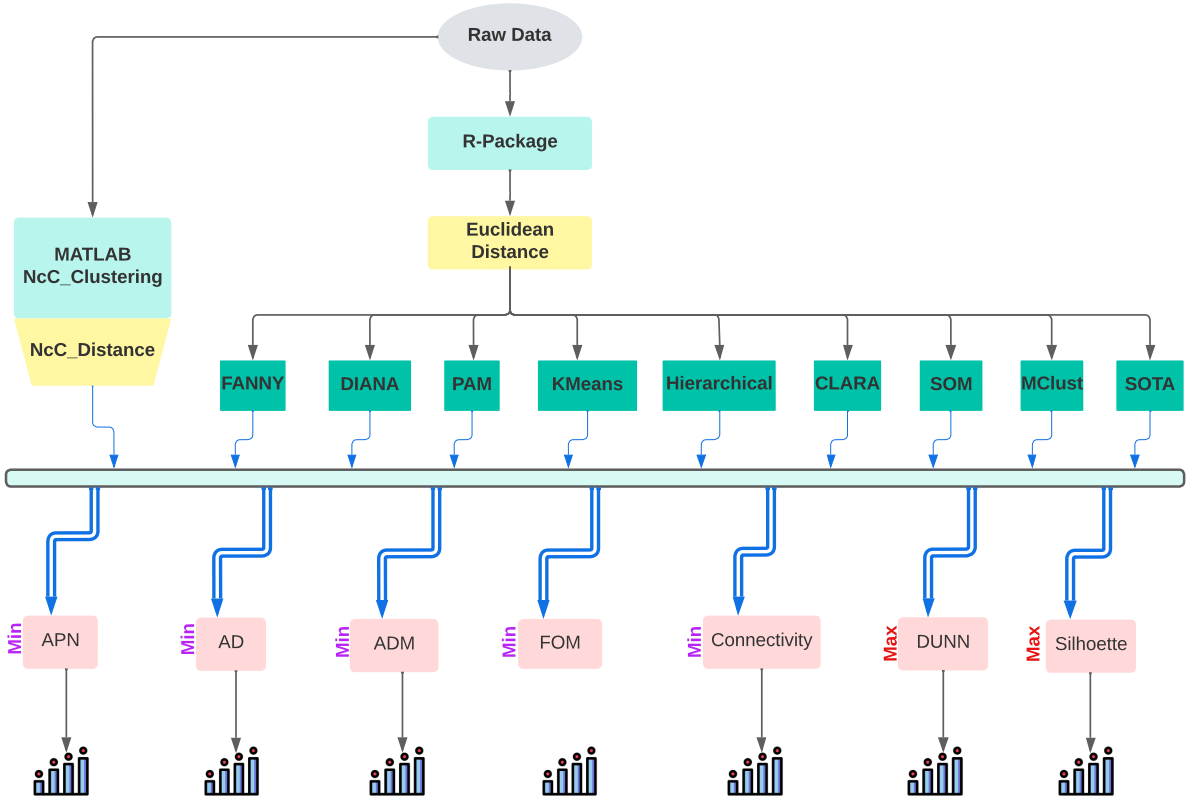

Figure 42 – Workflow of the experiment to evaluate the quality of Causal Feature Space compared to the standard Dimension Reduction methods in the literature.

We also designed the *experiment II* to evaluate the performance of ordinary methods using NcC_Distance. We want to assess whether or not NcC-distance can improve the performance of other methods. We fitted all methods with 26 clusters to compare and rank their performances as presented in Figure (43). We compared each metric using Euclidean versus NcC_distance for clustering. The ✓symbol indicates improvement in performance with NcC distance, and × otherwise.

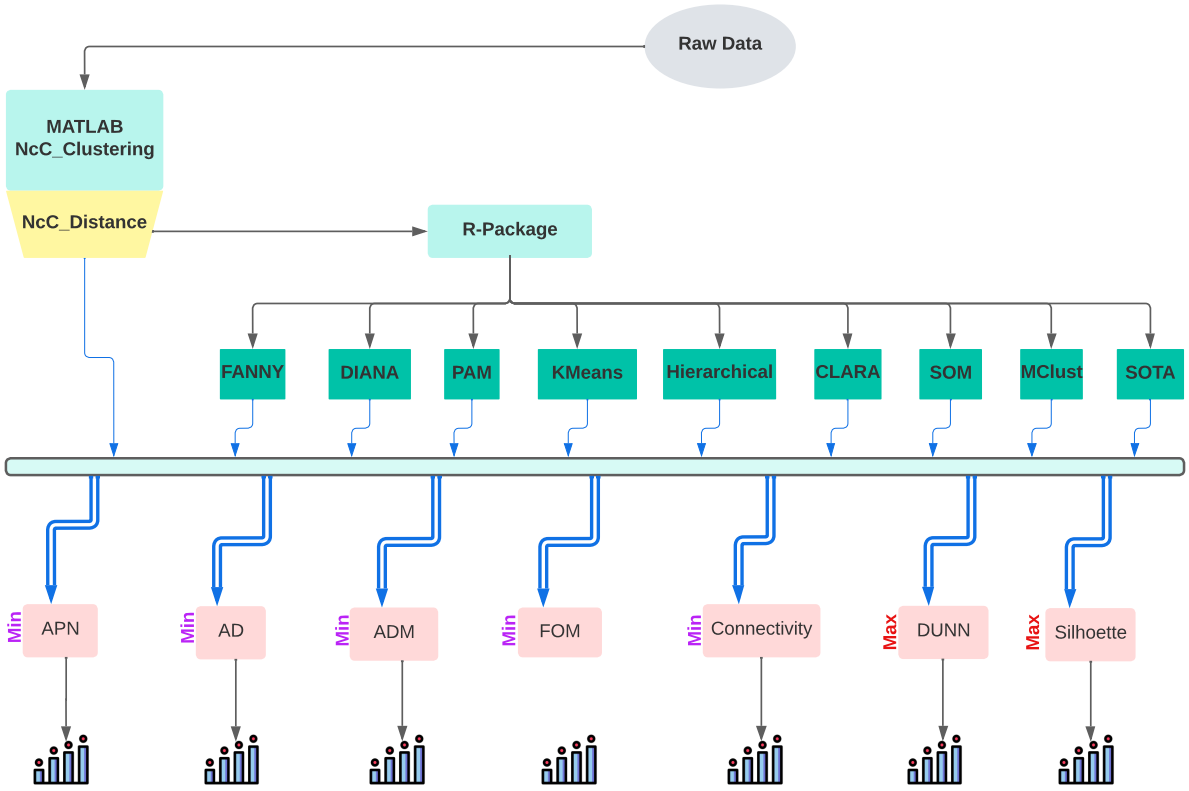

Figure 43 – Workflow of the experiments to evaluate the quality of NcC Clusters to the standard clustering methods without NcC_Distance.

8.5.1 Results of Experiment I

This section presents the results of the *experiment I*. The Figures 44, 45, 46, 47, 48, 49, and 50, explored the ranked values of metric assessments.

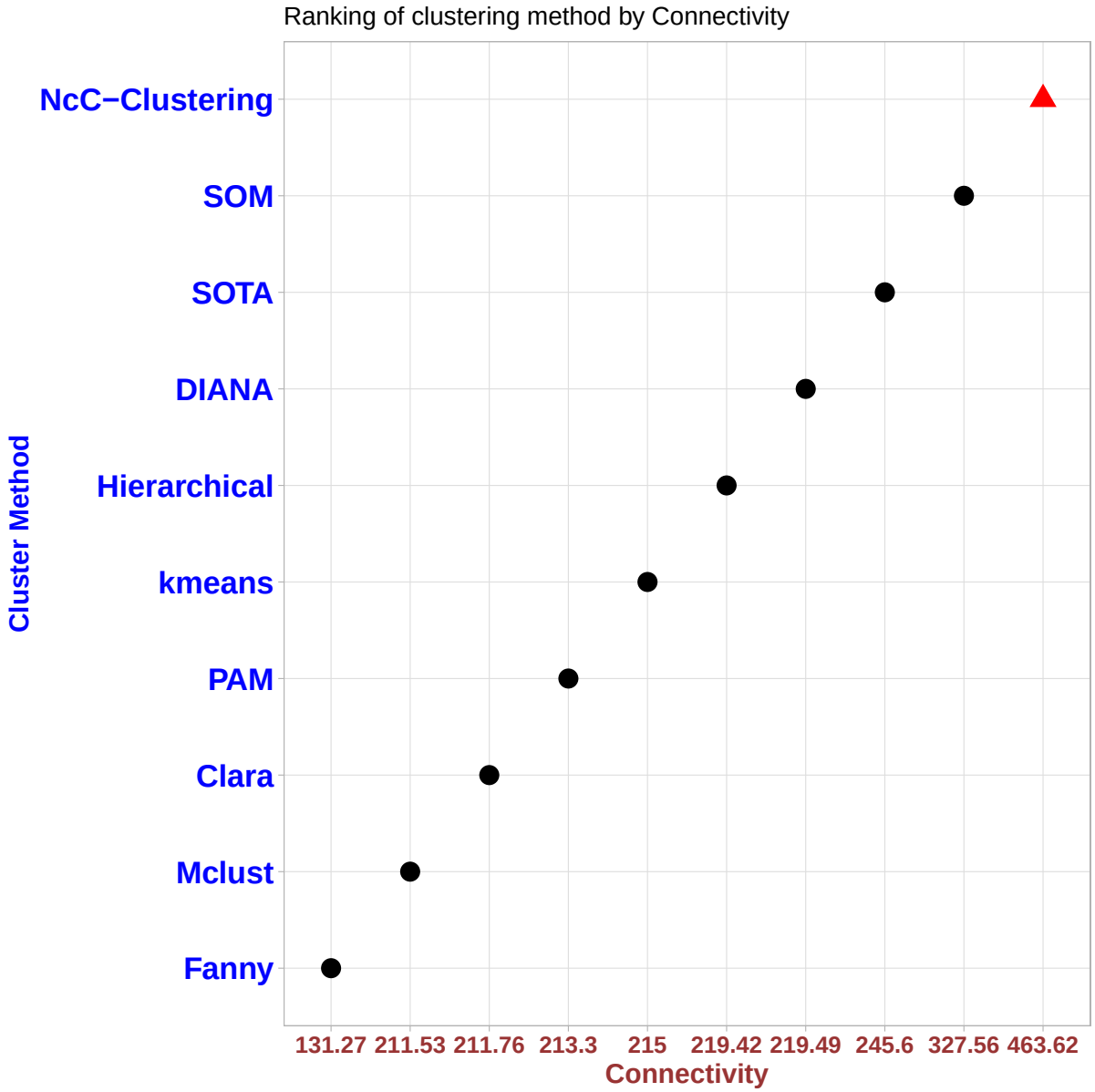

Figure 44 – Connectivity for each clustering method used in experimental data set with Euclidean-distance for the standard methods. NcC_Clustering is shown with the red point.

As illustrated in Figure 44, NcC_Clustering revealed a poor performance (the minimized value is desired) in this type of Connectivity assessment due to the induced geometry by NcC_-Distance, building nonlinear relations between observations. As the connectivity measure does not consider distance over a manifold, poor performance was expected because Euclidean neighbors strongly influenced this measure. In other words, the NcC_Distance's space is a manifold on euclidean space, and the distance over two points on this manifold should be interpreted based on its geometric shape.

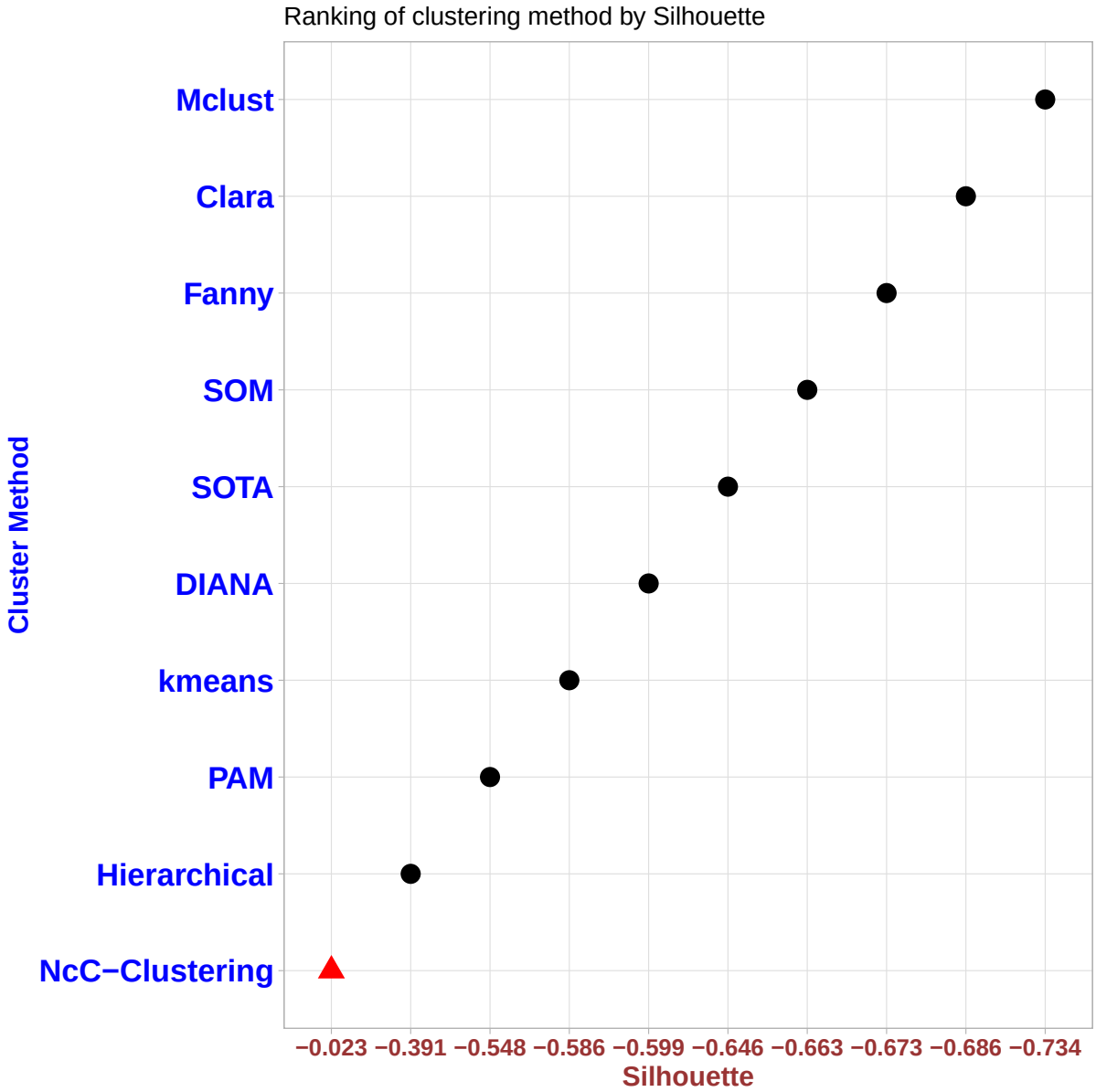

Figure 45 – Silhouette width for each clustering method used in experimental data set with Euclidean-distance for standard methods. NcC-Clustering is shown with the red point.

The ranking of clustering methods by Silhouette value was presented in Figure 45. Silhouette value computes how one cluster's members separate from the others, and the Maximum value is desired. NcC_Clustering indicated better performance in this metric.

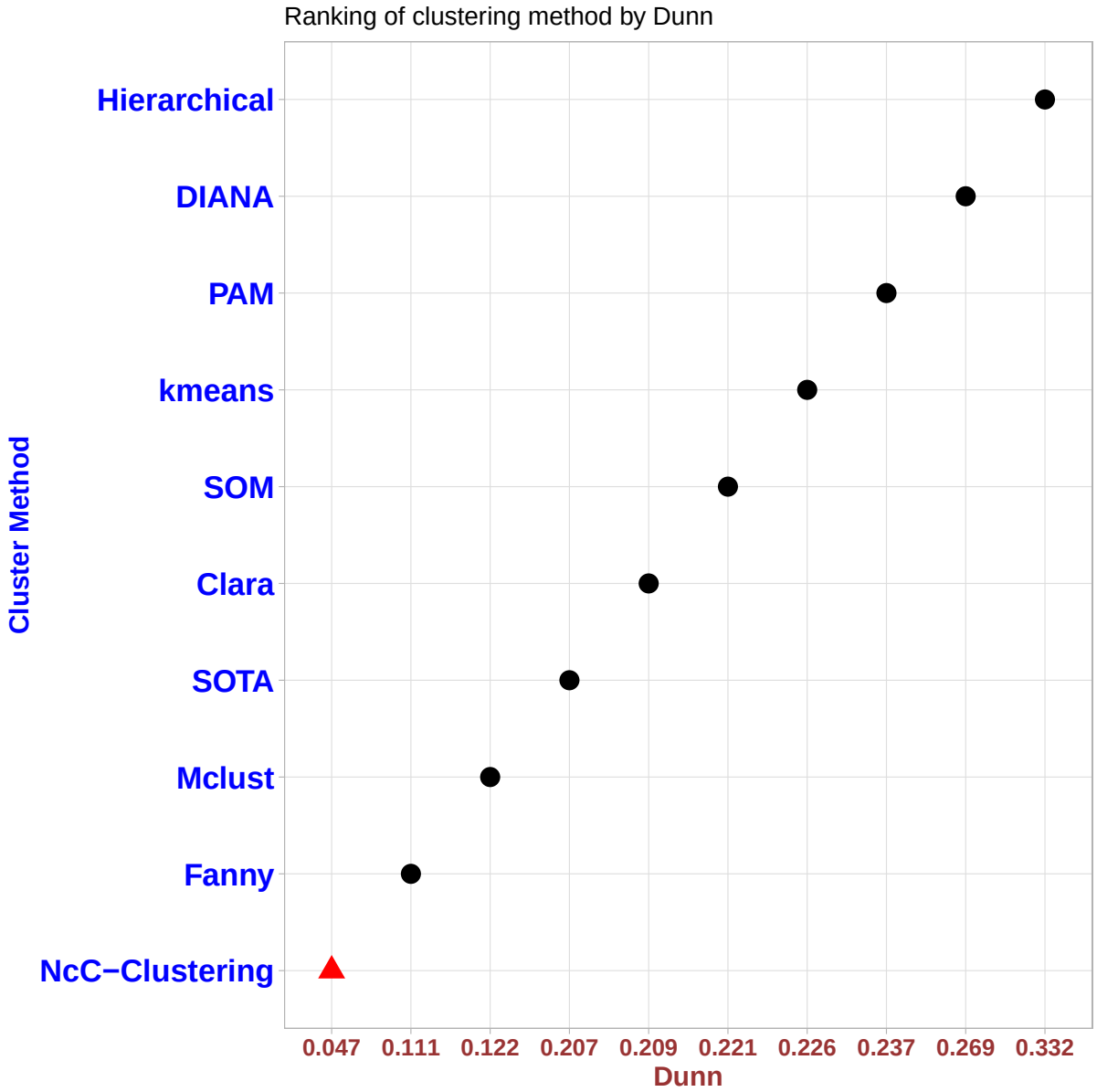

Figure 46 – Dunn index for each clustering method used in experimental data set with Euclidean-distance for standard methods. NcC-Clustering is shown with the red point.

We demonstrated Dunn index ranking in Figure 46, which is a ratio of the smallest distance between the clusters to the most considerable distance within the cluster. NcC_Clustering algorithm revealed a poor performance due to its characteristics to create a cluster with high mutual information and keep observations with low mutual information far from the shaped cluster. The distance between observations is affected by mutual information non-linearly.

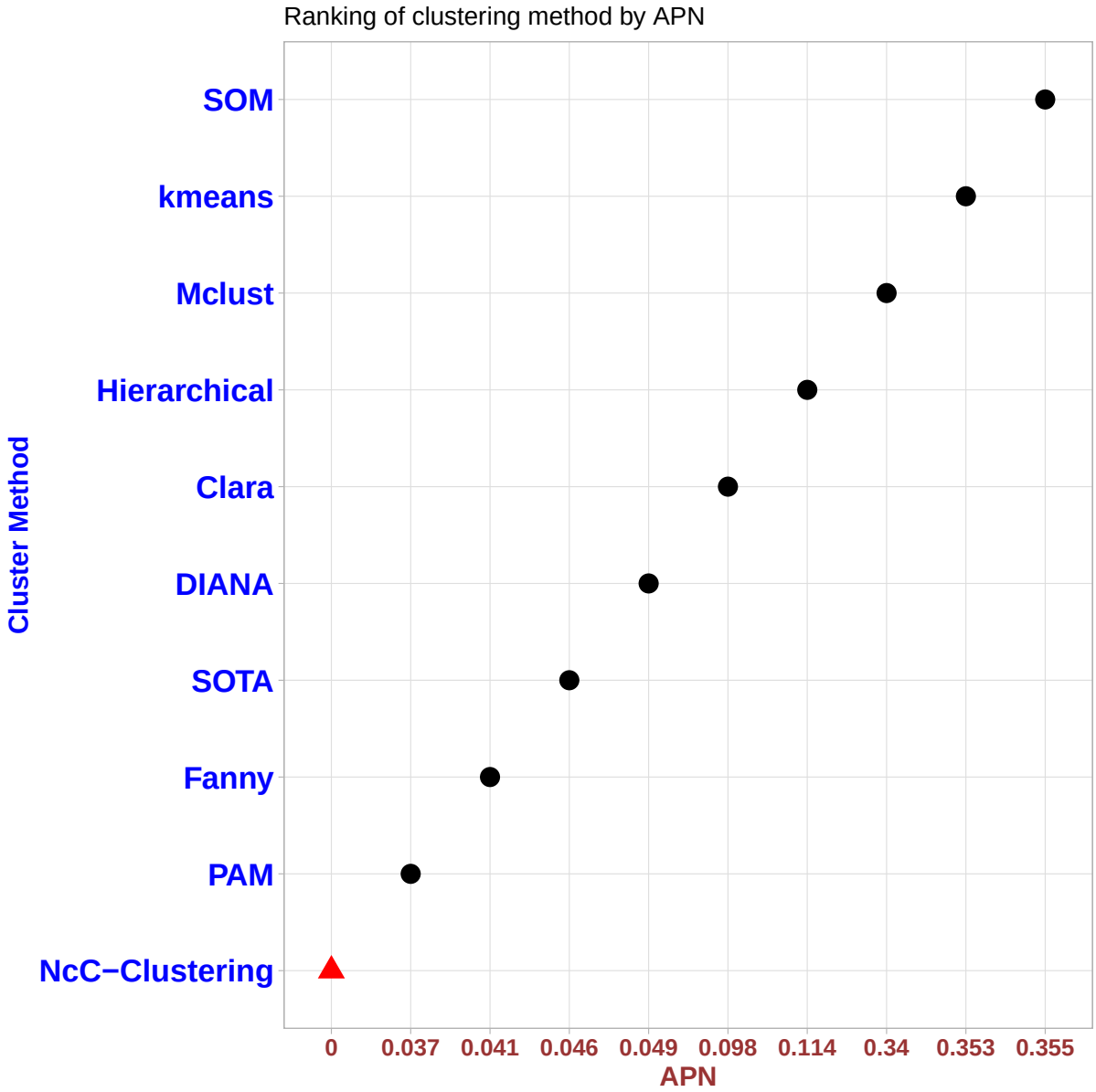

Figure 47 – APN for each clustering method used in experimental data set with Euclidean-distance for standard methods. NcC-Clustering is shown with the red point.

NcC_Clustering algorithm explored a considerable performance in APN ranking. It employs high mutual information to build clusters, the APN ranking for clustering methods is presented in Figure 47, which computes the stability of the cluster's observations. In other words, NcC is robust in the clustering of observations.

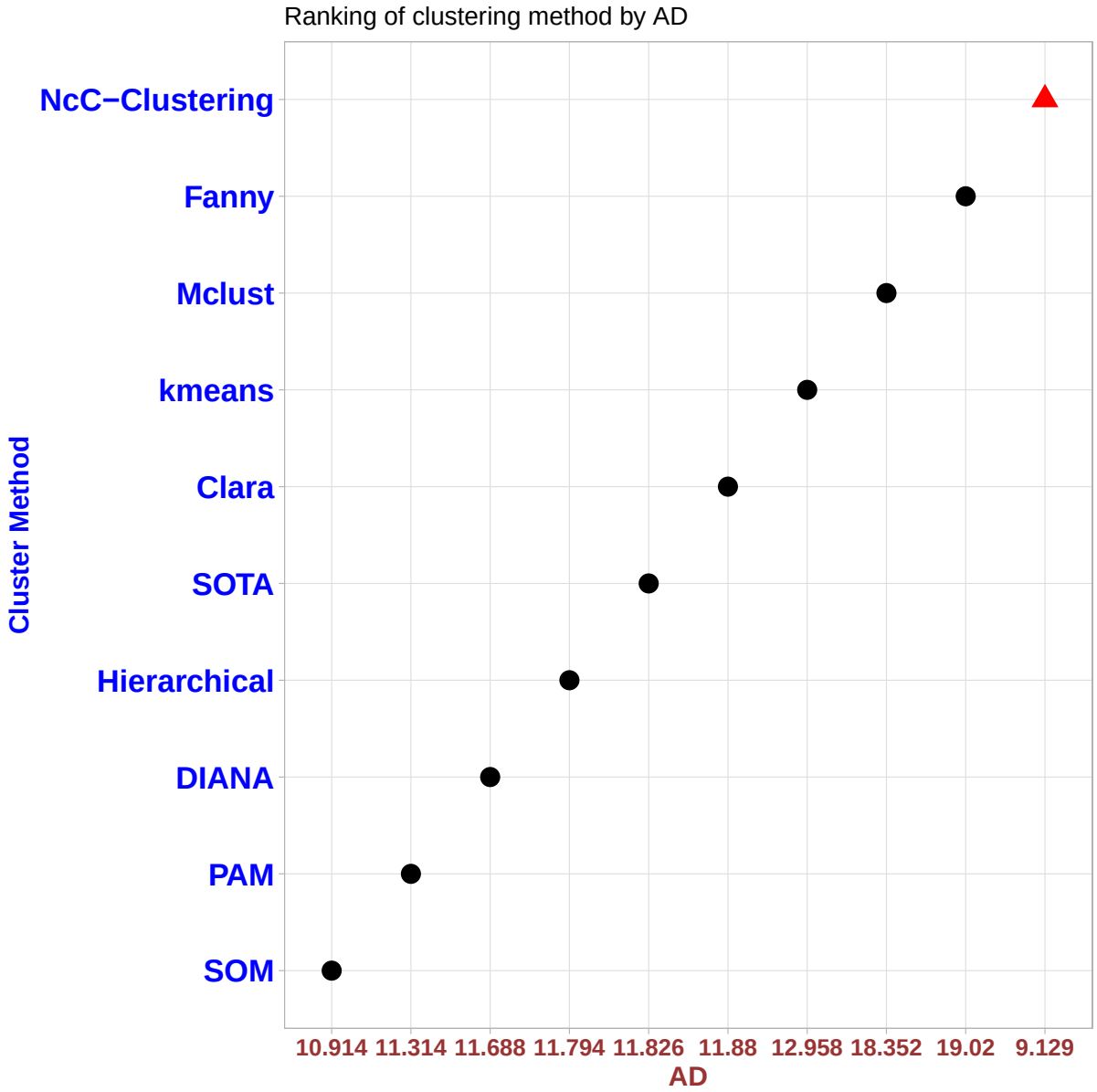

Figure 48 – AD for each clustering method used in experimental data set with Euclidean-distance for standard methods. NcC-Clustering is explored with the red point.

AD exhibited distance stability in the cluster when a feature was removed from the dataset. NcC_Clustering indicated poor performance (minimized value is desired) as presented in Figure 48 due to its nonlinear approach to measuring similarity and stability in the clustering process. In other words, generally, the NcC_clustering algorithm preserves the distances in the same cluster when one dimension drops.

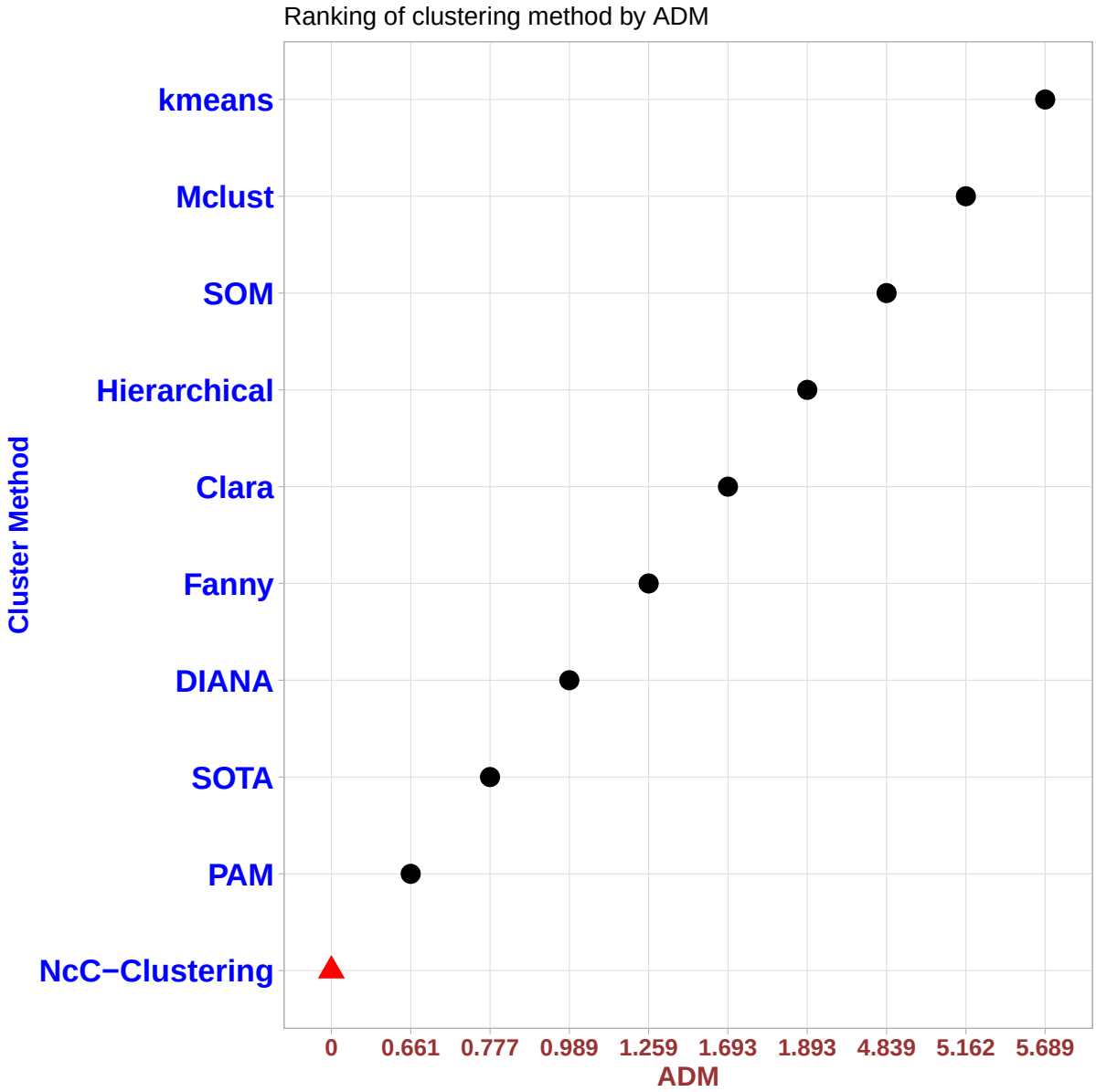

Figure 49 – ADM for each clustering method used in experimental data set with Euclidean-distance for standard methods. NcC-Clustering is identified with the red point.

Performances of clustering methods based on ADM measurement were ranked and explored in Figure 49. NcC algorithm revealed a significant performance that relies on its robustness in clustering besides the considerable distance between clusters and corresponding centroids.

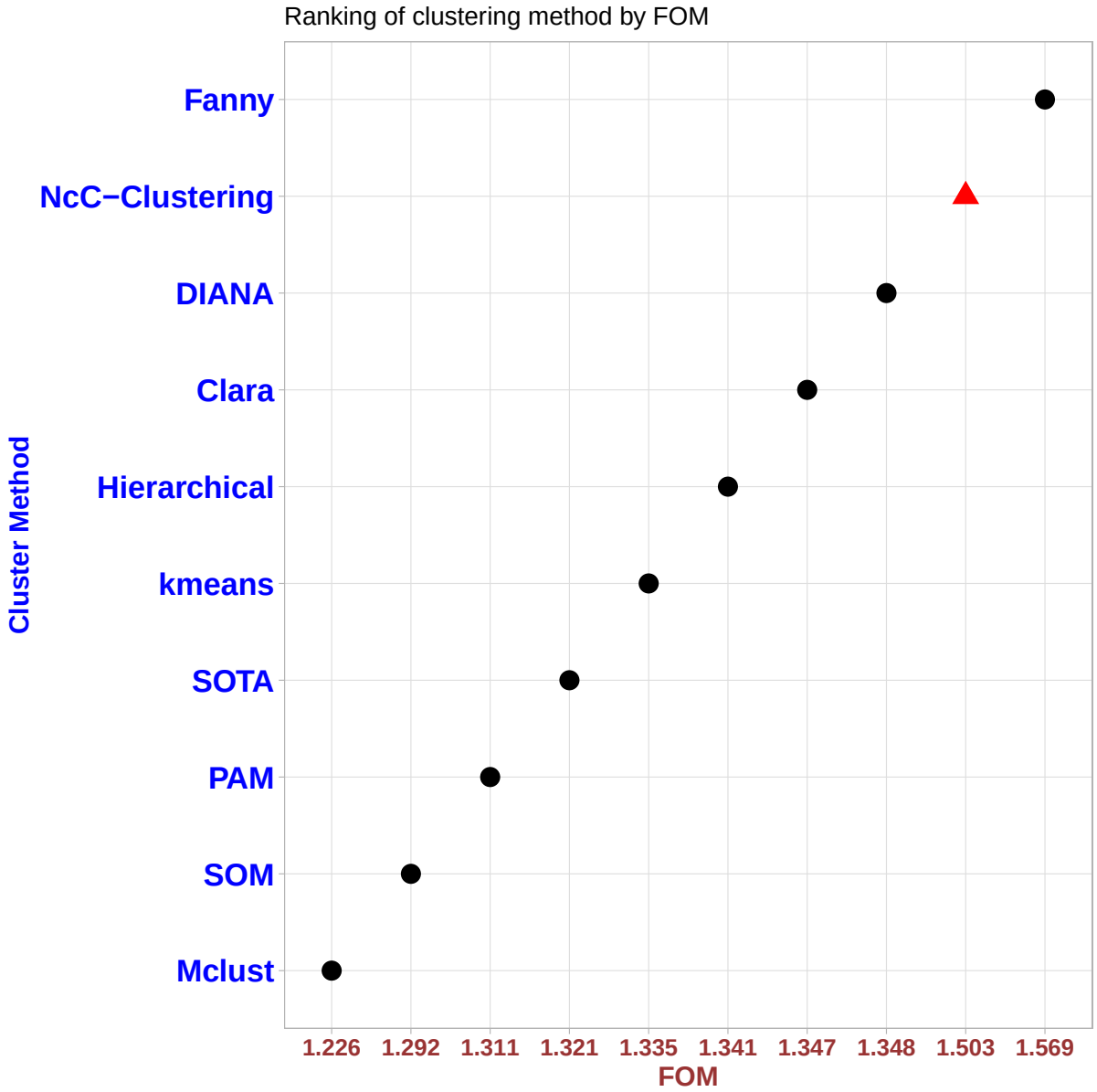

Figure 50 – FOM for each clustering method used in experimental data set with Euclidean-distance for standard methods. NcC-Clustering is depicted with the red point.

Figure of Merit (FOM) computes intra-cluster distance, as cluster methods performances illustrated in Figure 50. NcC algorithm revealed a poor performance due to its non-linearity measurement in similarity, which significantly influences distance matrices like Euclidean.

8.5.2 Results of Experiment II

This section explores the results and conclusions of the *experiment II*. Figures 51, 52, 53, 54, 55, 56, and 57, displays the ranked values of metric assessments.

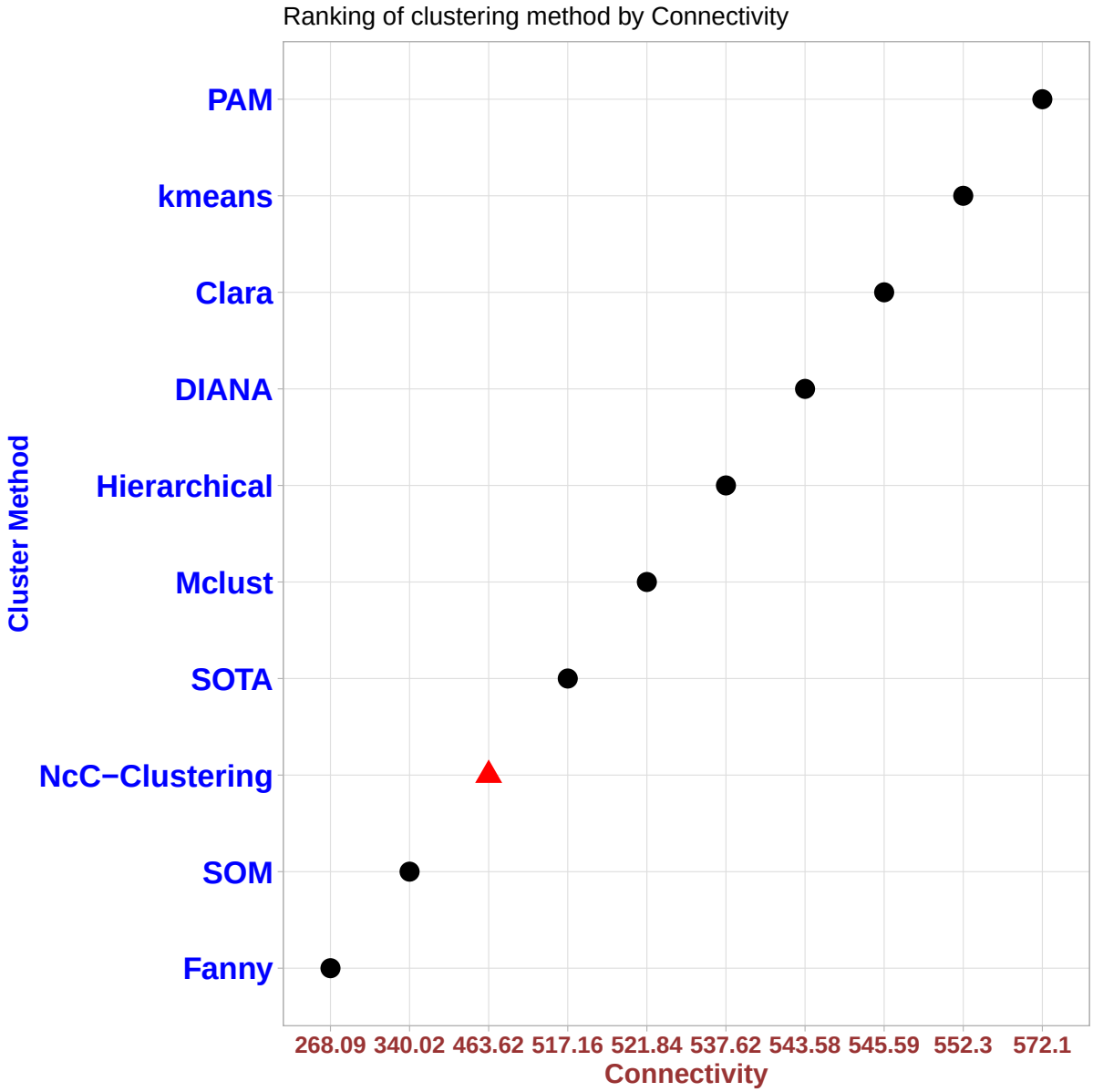

Figure 51 – Connectivity for each clustering method used in experimental data set with NcC-distance. NcC-Clustering is shown with the red point.

Connectivity ranked of clustering methods using NcC-Distance and NcC_Clustering indicated satisfactory performance as illustrated in Figure 51. Other methods were penalized in the connectivity measurement due to connectivity characteristics to ignoring distance non-linearity in a manifold. Compared with the *experiment I*, the NcC_distance negatively impacts the clustering performance in connectivity assessment. In other words, all clustering processes consider the similarity between observations over manifold instead of Euclidean space, against the connectivity assessment assumption.

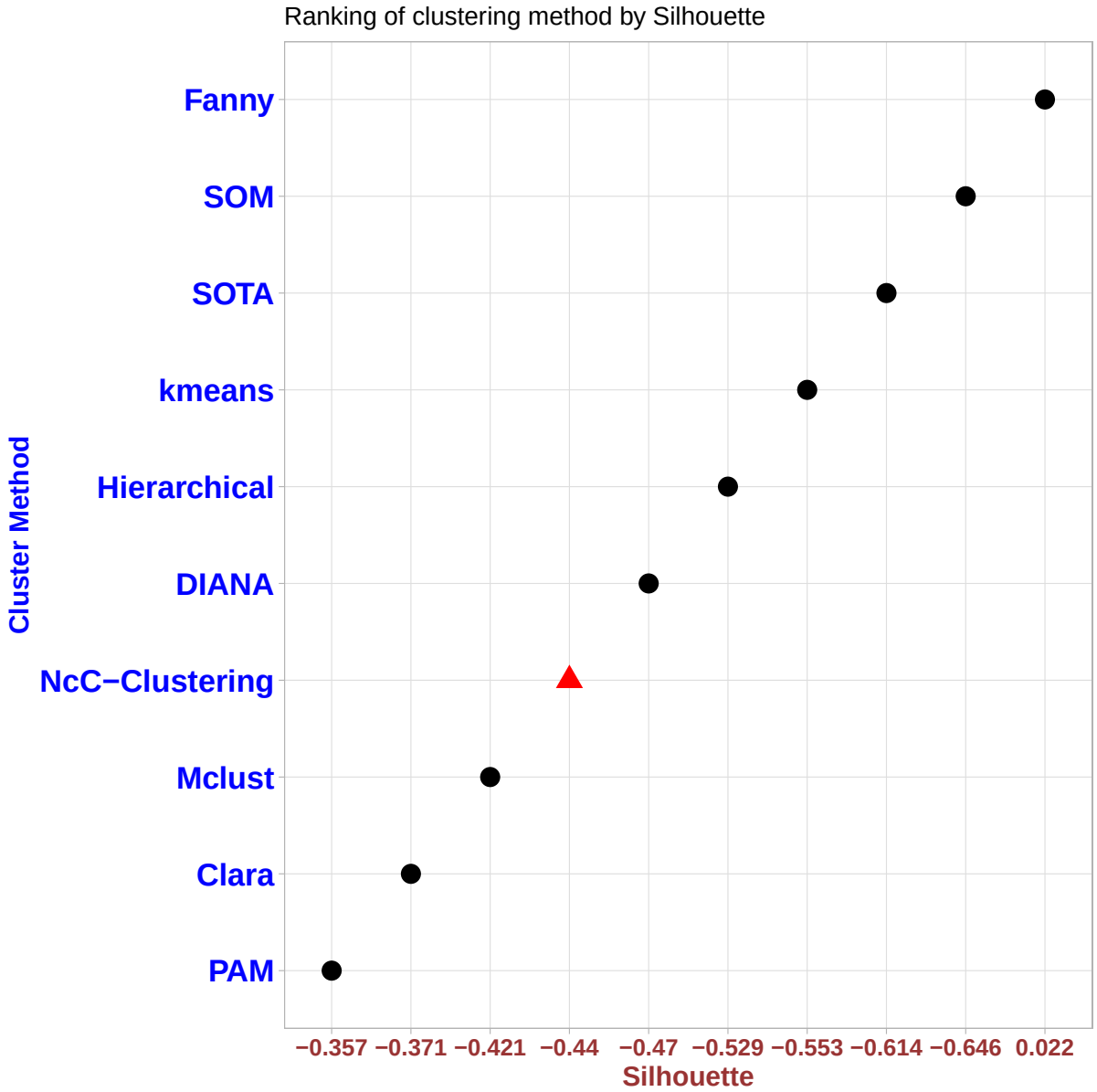

Figure 52 – Silhouette width for each clustering method used in experimental data set with NcC-distance. NcC-Clustering is identified with the red triangle.

Clustering methods using NcC-distance revealed significant improvement in performance over the Silhouette value assessment as illustrated in Figure 52. Computing the "closeness" based on mutual information in NcC-distance results in more homogeneous clusters in all methods and consequently enhances their performance in the Silhouette value assessment.

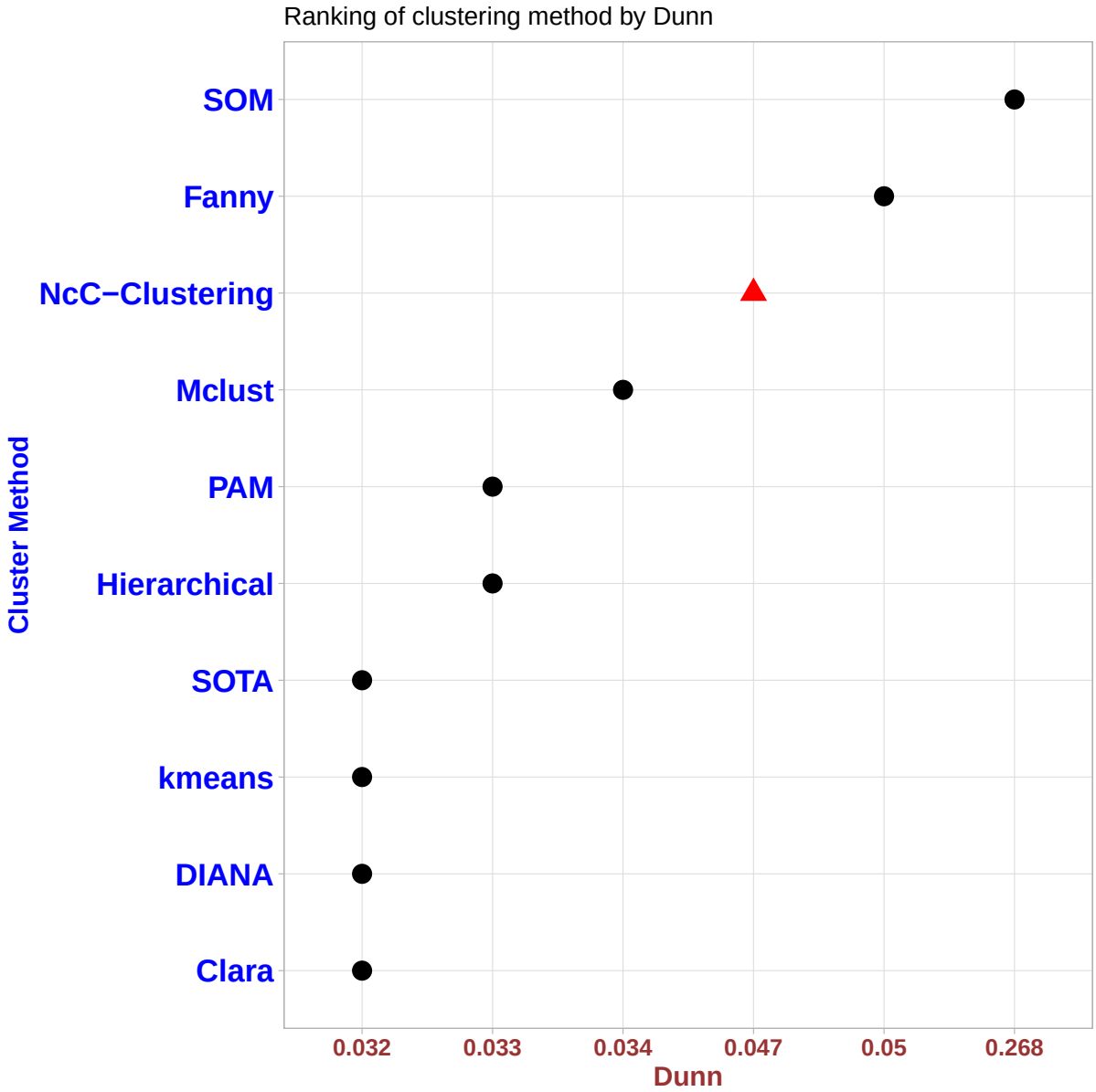

Figure 53 – Dunn index for each clustering method used in experimental data set with NcC-distance. NcC-Clustering is identified with the red triangle.

Using NcC_distance in the *experiment II* compared with the *experiment I* negatively impacts the performance of cluster methods in the Dunn index, as displayed in Figure 53. The non-linearity characteristics of the NcC-distance might affect observations' "closeness" in the context of Euclidean distance and consequently reduces their Dunn indices.

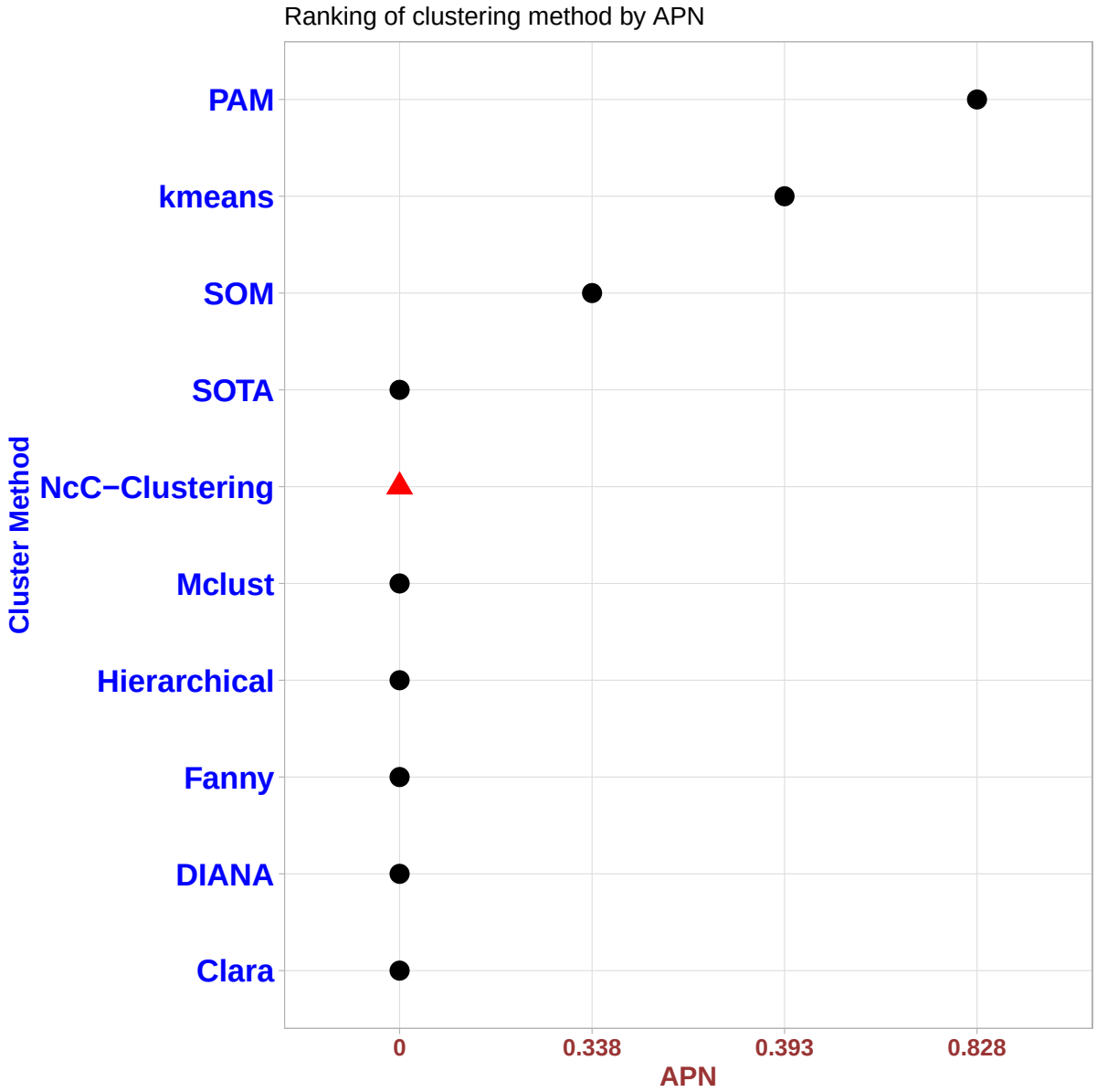

Figure 54 – APN for each clustering method used in experimental data set with NcC-distance. NcC-Clustering is identified with the red triangle.

As reported in *experiment I* NcC_distance, using mutual information leads to highly stable clusters. Supportively, Almost all methods revealed boosted stability in clusters when using NcC_distance. Therefore, we expected non-significant changes in cluster performance when one feature removes from the dataset, as illustrated in Figure 54.

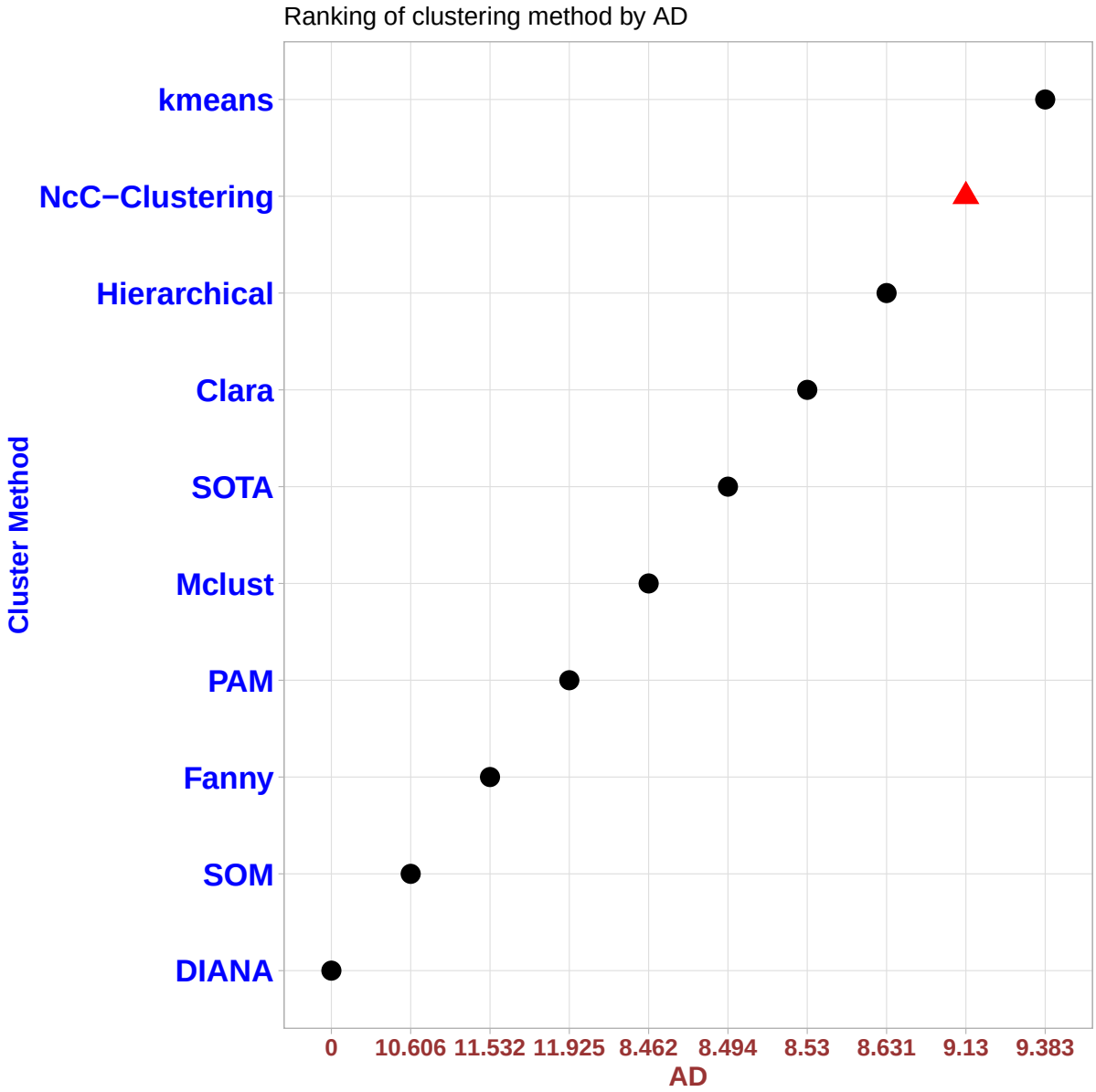

Figure 55 – AD for each clustering method used in experimental data set with NcC-distance. NcC-Clustering is identified with the red triangle.

Employing NcC-distance revealed a non-significant impact on the performance of AD assessment compared with the *experiment I*. In other words, NcC_distance is unable to improve the Average Distance assessment in the same clustering method. Therefore ranking positions are identical in the two experiments and are displayed in Figure 55.

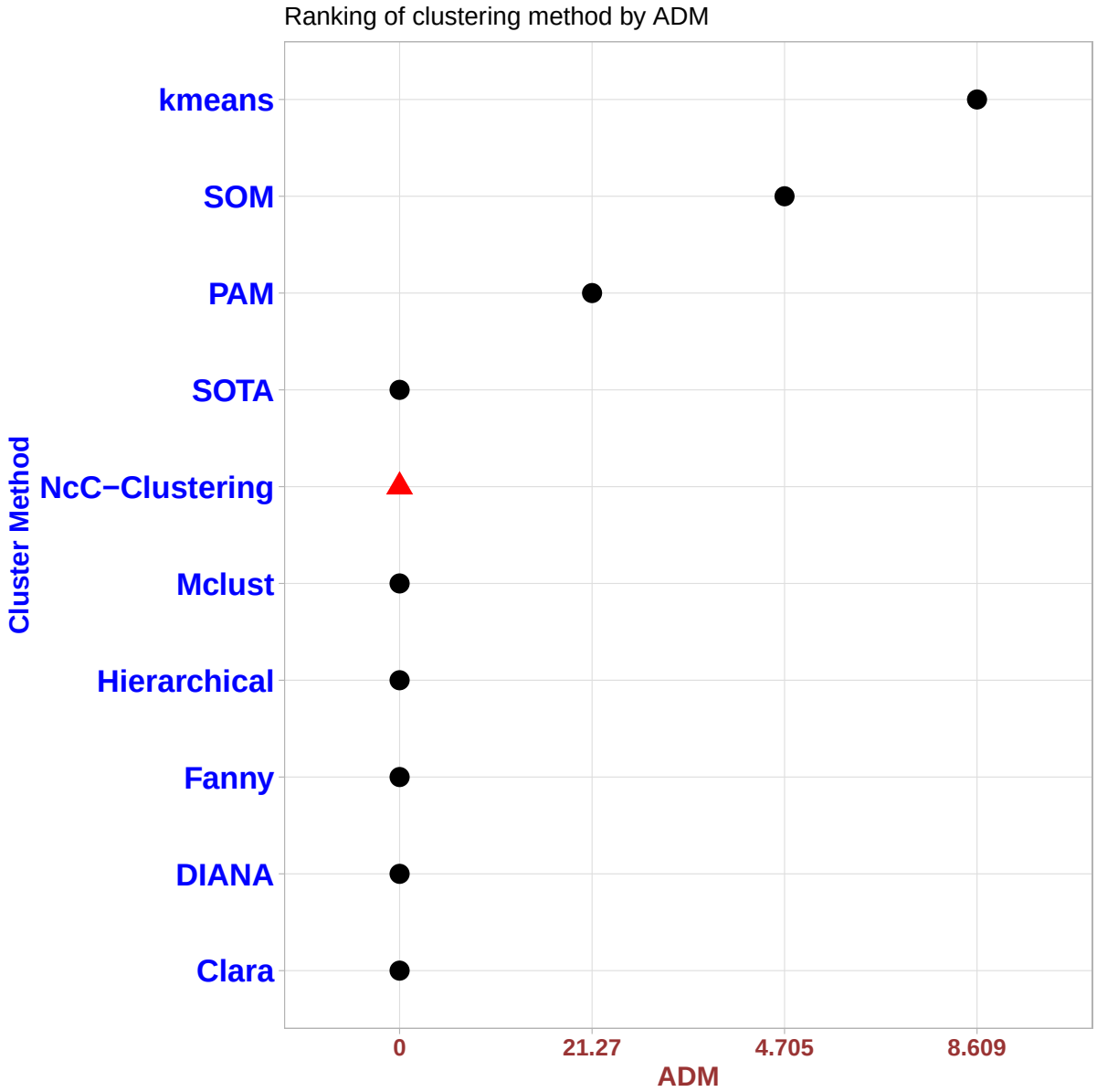

Figure 56 – ADM for each clustering method used in experimental data set with NcC-distance. NcC-Clustering is shown with the red triangle.

Clustering methods using NcC_distance explored better performance in Average Distance between Means (ADM) assessment compared with the *experiment I*, as illustrated in Figure 56. NcC_distance supports other methods to create more homogeneous clusters. Accordingly, the centroids become more distant, resulting in better performance in ADM evaluation.

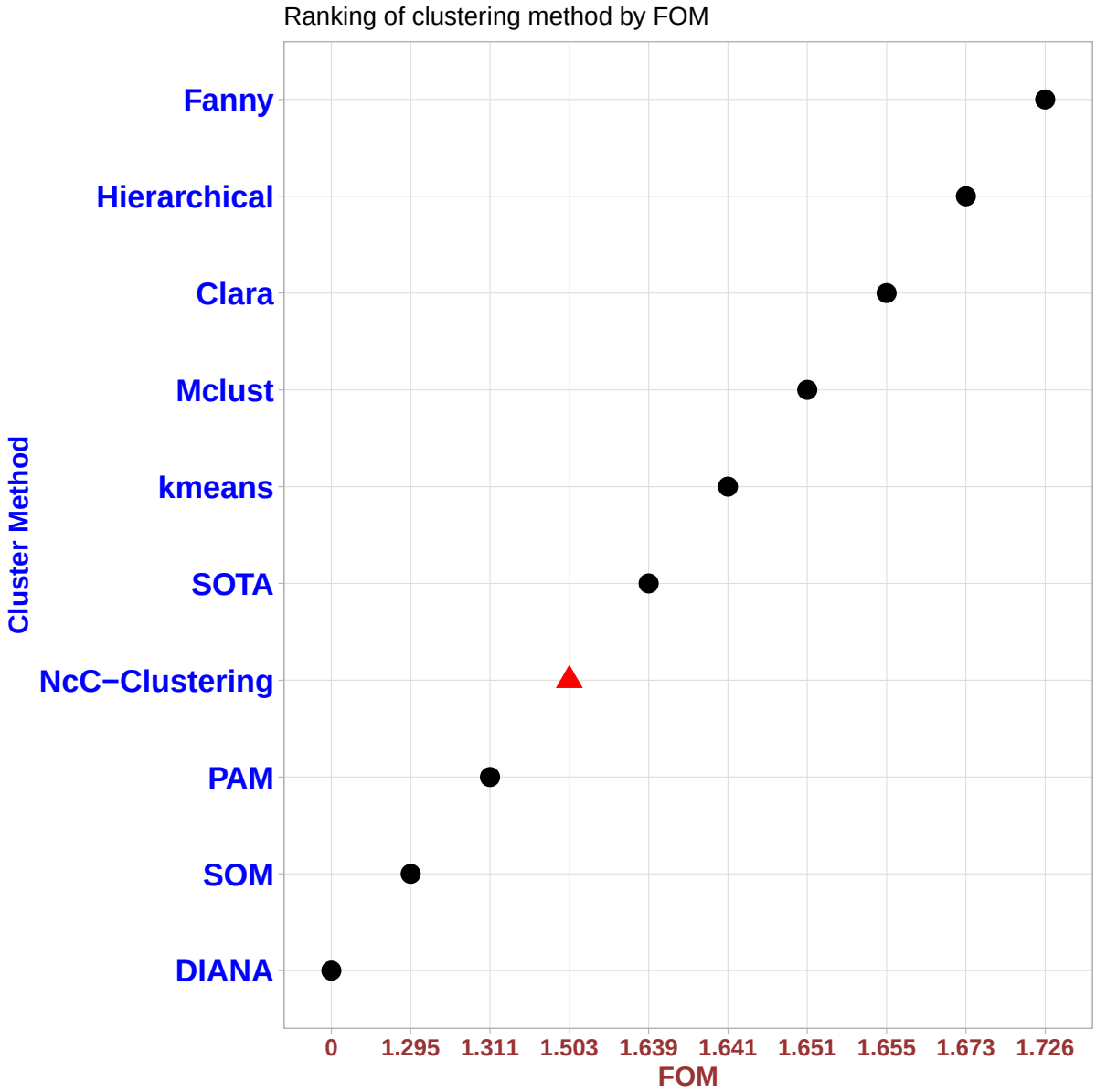

Figure 57 – FOM for each clustering method used in experimental data set with NcC-distance. NcC-Clustering is identified with the red triangle.

Clustering methods using NcC_distance demonstrated a reduction in performance due to its non-linearity characteristics compared with *experiment I*. Eventually, clusters are created based on the value of the mutual information between observations which does not guarantee their "closeness". Therefore, penalized the clustering methods performance in FOM evaluation as illustrated in Figure 57.

8.5.3 Conclusions of Performance evaluation

We conducted seven-evaluation metrics to compare clustering methods' performance using Euclidean versus NcC distances. We fitted 26 clusters in all applied methods in both experiments to make a reliable and fair evaluation.

Table 8 – Results of comparison clustering method using NcC_distance and Euclidean distance. ✓means NcC_distance increases performance, × does not increase.

Clustering Methods	**APN**	**AD**	**ADM**	**FOM**	**Connectivity**	**Dunn**	**Silhouette**
NcC-Clustering	N/A	N/A	N/A	N/A	N/A	N/A	N/A
Hierarchical	✓	×	✓	×	×	×	✓
kmeans	×	×	×	×	×	×	✓
DIANA	✓	✓	✓	✓	×	×	×
PAM	×	×	×	×	×	×	×
Clara	✓	×	✓	×	×	×	×
Fanny	✓	✓	✓	×	×	×	✓
SOM	✓	✓	✓	×	×	✓	✓
SOTA	✓	×	✓	×	×	×	✓
Mclust	✓	×	✓	×	×	×	×

Table 8 summarizes the influence of NcC_Distance on the applied methods. General improvements were revealed in the metrics that evaluate the distance between clusters, like a Silhouette, APN, and ADM, when using NcC-distance. On the other hand, metrics that compute distance inside the cluster showed non-significant improvement in performance. NcC_-distance supports homogeneous clusters but does not guarantee “Closeness” due to its non-linear characteristics of mutual information.

CHAPTER

9

SUPERVISED CAUSALITY NCC-DATADRIVEN MODELING

NcC_DataDriven employed mediatory models to support evidence for the causality relationship between the cognitive conceptual model compartments developed in (Chapter. 4) as a part of the NcC_Neurofunctional. Accordingly, in this chapter, we discussed the background of causality and multi-mediatory models and the inferential statistical model developed in the IBM-SPSS platform.

Background; A linear regression model represents an equation that links features (input) to a target variable (output) by a linear relationship. Linear regression analysis intends to estimate the regression model's various parameters to yield a reasonable estimation of the independent variables' target variable. The result of a regression model can test hypotheses about the processes that link predictors and target.

9.1 simple linear regression model

A simple linear regression model contains only a single predictor variable.

$$Y_j = \beta_0 + \beta X_j + \varepsilon_j \tag{9.1}$$

Y_j and X_j refer to case j's measurement and a target and predictor variable, respectively, b is the regression coefficient for predictor variable, b_0 is the intercept or regression constant, and e_j is the error of regression or residual. Suppose b_0 and b identified so we can generate an estimate of Y from X with a variant of this model:

$$\begin{aligned} \hat{Y}_j &= \hat{\beta}_0 + \hat{\beta} X_j \\ Y_j &= \hat{Y}_j + \hat{\varepsilon}_j \\ \hat{\varepsilon}_j &= Y_j - \hat{Y}_j \end{aligned} \tag{9.2}$$

optimum estimation will achieve when Ordinary Least Square (OLS)data is minimized.

$$OLS = SS_{\text{residual}} = \sum_{j=1}^{n} \left(Y_j - \hat{Y}_j\right)^2 = \sum_{j=1}^{n} \hat{\varepsilon}_j^2 \tag{9.3}$$

and the total some of square defines as

$$SS_{\text{total}} = \sum_{j=1}^{n} \left(Y_j - \bar{Y}\right)^2 \tag{9.4}$$

The simple linear regression model expresses a mathematical relationship between X to Y with a line equation. The regression coefficient corresponds to the line's slope and b_0 to intercept in the linear regression equation. Multiple Linear Regression The multiple linear regression model estimates a target variable using more than one predictor variable. In its most general form, a multiple linear regression model with k features variables takes the form

$$Y_j = \beta_0 + \beta_1 x_{1j} + \beta_2 x_{2j} + \ldots + \beta_k x_{kj} + \varepsilon_j \tag{9.5}$$

and in matrix notation is:

$$\begin{aligned} \mathbf{Y} &= \mathbf{x}'\beta + \varepsilon \quad \text{where} \quad \mathbf{x}' = \{1, x_1, x_2, \ldots, x_k\}' \\ \hat{\mathbf{Y}} &= \mathbf{x}'\hat{\beta} \end{aligned} \tag{9.6}$$

9.1.1 Model Fit Measurements

The multiple regression equation minimizes the Mean Square residuals (MS_{residual}), consequently obtains the best linear fitting model.

$$MS_{\text{residual}} = \frac{SS_{\text{residual}}}{n-k-1} \tag{9.7}$$

where n is the number of observations and k is the number of features, generally (n-k-1) is also called degrees of freedom. An alternative measure of fit is the standard error of estimate and defined as

$$\text{Standard error of estimate} = \sqrt{MS_{\text{residual}}} = \sqrt{\frac{SS_{\text{residual}}}{n-k-1}} \tag{9.8}$$

Multiple Correlation Coefficient (R) and R^2 represent the proportion of the variance in Y explained by the model and formulate as

$$R^2 = \frac{SS_{\text{total}} - SS_{\text{residual}}}{SS_{\text{total}}} \tag{9.9}$$

9.1.2 Assumptions for Interpretation and Statistical Inference

1. **Linearity**

   OLS regression assumes that all features **x** are individually related with the target variable Y linearly. Whenever the essential linearity assumption is violated makes the regression coefficient's interpretation meaningless (DARLINGTON; HAYES, 2016).

2. **Normality**
   The normality assumption asserts that the errors in estimating target variable Y, conditioned on **x**, are typically distributed. Simulation studies identified that only severe violations of the normality assumption considerably affect the validity of statistical inferences from a regression analysis unless the sample size is relatively small (DUNCAN; LAYARD, 1973; EDGELL; NOON, 1984; HAVLICEK; PETERSON, 1977; HAYES, 1996). However, non-normality can affect sampling variance in some situations, reducing hypothesis tests' power and the certainty of rejecting a nonsignificant null hypothesis.

3. **Homoscedasticity**
   The assumption of homoscedasticity states that the errors in the estimation of Y are equally variable conditioned on **x**. When it fails to detect, heteroscedasticity happens, affecting both the validity of inference and reducing hypothesis tests' statistical power. Therefore, influence the precision of confidence intervals for regression coefficients. An informal test of homoscedasticity is a visual inspection of the residuals' scatterplot as a function of $\hat{\varepsilon}$.

4. **Independence of observations**
   OLS regression assumes the errors in estimation are statistically independent. The errors in estimation are independent when there is no information available in the error of estimation of Y_i that could estimate the error of Y_j.

5. **Non-multicollinearity between the Features**
   Multicollinearity refers to a situation in which more than two features in a multiple regression model are extremely linearly related.

9.2 Mediator

An investigator to discover how X affects Y generally hypothesizes that mediating variables M can influence the relation between X and Y (Mediator models depicted in Figures (58, 59, and 60) (HAYES, 2017). Therefore, investigators are interested in measuring X's direct effect on Y, besides mediatory analyses and identifying causal relationships.(MACKINNON *et al.*, 2002; PREACHER; HAYES, 2004; PREACHER; HAYES, 2008; BARON; KENNY, 1986).

9.2.1 simple Mediator

Mediation analysis evaluates evidence from studies designed to test hypotheses about how features X causally transmit effects on a target variable Y. A simple mediation model contains two target variables (M) and (Y) and two features (X) and (M) whereas X causally affecting Y and M, and M causally affecting Y. A simple mediator model is a causal system that one causal feature X leads to an outcome Y through a single intermediary variable M. in other words, X from two unidirectional pathways can affect Y.

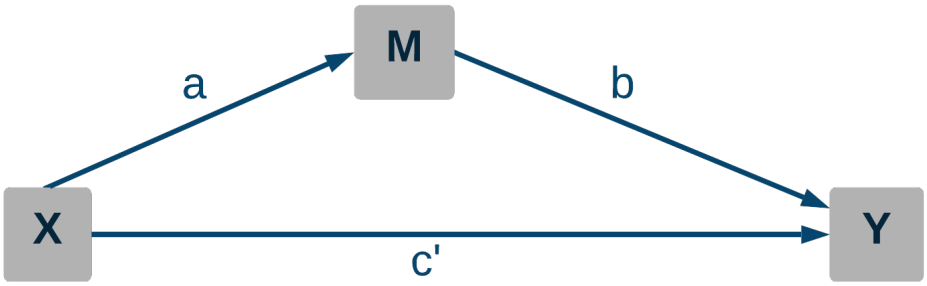

Figure 58 – Simple Mediator diagram, X, M, and Y represents Predictor, Mediator and Target variable, respectively.

- One leads from X to Y directly and is called the direct effect of X on Y.
- The second from X to Y is the indirect influence of X on Y over M.

Estimation of the Direct, Indirect, and Total Effects of X As there are two target variables in the simple mediator diagram (Figure 58), two linear models are needed, one for each target.

$$M = \beta_{0_M} + aX + \varepsilon_M \tag{9.10}$$

$$Y = \beta_{0_Y} + c'X + bM + \varepsilon_Y \tag{9.11}$$

$$Y = \beta_{0_Y} + c'X + b\,(\beta_{0_M} + aX + \varepsilon_M) + \varepsilon_Y$$

$$Y = (\beta_{0_Y} + b\beta_{0_M}) + (ab + c')X + (\varepsilon_Y + b\varepsilon_M)$$

$$c = c' + ab \tag{9.12}$$

$$Y = \beta_{0_{Y*}} + cX + \varepsilon_{Y*} \tag{9.13}$$

where β_{0_M} and β_{0_Y} are regression constants, ε_M and ε_Y are error in estimation of M and Y, respectively. a, b, and c' are the regression coefficients given to the features in the regression models to estimate target variables. c' estimates the direct effect of X on Y and a quantifies the effect of X on M, and c' represents the direct effect of M on Y. In the Equation(9.13), $c' + ab$ replaced with c . Errors of estimations and intercepts also integrated with $Y*$ for simplifications. It is essential to consider that this mathematics, whereby c applies when Y and M are estimated using OLS regression, meaning analyzed as continuous variables using the OLS criterion for maximizing the fit of the model. It also works when using a maximum-likelihood-based model of continuous outcomes, but it does not applicable for using other modeling methods like generalized linear modeling.

Statistical inference; Bootstrap Confidence Interval is a resampling method and needs high-speed computing, so as computer power has increased bootstrapping approach is implemented in modern statistical software. Bootstrapping is helpful when the behavior of a statistic over repeated sampling is either not known or highly depends on context. The original sample of

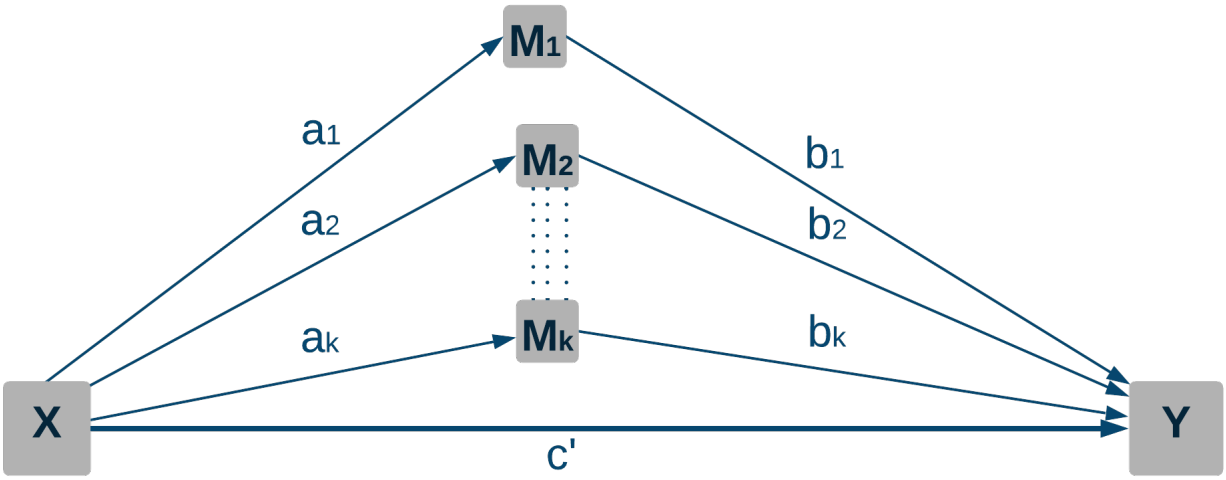

Figure 59 – Parallel Multi-Mediator diagram, parallel mediators $\{M_1, M_2, \ldots, M_k\}$ assumed has no influence on each others.

size n is treated as a small representation of the population initially sampled. Observations in this sample are then "resampled" with replacement, and some statistic of interest was calculated in the new sample of size n created by this resampling method.
In mediation analysis, bootstrapping is employed to make an empirical representation of the indirect effect's sampling distribution. This empirical representation is utilized to build a confidence interval for the null hypotheses that respect the irregularity of the sampling distribution of ab and yield accurate inferences.

9.2.2 Parallel Multi-Mediator

In parallel multiple mediator models, Predictor X affects target Y directly and indirectly through two or more mediators, with the condition that no mediator causally affects another. The statistical diagram of a parallel multi-mediator model with k isolated mediators that have no effects on each other (presented in Figure 59).

It does not mean mediators are independent. However, parallel multi-mediator in comparison to multiple single mediator models could boost power for tests of indirect effects if the mediators are highly correlated with Y but weakly correlated with each other. It also makes it possible to compare the sizes of the indirect effects through different mediators. As can be seen in Figure 59, a parallel multiple mediator models with k mediators have $k+1$ target variables and so requires

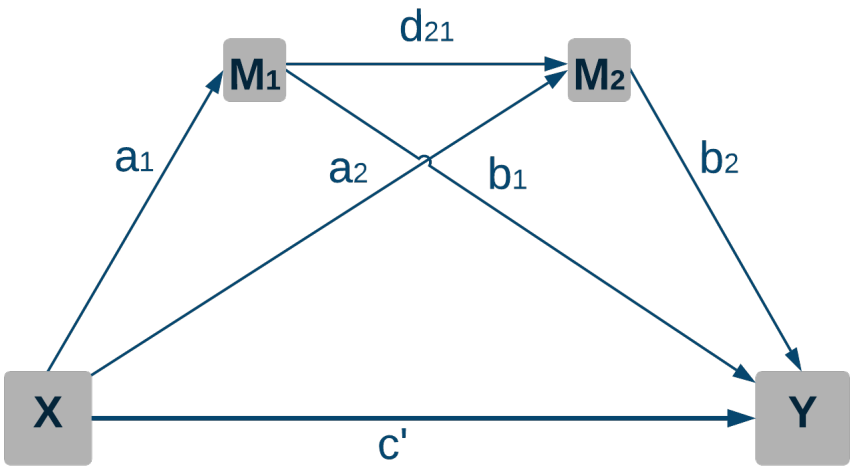

Figure 60 – Serial Multi-Mediator diagram demonstrated for two mediators for restriction in visualizations

$k+1$ equations to estimate all the causal effects of X on Y. These equations are

$$M_i = \beta_{0M_i} + a_i X + \varepsilon_{M_i} \quad \text{for all i =1 to k} \tag{9.14}$$

$$Y = \beta_{0_Y} + c'X + \sum_{i=1}^{k} b_i M_i + \varepsilon_Y \tag{9.15}$$

$$c = c' + \sum_{i=1}^{k} a_i b_i \tag{9.16}$$

where a_i measures the effect of X on M_i, b_i calculates the effect of M_i on Y examining for X and the other $(k-1)M$ variables. c' also assesses the effect of X on Y, holding all M mediator variables as constant. Furthermore, in the Equation(9.16), c is the total effect of X.

9.2.3 Serial Multi-Mediator

The serial multi-mediator model assumes no causal association between two or more mediators. The direct, indirect, and total effects of X on Y are investigated when consecutively hypothesized X causes M_1, then M_1 leads M_2, and so forth, achieving Y as the final target.

$$M_1 = \beta_{0M_1} + a_1 X + \varepsilon_{M_1}$$

$$M_i = \beta_{0M_i} + a_i X + \sum_{j=1}^{i=1} d_{ij} M_j + \varepsilon_{M_j} \quad \text{for all i = 2 to k} \tag{9.17}$$

$$Y = \beta_{0Y} + c'X + \sum_{i=1}^{k} b_i M_i + \varepsilon_Y \tag{9.18}$$

By integrating all introduced models here, we are able to make any diagram of complex unidirectional mediator models.

9.3 Introduction: Tinnitus Causality Model

Tinnitus Conceptual Cognitive Framework (CCF) introduced in (Chapter. 4) aims to illustrate causality (mediation) relationships. Thus, demand a methodology to evaluate causalities in theories and hypotheses. The tinnitus CCF supports data models for testing mediational relationships between independent variables and outcomes measured in retrospective studies. We presented causality relationship through multi-mediatory (causality) modeling approaches (HAYES, 2017)for Neutral (learning process) and Clinical (Maintenance) Tinnitus. NcC learning process employs mediator modeling to prove the concept for CCF for tinnitus besides constructing the causality graph for Causal Reinforcement Learning (Similar to cognitive Map). NcC mission-driven causality model illustrates how cognitive processes and their interactions emerge annoyance-distress reactions and lead to the development or maintenance of clinical tinnitus.

Questionnaire	**Item**	**Model Component**
Tinnitus Handicap Inventory (THI)	Sum of all questions	Distress **THIR**
Tinnitus Severity (TS)	Q2. How strong or loud is your tinnitus at present?	Tinnitus loudness **Ts2Pre**
	Q3. How uncomfortable is your tinnitus at present, if everything around you is quiet?	Cognitive value **Ts3Pre**
	Q4. How annoying is your tinnitus at present?	Annoyance **Ts4Pre**
	Q5. How easy is it for you to ignore your tinnitus at present?	Attentional Bias **Ts5Pre**
	Q6. How unpleasant is your tinnitus at present?	Emotional value **Ts6Pre**
	Average of [Q3 and Q6]	Cognitive-Emotional Value **Ts36Pre**

Table 9 – List of Questionnaires and corresponding questions for each model component

9.3.1 Preprocessing of the data

The data were anonymized to ensure blinding. Initially, those with missing values were omitted, which resulted in 112 and 134 session-wised questionnaires from the first and second studies, respectively. Primarily, data sets were aggregated and segmented based on tinnitus severity stages. Concerning tinnitus, scores of the THI questionnaire lower than 20 *(THI-R< 20)* were labeled as Neutral otherwise *(THI-R > = 20)* the Clinical. Following this segmentation, two sub-datasets (Tinnitus-Neutral and Tinnitus-Clinical) were provided to conduct statistical analysis.

9.3.2 Statistical analysis

We employed Durbin-Watson to test multicollinearity/autocorrelation between independent variables in each dataset segment. Results exhibited independence in residual.
SPSS v.26 and PROCESS macro (HAYES, 2017) were used for the data analysis. We customized all models with‘10,000’ bias-corrected bootstrap samples and the fixed random-seed (‘12020’). The confidence level was chosen at 95% with $p < 0.05$ significance. An investigated evidence for tinnitus Neutral and Clinical CCF within the data segments was investigated through hierarchical regression analyses. We developed Multiple mediation models to determine the mediating effects of tinnitus-related cognitive and emotional factors in annoyance and clinical distress. PROCESS macro computed standard errors, p-values, confidence intervals for direct effects, and bootstrap confidence intervals for conditional indirect effects.

9.3.3 Proposed Mediator Models

Fundamental Ideas and Postulations of Mediator Models

- Tinnitus loudness represents the CAAP of the tinnitus sound.
- Failure to ignore tinnitus describes attentional bias to tinnitus sound.
- Cognitive-emotional value is considered as a unified parameter.
- Used dataset does not support measuring factors related to the distorted perception of tinnitus.

The causality model of *Neutral tinnitus* aims to explore the *prepetual-learning proess* considering the role of evaluative conditional learning and negative appraisal (thought)that we coined as the term *cognitive-emotional evaluation*. The CAAP of tinnitus sound drives attentional bias and subsequently triggers the *cognitive-emotional evaluation* of the perceived sound, leading to annoyance. However, in the Neutral stage, merely tinnitus CAAP is incapable of generating

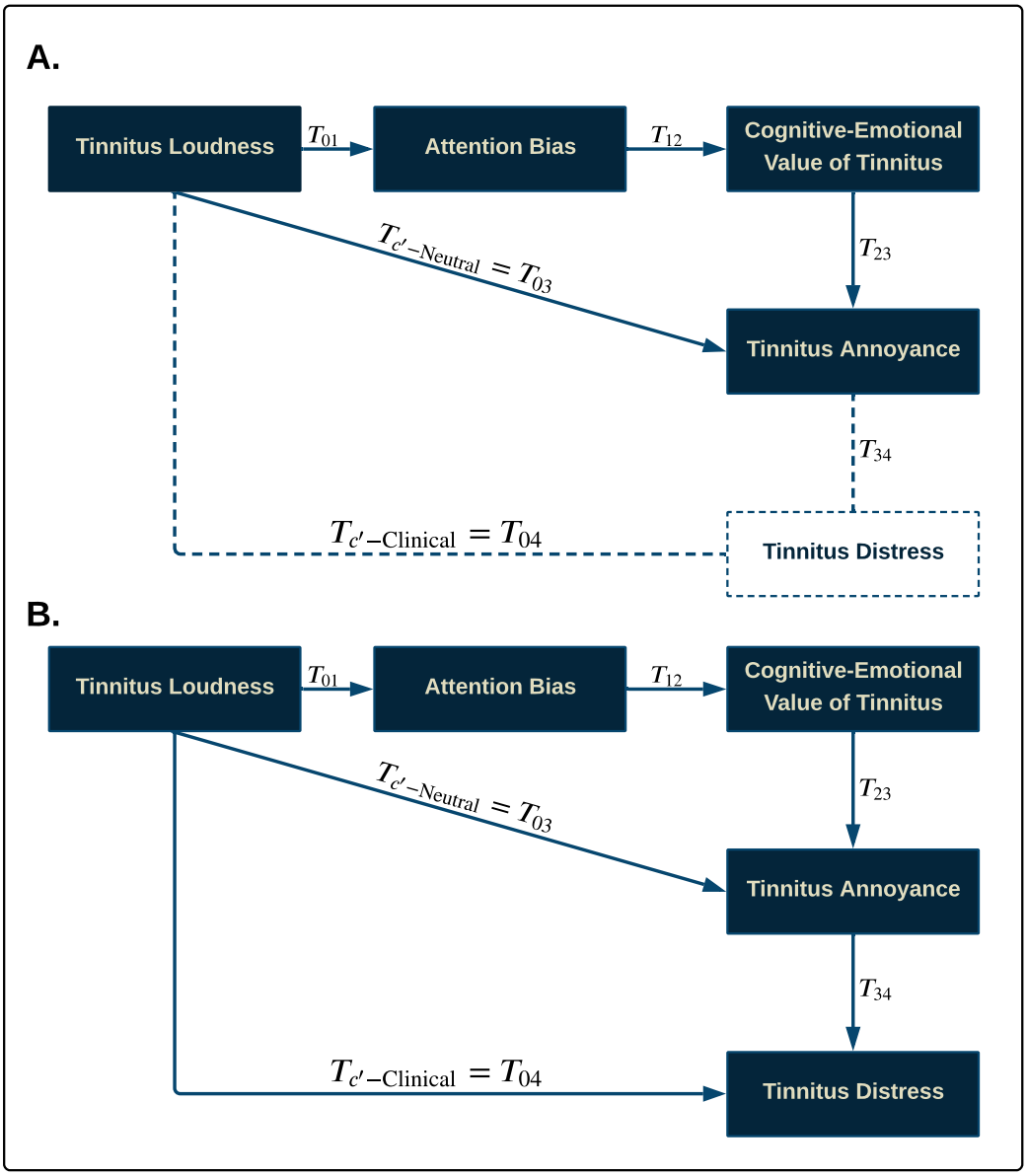

Figure 61 – **A: Neutral tinnitus mediator model** includes,
Direct effect of tinnitus loudness on tinnitus annoyance $(T_{c'-\text{Neutral}})$;
Ind-1$[T_{01} \rightarrow T_{12} \rightarrow T_{23}]$: Tinnitus Loudness $\rightarrow$ Attentional bias$\rightarrow$ Cognitive-emotional value of tinnitus$\rightarrow$ Tinnitus annoyance.

B: Clinical tinnitus mediator model includes,
Direct effect of tinnitus loudness on the Tinnitus Distress $(T_{c'-\text{Clinical}})$;
Ind-1 $[T_{01} \rightarrow T_{12} \rightarrow T_{23} \rightarrow T_{34}]$: Tinnitus Loudness $\rightarrow$ Attentional Bias $\rightarrow$ Cognitive-Emotional Value of Tinnitus $\rightarrow$ Tinnitus Annoyance $\rightarrow$ Tinnitus Distress;
Ind-2 $[T_{c'-\text{Neutral}} \rightarrow T_{34}]$: Tinnitus Loudness $\rightarrow$ Tinnitus Annoyance $\rightarrow$ Tinnitus Distress.

annoyance. The *perpetual-learning process* plays a crucial role in the transition from the Neutral stage to the Clinical one. The *neutral tinnitus model* is depicted in Figure 61-A.
The Clinical tinnitus causality model aims to reveal that clinical distress and handicap depend on the occurrence of tinnitus-related annoyance. However, in the Clinical stage, tinnitus-related annoyance arises either through *perpetual-learning process* or instantly after CAAP of tinnitus. Consequently, because of the accumulative characteristic of the ECL and appraisal in the severe Clinical stage, the CAAP of louder tinnitus leads to a more negative cognitive-emotional value resulting in severe tinnitus-related annoyance and reinforces the distress. The clinical tinnitus model is exhibited in Figure.61-B.
Higher distress levels distort perception leading to louder tinnitus CAAP, which is out of the scope of this model.

9.4 Results

9.4.1 Neutral Multi-mediation model

Multi-mediation regression analysis with the conventional least-squares method revealed that tinnitus loudness (CAAP) could lead to annoyance through either direct path or cascade mediators from attentional bias to cognitive-emotional value. The 95% confidence interval of bootstrap results of '**Ind-1;**$[T_{01} \times T_{12} \times T_{23}]$' revealed significantly different from zero , (0.236; between 0.142 to 0.350) in Full-dataset, (0.248; between 0.109 to 0.42) in Neutral-dataset, and (0.117; between 0.049 to 0.220) in Clinical-dataset.
There was no substantial evidence within the Neutral-dataset to show tinnitus loudness ($T_{C'\text{-Neutral}} = T_{03} = 0.110$, P-Value=0.202) from a direct path that might lead to tinnitus annoyance. However, the direct path from tinnitus loudness to annoyance in Full-dataset and Clinical-dataset were significant. As shown in Table 10, Table 11, and Table 12, in the full-dataset, Neutral dataset, and Clinical dataset, respectively.

9.4.2 Clinical Multi-mediation model

Multi-mediation regression analysis with the conventional least-squares method revealed that tinnitus loudness (CAAP) causes distress through either direct path or cascade mediators from attentional bias to cognitive-emotional value leading to annoyance. The 95% confidence interval of bootstrap results of '***Ind-1***;$[T_{01} \times T_{12} \times T_{23} \times T_{34}]$' revealed significantly different from zero (1.38; between 0.79 to 2.12) in Full-dataset and (0.573; between 0.211 to 1.207) in Clinical-dataset. Moreover, '***Ind-2***;$[(T_{c'-\text{Neutral}} = T_{03}) \times T_{34}]$' showed a significant difference from zero (2.114; between 1.067 to 3.50) in Full-dataset and (2.556; between 1.31 to 3.935) in Clinical-dataset. However, both the '***Ind-1***' and '***Ind-2***' were insignificant in Neutral-dataset. There was no substantial evidence to show tinnitus loudness from a direct path ($T_{c'-\text{Clinical}} = T_{04}$)

Paths and Effects	Coefficient	SE	t	LLCI	ULCI
Effect of tinnitus loudness on the attentional bias (T_{01})	0.7	0.076	9.2	0.55	0.85
Effect of attentional bias on the cognitive-emotional value of tinnitus (T_{12})	0.51	0.042	12.251	0.426	0.59
Effect of the cognitive-emotional value of tinnitus on tinnitus annoyance (T_{23})	0.667	0.04	16.65	0.588	0.745
Direct effect					
Effect of tinnitus loudness on tinnitus annoyance ($T_{c'-\text{Neutral}} = T_{03}$), [P-value < 0.01]	0.362	0.046	7.93	0.27	0.45
Indirect effects					

	Bootstrap estimate		95% CI	
	Effect	**SE**	**Lower**	**Upper**
Total indirect effect	0.236	0.054	0.142	0.35
"Ind-1": $T_{01} \rightarrow T_{12} \rightarrow T_{23}$	0.236	0.054	0.142	0.35

Table 10 – Mediator model of Neutral Tinnitus in the full dataset:
We set the Random seed number as "12020" with "10,000" Bootstrap samples.

could lead to tinnitus distress on tested datasets. As depicted in Table 10, Table 11, and Table 12, in the full-dataset, Neutral dataset, and Clinical dataset, respectively.

Paths and Effects	Coefficient	SE	t	LLCI	ULCI
Effect of tinnitus loudness on the attentional bias (T_{01})	0.584	0.144	4.05	0.296	0.872
Effect of attentional bias on the cognitive-emotional value of tinnitus (T_{12})	0.515	0.079	6,544	0.358	0.672
Effect of the cognitive-emotional value of tinnitus on tinnitus annoyance (T_{23})	0.824	0.082	10.04	0.66	0.99
Direct effect					
Effect of tinnitus loudness on tinnitus annoyance ($T_{c'-\text{Neutral}} = T_{03}$), [P-value =0.202]	0.11	0.085	1.3	-0.06	0.281
Indirect effects					

	Bootstrap estimate		95% CI	
	Effect	SE	Lower	Upper
Total indirect effect	0.248	0.079	0.109	0.42
"Ind-1": $T_{01} \rightarrow T_{12} \rightarrow T_{23}$	0.248	0.079	0.109	0.42

Table 11 – Mediator model of Neutral Tinnitus in the Neutral dataset:
We set the Random seed number as "12020" with "10,000" Bootstrap samples.

Paths and Effects	**Coefficient**	**SE**	**t**	**LLCI**	**ULCI**
Effect of tinnitus loudness on the attentional bias (T_{01})	0.573	0.089	6.44	0.398	0.748
Effect of attentional bias on the cognitive-emotional value of tinnitus (T_{12})	0.393	0.052	8	0.29	0.495
Effect of the cognitive-emotional value of tinnitus on tinnitus annoyance (T_{23})	0.52	0.05	10.331	0.421	0.619
Direct effect					
Effect of tinnitus loudness on tinnitus annoyance ($T_{c'-\text{Neutral}} = T_{03}$), [P-value < 0.01]	0.522	0.053	9.788	0.417	0.627
Indirect effects					

	Bootstrap estimate		**95% CI**	
	Effect	**SE**	**Lower**	**Upper**
Total indirect effect	0.117	0.044	0.049	0.22
"Ind-1": $T_{01} \rightarrow T_{12} \rightarrow T_{23}$	0.117	0.044	0.049	0.22

Table 12 – Mediator model of Neutral Tinnitus in the Clinical dataset:
We set the Random seed number as "12020" with "10,000" Bootstrap samples.

CHAPTER

10

NCC-LEARNING AND DEPLOYMENT SECTION: FUTURE CONCEPT

10.1 introduction

Fundamental elements of the human learning process are experimentation and observation. We already acknowledged that observing behaviors alone is insufficient to judge phenomena and their interactions with the environment to predict the outcome. Predictions' precision depends on unseen information. Therefore, the main questions are "how we integrate observation and experiment about one phenomenon to consolidate a piece of knowledge" and "how to generalize this knowledge to make the wisest decision in unexperienced situations." In the context of artificial intelligence (AI), particularly reinforcement learning (RL) analogously, "how offline data obtained from observations and be combined with online data from acquiring experiments to improve the performance of a learning agent?" The most used machine learning methodology for cognitive computing is Reinforcement Learning (RL) due to its simplistic algorithm using real-time *"trial and error"* experiments, it is depicted in Figure 62.
RL uses errors to compute trials' estimations quality and store them in the table-like data structures per the trials defined as state-action pairs. The table-like format embodies state-action data containers to compute quality functions. Therefore, RL with minimum historical data supports online learning, essential for self-adapting to the perpetual spatiotemporal fluctuation in cognitive demand. However, state-action table-like structures suffer from the curse of dimensionality. Deep Neural Network models are employed to eliminate table-like structures in the RL framework by developing efficient quality-function approximators; consequently, Deep Reinforcement Learning (DRL) is created at niche(ANDRYCHOWICZ *et al.*, 2017; IIDA; LASCHI, 2011).
Recently, Deep learning attempts to model high-level abstractions in the data by using either multiple processing layers with complex structures or multiple non-linear transformations (BENUWA *et al.*, 2016). Models conceptualized with multiple processing layers similar to the human

cerebral cortex are known as Deep Neural Network (DNN). DNNs merge feature extraction and prediction processes in a single structure using dense informative data sets. Moreover, preparing and learning strategies for complex DNN demands high computation to reach robust learning and rapid convergence towards the target. Through the Partially- Observable Markov Decision Process (POMDP), the agent observes part of the possible states of the environment leading to the flourishing ecosystem of offline reinforcement learning (LANGE; GABEL; RIEDMILLER, 2012; LEVINE *et al.*, 2020). In medicine, offline data collected from physicians might not include information from their patients' medical records and lifestyles. This lack creates confounding and will cause a naive decision support system to wrongly conclude that a treatment has positive health effects.

Of course, in such situations, the learning agent will ultimately infer the proper causal effects of taken actions if it feeds with enough online data from its interactions. Moreover, recognizing causal patterns underlying natural phenomena is essential to understanding and analyzing them. In practice for causal-pattern discovery, investigators design and execute controlled randomized experiments that induce feasibility challenges (BOLLEN, 1989; OPGEN-RHEIN; STRIMMER, 2007), Causal Reinforcement Learning (CRL) demands a prepared environment with Directed Acyclic Graph(DAGs)(PEARL, 2009) is the most practical approach. Causal pattern recognition from passively observational data becomes an attractive research field (PEARL, 2009; SPIRTES *et al.*, 2000; PETERS; JANZING; SCHÖLKOPF, 2017). Primarily, it aims to find the best-scored graph S(G), which typically is computed between the observed data prepared as Directed Acyclic Graphs (DAGs):

$$\underset{\mathscr{G}}{S(\mathscr{G})}, \text{subjet to } \mathscr{G} \in DAGs. \tag{10.1}$$

In the architecture of the NcC-learning and deployment section, we proposed a hierarchical structure in which segmented DRL layers outputs feed the CRL environment. Causality pattern discoveries can promote individualized treatment and closed-loop cognitive rehabilitation per patient or group of patients. The main contributions of the learning and deployment section are as follows

- Reinforcement learning architecture and advances
- Deep Reinforcement learning
- Causal Reinforcement learning

10.2 Reinforcement Learning

NcC mission is to solve non-trivial tasks similar to human cognition to take action upon continually varying environments. With the assistance of Reinforcement Learning, causal decision-maker agents develop a framework that can take and identify optimal action based on a certain reward (or loss) function. Therefore, Reinforcement Learning is a process where at

each state [s], the agent conducts an action [a], receiving a reward [r] from the environment. It decides the efficiency of the former state-action duets, and this process resumes until the agent adequately learns a policy. RL involves both explorations that indicate exploring different ways to achieve a particular task besides exploitation, which is the method of utilizing the current gained information and trying to increase reward at that given state.

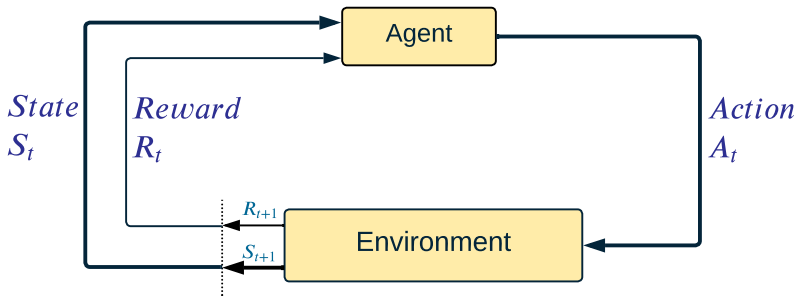

Figure 62 – Reinforcement learning, Agent at the Environment's State S_t, take action A_t to move to the next state S_{t+1},and receive Reward R_t.

NcC missions or intermediate Un/supervised data-driven models can be partially mapped as a 5-tuple function of Markov Decision Processes (MDP) in which

(i) S: set of states;

(ii) A: set of actions;

(iii) P: transition dynamics;

(iv) R: set of rewards;

(v) γ: discount factor.

The final state of Episodic MDPs occurs when the agent reaches the end of the learning procedure. The agent's goal is to interact with the controlled environment by taking actions to maximize future rewards. Episodic MDPs with time limit [T] end after T time steps eighter the goal is obtained or not.
In the RL framework, the transition construct with the 4-tuple $(s_t, a_t, r_{t+1}, s_{t+1})$. Several sequential transitions form a roll-out. A full sequence $(s_0, a_0, r_1, s_1, a_1, r_2, \ldots)$ shapes a trajectory. Consequently, a trajectory in a finite length τ is called an episode. trajectory distribution for given MDP and policy π defined as:

$$\tau_\pi = \prod_t \pi a_t|s_t) T(s_{t+1}|s_t, a_t) \tag{10.2}$$

For every episode, return is defined as the weighted sum of immediate rewards:

$$\Re = \sum_{t=0}^{\tau-1} \gamma^t r_{t+1} \tag{10.3}$$

Therefore, *expected reward maximization* is:

$$\mathbb{E}_{\tau_\Phi} \sum_{t=0}^{\tau-1} r_{t+1} \rightarrow \max_{\pi} \tag{10.4}$$

thus, given MDP and policy π, the discounted expected reward is defined:

$$G(\pi) = \mathbb{E}_{\tau_\Phi} \sum_{t=0}^{\tau-1} \gamma^t r_{t+1} \rightarrow \max_{\pi} \tag{10.5}$$

The target of the RL agent is to find an optimal policy π^*, to maximize the discounted expected reward. In the NcC, the information about the environment is gathered through clinical studies' surrogate endpoints or acquiring data sets, which are not enough to decide on the action (end of study).

RL employs Recurrent Neural Network (RNN) or accumulating observations up to that time step before processing. Maximizing the expected discount return of the weighted sum of received rewards by the agent is the objective of any RL tasks (SUTTON; BARTO, 2018). For this purpose, two types of policies

a) Stochastic $(\pi(a|s))$ where actions fit on a probability distribution;

b) Deterministic $(\mu(s))$ where they are explicitly selected for every state.

Value functions $(V_\pi(s))$ also represent the expected outcome from state s and follow policy π. Reinforcement Learning tasks classifies as model-oriented and model-free approaches. In model-based techniques, the agents learn optimal actions for every state regarding the rewards and observations. It is not necessary to learn a model for predicting the optimal actions. Supervised learning is employed to minimize a cost function based on what the agent observes from the environment.

10.3 Reinforcement Learning Algorithms

The RL agent can earn knowledge from the learning process by iteratively modeling the dynamics of the environment just by interacting with it (MOUSAVI; SCHUKAT; HOWLEY, 2017).

Generally, the learning process begins with no prior knowledge about the policy, so the action is taken randomly within the possible range. Through time the likelihood of taking random actions declines across the learning time. Consequently, action is progressively taken, reinforcing the

learned policy function.

In a nutshell, the probability of policy functions that achieve reasonable solutions increases over the learning mechanism and is exploited more frequently. The counterbalance between the random exploration of state–action space and exploitation of learned policy function through the learning models with The ε- greedy algorithm for choosing actions (LIANG *et al.*, 2019). The ability to conduct exploration in RL algorithms should always retain to achieve robust decisions to react against potential unseen states in a controlled environment.

The classical RL agent receives a piece of reward after taking each action in the controlled environment. The RL agent aims to learn an optimal policy, maximizing the discounted cumulative reward within the learning process through replicated interactions with the environment (MOUSAVI; SCHUKAT; HOWLEY, 2017). However, the Q-learning algorithm is increasingly being used based on value-based, or off-policy RL method (CHIN *et al.*, 2012) due to its efficiency and simple architecture, which does not explicitly describe policy function. The Q-learning uses the step-wise experience to formulate and update the state–action value function (WATKINS; DAYAN, 1992). The optimal Quality-value recalculates using per new learning sample (s_t, a_t, s_{t+1}, r_t). Based on the Bellman equation

$$Q^*(s_t, a_t) = Q(s_t, a_t) + \alpha_n(r_t + \gamma \max_{a' \in A} Q(s_{t+1}, a') - Q(s_t, a_t)) \tag{10.6}$$

where $Q^*(s_t, a_t)$ is a new Q-value, $Q(s_t, a_t)$ is the current Q-value of the state-action pair, α_n is the learning rate, r_t is the reward received from the environment, γ is the discount rate which can be static or change over time in order to model process in which the earlier rewards are worthier than the rewards in the future, $\max_{a' \in A} Q(s_{t+1}, a')$ is the maximum anticipated future reward, and A represents possible action space.

Following every learning iteration, Q-values are recalculated and stored in a Q-table under equal state-action pairs. Q-values for each state-action pair represent their anticipated future rewards acquired as the long-term accumulative rewards.

RL Algorithms are mainly categorized as below.

10.3.1 Value-based Methods

The value-based method based on Bellman's Equations calculates the probability of being in a given state and determines the corresponding action and policy that needs to be taken in a sequence to maximize the reward. Value-based RL algorithms include State-Action-Reward-State-Action (SARSA) and Q-Learning. SARSA is an on-policy method where the value estimations are updated towards a policy.

Q-learning is the off-policy RL algorithm that can efficiently be updated with the bootstrapped sampling of Experience Replay (ER). The one-timestamp temporal difference derives updates into achieving good convergence relying on a stationary MDP transition (CHU *et al.*, 2019).

10.3.2 Policy-based Methods

Policy-based methods are developed to directly formulate and update the policy with a sampled reward at the end of each episode (WILLIAMS, 1992). Therefore, policy-based algorithms demand numerous episodes besides a proper scoring function to converge towards the desired results. They perform in two main approaches, gradient-based and gradient-free (FU; GLOVER; APRIL, 2005; SZITA; LÖRINCZ, 2006)strategies of parameterization. In gradient-based methods, the drop-in gradient uses for optimizing the objective function.

$$J(\pi_\theta) = \mathbb{E}_{\pi_\theta}\left[f_{\pi_\theta}(.)\right] \tag{10.7}$$

where the score function (SCHULMAN *et al.*, 2015) for the policy π_θ is given by $f_{\pi_\theta}(.)$. The model's performance can be evaluated using the Equation. (10.7).

10.3.3 Reinforcement Learning Challenges

The conventional Q-learning algorithm in iteratively learning processes demands a comprehensive exploration within the entire Q-table. Exponential increases of the Q-table in NcC missions occur due to the quantization of the action space since the Mission-driven decisions must be made in similar time intervals. The quantization of Mission-driven actions is also crucial for simplifying simulation environments. It is possible to conclude that the Q-table in most of the NcC Mission-driven problems for cognitive rehabilitation can be influenced by high dimensionality. Due to the curse of dimensionality, searching between state-action pairs within table-like structures can become a problematic challange(IIDA; LASCHI, 2011). Numerous non-linear function approximation methods have been considered to avoid computing the exact Q-value within continuous space.

Usually, approximator functions segment the state-action space to compute scalable fitting distribution over continuous states and features. Function approximation methods are also suitable for estimating the Q-values of unseen regions of the state-action space during the learning process (SCHMIDHUBER, 2015).

10.4 Advanced algorithms in Deep Reinforcement Learning

The primary purpose of DRL is to integrate the policy function approximation using DNN models. DNN models for DRL relying on Convolution layers, which are superimposed along with the flattened one and several Fully Connected (FC) layers. The flattened layer converts two-dimensional features calculated by convolution layers into the one-dimensional vector that feeds FC layers. DNN models acknowledge as the Convolutional Neural Networks (CNN) contain convolution layers that manage feature extraction from the image-like inputs by mimicking

biological convolution processes in the human visual cortex (KIRAN; THOMAS; PARAKKAL, 2018). CNN model enables high-level features development by sub-sampling from the extracted features in low-level layers to improve the overall performance (GENDERS; RAZAVI, 2016). The FC layers frame structure for classifying conditions and evaluating the probability of taking each possible action regarding the transferred inputs to the CNN.
Long Short-Term Memory (LSTM) layers and the ResNet architecture in the CNN models are proposed to handle the vanishing gradient problem and induce more stable learning process.
DRL framework for cognitive rehabilitation employs CNN models within the all mentioned layers based on RNN architecture besides benefit from LSTM layers to process data sequentially and keep hidden states through time.
Furthermore, The ResNet architecture (LI, 2017) for CNN models grants a jumping connection among a group of layers (ResNet blocks) to skip beyond some layers and reuse activations from a previous layer that forced skip until the neighboring layer learns its weights. Moreover, Batch Normalization (BN) process forms an added normalization process between layers in DNN models to adjust and scale activation of layers, improving the stability and speed of DNN (LIN *et al.*, 2018). Integrating complex DNN models with the RL enhances the learning capacity to tackle complex tasks such as cognitive rehabilitation. Generally, RL approaches can be extended by using DNN models for the sake of NcC mission-driven actions through value-based, policy-based, and Actor-Critic methods (BHAGAT *et al.*, 2019). Deep Q-learning (DQL) is an enlargement of the value-based Q-learning algorithm where $Q(s_t, a_t)$ is approximated using the DNN model with weights θ;

$$Q(s_t, a_t; \theta) = Q^*(s_t, a_t) \tag{10.8}$$

The DNN receive states as input that are prepared similar to an image-like matrix or one-dimensional vectors containing various channels (*Tensor*) if needed. Regularly, matrices are populated with different mission-driven features parametrizing the same mission-driven scenario in the current action episode. The DNN model has a preset output range proportional to the possible action range. The Q-value is calculated for each action per learning iteration. The DNN model is learned to minimize the expected squared error (loss) between the predicted Q-value and the target Q-value, as characterized by the following Equation:

$$L = \mathbb{E}\left[\left(r_{t+1} + \gamma \max_{a' \in A} Q(s_{t+1}, a') - Q(s_t, a_t; \theta)\right)^2\right] \tag{10.9}$$

Target Q_{target}-values are usually calculated with similar architecture but separated from the Q-value DNN model. The Target DNN model's weighting coefficients are frequently changed by transferred coefficients θ' from the Q-value DNN model. Retaining unchanged the coefficients in the target DNN model for a preset time secures a temporally static Q-value target. That prevents the *moving target problem* and, consequently, sustains the DQL learning process and reduces drastic oscillations around taken action due to the small changes in q-value(CASAS, 2017). The

two DNN models in the DQL framework are named Double DQL. It is shown that *Double DQL* effectively mitigates the over-estimation of rewards in noisy environments, improving its overall performance (LIANG *et al.*, 2019). The target Q-value describes as

$$Q_{target}(s_t, a_t) = r_t + \gamma\, Q(s_{t+1}, \underset{a' \in A}{argmax}\; Q(s_{t+1}, a'; \theta); \theta') \tag{10.10}$$

In the *Double DQL* framework, a significant part is Experience Replay (ER). The ER supports the memory buffer for collecting the experience tuples (s_t, a_t, r_t, s_{t+1}) during the observation phase in the DQL learning process. The observation phase begins with the operational work of DQL and ends when the ER, with predefined size, is full. By the termination of the observation phase, it is possible to sample Mini-Batches from ER. Mini-Batches uses for the learning sets of inputs in the Q-value DNN model. The ER has a predefined size.

10.4.1 Prioritized Experience Memory

It enables the RL agent to learn weighted state–action transitions with the repeated experiences (CALVO; DUSPARIC, 2018). It improves the learning convergence based on the raised replay probability of samples stored in RM with a high Temporal-Difference (TD) error. TD error is the difference between the current and targeted Q-values. PER also can lead to a loss of diversity and biased outputs that can optimize by stochastic prioritization and importance sampling, respectively(SCHAUL *et al.*, 2015).

10.4.2 Dueling Deep Q-Networks

It represents the particular architecture of DNN models applied in the DQL framework. It is illustrated in figure 63. The value of each action's current state and the advantage of each action in states contribute to Q-value computation. The value of state $V(s;\theta)$ is the total expected reward in taking the likelihood action in the future steps. Advantage, expressed by $A(s,a;\theta)$, is calculated for all possible actions under the given state and taken action. The main objective is to define how significant unique action contributes to the value function compared to the other actions(WANG *et al.*, 2016; LIANG *et al.*, 2019). Therefore the Q-value is computed

$$Q^*(s_t, a_t) = A^*(s,a) + V^*(s) \tag{10.11}$$

in practical implementation, dueling DQL is computed as bellow:

$$Q^*(s_t, a_t) = V^*(s_t) + A^*(s_t, a_t) - \underset{a_{t+1}}{mean} A^*(s_t, a_{t+1}) \tag{10.12}$$

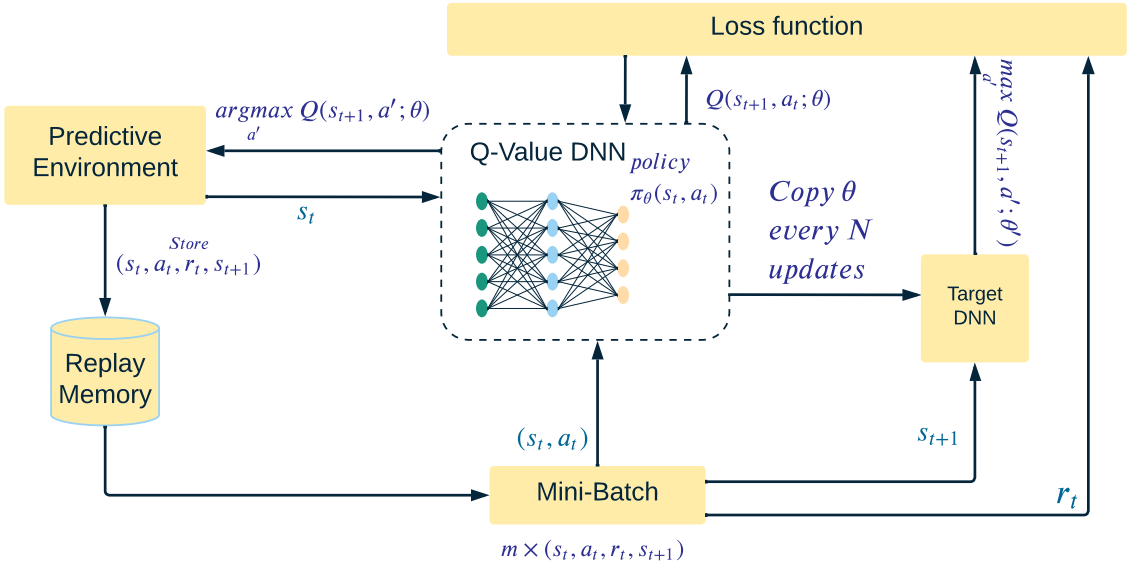

Figure 63 – The architecture of Dueling Deep Q-Network.

10.4.3 Actor-critic DRL algorithm

Actor-Critic architecture is developed based on the discrete state representation in the DRL frameworks. The architectural methodology uses two DNN models with updatable on-policy algorithms such as REINFORCE at each time step. One of these two DNN models performs the Critic's role, approximating the value function for each learning stage. This value function is adopted in the policy gradient approach. The impact of the current state on supporting the agent policy to be closer to its long-term objective assesses with TD error as described bellow.

$$TD = r_{t+1} + \gamma V(s_{t+1}) - V(s_t), \;\; 0 \leq \gamma \leq 1 \tag{10.13}$$

Actor, the second DNN model, is employed as a policy function approximator and governs how agents select actions. Generally, both DNN models train and optimize independently. A novel strategy in Actor-Critic DNN model architecture is to share convolution layers between the Actor and Critic parts in the same DNN model at the lower layer. However, at the higher layers, LSTM differentiates them (YANG *et al.*, 2019). The Actor-Critic architecture delivers current state representation from the controlled environment to both models. Based on the current state, the policy (Actor) model computes the action, changes the environment, and induces a new state for the following action interval. This new state estimates the relevant reward. The estimated reward and the new state transform into the value (Critic) model. Critic measures the Quality (Q-value) of transition from action to that state. The Actor takes the following action relying on the updated Q-value and new state, and at the same time Critic model updates its wights. At the same time, the Actor recalculates its policy parameters using Q-value. Actor-Critic architecture has two possible modifications grounded on advantage function application to reduce the value-based

method's variability and increase its learning stability. Both focus on parallel learning in the multi-agent framework.

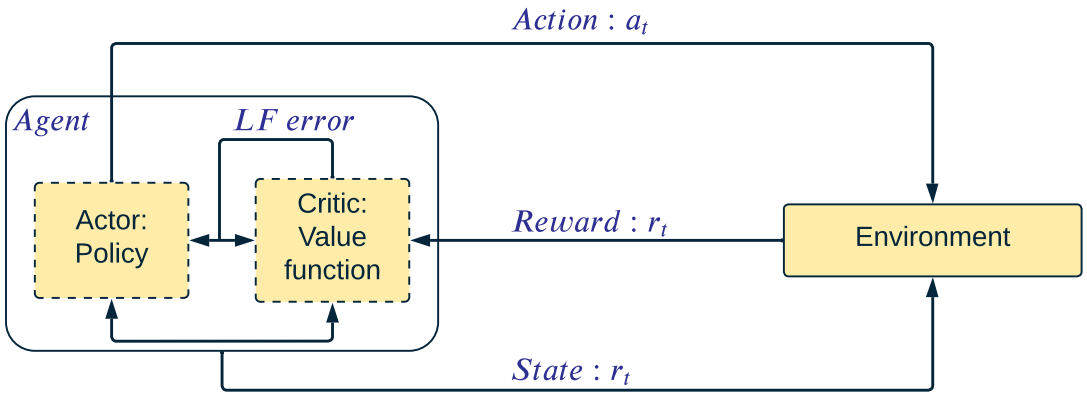

Figure 64 – The architecture of AC. The actor is to choose an action, and the critic to evaluate the advantage of the action chosen by the actor.

10.4.3.1 Advantage Actor-Critic

Mnih et al.(2016) implemented the coordinator module between the Actor's performance and global DNN model parameters, which waits for all agents to finish their share of experience before refreshing the global DNN model(MNIH *et al.*, 2016).
This approach enables all agents to begin concurrently with a similar policy. In Advantage Actor-Critic (A2C), all agents are identical with an equal set of weights and are updated simultaneously. This method demands several versions of the environment that must be executed in parallel. Knowledge only about the current state puts MDP at risk of becoming non-stationary (CHU *et al.*, 2019), particularly in complex spatiotemporal datasets such as brain networks. Furthermore, it is infeasible to insert all historical inputs to A2C; thus, include LSTM layers in its DNN models, keeping hidden states to retain short history (HOCHREITER; SCHMIDHUBER, 1997). Consequently, A2C learns more cohesively and faster through the following steps:

step 1: advantage function calculation:

$$A^{\pi}(s_t, a_t) = R(s_t, s_{t+1}) + \gamma V_w^{\pi}(s_{t+1}) - V_w^{\pi}(s_t))$$

Step 2: Target Calculation:

$$\mathscr{Y} = R(s_t, s_{t+1}) + \gamma V_w^{\pi}(s_{t+1})$$

Step 3: Critic Loss calculation with MSE loss:

$$\mathscr{L} = \frac{1}{B}\sum_{T} \|\mathscr{Y} - V^{\pi}(s_t)\|$$

Where B is batch size and $V^{\pi}(s_t)$ is denoted as:

$$v^{\pi}(s_t) = \mathbb{E}_{a_t \sim \pi(a_t|s_t)} \mathbb{E}_{s_{t+1} \sim T(s_{t+1}|a_t, s_t)} (R(s_t, s_{t+1}) + \gamma V^{\pi}|(s_{t+1}))$$

Step 4: Critic gradient Calculation:

$$\bigtriangledown^{critic} = \frac{\partial \mathscr{L}}{\partial w}$$

step 5: Actor gradient calculation:

$$\bigtriangledown^{actor} = \frac{1}{B}\sum_{T} \bigtriangledown_{\theta} \log \pi(a_t|s_t) A^{\pi}(s_t, a_t)$$

10.4.3.2 Asynchronous Advantage Actor-Critic (A3C)

Mnih et al. (2016) performed another strategy to execute an actor-critic agent. To achieve memory efficiency, Asynchronous Advantage Actor-Critic (A3C) asynchronously runs several agents in parallel on multiple instances in the environment(MNIH *et al.*, 2016). Since A3C is asynchronous, some workers carry older values of the parameters; thus, updating with the global DNN model is not optimal. There can be an issue related to policy inconsistency among some workers Considering independent exchange data between agents and the global parameters.

10.5 Causal Reinforcement learning

10.5.1 Causality Framework

Several frameworks are used for reasoning about causality (PEARL, 2009; IMBENS; RUBIN, 2015; HAYES, 2017). We introduced the causality ladder framework of Judea Pearl shortly. Association, the ladder's first level, relates to observing an external agent taking action in the environment. In contrast, intervention, the second level, describes what change happens to the environment based on only actions' occurrence. The tool of do-calculus (PEARL, 2012) builds a bridge between the two ladder levels and describes observational distributions, such as $p(y|x)$, and interventional distributions, such as $p(y|do(x))$, in a casual environment prepared like DAGs. The do-calculus can measure changes in random variables' distribution $X, Y, Z, \ldots$ when one does an unpredictable intervention do(x), which forces some variables to become values $X = x$ despite their causal ancestors. It is grounded on a comprehensive set of rules (HUANG; VALTORTA, 2012; SPENCER *et al.*, 2021), which make possible the following rules when specific structural conditions are met in the causal DAG:

R1: insertion/deletion of observations

$$p(y|do(x), z, w) = p(y|do(x), w)$$

R2: action/observation exchange

$$p(y|do(x), do(z), w) = p(y|do(x), z, w)$$

R3: insertion/deletion of actions

$$p(y|do(x),do(z),w) = p(y|do(x),w).$$

For further information about do-calculus, we refer to Pearl (PEARL, 2012). We utilize these rules to derive formal solutions to model-based CRL in multiple POMDP settings. It is depicted in Figure 65.

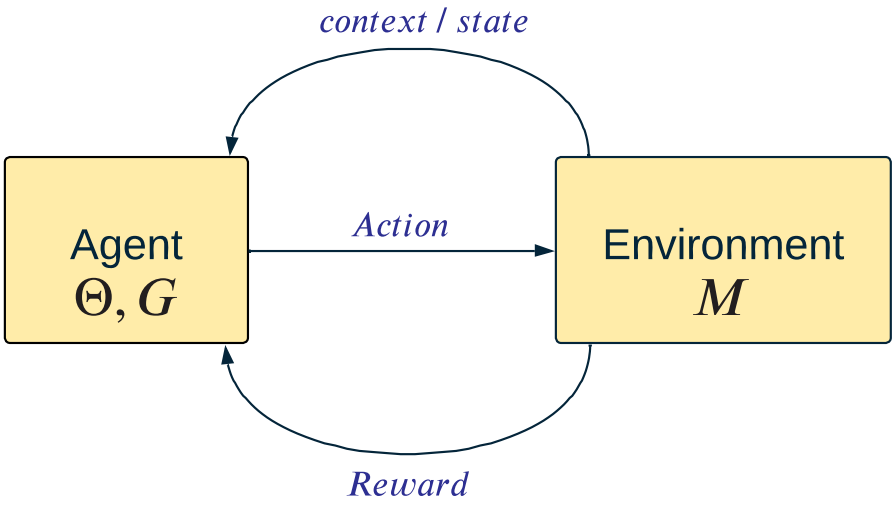

Figure 65 – The architecture of the Causal Reinforcement Learning.

10.5.2 Partially-Observable Markov Decision Processes (POMDPs)

of the 7-tuple function M = $(S, A, O, p_{trans}, r, P_{obs}, Pinit)$, as it is defined:

- Finite set of states, S
- Finite set of actions, A
- Finite set of Observation, O
- Probabilistic state-action transition, T, $p_{trans}(s_{t+1}|s_t, a_t)$
- Reward for each state/action pair*: $r(s,a)$
- conditional observation probabilities : $p_{obs}(o|s)$
- Distribution of initial state $P_{init} = (s_0)$

A standard scenario for POMDPs is when actions are taken considering all the available information from the past (ZHOU *et al.*, 2021). The stochastic policy $\pi(a_t|h_t)$ together with the POMDP

dynamics $p_{init}, p_{obs} and p_{trans}$ defines a probability distribution over trajectories τ as a control mechanism:

$$p_{std}(\tau) = \sum_{s_0 \to |\tau|}^{S^{|\tau|+1}} p_{init}(s_0) p_{obs}(o_0|s_0) \prod_{t=0}^{|\tau|-1} \pi(a_t|h_t) p_{trans}(s_{t+1}|s_t, a_t) p_{obs}(o_{t+1}|s_{t+1}) \quad (10.14)$$

10.6 NcC-Learning conceptual Process of Reinforcement Learning for cluster prediction; Future Trends

In NcC-Learning architecture, We defined and conceptualized an architecture to achieve mission-driven targets (unsupervised clustering)based on Deep Reinforcement Learning. We selected the one-step hierarchical Asynchronous Advantage Actor-Critic (A3C) strategy for DRL in NcC_Clustering optimization. Primarily suggesting DRL can optimize clustering with training dataset and train the agents to develop actions and policies for prediction through un/partially seen observations. After the training phase, agents use the predictive DRL with the similar A3C strategy and continue learning to improve the trained actions to update clusters patterns or emerge new actions and policies.

Therefore, we constructed the NcC Cluster pattern from the discovered Medoids as the initial core of policies and initial states in the environment ($\mathscr{E}$). DRL agent receives the training dataset randomly to take action a and find the next State that maximizes the received reward. We consider a 4-tuple $\overset{c}{MDP}(S, A, R, \gamma)$, where:

- Policy (c in $\overset{c}{\pi}$)
  In NcC Projected Model **c** is a cluster number (pointer) formed by the NcC_Clutering, and the medoid belongs to that to perform robust and homogeneous segments in the environment.

- State (S)
  We defined S based on observations in the training data, ordered randomly, and the sample size can be boosted with bootstrap. Each observation will be represented in n-step and 4-tuple [CF_n, CDF_Lb, CDF_Ub, PDF] and n = | NcC_Causal Feature |. During the DRL training phase, the possible initial states are cluster patterns.

- Action (A)
  We proposed A as a set of actions the agent can take to identify the observations' cluster and accumulate rewards through state steps.

- Reward(R)
  We projected reward for transactions from State t to the state t+1 accumulating based on the partially received at each step of step(n). At each step, the reward is calculated based on the multiplication of three factors as bellow

1. **Ratio of the Quanta's number of repetition** ($\overset{c}{R}_{f_1,n}$)

$$\overset{c}{R}_{f_1,n} = \frac{\overline{Q_{S_{tm,n}}}}{\overline{Max(Q_{S_{t,n}})}}, \text{When} \quad Q_{S_{tm,n}} == Q_{S_{t+1,n}} \tag{10.15}$$

2. **Ratio of the Quanta value** ($\overset{c}{R}_{f_2,n}$)

$$\overset{c}{R}_{f_2,n} = \frac{Q_{S_{tm,n}}}{\sum(\exists! Q_{S_{t,n}})}, \text{When} \quad Q_{S_{tm,n}} == Q_{S_{t+1,n}} \tag{10.16}$$

3. **Normalized Mutual information between the Steps** ($\overset{c}{R}_{f_3,n}$)
it is a global factor and independent of policy ($\overset{c}{\pi}$)

$$\overset{c}{R}_{f_3,n} = I(D_n; D_{n+1}) \tag{10.17}$$

Consequently,

$$\overset{\mathbf{c}}{\mathbf{R}} = \sum_{n=1}^{D} (\overset{c}{R}_{f_1,n} \times \overset{c}{R}_{f_2,n} \times \overset{c}{R}_{f_3,n}) \tag{10.18}$$

Reward also is a dependent value to the policy.

- Discount Factor (γ)
W defined the Discount factor (0,1] based on the inverse of NcC_Distance between new observation and Cluster pattern:

$$\gamma = \begin{cases} 1 & D = 0 \\ \\ \frac{1}{D} & D \neq 0 \end{cases} \tag{10.19}$$

We suggest Convolutional Neural Networks (CNN) form Q value, which is the part of Asynchronous Advantage Actor-Critic (A3C) architecture. A3C preserves a policy $\pi(a_t|s_t;\theta)$ and an estimate of the value function $V(s_t;\theta_v)$. The variant of actor-critic works in the forward view and utilizes the mix of n-step accumulated rewards to update the policy and value-function. The policy and value-function are updated after every t_{max} action or at the terminal state. The update accomplished by the algorithm can be seen as $\bigtriangledown_{\theta'} log\pi(a_t|s_t;\theta')A(s_t,a_t;\theta,\theta_v)$ where $A(s_t,a_t;\theta,\theta_v)$ is an estimate of the advantage function given by

$$\sum_{i=1}^{k-1} \left\{ r_t + (\bigcap_{p=1}^{i} \gamma_p) r_{t+i} + (\bigcap_{p=1}^{k} \gamma_p) V(s_{t+k};\theta_v) - V(s_t;\theta_v) \right\}, \tag{10.20}$$

where k can vary from state to state and is upper bounded by t_{max}, based on the NcC Mission-driven problems (Cluster optimization).In other words, the maximum number of cluster members

can update the policy regulating the k. We already presented the pseudo-code for the algorithm in **algorithm 3** in which the policy(cluster pattern) updates with each new member due to the current averaging distance strategy of NcC_clustering. However, if instead, we employ distance from cluster pattern strategy k can regulate the minimum members are needed to be marked with the current policy(cluster) before updating Cluster pattern and policy.

Parameters θ of the policy and $\theta_v$of the value function are considered separate for generality, but we always share some factors in practice. We generally operate a Convolutional Neural Networks with one particular output for the policy $\pi(a_t|s_t;\theta)$ and one linear output for the value function $V(s_t;\theta_v)$, sharing all non-output layers. Similar to the value-based strategies, we rely on parallel actor-learners and integrated updates to enhance training stability.
Previous studies (MNIH *et al.*, 2016)showed that adding the policy's entropy to the objective function might enhance exploration by discouraging premature convergence to suboptimal deterministic policies. Williams et al. (1991) documented that including entropy is beneficial for tasks requiring hierarchical behavior. The gradient of the entire objective function, including the entropy regularization term concerning the policy parameters, takes the form

$$\bigtriangledown_{\theta'} log\pi(a_t|s_t;\theta')(R_t - V(s_t;\theta_v)) + \beta \bigtriangledown_{\theta'} H(\pi(s_t;\theta')) \tag{10.21}$$

where H is the entropy. The hyper-parameter governs the strength of the entropy regularization term. Further optimization strategies are required to improve the method in higher-step Asynchronous Advantage Actor-Critic (A3C), but in the suggested one-step A3C, recursive greedy algorithm as we introduced can optimize the NcC mission in clustering optimization and predictive analytics for unseen data in Future. We also consider the maximum distance and the minimum reward satisfactory levels as meta-information to support the regulatory factors for the agent learning quality evaluation in the Future deploying Deep Reinforcement Learning (DRL) applications.

10.6.1 Conceptual algorithm for Hierarchical Asynchronous Advantage Actor-Critics

Algorithm 3 One-step Hierarchical Actor-critics for Unbalanced NcC_DRL-Clustering (Training and Optimization)

Assume global shared parameter vectors θ, θ_v, and $r_{min} = NaN$ are global counter $T = 0$.
Assume Thread-specific parameter vector θ' and θ'_V for each cluster
NcC_Clustering makes Policies and one-to-one actions for cluster discovery.
Initiate state s_t for each policy is its Cluster Pattern $_j$)
repeat
  Reset Gradients: $d\theta \leftarrow 0$ and $d\theta_v \leftarrow 0$
  Synchronize Thread-specific parameters $\theta' = \theta$ and $\theta'_v = \theta_v$
  $t_{\text{start}} = t$, relies on Cluster and is equal to corresponding(Thread) Cluster pattern
  Get the state s_t
  for $s_t \in ClusterPatterns(\pi_j)$ **do**
    for $s_{t+1} \in Training\_Set$ **do**
      Perform a_j in policy $\overset{c}{\pi}_j(a_j|s_t;\theta'_t)$, c_j shows jth NcC_CPat (π_j) and drive action a_j
      Receive reward $r_{t,j}$ and new state $s_{t+1,j}$
      Save results to Replay Memory, $Rem_j \leftarrow (s_{t,j}, a_j, r_{t,j}, \theta'_{t,j}, s_{t+1,j})$, and $\theta' = \theta$
    Sort Rem_j descendingly based on the values of $r_{t,j}$
  Copy all rem_{j1} to a buffer, $BF = (s_{t+j1}, a_{j1}, r_{t,j1}, \theta'_{t,j1}, s_{t+1,j1})$
  Sort BF descendingly based on the values of $r_{t,j}$
  for $k \in BF$ **do**
    if $(\overset{*}{s}_{t+1})_{j,k} == (s_{t+1})_l, 1 \le l \le k-1$ **then**
      $d = 2, m = 0$
      repeat
        if $(\overset{*}{s}_{t+1})_{Rem_{jd}} \neq (s_{t+1})_{BF(l)}, 1 \le l \le k-1$ **then**
          if $(\overset{*}{r}_t)_{Rem_{jd}} \ge Max((r_t)_{BF(l)}), k < l \le |BF|$ **then**
            Copy Rem_{jd} to the end of BF, and descendingly sort $BF(l), k < l \le |BF|$
            $m \leftarrow 1$
        $d \leftarrow d + 1$
      until *($d == |Rem_j|$ or $m == 1$)*
      Delete $BF(k)$
  for $U_{j,k} \in BF$ **do**
    $R = V_j(S_{t,j}, \theta'_{v,j})$
    $R \leftarrow r_{t,j} + \gamma R$
    Accumulate gradients W.r.t : $\theta'_j : d\theta_j \leftarrow d\theta_j + \nabla_{\theta'_{t,j1}} log\pi(a_j|S_{t,j};\theta'_{t,j})(R - V_j(S_{t,j};\theta'_{v,j}))$
    Accumulation gradients W.r.t :$\theta'_{v,j} : d\theta_{v,j} \leftarrow d\theta_{v,j} + \partial(R - V(S_{t,j};\theta'_{v,j}))^2/\partial\theta'_{v,j}$
    Update π_j and corresponding cluster Pattern
    $r_{min} = min(r_{min}, r_t)$
  $Training\_set(s_{t+1} \in BF) = NaN$
  Reset All Rem_j and BF
until *($Training\_Set \neq NaN$)*

10.7 Conclusions and Future Trends

In the Proposed Hierarchical Actor-critics, Agents can learn and update the cluster patterns (Policy) with new data. Relying on developed NcC algorithms, the A3C-DRL provides the following advantages:

- after initial training phased replay memory is unnecessary.
- unbalanced clusters can be emerged and be updated during the agent lifetime.
- unsupervised classification (Clustering) is unaffected by noisy data.
- since the distribution of the causal features is significantly unchanged, alterations in quantization do not affect the prediction and classification quality.
- similar method can be generalized for multichannel tensor time-series by increasing the steps before each update associated with the intrinsic of the environment.

NcC_clusters classify homogenous data, which can fuel decision-making based on the mission-driven task of neurocognitive computing. Considering cluster policy(Cluster pattern) dependency on saving raw data and relying on DRL for updating, future additional features can update patterns without extinguishing and retraining the current patterns. Furthermore, Closed-loop control of the electrical stimulation with the suggested DRL algorithm is feasible for dose diet control to improve the individualized electrical stimulation efficacy in the future. All the abovementioned advantages are achievable within the suggested Neurocognitive computing architecture. Future scholars and students can implement and deploy NcC in various fields and applications or optimize its calculation and time demand performance.

CHAPTER

11

LISTAS

11.1 list of abbreviations

\

#1 functional Magnetic Resonance Imaging; *Chapter(1, 2, 3)* (fMRI)

Cognitive Computing; *Chapter(1)* (CC)

Neurocognitive Computing; *Chapter(1, 7, 8, 9, 10)* (NcC)

Application Programming Interface; *Chapter(1)* (API)

Feature Selection; *Chapter(1, 7, 8)* (FS)

Feature Transformation; *Chapter(1, 7,8)* (FT)

integrated Cognitive Rehabilitation Platform; *Chapter(2, 5, 6)* (iCRP)

Electroencephalogeraphy; *Chapter(2, 3, 5)* (EEG)

magnetoencephalography; *Chapter(2, 3)* (MEG)

Thalamic reticular nucleus; *Chapter(2, 3)* (TRN)

pre-frontal cortex; *Chapter(2, 3)* (PFC)

medial geniculate body; *Chapter(2, 3)* (MGB)

dorsomedial; *Chapter(2, 3)* (DM)

nucleus accumbens; *Chapter(2, 3)* (NAc)

ventral pallidum; *Chapter(2,3)* (VP)

medial geniculate nucleus; *Chapter(2,3)* (MGN)

posterior orbitofrontal cortex; *Chapter(2,3)* (pOFC)

ventromedial; *Chapter(2, 3)* (vm)

Gamma-aminobutyric acid; *Chapter(2, 3)* (GABA)

inferior colliculus; *Chapter(2, 3)* (IC)

intercalated cells; *Chapter(2, 3)* (ITC)

superior olivary complex; *Chapter(2,3)* (SOC)

basolateral amygdala; *Chapter(3)* (BLA)

blood oxygen level-dependent; *Chapter(2)* (BOLD)

mediodorsal nucleus; *Chapter(2, 3)* (MDN)

dorsal cochlear nucleus; *Chapter(2, 3)* (DCN)

anterior cingulate cortex; *Chapter(2, 3, 3)* (ACC)

Lateral PFC; *Chapter(2, 3, 5)* (lPFC)

conscious perception process; *Chapter(2, 3)* (CPP)

Single-photon emission computed tomography; *Chapter(3)* (SPECT)

Positron emission tomography; *Chapter(3)* (PET)

Evaluative Conditional Learning; *Chapter(2, 3, 4, 5)* (ECL)

anterior cingulate cortex; *Chapter(2)* (ACC)

Conditional Stimulus; *Chapter(2, 3, 4)* (CS)

Unconditional Stimulus; *Chapter(2, 3, 4)* (US)

transcranial Direct Current Stimulation; *Chapter(2, 4, 5)* (tDCS)

High Definition; *Chapter(2, 4, 5)* (HD)

Neurofunctional Tinnitus Model; *Chapter(3, 5)* (NfTM)

Conceptual Cognitive Framework; *Chapter(4, 9)* (CCF)

Cognitive Behavioural Therapy; *Chapter(4)* (CBT)

Mindfulness-Based Cognitive Therapy; *Chapter(4)* (MBCT)

Mindfulness-based interventions; *Chapter(4)* (MBI)

Food and Drug Administration; *Chapter(5)* (FDA)

Mili Amper; *Chapter(5)* (mA)

Tinnitus Loudness Questionnaire; *Chapter(5, 6)* (TLQ)

positive emotion induction; *Chapter(5, 6)* (PEI)

Hearing Threshold Level; *Chapter(5)* (HTL)

Loudness Match Test; *Chapter(5)* (LMT)

Minimal Masking Level; *Chapter(5)* (MML)

Pitch Matching test; *Chapter(5)* (PMT)

Discomfort Level; *Chapter(5)* (DL)

Tinnitus Handicap Inventory; *Chapter(5, 6, 9)* (THI)

Minimum Clinical Efficacy; *Chapter(5)* (δ)

"Sham concurrent with PEI (SP)"; *Chapter(5, 6)* ("SP")

"tDCS concurrent with PEI (tP)"; *Chapter(5)* ("tP")

Coefficient of Variance; *Chapter(5)* (CV)

Adaptive-Seamless Bayesian; *Chapter(5)* (ASB)

Minutes; *Chapter(5)* (Min)

Conscious Attended-Awareness Perception; *Chapter(4, 5, 9)* (CAAP)

Region Of Interest; *Chapter(5)* (ROI)

Dorsolateral Prefrontal Cortex; *Chapter(5)* (dlPFC)

Emotional Stroop Task; *Chapter(4, 5)* (EST)

Neurofunctional Tinnitus Model; *Chapter(5)* (NfTM)

Tinnitus Impairment Questionnaire; *Chapter(5, 6)* (TBF-12)

Major Depression Inventory; *Chapter(5, 6)* (MDI)

State Trait Anxiety Inventory Small Questions; *Chapter(5, 6)* (STAI-S6)

Clinical Global Impression; *Chapter(5, 6)* (CGI)

Mini Sleep Questionnaire; *Chapter(5, 6)* (MSQ)

Nencki Affective Picture System; *Chapter(5)* (NAPS)

arousal-ratio; *Chapter(5)* (Ar)

Valence-ratio; *Chapter(5)* (Vr)

resting-state; *Chapter(5)* (rs)

event-related potential; *Chapter(5)* (ERP)

Late Positive Potential; *Chapter(5)* (LPP)

high-arousal-valence pictures; *Chapter(5)* (HAV)

high-valence Pictures; *Chapter(5)* (HV)

Electronic Geodesic Incorporation; *Chapter(5)* (EGI)

Tinnitus Sample Case History Questionnaire; *Chapter(6)* (TSCHQ)

Tinnitus Severity; *Chapter(6)* (TS)

principal component analysis; *Chapter(7)* (PCA)

Kernel Principal Component Analysis; *Chapter(7)* (kPCA)

Locally Linear Embedding; *Chapter(7)* (LLE)

t-Distributed Stochastic Neighbor Embedding; *Chapter(7)* (t-SNE)

Independent Component Analysis; *Chapter(7)* (ICA)

Dimensionality Reduction via Regression; *Chapter(7)* (DRR)

mutual information; *Chapter(7)* (MI)

quanta; *Chapter(7)* (q)

Minimum Squared Error; *Chapter(7)* (MSE)

Mutual Information; *Chapter(7)* (MI)

Normalized MI; *Chapter(7)* (NMI)

CausalSpace Toolbox; *Chapter(7)* (CST)

Principal Components Analysis; *Chapter(7)* (PCA)

Independent Component Analysis; *Chapter(7)* (FastICA)

Locally Linear Embedding; *Chapter(7)* (LLE)

Non-Negative Matrix Factorization; *Chapter(7)* (NNMF)

Dimensionality Reduction via Regression; *Chapter(7)* (DRR)

Fruchterman Reingold Graph Layout; *Chapter(7)* (Fruchterman Reingold)

Kernel Principal Component Analysis; *Chapter(7)* (kPCA)

Non-Metric Dimensional Scaling; *Chapter(7)* (nMDS)

Distributed Recursive Graph Layout; *Chapter(7)* (DrL)

Self-Organized Tree Algorithm; *Chapter(7, 8)* (SOTA)

Average Distance; *Chapter(7, 8)* (AD)

Figure of Merit; *Chapter(7, 8)* (FOM)

Average Proportion of Non-overlap; *Chapter(7, 8)* (APN)

Average Distance between Means; *Chapter(7, 8)* (ADM) Cognitive-Behavioral Model; *Chapter(7)* (CBM)

Fresh noise; *Chapter(5)* (FN)

Hearing Level; *Chapter(5)* (HL)

Testing Tone; *Chapter(5)* (TT)

transcranial Electrical Stimulation; *Chapter(5)* (tES)

Loudness Misperception Correction; *Chapter(5)* (LMC)

Pure-tone audiometry; *Chapter(5)* (PTA)

narrow-band noise; *Chapter(5)* (NBN)

loudness discomfort level; *Chapter(5)* (LDL)

Brodmann areas; *Chapter(5)* (BA)

computer-aided design; *Chapter(5)* (CAD)

Finite element; *Chapter(5)* (FE)

electric field; *Chapter(5)* (EF)

Ordinary Least Square; *Chapter(5)* (OLS)

Non-invasive Brain Stimulation; *Chapter(5)* (NIBS)

Deep Neural Network; *Chapter(1, 10)* (DNN)

Reinforcement Learning; *Chapter(1, 10)* (RL)

Causal Reinforcement Learning; *Chapter(10)* (CRL)

Deep Reinforcement Learning; *Chapter(1, 8, 10)* (DRL)

Recurrent Neural Network; *Chapter(10)* (RNN)

Markov Decision Processes; *Chapter(10)* (MDP)

State-Action-Reward-State-Action; *Chapter(10)* (SARSA)

Experience Replay; *Chapter(10)* (ER)

Fully Connected; *Chapter(10)* (FC)

Convolutional Neural Networks; *Chapter(10)* (CNN)

Long Short-Term Memory; *Chapter(10)* (LSTM)

Batch Normalization; *Chapter(10)* (BN)

Deep Q-learning; *Chapter(10)* (DQL)

Partially- Observable Markov Decision Process; *Chapter(10)* (POMDP)

Directed acyclic graph; *Chapter(10)* (DAG)

Mathews Correlation Coefficient; *Chapter(10)* (MCC)

Advantage Actor-Critic; *Chapter(10)* (A2C)

Asynchronous Advantage Actor-Critic; *Chapter(10)* (A3C)

11.2 symbols and Notations

$\backslash$

#1

$\mathfrak{R}^d$

$\mathscr{H}$

$\Phi(\cdot)$

$N_{\mathscr{H}}$

$d_{ij}^{\mathfrak{X}}, d^{\mathfrak{X}}(\mathbf{x}_i, \mathbf{x}_j)$

N_i^k

N_i^{ε}

$\mathfrak{Y}$

$\mathscr{M}$

$\mathscr{N} - pdf$

$q_{k,l}$

$TPQ_{[X,Y]}$

$TPQ_{[X_1,X_2,\ldots,X_n]}$

$H(X)$

$H(X,Y)$

$MI(X,Y)$

$\Pi_j^{(n)}, \Pi_j(X_1,\ldots,X_n)$

$N_{n,j}, |\Pi_j^{(n)}|$

$x_{\pi_j^{(n)}(i)}$

$\mathfrak{X}$

$\mathscr{Y}$

$\mathscr{U}$

$\mathscr{M}^{(k)}$

$X_{S_i^{(k)}}$

$\mathscr{P}^{(k)}$

$\mathscr{U}^{(k)}$

N_{Opt}

$\mathscr{N}^{(k)}$

$\mathscr{F}$

$a_i^{(k)}$

$b_i^{(k)}$

$c_i^{(k)}$

$a_{-i}^{(k)}$

$b_{-i}^{(k)}$

$c_{-i}^{(k)}$

$\mathscr{C}_k$

$\mathscr{P}(\hat{X}_k)$

$d_j^{(k)}$

$e_j^{(k)}$

$f_j^{(k)}$

$u_j^{(k)}$

$v_j^{(k)}$

$w_j^{(k)}$

α

β

f_M

ρ_{Total}

$dCorr(X,Y)$

$dCov(X,Y)$

$dVar(X)$

Q_{local}

Q_{global}

$R_{NX}(k)$

$r^2(D,\hat{D})$

$d_{Eu}(x,y)$

$d_1(O_i,O_j)$

$H(O_{i_f},O_{j_f})$

$MI(O_{i_f}, O_{j_f})$

$F(O_{i_f}^{-})$

$p_H(O_{i_f})$

$d_2(O_i, O_j)$

$\mathscr{O}$

$d(O_i, O_j)$

$\mathscr{C}$

$O(m)$

$D_1(O_i, \mathscr{C})$

$D_2(O_i, \mathscr{C})$

$D(O_i, \mathscr{C})$

$\mathfrak{M}^{(k)}$

C_k

n_k

$O_{S_i^{(k)}}$

$\mathscr{S}$

$p_{Optimal}$

$n^{(k)}$

$O_i^{(k)}$

$\mathscr{S}^{(k)}$

$\mathscr{S}^{(k)}$

C_{-l}

$x_{i,nn(j)}$

$n(C(i))$

$S(i)$

$D(\mathscr{C})$

$C^{i,l}$

$C^{i,0}$

$APN(\mathscr{C})$

$AD(\mathscr{C})$

$\bar{x}_{C^{i,0}}$

$\bar{x}_{C^{i,l}}$

BIBLIOGRAPHY

ABE, K. Modulation of hippocampal long-term potentiation by the amygdala: a synaptic mechanism linking emotion and memory. **Jpn J Pharmacol**, v. 86, n. 1, p. 18–22, 2001. ISSN 0021-5198 (Print) 0021-5198 (Linking). Abe, K Japan Jpn J Pharmacol. 2001 May;86(1):18-22. Available: <http://www.ncbi.nlm.nih.gov/pubmed/11430468https://www.jstage.jst.go.jp/article/jjp/86/1/86_1_18/_pdf>. Citation on page 62.

ADJAMIAN, P.; SEREDA, M.; HALL, D. A. The mechanisms of tinnitus: perspectives from human functional neuroimaging. **Hear Res**, v. 253, n. 1-2, p. 15–31, 2009. ISSN 1878-5891 (Electronic) 0378-5955 (Linking). Adjamian, Peyman Sereda, Magdalena Hall, Deborah A Netherlands Hear Res. 2009 Jul;253(1-2):15-31. Epub 2009 Apr 11. Available: <http://www.ncbi.nlm.nih.gov/pubmed/19364527http://ac.els-cdn.com/S0378595509000860/1-s2.0-S0378595509000860-main.pdf?_tid=3f4d43a87c6b2f517a1e5fca0055458a&acdnat=1340992235_c847e875d3cdc37bc2e9e088c23b2fbb>. Citations on pages 77 and 87.

ALSTER, J.; SHEMESH, Z.; ORNAN, M.; ATTIAS, J. Sleep disturbance associated with chronic tinnitus. **Biol Psychiatry**, v. 34, n. 1-2, p. 84–90, 1993. ISSN 0006-3223 (Print) 0006-3223 (Linking). Alster, J Shemesh, Z Ornan, M Attias, J Biol Psychiatry. 1993 Jul 1-15;34(1-2):84-90. Available: <http://www.ncbi.nlm.nih.gov/pubmed/8373941http://ac.els-cdn.com/000632239390260K/1-s2.0-000632239390260K-main.pdf?_tid=86c89760-892d-11e2-ad87-00000aab0f26&acdnat=1362884120_305b02ff8589fbad9b3e6f68765f301d>. Citation on page 64.

ALVAREZ, J. A.; EMORY, E. Executive function and the frontal lobes: a meta-analytic review. **Neuropsychol Rev**, v. 16, n. 1, p. 17–42, 2006. ISSN 1040-7308 (Print) 1040-7308 (Linking). Alvarez, Julie A Emory, Eugene R01 MH 64732/MH/NIMH NIH HHS/ Neuropsychol Rev. 2006 Mar;16(1):17-42. Available: <http://www.ncbi.nlm.nih.gov/pubmed/16794878http://download.springer.com/static/pdf/76/art%253A10.1007%252Fs11065-006-9002-x.pdf?auth66=1365515490_cc8eca13a24c7441e45dc3f883545dfc&ext=.pdf>. Citation on page 63.

AMBROGGI, F.; ISHIKAWA, A.; FIELDS, H. L.; NICOLA, S. M. Basolateral amygdala neurons facilitate reward-seeking behavior by exciting nucleus accumbens neurons. **Neuron**, v. 59, n. 4, p. 648–61, 2008. ISSN 1097-4199 (Electronic) 0896-6273 (Linking). Ambroggi, Frederic Ishikawa, Akinori Fields, Howard L Nicola, Saleem M DA019473/DA/NIDA NIH HHS/ R01 DA019473-01A1/DA/NIDA NIH HHS/ R01 DA019473-02/DA/NIDA NIH HHS/ R01 DA019473-03/DA/NIDA NIH HHS/ R01 DA019473-04/DA/NIDA NIH HHS/ Neuron. 2008 Aug 28;59(4):648-61. doi: 10.1016/j.neuron.2008.07.004. Available: <http://www.ncbi.nlm.nih.gov/pubmed/18760700http://ac.els-cdn.com/S0896627308005734/1-s2.0-S0896627308005734-main.pdf?_tid=285ca094-892e-11e2-8b5f-00000aacb35e&acdnat=1362884391_8f2bcc2d3fd2bcbf736a19abe738bf51>. Citation on page 64.

ANDERSON, B. A.; LAURENT, P. A.; YANTIS, S. Value-driven attentional capture. **Proc Natl Acad Sci U S A**, v. 108, n. 25, p. 10367–71, 2011. ISSN 1091-6490 (Electronic) 0027-8424 (Linking). Anderson, Brian A Laurent, Patryk A Yantis, Steven R01-DA013165/DA/NIDA NIH HHS/ Proc Natl Acad Sci U S A. 2011 Jun 21;108(25):10367-71. doi: 10.1073/pnas.1104047108.

Epub 2011 Jun 6. Available: <http://www.ncbi.nlm.nih.gov/pubmed/21646524http://www.pnas.org/content/108/25/10367.full.pdf>. Citation on page 68.

ANDERSON, J. R. **The architecture of cognition**. [S.l.]: Psychology Press, 1996. Citation on page 45.

ANDERSSON, G.; BAKHSH, R.; JOHANSSON, L.; KALDO, V.; CARLBRING, P. Stroop facilitation in tinnitus patients: an experiment conducted via the world wide web. **Cyberpsychol Behav**, v. 8, n. 1, p. 32–8, 2005. ISSN 1094-9313 (Print) 1094-9313 (Linking). Andersson, Gerhard Bakhsh, Raghad Johansson, Linda Kaldo, Viktor Carlbring, Per Cyberpsychol Behav. 2005 Feb;8(1):32-8. Available: <http://www.ncbi.nlm.nih.gov/pubmed/15738691http://www.liebertonline.com/doi/abs/10.1089/cpb.2005.8.32http://www.liebertonline.com/doi/pdfplus/10.1089/cpb.2005.8.32>. Citation on page 91.

ANDERSSON, G.; JURIS, L.; CLASSON, E.; FREDRIKSON, M.; FURMARK, T. Consequences of suppressing thoughts about tinnitus and the effects of cognitive distraction on brain activity in tinnitus patients. **Audiol Neurootol**, v. 11, n. 5, p. 301–9, 2006. ISSN 1420-3030 (Print) 1420-3030. Citation on page 92.

ANDERSSON, G.; KALDO, V. Internet-based self-help treatment of tinnitus. **Tinnitus treatment: Clinical protocols**, p. 29–40, 2006. Citation on page 94.

ANDERSSON, G.; LYTTKENS, L. A meta-analytic review of psychological treatments for tinnitus. **British journal of audiology**, Taylor & Francis, v. 33, n. 4, p. 201–210, 1999. Citation on page 93.

ANDERSSON, G.; LYTTKENS, L.; HIRVELA, C.; FURMARK, T.; TILLFORS, M.; FREDRIKSON, M. Regional cerebral blood flow during tinnitus: a pet case study with lidocaine and auditory stimulation. **Acta Otolaryngol**, v. 120, n. 8, p. 967–72, 2000. ISSN 0001-6489 (Print) 0001-6489 (Linking). Andersson, G Lyttkens, L Hirvela, C Furmark, T Tillfors, M Fredrikson, M Norway Acta Otolaryngol. 2000 Oct;120(8):967-72. Available: <http://www.ncbi.nlm.nih.gov/pubmed/11200593>. Citations on pages 78 and 91.

ANDERSSON, G.; MCKENNA, L. The role of cognition in tinnitus. **Acta Oto-Laryngologica**, Taylor & Francis, v. 126, n. sup556, p. 39–43, 2006. Citation on page 87.

ANDERSSON, G.; WESTIN, V. Understanding tinnitus distress: introducing the concepts of moderators and mediators. **Int J Audiol**, v. 47 Suppl 2, p. S106–11, 2008. ISSN 1708-8186 (Electronic) 1499-2027 (Linking). Andersson, Gerhard Westin, Vendela England Int J Audiol. 2008 Nov;47 Suppl 2:S106-11. Available: <http://www.ncbi.nlm.nih.gov/pubmed/19012118http://informahealthcare.com/doi/pdfplus/10.1080/14992020802301670>. Citation on page 93.

ANDRYCHOWICZ, M.; WOLSKI, F.; RAY, A.; SCHNEIDER, J.; FONG, R.; WELINDER, P.; MCGREW, B.; TOBIN, J.; ABBEEL, P.; ZAREMBA, W. Hindsight experience replay. **arXiv preprint arXiv:1707.01495**, 2017. Citations on pages 51 and 207.

ANGELUCCI, F.; FIORE, M.; RICCI, E.; PADUA, L.; SABINO, A.; TONALI, P. A. Investigating the neurobiology of music: brain-derived neurotrophic factor modulation in the hippocampus of young adult mice. **Behav Pharmacol**, v. 18, n. 5-6, p. 491–6, 2007. ISSN 0955-8810 (Print) 0955-8810 (Linking). Angelucci, Francesco Fiore, Marco Ricci, Enzo Padua, Luca Sabino, Andrea Tonali, Pietro Attilio England Behav Pharmacol. 2007 Sep;18(5-6):491-6. Available: <http://www.ncbi.nlm.nih.gov/pubmed/17762517>. Citation on page 63.

ARMONY, J. L.; QUIRK, G. J.; LEDOUX, J. E. Differential effects of amygdala lesions on early and late plastic components of auditory cortex spike trains during fear conditioning. **J Neurosci**, v. 18, n. 7, p. 2592–601, 1998. ISSN 0270-6474 (Print) 0270-6474 (Linking). Armony, J L Quirk, G J LeDoux, J E MH00956/MH/NIMH NIH HHS/ MH38774/MH/NIMH NIH HHS/ MH46516/MH/NIMH NIH HHS/ J Neurosci. 1998 Apr 1;18(7):2592-601. Available: <http://www.ncbi.nlm.nih.gov/pubmed/9502818http://www.jneurosci.org/content/18/7/2592.full.pdf>. Citation on page 61.

ARNOLD, W.; BARTENSTEIN, P.; OESTREICHER, E.; ROMER, W.; SCHWAIGER, M. Focal metabolic activation in the predominant left auditory cortex in patients suffering from tinnitus: a pet study with [18f]deoxyglucose. **ORL J Otorhinolaryngol Relat Spec**, v. 58, n. 4, p. 195–9, 1996. ISSN 0301-1569 (Print) 0301-1569 (Linking). Arnold, W Bartenstein, P Oestreicher, E Romer, W Schwaiger, M SWITZERLAND ORL J Otorhinolaryngol Relat Spec. 1996 Jul-Aug;58(4):195-9. Available: <http://www.ncbi.nlm.nih.gov/pubmed/8883104http://content.karger.com/ProdukteDB/produkte.asp?doi=10.1159/000276835>. Citation on page 78.

ASNIS, G. M.; MAJEED, K.; HENDERSON, M. A.; SYLVESTER, C.; THOMAS, M.; GARZA, R. D. L. An examination of the relationship between insomnia and tinnitus: A review and recommendations. **Clinical Medicine Insights: Psychiatry**, v. 9, p. 1179557318781078, 2018. ISSN 1179-5573. Available: <https://doi.org/10.1177/1179557318781078>. Citation on page 90.

AUERBACH, B. D.; RODRIGUES, P. V.; SALVI, R. J. Central gain control in tinnitus and hyperacusis. **Front Neurol**, v. 5, p. 206, 2014. ISSN 1664-2295 (Electronic) 1664-2295 (Linking). Auerbach, Benjamin D Rodrigues, Paulo V Salvi, Richard J eng R01 DC011808/DC/NIDCD NIH HHS/ Review Switzerland 2014/11/12 06:00 Front Neurol. 2014 Oct 24;5:206. doi: 10.3389/fneur.2014.00206. eCollection 2014. Available: <http://www.ncbi.nlm.nih.gov/pubmed/25386157>. Citation on page 78.

BAGULEY, D.; MCFERRAN, D.; HALL, D. Tinnitus. **The Lancet**, Elsevier, v. 382, n. 9904, p. 1600–1607, 2013. Citations on pages 87 and 101.

BALDAUF, Z. B. Dual chemoarchitectonic lamination of the visual sector of the thalamic reticular nucleus. **Neuroscience**, v. 165, n. 3, p. 801–18, 2010. ISSN 1873-7544 (Electronic) 0306-4522 (Linking). Baldauf, Z B NS35377/NS/NINDS NIH HHS/ R01 NS035377-07/NS/NINDS NIH HHS/ Neuroscience. 2010 Feb 3;165(3):801-18. doi: 10.1016/j.neuroscience.2009.11.010. Epub 2009 Nov 10. Available: <http://www.ncbi.nlm.nih.gov/pubmed/19909790http://ac.els-cdn.com/S0306452209018272/1-s2.0-S0306452209018272-main.pdf?_tid=3d0fbaf8-892e-11e2-acb3-00000aacb35d&acdnat=1362884426_93814c207f7a11ba7d94439764bf658e>. Citation on page 58.

BALLEINE, B. W.; KILLCROSS, S. Parallel incentive processing: an integrated view of amygdala function. **Trends Neurosci**, v. 29, n. 5, p. 272–9, 2006. ISSN 0166-2236 (Print) 0166-2236 (Linking). Balleine, Bernard W Killcross, Simon NIH 56446/PHS HHS/ England Trends Neurosci. 2006 May;29(5):272-9. Epub 2006 Mar 20. Available: <http://www.ncbi.nlm.nih.gov/pubmed/16545468http://ac.els-cdn.com/S0166223606000506/1-s2.0-S0166223606000506-main.pdf?_tid=05515d6a-892e-11e2-855b-00000aacb361&acdnat=1362884332_8c872b2fd2b29a240ec2a59109b5eb38>. Citation on page 61.

BAR-ANAN, Y.; HOUWER, J. D.; NOSEK, B. A. Evaluative conditioning and conscious knowledge of contingencies: a correlational investigation with large samples. **Q J Exp Psychol**

(Hove), v. 63, n. 12, p. 2313–35, 2010. ISSN 1747-0226 (Electronic) 1747-0218 (Linking). Bar-Anan, Yoav De Houwer, Jan Nosek, Brian A eng R01 MH68447/MH/NIMH NIH HHS/ Research Support, N.I.H., Extramural Research Support, Non-U.S. Gov't England 2010/06/15 06:00 Q J Exp Psychol (Hove). 2010 Dec;63(12):2313-35. doi: 10.1080/17470211003802442. Epub 2010 Jun 11. Available: <http://www.ncbi.nlm.nih.gov/pubmed/20544561>. Citation on page 70.

BAR, M. A cognitive neuroscience hypothesis of mood and depression. **Trends Cogn Sci**, v. 13, n. 11, p. 456–63, 2009. ISSN 1879-307X (Electronic) 1364-6613 (Linking). Bar, Moshe R01 NS050615-05/NS/NINDS NIH HHS/ R01NS050615/NS/NINDS NIH HHS/ England Trends Cogn Sci. 2009 Nov;13(11):456-63. doi: 10.1016/j.tics.2009.08.009. Epub 2009 Oct 12. Available: <http://www.ncbi.nlm.nih.gov/pubmed/19819753http://ac.els-cdn.com/S1364661309001764/1-s2.0-S1364661309001764-main.pdf?_tid=2f2baad2-892e-11e2-a368-00000aab0f01&acdnat=1362884402_c1f52a13d2324f5fc687df32a7badf2d>. Citations on pages 59 and 60.

BARBAS, H.; ZIKOPOULOS, B.; TIMBIE, C. Sensory pathways and emotional context for action in primate prefrontal cortex. **Biol Psychiatry**, v. 69, n. 12, p. 1133–9, 2011. ISSN 1873-2402 (Electronic) 0006-3223 (Linking). Barbas, Helen Zikopoulos, Basilis Timbie, Clare Biol Psychiatry. 2011 Jun 15;69(12):1133-9. doi: 10.1016/j.biopsych.2010.08.008. Epub 2010 Oct 2. Available: <http://www.ncbi.nlm.nih.gov/pubmed/20889144http://ac.els-cdn.com/S0006322310008425/1-s2.0-S0006322310008425-main.pdf?_tid=5716e32c-892e-11e2-8cc2-00000aacb361&acdnat=1362884469_143fa4789d47fdf8118667c2cb572940>. Citation on page 59.

BARON, R. M.; KENNY, D. A. The moderator–mediator variable distinction in social psychological research: Conceptual, strategic, and statistical considerations. **Journal of personality and social psychology**, American Psychological Association, v. 51, n. 6, p. 1173, 1986. Citation on page 195.

BAXTER, M. G.; MURRAY, E. A. The amygdala and reward. **Nat Rev Neurosci**, v. 3, n. 7, p. 563–73, 2002. ISSN 1471-003X (Print) 1471-003X (Linking). Baxter, Mark G Murray, Elisabeth A England Nat Rev Neurosci. 2002 Jul;3(7):563-73. Available: <http://www.ncbi.nlm.nih.gov/pubmed/12094212http://www.nature.com/nrn/journal/v3/n7/pdf/nrn875.pdf>. Citation on page 60.

BECHARA, A.; DAMASIO, H.; DAMASIO, A. R. Role of the amygdala in decision-making. **Ann N Y Acad Sci**, v. 985, p. 356–69, 2003. ISSN 0077-8923 (Print) 0077-8923 (Linking). Bechara, Antoine Damasio, Hanna Damasio, Antonio R DA12487-03/DA/NIDA NIH HHS/ P01 NS19632/NS/NINDS NIH HHS/ R01 DA11779-02/DA/NIDA NIH HHS/ Ann N Y Acad Sci. 2003 Apr;985:356-69. Available: <http://www.ncbi.nlm.nih.gov/pubmed/12724171http://onlinelibrary.wiley.com/store/10.1111/j.1749-6632.2003.tb07094.x/asset/j.1749-6632.2003.tb07094.x.pdf?v=1&t=hza00zqu&s=a83ad0209f6d81035e9238e77d353b7c8c196118>. Citation on page 61.

BECK, A. T.; CLARK, D. A. An information processing model of anxiety: Automatic and strategic processes. **Behaviour research and therapy**, Elsevier, v. 35, n. 1, p. 49–58, 1997. Citation on page 91.

BELKIN, M.; NIYOGI, P. Laplacian eigenmaps for dimensionality reduction and data representation. **Neural computation**, MIT Press, v. 15, n. 6, p. 1373–1396, 2003. Citation on page 133.

BENUWA, B. B.; ZHAN, Y. Z.; GHANSAH, B.; WORNYO, D. K.; KATAKA, F. B. A review of deep machine learning. **International Journal of Engineering Research in Africa**, Trans Tech Publ, v. 24, p. 124–136, 2016. Citation on page 207.

BERGMAN, P.; VäSTFJäLL, D.; TAJADURA-JIMéNEZ, A.; ASUTAY, E. Auditory-induced emotion mediates perceptual categorization of everyday sounds. **Frontiers in Psychology**, v. 7, n. 1565, 2016. ISSN 1664-1078. Available: <https://www.frontiersin.org/article/10.3389/fpsyg.2016.01565>. Citation on page 96.

BHAGAT, S.; BANERJEE, H.; TSE, Z. T. H.; REN, H. Deep reinforcement learning for soft, flexible robots: Brief review with impending challenges. **Robotics**, Multidisciplinary Digital Publishing Institute, v. 8, n. 1, p. 4, 2019. Citation on page 213.

BIKSON, M.; RAHMAN, A. Origins of specificity during tdcs: anatomical, activity-selective, and input-bias mechanisms. **Frontiers in human neuroscience**, Frontiers, v. 7, p. 688, 2013. Citation on page 102.

BLOOD, A. J.; ZATORRE, R. J. Intensely pleasurable responses to music correlate with activity in brain regions implicated in reward and emotion. **Proc Natl Acad Sci U S A**, v. 98, n. 20, p. 11818–23, 2001. ISSN 0027-8424 (Print) 0027-8424 (Linking). Blood, A J Zatorre, R J Proc Natl Acad Sci U S A. 2001 Sep 25;98(20):11818-23. Available: <http://www.ncbi.nlm.nih.gov/pubmed/11573015http://www.pnas.org/content/98/20/11818.full.pdf>. Citation on page 64.

BLOOD, A. J.; ZATORRE, R. J.; BERMUDEZ, P.; EVANS, A. C. Emotional responses to pleasant and unpleasant music correlate with activity in paralimbic brain regions. **Nat Neurosci**, v. 2, n. 4, p. 382–7, 1999. ISSN 1097-6256 (Print) 1097-6256 (Linking). Blood, A J Zatorre, R J Bermudez, P Evans, A C Nat Neurosci. 1999 Apr;2(4):382-7. Available: <http://www.ncbi.nlm.nih.gov/pubmed/10204547>. Citations on pages 59, 60, and 64.

BOLLEN, K. A. **Structural equations with latent variables**. [S.l.]: John Wiley & Sons, 1989. Citation on page 208.

BOSO, M.; POLITI, P.; BARALE, F.; ENZO, E. Neurophysiology and neurobiology of the musical experience. **Funct Neurol**, v. 21, n. 4, p. 187–91, 2006. ISSN 0393-5264 (Print) 0393-5264 (Linking). Boso, Marianna Politi, Pierluigi Barale, Francesco Enzo, Emanuele Italy Funct Neurol. 2006 Oct-Dec;21(4):187-91. Available: <http://www.ncbi.nlm.nih.gov/pubmed/17367577http://www.functionalneurology.com/common/php/portiere.php?ID=56baba9c9d6e917c88fbbf20aba16979>. Citation on page 61.

BOYEN, K.; LANGERS, D. R.; KLEINE, E. de; DIJK, P. van. Gray matter in the brain: Differences associated with tinnitus and hearing loss. **Hear Res**, 2012. ISSN 1878-5891 (Electronic) 0378-5955 (Linking). Boyen, Kris Langers, Dave R M de Kleine, Emile van Dijk, Pim Hear Res. 2012 Mar 15. Available: <http://www.ncbi.nlm.nih.gov/pubmed/22446179http://ac.els-cdn.com/S0378595512000469/1-s2.0-S0378595512000469-main.pdf?_tid=7c7025648d9f7e6a3141192ff84f711c&acdnat=1345695809_e19c90a1e4ee3f0a24ba389627f31e5e>. Citation on page 78.

BRADLEY, M. M.; LANG, P. J. Measuring emotion: the self-assessment manikin and the semantic differential. **Journal of behavior therapy and experimental psychiatry**, Pergamon, v. 25, n. 1, p. 49–59, 1994. Citations on pages 88 and 101.

____. Measuring emotion: the self-assessment manikin and the semantic differential. **J Behav Ther Exp Psychiatry**, v. 25, n. 1, p. 49–59, 1994. ISSN 0005-7916 (Print) 0005-7916 (Linking). Bradley, M M Lang, P J eng NIMH MH37757/MH/NIMH NIH HHS/ NIMH MH41950/MH/NIMH NIH HHS/ NIMH MH43975/MH/NIMH NIH HHS/ etc. Comparative Study Research Support, U.S. Gov't, P.H.S. Netherlands J Behav Ther Exp Psychiatry. 1994 Mar;25(1):49-59. doi: 10.1016/0005-7916(94)90063-9. Available: <https://www.ncbi.nlm.nih.gov/pubmed/7962581>. Citation on page 91.

BREIT, S.; SCHULZ, J. B.; BENABID, A.-L. Deep brain stimulation. **Cell and tissue research**, Springer, v. 318, n. 1, p. 275–288, 2004. Citation on page 101.

BREITER, H. C.; AHARON, I.; KAHNEMAN, D.; DALE, A.; SHIZGAL, P. Functional imaging of neural responses to expectancy and experience of monetary gains and losses. **Neuron**, v. 30, n. 2, p. 619–39, 2001. ISSN 0896-6273 (Print) 0896-6273 (Linking). Breiter, H C Aharon, I Kahneman, D Dale, A Shizgal, P 00265/PHS HHS/ 09467/PHS HHS/ P41-RR14075/RR/NCRR NIH HHS/ R01-NS39581/NS/NINDS NIH HHS/ R01-RR13609/RR/NCRR NIH HHS/ Neuron. 2001 May;30(2):619-39. Available: <http://www.ncbi.nlm.nih.gov/pubmed/11395019http://ac.els-cdn.com/S0896627301003038/1-s2.0-S0896627301003038-main.pdf?_tid=ba7f5c2e-892d-11e2-9ea4-00000aab0f26&acdnat=1362884207_7252d6aede78b6073c4889eb518fd0ac>. Citations on pages 59 and 60.

BROWN, P.; MOLLIVER, M. E. Dual serotonin (5-ht) projections to the nucleus accumbens core and shell: relation of the 5-ht transporter to amphetamine-induced neurotoxicity. **J Neurosci**, v. 20, n. 5, p. 1952–63, 2000. ISSN 1529-2401 (Electronic) 0270-6474 (Linking). Brown, P Molliver, M E DA 04431/DA/NIDA NIH HHS/ DA 08692/DA/NIDA NIH HHS/ N01DA 3-7301/DA/NIDA NIH HHS/ J Neurosci. 2000 Mar 1;20(5):1952-63. Available: <http://www.ncbi.nlm.nih.gov/pubmed/10684896http://www.jneurosci.org/content/20/5/1952.full.pdf>. Citation on page 64.

BROZOSKI, T. J.; BAUER, C. A.; CASPARY, D. M. Elevated fusiform cell activity in the dorsal cochlear nucleus of chinchillas with psychophysical evidence of tinnitus. **J Neurosci**, v. 22, n. 6, p. 2383–90, 2002. ISSN 1529-2401 (Electronic) 0270-6474 (Linking). Brozoski, T J Bauer, C A Caspary, D M eng DC00-151/DC/NIDCD NIH HHS/ DC96-003/DC/NIDCD NIH HHS/ R01 DC000151/DC/NIDCD NIH HHS/ Research Support, U.S. Gov't, P.H.S. 2002/03/16 10:00 J Neurosci. 2002 Mar 15;22(6):2383-90. Available: <http://www.ncbi.nlm.nih.gov/pubmed/11896177>. Citations on pages 73 and 78.

BURGESS, N.; MAGUIRE, E. A.; O'KEEFE, J. The human hippocampus and spatial and episodic memory. **Neuron**, v. 35, n. 4, p. 625–41, 2002. ISSN 0896-6273 (Print) 0896-6273 (Linking). Burgess, Neil Maguire, Eleanor A O'Keefe, John Neuron. 2002 Aug 15;35(4):625-41. Available: <http://www.ncbi.nlm.nih.gov/pubmed/12194864http://ac.els-cdn.com/S0896627302008309/1-s2.0-S0896627302008309-main.pdf?_tid=bdda8e0c-892d-11e2-8942-00000aacb35d&acdnat=1362884212_eb87bcea4e096779d5eba11209dc389d>. Citation on page 62.

BUSEMEYER, J. R.; DIEDERICH, A. **Cognitive modeling**. [S.l.]: Sage, 2010. Citations on pages 55 and 56.

CAI, D.; ZHANG, C.; HE, X. Unsupervised feature selection for multi-cluster data. In: **Proceedings of the 16th ACM SIGKDD international conference on Knowledge discovery and data mining**. [S.l.: s.n.], 2010. p. 333–342. Citations on pages 129 and 130.

CALVO, J. A.; DUSPARIC, I. Heterogeneous multi-agent deep reinforcement learning for traffic lights control. In: **AICS**. [S.l.: s.n.], 2018. p. 2–13. Citation on page 214.

CARMONA, P. L.; SOTOCA, J. M.; PLA, F. Filter-type variable selection based on information measures for regression tasks. **Entropy**, Molecular Diversity Preservation International, v. 14, n. 2, p. 323–343, 2012. Citation on page 135.

CASAS, N. Deep deterministic policy gradient for urban traffic light control. **arXiv preprint arXiv:1703.09035**, 2017. Citation on page 213.

CHANG, H.; CHEN, K.; KALTENBACH, J. A.; ZHANG, J.; GODFREY, D. A. Effects of acoustic trauma on dorsal cochlear nucleus neuron activity in slices. **Hear Res**, v. 164, n. 1-2, p. 59–68, 2002. ISSN 0378-5955 (Print) 0378-5955 (Linking). Chang, Henry Chen, Kejian Kaltenbach, James A Zhang, Jinsheng Godfrey, Donald A eng Research Support, Non-U.S. Gov't Netherlands 2002/04/13 10:00 Hear Res. 2002 Feb;164(1-2):59-68. Available: <http://www.ncbi.nlm.nih.gov/pubmed/11950525>. Citations on pages 73 and 78.

CHEN, G. D.; JASTREBOFF, P. J. Salicylate-induced abnormal activity in the inferior colliculus of rats. **Hear Res**, v. 82, n. 2, p. 158–78, 1995. ISSN 0378-5955 (Print) 0378-5955 (Linking). Chen, G D Jastreboff, P J eng R01 DC00299/DC/NIDCD NIH HHS/ Comparative Study Research Support, U.S. Gov't, P.H.S. NETHERLANDS 1995/02/01 Hear Res. 1995 Feb;82(2):158-78. Available: <http://www.ncbi.nlm.nih.gov/pubmed/7775282>. Citations on pages 73 and 78.

CHIN, Y. K.; KOW, W. Y.; KHONG, W. L.; TAN, M. K.; TEO, K. T. K. Q-learning traffic signal optimization within multiple intersections traffic network. In: IEEE. **2012 Sixth UKSim/AMSS European Symposium on Computer Modeling and Simulation**. [S.l.], 2012. p. 343–348. Citation on page 211.

CHIPMAN, S. E. **The Oxford handbook of cognitive science**. [S.l.]: Oxford University Press, 2016. Citation on page 45.

CHOW, S.; SHAO, J.; WANG, H.; LOKHNYGINA, Y. **Sample Size Calculations in Clinical Research**. CRC Press, 2017. (Chapman & Hall/CRC Biostatistics Series). ISBN 9781351727112. Available: <https://books.google.com.br/books?id=7_0wDwAAQBAJ>. Citation on page 107.

CHOW, S.-C.; TU, Y.-H. On two-stage seamless adaptive design in clinical trials. **Journal of the Formosan Medical Association**, Elsevier, v. 107, n. 12, p. S52–S60, 2008. Citation on page 107.

CHU, T.; WANG, J.; CODECÀ, L.; LI, Z. Multi-agent deep reinforcement learning for large-scale traffic signal control. **IEEE Transactions on Intelligent Transportation Systems**, IEEE, v. 21, n. 3, p. 1086–1095, 2019. Citations on pages 211 and 216.

CHURCHILL, L.; ZAHM, D. S.; DUFFY, P.; KALIVAS, P. W. The mediodorsal nucleus of the thalamus in rats–ii. behavioral and neurochemical effects of gaba agonists. **Neuroscience**, v. 70, n. 1, p. 103–12, 1996. ISSN 0306-4522 (Print) 0306-4522 (Linking). Churchill, L Zahm, D S Duffy, P Kalivas, P W DA-00158/DA/NIDA NIH HHS/ DA-03906/DA/NIDA NIH HHS/ MH-40817/MH/NIMH NIH HHS/ etc. Neuroscience. 1996 Jan;70(1):103-12. Available: <http://www.ncbi.nlm.nih.gov/pubmed/8848116http://ac.els-cdn.com/030645229500352J/1-s2.0-030645229500352J-main.pdf?_tid=b700f512-892d-11e2-acb1-00000aab0f02&acdnat=1362884201_5ed96a823086758893bd2484ac53bcd5>. Citation on page 58.

CHURCHILL, L.; ZAHM, D. S.; KALIVAS, P. W. The mediodorsal nucleus of the thalamus in rats–i. forebrain gabaergic innervation. **Neuroscience**, v. 70, n. 1, p. 93–102, 1996. ISSN 0306-4522 (Print) 0306-4522 (Linking). Churchill, L Zahm, D S Kalivas, P W DA-00158/DA/NIDA NIH HHS/ DA-03906/DA/NIDA NIH HHS/ MH-40817/MH/NIMH NIH HHS/ etc. Neuroscience. 1996 Jan;70(1):93-102. Available: <http://www.ncbi.nlm.nih.gov/pubmed/8848140http://ac.els-cdn.com/030645229500351I/1-s2.0-030645229500351I-main.pdf?_tid=8d02d23a-892d-11e2-b46f-00000aacb35f&acdnat=1362884130_5676b12a5f2d0a2b4dc63cd5666cfbf9>. Citation on page 58.

CIMA, R. F.; CROMBEZ, G.; VLAEYEN, J. W. Catastrophizing and fear of tinnitus predict quality of life in patients with chronic tinnitus. **Ear and hearing**, LWW, v. 32, n. 5, p. 634–641, 2011. Citation on page 92.

CITRON, F. M.; GRAY, M. A.; CRITCHLEY, H. D.; WEEKES, B. S.; FERSTL, E. C. Emotional valence and arousal affect reading in an interactive way: neuroimaging evidence for an approach-withdrawal framework. **Neuropsychologia**, Elsevier, v. 56, p. 79–89, 2014. Citation on page 105.

COELHO, C. B.; SANCHEZ, T. G.; TYLER, R. S. Tinnitus in children and associated risk factors. **Prog Brain Res**, v. 166, p. 179–91, 2007. ISSN 0079-6123 (Print) 0079-6123 (Linking). Coelho, Claudia Barros Sanchez, Tanit Ganz Tyler, Richard S Netherlands Prog Brain Res. 2007;166:179-91. Available: <http://www.ncbi.nlm.nih.gov/pubmed/17956782http://www.sciencedirect.com/science?_ob=MiamiImageURL&_cid=273019&_user=501045&_pii=S0079612307660166&_check=y&_origin=article&_zone=toolbar&_coverDate=31-Dec-2007&view=c&originContentFamily=serial&wchp=dGLbVlB-zSkWb&md5=a27086eaffb0106363f1bb6f1b024559/1-s2.0-S0079612307660166-main.pdf>. Citation on page 57.

COHEN, M. A.; CAVANAGH, P.; CHUN, M. M.; NAKAYAMA, K. The attentional requirements of consciousness. **Trends Cogn Sci**, v. 16, n. 8, p. 411–7, 2012. ISSN 1879-307X (Electronic) 1364-6613 (Linking). Cohen, Michael A Cavanagh, Patrick Chun, Marvin M Nakayama, Ken EY01363/EY/NEI NIH HHS/ EY014193/EY/NEI NIH HHS/ EY09258/EY/NEI NIH HHS/ England Trends Cogn Sci. 2012 Aug;16(8):411-7. Epub 2012 Jul 12. Available: <http://www.ncbi.nlm.nih.gov/pubmed/22795561http://ac.els-cdn.com/S1364661312001519/1-s2.0-S1364661312001519-main.pdf?_tid=5dac9a10-892e-11e2-b9a1-00000aacb35d&acdnat=1362884480_94bbfbbfd20c6cf9862a565698461e42>. Citation on page 68.

COIFMAN, R. R.; LAFON, S. Diffusion maps. **Applied and computational harmonic analysis**, Elsevier, v. 21, n. 1, p. 5–30, 2006. Citations on pages 129, 130, and 134.

COMPTON, R. J. The interface between emotion and attention: a review of evidence from psychology and neuroscience. **Behav Cogn Neurosci Rev**, v. 2, n. 2, p. 115–29, 2003. ISSN 1534-5823 (Print) 1534-5823 (Linking). Compton, Rebecca J Behav Cogn Neurosci Rev. 2003 Jun;2(2):115-29. Available: <http://www.ncbi.nlm.nih.gov/pubmed/13678519http://bcn.sagepub.com/content/2/2/115>. Citation on page 60.

COMPTON, R. J.; BANICH, M. T.; MOHANTY, A.; MILHAM, M. P.; HERRINGTON, J.; MILLER, G. A.; SCALF, P. E.; WEBB, A.; HELLER, W. Paying attention to emotion: an fmri investigation of cognitive and emotional stroop tasks. **Cogn Affect Behav Neurosci**, v. 3, n. 2, p. 81–96, 2003. ISSN 1530-7026 (Print) 1530-7026 (Linking). Compton, Rebecca J Banich, Marie T Mohanty, Aprajita Milham, Michael P Herrington, John Miller, Gregory A Scalf, Paige E

Webb, Andrew Heller, Wendy MH19554/MH/NIMH NIH HHS/ R01 MH61358/MH/NIMH NIH HHS/ R21 DA14111/DA/NIDA NIH HHS/ Cogn Affect Behav Neurosci. 2003 Jun;3(2):81-96. Available: <http://www.ncbi.nlm.nih.gov/pubmed/12943324>. Citation on page 60.

CONRAD, I.; KLEINSTAUBER, M.; JASPER, K.; HILLER, W.; ANDERSSON, G.; WEISE, C. The role of dysfunctional cognitions in patients with chronic tinnitus. **Ear Hear**, v. 36, n. 5, p. e279–89, 2015. ISSN 0196-0202. Citation on page 93.

CRONLEIN, T.; LANGGUTH, B.; GEISLER, P.; HAJAK, G. Tinnitus and insomnia. **Prog Brain Res**, v. 166, p. 227–33, 2007. ISSN 0079-6123 (Print) 0079-6123 (Linking). Cronlein, Tatjana Langguth, Berthold Geisler, Peter Hajak, Goran Netherlands Prog Brain Res. 2007;166:227-33. Available: <http://www.ncbi.nlm.nih.gov/pubmed/17956787http://www.sciencedirect.com/science/article/pii/S007961230766021X>. Citation on page 78.

CZISCH, M.; WEHRLE, R.; STIEGLER, A.; PETERS, H.; ANDRADE, K.; HOLSBOER, F.; SAMANN, P. G. Acoustic oddball during nrem sleep: a combined eeg/fmri study. **PLoS One**, v. 4, n. 8, p. e6749, 2009. ISSN 1932-6203 (Electronic) 1932-6203 (Linking). Czisch, Michael Wehrle, Renate Stiegler, Andrea Peters, Henning Andrade, Katia Holsboer, Florian Samann, Philipp G PLoS One. 2009 Aug 25;4(8):e6749. doi: 10.1371/journal.pone.0006749. Available: <http://www.ncbi.nlm.nih.gov/pubmed/19707599http://www.plosone.org/article/fetchObjectAttachment.action?uri=info%3Adoi%2F10.1371%2Fjournal.pone.0006749&representation=PDF>. Citation on page 61.

DALGLEISH, T.; WATTS, F. N. Biases of attention and memory in disorders of anxiety and depression. **Clinical Psychology Review**, Elsevier, v. 10, n. 5, p. 589–604, 1990. Citation on page 91.

DARLINGTON, R. B.; HAYES, A. F. **Regression analysis and linear models: Concepts, applications, and implementation**. [S.l.]: Guilford Publications, 2016. Citation on page 194.

DAVIDSON, R. J.; PUTNAM, K. M.; LARSON, C. L. Dysfunction in the neural circuitry of emotion regulation–a possible prelude to violence. **science**, American Association for the Advancement of Science, v. 289, n. 5479, p. 591–594, 2000. Citations on pages 87, 101, and 102.

DAVIS, M.; WHALEN, P. J. The amygdala: vigilance and emotion. **Mol Psychiatry**, v. 6, n. 1, p. 13–34, 2001. ISSN 1359-4184 (Print) 1359-4184 (Linking). Davis, M Whalen, P J MH 01866/MH/NIMH NIH HHS/ MH 47840/MH/NIMH NIH HHS/ MH 52384/MH/NIMH NIH HHS/ MH 57250/MH/NIMH NIH HHS/ MH 58922/MH/NIMH NIH HHS/ MH 59906/MH/NIMH NIH HHS/ England Mol Psychiatry. 2001 Jan;6(1):13-34. Available: <http://www.ncbi.nlm.nih.gov/pubmed/11244481http://www.nature.com/mp/journal/v6/n1/pdf/4000812a.pdf>. Citation on page 60.

DEVITO, L. M.; EICHENBAUM, H. Distinct contributions of the hippocampus and medial prefrontal cortex to the "what-where-when" components of episodic-like memory in mice. **Behav Brain Res**, v. 215, n. 2, p. 318–25, 2010. ISSN 1872-7549 (Electronic) 0166-4328 (Linking). DeVito, Loren M Eichenbaum, Howard R01 MH059357-05/MH/NIMH NIH HHS/ Netherlands Behav Brain Res. 2010 Dec 31;215(2):318-25. doi: 10.1016/j.bbr.2009.09.014. Epub 2009 Sep 17. Available: <http://www.ncbi.nlm.nih.gov/pubmed/19766146http://ac.els-cdn.com/S0166432809005294/1-s2.0-S0166432809005294-main.pdf?_tid=44c98c2e-892e-11e2-bc1f-00000aab0f02&acdnat=1362884439_ed0b03a05a003ba9d0b143419fce5a31>. Citations on pages 61 and 62.

DIVAC, I.; MOGENSEN, J.; MARINKOVIC, S.; MARTENSSON, R. On the projections from the neostriatum to the cerebral cortex: the "displaced" neurons. **Neuroscience**, v. 21, n. 1, p. 197–205, 1987. ISSN 0306-4522 (Print) 0306-4522 (Linking). Divac, I Mogensen, J Marinkovic, S Martensson, R ENGLAND Neuroscience. 1987 Apr;21(1):197-205. Available: <http://www.ncbi.nlm.nih.gov/pubmed/3601075http://ac.els-cdn.com/0306452287903332/1-s2.0-0306452287903332-main.pdf?_tid=82cb3be0-892d-11e2-b492-00000aab0f6c&acdnat=1362884113_439715e27606a474a765485fb7e67f0e>. Citation on page 60.

DMOCHOWSKI, J. P.; DATTA, A.; BIKSON, M.; SU, Y.; PARRA, L. C. Optimized multi-electrode stimulation increases focality and intensity at target. **Journal of neural engineering**, IOP Publishing, v. 8, n. 4, p. 046011, 2011. Citation on page 102.

DOMINGUEZ, M.; BECKER, S.; BRUCE, I.; READ, H. A spiking neuron model of cortical correlates of sensorineural hearing loss: Spontaneous firing, synchrony, and tinnitus. **Neural Comput**, v. 18, n. 12, p. 2942–58, 2006. ISSN 0899-7667 (Print) 0899-7667 (Linking). Dominguez, Melissa Becker, Suzanna Bruce, Ian Read, Heather Neural Comput. 2006 Dec;18(12):2942-58. Available: <http://www.ncbi.nlm.nih.gov/pubmed/17052154http://www.mitpressjournals.org/doi/pdfplus/10.1162/neco.2006.18.12.2942>. Citation on page 78.

DOPAZO, J.; CARAZO, J. M. Phylogenetic reconstruction using an unsupervised growing neural network that adopts the topology of a phylogenetic tree. **Journal of molecular evolution**, Springer, v. 44, n. 2, p. 226–233, 1997. Citation on page 168.

DREVETS, W. C.; PRICE, J. L.; SIMPSON J. R., J.; TODD, R. D.; REICH, T.; VANNIER, M.; RAICHLE, M. E. Subgenual prefrontal cortex abnormalities in mood disorders. **Nature**, v. 386, n. 6627, p. 824–7, 1997. ISSN 0028-0836 (Print) 0028-0836 (Linking). Drevets, W C Price, J L Simpson, J R Jr Todd, R D Reich, T Vannier, M Raichle, M E ENGLAND Nature. 1997 Apr 24;386(6627):824-7. Available: <http://www.ncbi.nlm.nih.gov/pubmed/9126739http://www.nature.com/nature/journal/v386/n6627/abs/386824a0.htmlhttp://www.nature.com/nature/journal/v386/n6627/pdf/386824a0.pdf>. Citation on page 64.

DU, S.; MA, Y.; LI, S.; MA, Y. Robust unsupervised feature selection via matrix factorization. **Neurocomputing**, Elsevier, v. 241, p. 115–127, 2017. Citations on pages 129 and 130.

DUNCAN, G.; LAYARD, M. A monte-carlo study of asymptotically robust tests for correlation coefficients. **Biometrika**, Oxford University Press, v. 60, n. 3, p. 551–558, 1973. Citation on page 195.

DURAI, M.; O'KEEFFE, M. G.; SEARCHFIELD, G. D. Examining the short term effects of emotion under an adaptation level theory model of tinnitus perception. **Hearing Research**, v. 345, p. 23–29, 2017. ISSN 0378-5955. Available: <http://www.sciencedirect.com/science/article/pii/S0378595516303033>. Citation on page 93.

EDGELL, S. E.; NOON, S. M. Effect of violation of normality on the t test of the correlation coefficient. **Psychological bulletin**, v. 95, n. 3, 1984. Citation on page 195.

EGGERMONT, J. J. Cortical tonotopic map reorganization and its implications for treatment of tinnitus. **Acta Otolaryngol Suppl**, n. 556, p. 9–12, 2006. ISSN 0365-5237 (Print) 0365-5237 (Linking). Eggermont, J J eng Research Support, Non-U.S. Gov't Review Norway 2006/11/23 09:00 Acta Otolaryngol Suppl. 2006 Dec;(556):9-12. Available: <http://www.ncbi.nlm.nih.gov/pubmed/17114136>. Citations on pages 65 and 78.

____. Correlated neural activity as the driving force for functional changes in auditory cortex. **Hear Res**, v. 229, n. 1-2, p. 69–80, 2007. ISSN 0378-5955 (Print) 0378-5955 (Linking). Eggermont, Jos J Netherlands Hear Res. 2007 Jul;229(1-2):69-80. Epub 2007 Jan 16. Available: <http://www.ncbi.nlm.nih.gov/pubmed/17296278http://www.sciencedirect.com/science?_ob=MImg&_imagekey=B6T73-4MV0M97-9-1&_cdi=5047&_user=5674931&_pii=S0378595507000238&_origin=&_coverDate=07%2F31%2F2007&_sk=997709998&view=c&wchp=dGLzVzb-zSkWA&md5=7c8c0987bc67269819ad293c2cc02f5d&ie=/sdarticle.pdf>. Citations on pages 65 and 78.

EGGERMONT, J. J.; KOMIYA, H. Moderate noise trauma in juvenile cats results in profound cortical topographic map changes in adulthood. **Hear Res**, v. 142, n. 1-2, p. 89–101, 2000. ISSN 0378-5955 (Print) 0378-5955 (Linking). Eggermont, J J Komiya, H eng Research Support, Non-U.S. Gov't NETHERLANDS 2000/04/05 09:00 Hear Res. 2000 Apr;142(1-2):89-101. Available: <http://www.ncbi.nlm.nih.gov/pubmed/10748332>. Citations on pages 73 and 78.

EGGERMONT, J. J.; ROBERTS, L. E. The neuroscience of tinnitus. **Trends Neurosci**, v. 27, n. 11, p. 676–82, 2004. ISSN 0166-2236 (Print) 0166-2236 (Linking). Eggermont, Jos J Roberts, Larry E eng Research Support, Non-U.S. Gov't Review England 2004/10/12 09:00 Trends Neurosci. 2004 Nov;27(11):676-82. Available: <http://www.ncbi.nlm.nih.gov/pubmed/15474168>. Citations on pages 65 and 78.

EICHENBAUM, H. Hippocampus: cognitive processes and neural representations that underlie declarative memory. **Neuron**, v. 44, n. 1, p. 109–20, 2004. ISSN 0896-6273 (Print) 0896-6273 (Linking). Eichenbaum, Howard Neuron. 2004 Sep 30;44(1):109-20. Available: <http://www.ncbi.nlm.nih.gov/pubmed/15450164http://ac.els-cdn.com/S089662730400529X/1-s2.0-S089662730400529X-main.pdf?_tid=ddc91882-892d-11e2-84b3-00000aab0f6b&acdnat=1362884266_cddaedacc71d1263f9b0461a5408938a>. Citations on pages 61 and 62.

EKHTIARI, H.; GHOBADI-AZBARI, P.; THIELSCHER, A.; ANTAL, A.; LI, L. M.; SHEREEN, A. D.; CABRAL-CALDERIN, Y.; KEESER, D.; BERGMANN, T. O.; JAMIL, A. *et al.* A checklist for assessing the methodological quality of concurrent tes-fmri studies (contes checklist): a consensus study and statement. **Nature protocols**, Nature Publishing Group, v. 17, n. 3, p. 596–617, 2022. Citation on page 52.

ELHAMIFAR, E.; VIDAL, R. Sparse subspace clustering: Algorithm, theory, and applications. **IEEE transactions on pattern analysis and machine intelligence**, IEEE, v. 35, n. 11, p. 2765–2781, 2013. Citation on page 129.

EYSEL-GOSEPATH, K.; GERHARDS, F.; SCHICKETANZ, K.; TEICHMANN, K.; BENTHIEN, M. Attention diversion in tinnitus therapy. comparison of the effects of different treatment methods. **Hno**, v. 52, n. 5, p. 431–439, 2004. ISSN 0017-6192. Citation on page 94.

FARROKHI, H.; TOOSTANI, I. G.; FARASATKHAH, M.; EKHTIARI, H. Sustainable development of cognitive science and technology ecosystem; an overview to the "human brain project" as a functioning sample. **Basic and Clinical Neuroscience**, Iranian Neuroscience Society, v. 5, n. 1, p. 4, 2014. Citation on page 51.

FERRY, A. T.; ONGUR, D.; AN, X.; PRICE, J. L. Prefrontal cortical projections to the striatum in macaque monkeys: evidence for an organization related to prefrontal networks. **J Comp Neurol**, v. 425, n. 3, p. 447–70, 2000. ISSN 0021-9967 (Print) 0021-9967 (Linking). Ferry, A T Ongur, D An, X Price, J L R01-00093/PHS HHS/ J Comp Neurol. 2000 Sep 25;425(3):447-70.

Available: <http://www.ncbi.nlm.nih.gov/pubmed/10972944http://onlinelibrary.wiley.com/store/10.1002/1096-9861(20000925)425:3<447::AID-CNE9>3.0.CO;2-V/asset/9_ftp.pdf?v=1&t=hhalpkdn&s=a3b4931a4ac289ed631512e33518b4d11f9b0f99>. Citation on page 60.

FLOR, H.; SCHWARTZ, M. Tinnitus: Nothing is as loud as a sound you are trying not to hear. **Biofeedback: A practitioner's guide**, v. 3, 2003. Citation on page 92.

FOLMER, R. L.; GRIEST, S. E. Tinnitus and insomnia. **Am J Otolaryngol**, v. 21, n. 5, p. 287–93, 2000. ISSN 0196-0709 (Print) 0196-0709 (Linking). Folmer, R L Griest, S E Am J Otolaryngol. 2000 Sep-Oct;21(5):287-93. Available: <http://www.ncbi.nlm.nih.gov/pubmed/11032291http://ac.els-cdn.com/S019607090098757X/1-s2.0-S019607090098757X-main.pdf?_tid=ad4b356e-892d-11e2-a5a2-00000aacb361&acdnat=1362884184_1fd5dcdf32407b2700625d67e24fb9ea>. Citation on page 64.

FORD, M. **Architects of Intelligence: The truth about AI from the people building it**. [S.l.]: Packt Publishing Ltd, 2018. Citation on page 49.

FRANK, E.; SCHECKLMANN, M.; LANDGREBE, M.; BURGER, J.; KREUZER, P.; POEPPL, T. B.; KLEINJUNG, T.; HAJAK, G.; LANGGUTH, B. Treatment of chronic tinnitus with repeated sessions of prefrontal transcranial direct current stimulation: outcomes from an open-label pilot study. **Journal of Neurology**, Springer, v. 259, n. 2, p. 327–333, 2012. Citation on page 96.

FRANKLIN, S.; MADL, T.; D'MELLO, S.; SNAIDER, J. Lida: A systems-level architecture for cognition, emotion, and learning. **IEEE Transactions on Autonomous Mental Development**, IEEE, v. 6, n. 1, p. 19–41, 2013. Citation on page 45.

FREGNI, F.; BOGGIO, P. S.; NITSCHE, M.; BERMPOHL, F.; ANTAL, A.; FEREDOES, E.; MARCOLIN, M. A.; RIGONATTI, S. P.; SILVA, M. T.; PAULUS, W. *et al.* Anodal transcranial direct current stimulation of prefrontal cortex enhances working memory. **Experimental brain research**, Springer, v. 166, n. 1, p. 23–30, 2005. Citation on page 102.

FRIEDMAN, J.; HASTIE, T.; TIBSHIRANI, R. *et al.* **The elements of statistical learning**. [S.l.]: Springer series in statistics New York, 2001. Citations on pages 163 and 168.

FRIJDA, N. H. Comment on oatley and johnson-laird's "towards a cognitive theory of emotions". **Cognition and Emotion**, v. 1, n. 1, p. 51–58, 1987. ISSN 0269-9931. Citation on page 92.

FROEMKE, R. C.; MARTINS, A. R. Spectrotemporal dynamics of auditory cortical synaptic receptive field plasticity. **Hear Res**, v. 279, n. 1-2, p. 149–61, 2011. ISSN 1878-5891 (Electronic) 0378-5955 (Linking). Froemke, Robert C Martins, Ana Raquel O R00 DC009635-04/DC/NIDCD NIH HHS/ Netherlands Hear Res. 2011 Sep;279(1-2):149-61. doi: 10.1016/j.heares.2011.03.005. Epub 2011 Mar 21. Available: <http://www.ncbi.nlm.nih.gov/pubmed/21426927http://ac.els-cdn.com/S0378595511000761/1-s2.0-S0378595511000761-main.pdf?_tid=54425230-892e-11e2-8479-00000aacb35e&acdnat=1362884465_1e503d0e672110bb9068fe8672edfd21>. Citation on page 61.

FU, M. C.; GLOVER, F. W.; APRIL, J. Simulation optimization: a review, new developments, and applications. In: IEEE. **Proceedings of the Winter Simulation Conference, 2005.** [S.l.], 2005. p. 13–pp. Citation on page 212.

GARDNER, A.; PAGANI, M.; JACOBSSON, H.; LINDBERG, G.; LARSSON, S. A.; WAGNER, A.; HALLSTROM, T. Differences in resting state regional cerebral blood flow assessed with 99mtc-hmpao spect and brain atlas matching between depressed patients with and without tinnitus. **Nucl Med Commun**, v. 23, n. 5, p. 429–39, 2002. ISSN 0143-3636 (Print) 0143-3636 (Linking). Gardner, A Pagani, M Jacobsson, H Lindberg, G Larsson, S A Wagner, A Hallstrom, T England Nucl Med Commun. 2002 May;23(5):429-39. Available: <http://www.ncbi.nlm.nih.gov/pubmed/11973483>. Citation on page 78.

GELMAN, A.; CARLIN, J. B.; STERN, H. S.; DUNSON, D. B.; VEHTARI, A.; RUBIN, D. B. **Bayesian data analysis**. [S.l.]: CRC press, 2013. Citations on pages 18, 107, and 109.

GENDERS, W.; RAZAVI, S. Using a deep reinforcement learning agent for traffic signal control. **arXiv preprint arXiv:1611.01142**, 2016. Citation on page 213.

GHASHGHAEI, H. T.; HILGETAG, C. C.; BARBAS, H. Sequence of information processing for emotions based on the anatomic dialogue between prefrontal cortex and amygdala. **NeuroImage**, v. 34, n. 3, p. 905–23, 2007. ISSN 1053-8119 (Print) 1053-8119 (Linking). Ghashghaei, H T Hilgetag, C C Barbas, H R01 MH057414-07/MH/NIMH NIH HHS/ R01 NS024760-17/NS/NINDS NIH HHS/ Neuroimage. 2007 Feb 1;34(3):905-23. Epub 2006 Nov 27. Available: <http://www.ncbi.nlm.nih.gov/pubmed/17126037http://ac.els-cdn.com/S105381190600989X/1-s2.0-S105381190600989X-main.pdf?_tid=17dfd326-892e-11e2-adb2-00000aacb35f&acdnat=1362884363_ed9438758998df3ca22b41e9bb3bddc6>. Citation on page 67.

GHODRATITOOSTANI, I.; DELBEM, A. C.; TORABI-NAMI, M.; MAKKIABADI, B.; JALILVAND, H.; SANCHEZ, T. Theoretical tinnitus multimodality framework: A neurofunctional model. **Journal of Advanced Medical Sciences and Applied Technologies**, v. 2, n. 1, 2016. Citations on pages 15, 45, 52, 62, 68, 73, 74, 76, 87, 88, and 101.

GHODRATITOOSTANI, I.; DELBEM, A. C.; TORABI-NAMI, M.; MAKKIABADI, B.; JALILVAND, H.; SANCHEZ, T. G. Theoretical tinnitus multimodality framework: a neurofunctional model. **Journal of Advanced Medical Sciences and Applied Technologies**, Shiraz University of Medical Sciences, v. 2, n. 1, p. 181–189, 2016. Citation on page 52.

GHODRATITOOSTANI, I.; JR, O. A. G.; VAZIRI, Z.; DELBEM, A. C.; MAKKIABADI, B.; DATTA, A.; THOMAS, C.; HYPPOLITO, M. A.; SANTOS, A. C.; LOUZADA, F. *et al.* Dose-response transcranial electrical stimulation study design: A well-controlled adaptive seamless bayesian method to illuminate negative valence role in tinnitus perception. **Frontiers in Human Neuroscience**, Frontiers Media SA, v. 16, 2022. Citation on page 52.

GHODRATITOOSTANI, I.; KAMALI, A.-M.; TAHAMTAN, M.; MOHAMMADI, N.; ALIGHOLI, H.; NAMI, M. The substrates of integrated neurocognitive rehabilitation platforms (incrps). **arXiv preprint arXiv:1906.02558**, 2019. Citations on pages 51 and 55.

GHODRATITOOSTANI, I.; ZANA, Y.; DELBEM, A. C.; SANI, S. S.; EKHTIARI, H.; SANCHEZ, T. G. Theoretical tinnitus framework: A neurofunctional model. **Front Neurosci**, v. 10, p. 370, 2016. ISSN 1662-4548 (Print) 1662-453X (Linking). Ghodratitoostani, Iman Zana, Yossi Delbem, Alexandre C B Sani, Siamak S Ekhtiari, Hamed Sanchez, Tanit G eng Switzerland 2016/09/07 06:00 Front Neurosci. 2016 Aug 19;10:370. doi: 10.3389/fnins.2016.00370. eCollection 2016. Available: <https://www.ncbi.nlm.nih.gov/pubmed/27594822>. Citations on pages 15, 45, 68, 69, 70, 71, 73, 74, 77, 78, 83, 84, 85, 86, 87, 88, 89, 91, 92, 101, and 102.

GOLDSWORTHY, M. R.; HORDACRE, B. Dose dependency of transcranial direct current stimulation: implications for neuroplasticity induction in health and disease. **The Journal of Physiology**, Wiley-Blackwell, v. 595, n. 11, p. 3265, 2017. Citation on page 103.

GOLM, D.; SCHMIDT-SAMOA, C.; DECHENT, P.; KROENER-HERWIG, B. Tinnitus- related distress: evidence from fmri of an emotional stroop task. **BMC Ear, Nose & Throat Disorders**, v. 16, 2016. ISSN 1472-6815. Citation on page 91.

GONG, Y.; KUMAR, S.; VERMA, V.; LAZEBNIK, S. Angular quantization-based binary codes for fast similarity search. 2012. Citation on page 164.

GOTO, Y.; O'DONNELL, P. Network synchrony in the nucleus accumbens in vivo. **J Neurosci**, v. 21, n. 12, p. 4498–504, 2001. ISSN 1529-2401 (Electronic) 0270-6474 (Linking). Goto, Y O'Donnell, P MH57683/MH/NIMH NIH HHS/ MH60131/MH/NIMH NIH HHS/ J Neurosci. 2001 Jun 15;21(12):4498-504. Available: <http://www.ncbi.nlm.nih.gov/pubmed/11404437http://www.jneurosci.org/content/21/12/4498.full.pdf>. Citation on page 63.

GRASSBERGER, P. Generalizations of the hausdorff dimension of fractal measures. **Physics Letters A**, Elsevier, v. 107, n. 3, p. 101–105, 1985. Citation on page 134.

GRAZIANO, M. S.; WEBB, T. W. The attention schema theory: a mechanistic account of subjective awareness. **Front Psychol**, v. 6, p. 500, 2015. ISSN 1664-1078 (Electronic) 1664-1078 (Linking). Graziano, Michael S A Webb, Taylor W eng Switzerland 2015/05/09 06:00 Front Psychol. 2015 Apr 23;6:500. doi: 10.3389/fpsyg.2015.00500. eCollection 2015. Available: <http://www.ncbi.nlm.nih.gov/pubmed/25954242>. Citation on page 68.

GROSS, J. J. The emerging field of emotion regulation: An integrative review. **Review of general psychology**, SAGE Publications Sage CA: Los Angeles, CA, v. 2, n. 3, p. 271–299, 1998. Citations on pages 88 and 101.

____. The emerging field of emotion regulation: An integrative review. **Review of general psychology**, v. 2, n. 3, p. 271, 1998. ISSN 155798560X. Citation on page 88.

____. **Handbook of emotion regulation**. [S.l.]: Guilford publications, 2013. Citations on pages 87, 88, and 101.

GRUBER, A. J.; HUSSAIN, R. J.; O'DONNELL, P. The nucleus accumbens: a switchboard for goal-directed behaviors. **PLoS One**, v. 4, n. 4, p. e5062, 2009. ISSN 1932-6203 (Electronic) 1932-6203 (Linking). Gruber, Aaron J Hussain, Rifat J O'Donnell, Patricio MH60131/MH/NIMH NIH HHS/ PLoS One. 2009;4(4):e5062. doi: 10.1371/journal.pone.0005062. Epub 2009 Apr 7. Available: <http://www.ncbi.nlm.nih.gov/pubmed/19352511http://www.plosone.org/article/fetchObjectAttachment.action?uri=info%3Adoi%2F10.1371%2Fjournal.pone.0005062&representation=PDF>. Citation on page 64.

GU, J. W.; HALPIN, C. F.; NAM, E. C.; LEVINE, R. A.; MELCHER, J. R. Tinnitus, diminished sound-level tolerance, and elevated auditory activity in humans with clinically normal hearing sensitivity. **J Neurophysiol**, v. 104, n. 6, p. 3361–70, 2010. ISSN 1522-1598 (Electronic) 0022-3077 (Linking). Gu, Jianwen Wendy Halpin, Christopher F Nam, Eui-Cheol Levine, Robert A Melcher, Jennifer R P30 DC-005209/DC/NIDCD NIH HHS/ P41RR14075/RR/NCRR NIH HHS/ T32 DC-00038/DC/NIDCD NIH HHS/ J Neurophysiol. 2010 Dec;104(6):3361-70. Epub 2010 Sep 29. Available: <http://www.ncbi.nlm.nih.gov/pubmed/20881196http://jn.physiology.org/content/104/6/3361.full.pdf>. Citation on page 59.

GUILLERY, R. W.; SHERMAN, S. M. Thalamic relay functions and their role in corticocortical communication: generalizations from the visual system. **Neuron**, v. 33, n. 2, p. 163–75, 2002. ISSN 0896-6273 (Print) 0896-6273 (Linking). Guillery, R W Sherman, S Murray EY0308/EY/NEI NIH HHS/ EY11409/EY/NEI NIH HHS/ EY11494/EY/NEI NIH HHS/ EY12936/EY/NEI NIH HHS/ Neuron. 2002 Jan 17;33(2):163-75. Available: <http://www.ncbi.nlm.nih.gov/pubmed/11804565http://ac.els-cdn.com/S0896627301005827/1-s2.0-S0896627301005827-main.pdf?_tid=c375dfce-892d-11e2-b9a1-00000aacb35d&acdnat=1362884222_6d489c76ca7a1d2f8b1412a290a5f456>. Citation on page 64.

GUSNARD, D. A.; RAICHLE, M. E. Searching for a baseline: functional imaging and the resting human brain. **Nat Rev Neurosci**, v. 2, n. 10, p. 685–94, 2001. ISSN 1471-003X (Print) 1471-003X (Linking). Gusnard, D A Raichle, M E England Nat Rev Neurosci. 2001 Oct;2(10):685-94. Available: <http://www.ncbi.nlm.nih.gov/pubmed/11584306http://www.nature.com/nrn/journal/v2/n10/pdf/nrn1001-685a.pdf>. Citation on page 59.

HALE, J. B.; FIORELLO, C. A.; BROWN, L. Determining medication treatment effects using teacher ratings and classroom observations of children with adhd: Does neuropsychological impairment matter. **Educational and Child Psychology**, v. 22, n. 2, p. 39–61, 2005. Citation on page 45.

HALE, J. B.; REDDY, L. A.; SEMRUD-CLIKEMAN, M.; HAIN, L. A.; WHITAKER, J.; MORLEY, J.; LAWRENCE, K.; SMITH, A.; JONES, N. Executive impairment determines adhd medication response: implications for academic achievement. **Journal of Learning Disabilities**, Sage Publications Sage CA: Los Angeles, CA, v. 44, n. 2, p. 196–212, 2011. Citation on page 45.

HALFORD, J. B.; ANDERSON, S. D. Anxiety and depression in tinnitus sufferers. **J Psychosom Res**, v. 35, n. 4-5, p. 383–90, 1991. ISSN 0022-3999 (Print) 0022-3999 (Linking). Halford, J B Anderson, S D ENGLAND J Psychosom Res. 1991;35(4-5):383-90. Available: <http://www.ncbi.nlm.nih.gov/pubmed/1920169http://ac.els-cdn.com/002239999190033K/1-s2.0-002239999190033K-main.pdf?_tid=d828e087423739ae01a77188275b9af9&acdnat=1340992022_01faf2e752c4e93bb88064ed4e6a28c3>. Citations on pages 59, 60, and 77.

____. Tinnitus severity measured by a subjective scale, audiometry and clinical judgement. **J Laryngol Otol**, v. 105, n. 2, p. 89–93, 1991. ISSN 0022-2151 (Print) 0022-2151 (Linking). Halford, J B Anderson, S D ENGLAND J Laryngol Otol. 1991 Feb;105(2):89-93. Available: <http://www.ncbi.nlm.nih.gov/pubmed/2013737>. Citations on pages 59 and 60.

HALLAM, R.; MCKENNA, L.; SHURLOCK, L. Tinnitus impairs cognitive efficiency. **International journal of audiology**, Taylor & Francis, v. 43, n. 4, p. 218–226, 2004. Citation on page 87.

HALLAM, R. S. Correlates of sleep disturbance in chronic distressing tinnitus. **Scand Audiol**, v. 25, n. 4, p. 263–6, 1996. ISSN 0105-0397 (Print) 0105-0397 (Linking). Hallam, R S DENMARK Scand Audiol. 1996;25(4):263-6. Available: <http://www.ncbi.nlm.nih.gov/pubmed/8975999>. Citation on page 64.

HANDSCOMB, L. E.; HALL, D. A.; SHORTER, G. W.; HOARE, D. J. Positive and negative thinking in tinnitus: factor structure of the tinnitus cognitions questionnaire. **Ear and hearing**, Wolters Kluwer Health, v. 38, n. 1, p. 126, 2017. Citations on pages 88 and 101.

HANNULA, D. E.; GREENE, A. J. The hippocampus reevaluated in unconscious learning and memory: at a tipping point? **Front Hum Neurosci**, v. 6, p. 80, 2012. ISSN 1662-5161 (Electronic) 1662-5161 (Linking). Hannula, Deborah E Greene, Anthony J Switzerland Front Hum Neurosci. 2012;6:80. doi: 10.3389/fnhum.2012.00080. Epub 2012 Apr 12. Available: <http://www.ncbi.nlm.nih.gov/pubmed/22518102http://www.frontiersin.org/Journal/DownloadFile/1/94307/17700/1/21/fnhum-06-00080_pdf>. Citation on page 69.

HARE, T. A.; CAMERER, C. F.; RANGEL, A. Self-control in decision-making involves modulation of the vmpfc valuation system. **Science**, v. 324, n. 5927, p. 646–8, 2009. ISSN 1095-9203 (Electronic) 0036-8075 (Linking). Hare, Todd A Camerer, Colin F Rangel, Antonio New York, N.Y. Science. 2009 May 1;324(5927):646-8. doi: 10.1126/science.1168450. Available: <http://www.ncbi.nlm.nih.gov/pubmed/19407204http://www.sciencemag.org/content/324/5927/646http://www.sciencemag.org/content/324/5927/646.full.pdf>. Citation on page 68.

HARIRI, A. R.; MATTAY, V. S.; TESSITORE, A.; FERA, F.; WEINBERGER, D. R. Neocortical modulation of the amygdala response to fearful stimuli. **Biol Psychiatry**, v. 53, n. 6, p. 494–501, 2003. ISSN 0006-3223 (Print) 0006-3223 (Linking). Hariri, Ahmad R Mattay, Venkata S Tessitore, Alessandro Fera, Francesco Weinberger, Daniel R Biol Psychiatry. 2003 Mar 15;53(6):494-501. Available: <http://www.ncbi.nlm.nih.gov/pubmed/12644354http://ac.els-cdn.com/S0006322302017869/1-s2.0-S0006322302017869-main.pdf?_tid=d70c4b90-892d-11e2-b594-00000aacb35d&acdnat=1362884254_62003cac70cbf61b2568f27a9fad7126>. Citation on page 61.

HAVLICEK, L. L.; PETERSON, N. L. Effect of the violation of assumptions upon significance levels of the pearson r. **Psychological Bulletin**, American Psychological Association, v. 84, n. 2, p. 373, 1977. Citation on page 195.

HAYES, A. F. Permutation test is not distribution-free: Testing h: $\rho = 0$. **Psychological Methods**, American Psychological Association, v. 1, n. 2, p. 184, 1996. Citation on page 195.

____. Book. **Introduction to mediation, moderation, and conditional process analysis: A regression-based approach**. [S.l.]: Guilford publications, 2017. ISBN 1462534651. Citations on pages 195, 199, 200, and 217.

HE, D. F.; CHEN, F. J.; ZHOU, S. C. Gaba mediaties the inhibitory effect of lateral amygdaloid nucleus stimulation on the acoustic response of neurons in a i cortex: An in vivo microiontophoretic study. **Sheng Li Xue Bao**, v. 56, n. 3, p. 374–8, 2004. ISSN 0371-0874 (Print) 0371-0874 (Linking). He, De-Fu Chen, Fu-Jun Zhou, Shao-Ci China Sheng Li Xue Bao. 2004 Jun 25;56(3):374-8. Available: <http://www.ncbi.nlm.nih.gov/pubmed/15224153>. Citation on page 61.

HEINECKE, K.; WEISE, C.; SCHWARZ, K.; RIEF, W. Physiological and psychological stress reactivity in chronic tinnitus. **J Behav Med**, v. 31, n. 3, p. 179–88, 2008. ISSN 0160-7715 (Print) 0160-7715. Citation on page 93.

HENKE, K. A model for memory systems based on processing modes rather than consciousness. **Nat Rev Neurosci**, v. 11, n. 7, p. 523–32, 2010. ISSN 1471-0048 (Electronic) 1471-003X (Linking). Henke, Katharina England Nat Rev Neurosci. 2010 Jul;11(7):523-32. doi: 10.1038/nrn2850. Available: <http://www.ncbi.nlm.nih.gov/pubmed/20531422http://www.nature.com/nrn/journal/v11/n7/pdf/nrn2850.pdf>. Citations on pages 69, 70, and 84.

HENRY, J. L.; WILSON, P. H. An evaluation of two types of cognitive intervention in the management of chronic tinnitus. **Behaviour Therapy**, v. 27, n. 4, p. 156–166, 1998. ISSN 0284-5717. Citation on page 94.

HERRERO, J.; VALENCIA, A.; DOPAZO, J. A hierarchical unsupervised growing neural network for clustering gene expression patterns. **Bioinformatics**, Oxford University Press, v. 17, n. 2, p. 126–136, 2001. Citation on page 168.

HESSER, H.; WEISE, C.; WESTIN, V. Z.; ANDERSSON, G. A systematic review and meta-analysis of randomized controlled trials of cognitive–behavioral therapy for tinnitus distress. **Clinical psychology review**, v. 31, n. 4, p. 545–553, 2011. ISSN 0272-7358. Citation on page 95.

HINTON, G.; ROWEIS, S. T. Stochastic neighbor embedding. In: CITESEER. **NIPS**. [S.l.], 2002. v. 15, p. 833–840. Citations on pages 129, 130, 134, and 138.

HOCHREITER, S.; SCHMIDHUBER, J. Long short-term memory. **Neural computation**, MIT Press, v. 9, n. 8, p. 1735–1780, 1997. Citation on page 216.

HOFFMAN, H.; REED, G. Epidemiology of tinnitus. In: ____. **Tinnitus: Theory and Management.** [S.l.: s.n.], 2004. p. 16e41. Citation on page 64.

HORSTMANN, G.; HERWIG, A. Novelty biases attention and gaze in a surprise trial. **Attention, Perception, & Psychophysics**, Springer, v. 78, n. 1, p. 69–77, 2016. Citation on page 90.

HOUWER, J. D.; THOMAS, S.; BAEYENS, F. Association learning of likes and dislikes: A review of 25 years of research on human evaluative conditioning. **Psychological bulletin**, American Psychological Association, v. 127, n. 6, p. 853, 2001. Citation on page 105.

____. Associative learning of likes and dislikes: a review of 25 years of research on human evaluative conditioning. **Psychol Bull**, v. 127, n. 6, p. 853–69, 2001. ISSN 0033-2909 (Print) 0033-2909 (Linking). De Houwer, J Thomas, S Baeyens, F eng Research Support, Non-U.S. Gov't Review Psychol Bull. 2001 Nov;127(6):853-69. doi: 10.1037/0033-2909.127.6.853. Available: <https://www.ncbi.nlm.nih.gov/pubmed/11726074>. Citations on pages 70, 88, 89, 91, 92, and 101.

HUANG, Y.; VALTORTA, M. Pearl's calculus of intervention is complete. **arXiv preprint arXiv:1206.6831**, 2012. Citation on page 217.

HURWITZ, J.; KAUFMAN, M.; BOWLES, A.; NUGENT, A.; KOBIELUS, J. G.; KOWOLENKO, M. D. **Cognitive computing and big data analytics**. [S.l.]: Wiley Online Library, 2015. Citation on page 46.

HUSAIN, F. T.; PAJOR, N. M.; SMITH, J. F.; KIM, H. J.; RUDY, S.; ZALEWSKI, C.; BREWER, C.; HORWITZ, B. Discrimination task reveals differences in neural bases of tinnitus and hearing impairment. **PLoS One**, v. 6, n. 10, p. e26639, 2011. ISSN 1932-6203 (Electronic) 1932-6203 (Linking). Husain, Fatima T Pajor, Nathan M Smith, Jason F Kim, H Jeff Rudy, Susan Zalewski, Christopher Brewer, Carmen Horwitz, Barry PLoS One. 2011;6(10):e26639. Epub 2011 Oct 31. Available: <http://www.ncbi.nlm.nih.gov/pubmed/22066003http://www.plosone.org/article/fetchObjectAttachment.action?uri=info%3Adoi%2F10.1371%2Fjournal.pone.0026639&representation=PDF>. Citation on page 78.

HUSAIN, F. T.; ZIMMERMAN, B.; TAI, Y.; FINNEGAN, M. K.; KAY, E.; KHAN, F.; MENARD, C.; GOBIN, R. L. Assessing mindfulness-based cognitive therapy intervention for tinnitus using behavioural measures and structural mri: a pilot study. **International Journal of Audiology**, v. 58, n. 12, p. 889–901, 2019. ISSN 1499-2027. Citation on page 95.

HUTTER, M.; SWELDENS, S. Implicit misattribution of evaluative responses: contingency-unaware evaluative conditioning requires simultaneous stimulus presentations. **J Exp Psychol Gen**, v. 142, n. 3, p. 638–43, 2013. ISSN 1939-2222 (Electronic) 0022-1015 (Linking). Hutter, Mandy Sweldens, Steven eng Research Support, Non-U.S. Gov't 2012/09/06 06:00 J Exp Psychol Gen. 2013 Aug;142(3):638-43. doi: 10.1037/a0029989. Epub 2012 Sep 3. Available: <http://www.ncbi.nlm.nih.gov/pubmed/22946896>. Citation on page 70.

HYVARINEN, A. Fast and robust fixed-point algorithms for independent component analysis. **IEEE transactions on Neural Networks**, IEEE, v. 10, n. 3, p. 626–634, 1999. Citations on pages 129, 130, and 134.

IIDA, F.; LASCHI, C. Soft robotics: Challenges and perspectives. **Procedia Computer Science**, Elsevier, v. 7, p. 99–102, 2011. Citations on pages 51, 207, and 212.

IMBENS, G. W.; RUBIN, D. B. **Causal inference in statistics, social, and biomedical sciences**. [S.l.]: Cambridge University Press, 2015. Citation on page 217.

ISING, H.; KRUPPA, B. Health effects caused by noise: evidence in the literature from the past 25 years. **Noise Health**, v. 6, n. 22, p. 5–13, 2004. ISSN 1463-1741 (Print) 1463-1741 (Linking). Ising, H Kruppa, B England Noise Health. 2004 Jan-Mar;6(22):5-13. Available: <http://www.ncbi.nlm.nih.gov/pubmed/15070524http://www.noiseandhealth.org/article.asp?issn=1463-1741;year=2004;volume=6;issue=22;spage=5;epage=13;aulast=Ising>. Citation on page 61.

JACKSON, M. P.; RAHMAN, A.; LAFON, B.; KRONBERG, G.; LING, D.; PARRA, L. C.; BIKSON, M. Animal models of transcranial direct current stimulation: methods and mechanisms. **Clinical Neurophysiology**, Elsevier, v. 127, n. 11, p. 3425–3454, 2016. Citation on page 102.

JACOB, H.; BRÜCK, C.; DOMIN, M.; LOTZE, M.; WILDGRUBER, D. I can't keep your face and voice out of my head: neural correlates of an attentional bias toward nonverbal emotional cues. **Cerebral Cortex**, Oxford University Press, v. 24, n. 6, p. 1460–1473, 2014. Citation on page 101.

JAIN, A. K. Data clustering: 50 years beyond k-means pattern recognition letters. **Corrected Proof**, 2009. Citation on page 163.

JAIN, A. K.; DUBES, R. C. **Algorithms for clustering data**. [S.l.]: Prentice-Hall, Inc., 1988. Citation on page 163.

JAMIL, A.; BATSIKADZE, G.; KUO, H.-I.; LABRUNA, L.; HASAN, A.; PAULUS, W.; NITSCHE, M. A. Systematic evaluation of the impact of stimulation intensity on neuroplastic after-effects induced by transcranial direct current stimulation. **The Journal of physiology**, Wiley Online Library, v. 595, n. 4, p. 1273–1288, 2017. Citations on pages 102 and 103.

JASTREBOFF, P.; JASTREBOFF, M. Tinnitus retraining therapy: a different view on tinnitus. **Orl**, v. 68, n. 1, p. 23, 2006. ISSN 0301-1569. Citation on page 79.

JASTREBOFF, P. J. Phantom auditory perception (tinnitus): mechanisms of generation and perception. **Neurosci Res**, v. 8, n. 4, p. 221–54, 1990. ISSN 0168-0102 (Print) 0168-0102 (Linking). Jastreboff, P J DC00299/DC/NIDCD NIH HHS/ IRELAND Neurosci Res. 1990 Aug;8(4):221-54. Available: <http://www.ncbi.nlm.nih.gov/pubmed/2175858http://ac.els-cdn.com/0168010290900319/1-s2.0-0168010290900319-main.pdf?_tid=b8eedd9fc31c4ed1cb05483a6429f7e6&acdnat=1340992151_6fbbe72a859f37cc0e5645c4bd4b550f>. Citations on pages 15, 79, 84, 87, and 101.

JASTREBOFF, P. J.; BRENNAN, J. F.; COLEMAN, J. K.; SASAKI, C. T. Phantom auditory sensation in rats: an animal model for tinnitus. **Behav Neurosci**, v. 102, n. 6, p. 811–22, 1988. ISSN 0735-7044 (Print) 0735-7044 (Linking). Jastreboff, P J Brennan, J F Coleman, J K Sasaki, C T NS 16288/NS/NINDS NIH HHS/ NS 22024/NS/NINDS NIH HHS/ Behav Neurosci. 1988 Dec;102(6):811-22. Available: <http://www.ncbi.nlm.nih.gov/pubmed/3214530http://psycnet.apa.org/journals/bne/102/6/811.pdf>. Citation on page 78.

JASTREBOFF, P. J.; HAZELL, J. W. A neurophysiological approach to tinnitus: clinical implications. **British journal of audiology**, Taylor & Francis, v. 27, n. 1, p. 7–17, 1993. Citation on page 94.

____. Book. **Tinnitus Retraining Therapy: Implementing the Neurophysiological Model**. United States of America by Cambridge University Press, New York: Cambridge university press, 2004. ISBN 978-0-521-59256-7. Citation on page 78.

JASTREBOFF, P. J.; SASAKI, C. T. Salicylate-induced changes in spontaneous activity of single units in the inferior colliculus of the guinea pig. **J Acoust Soc Am**, v. 80, n. 5, p. 1384–91, 1986. ISSN 0001-4966 (Print) 0001-4966 (Linking). Jastreboff, P J Sasaki, C T eng NS 16288/NS/NINDS NIH HHS/ NS 22024/NS/NINDS NIH HHS/ Research Support, U.S. Gov't, P.H.S. 1986/11/01 J Acoust Soc Am. 1986 Nov;80(5):1384-91. Available: <http://www.ncbi.nlm.nih.gov/pubmed/3782617>. Citations on pages 73 and 78.

JAY, T. M.; WITTER, M. P. Distribution of hippocampal ca1 and subicular efferents in the prefrontal cortex of the rat studied by means of anterograde transport of phaseolus vulgaris-leucoagglutinin. **J Comp Neurol**, v. 313, n. 4, p. 574–86, 1991. ISSN 0021-9967 (Print) 0021-9967 (Linking). Jay, T M Witter, M P J Comp Neurol. 1991 Nov 22;313(4):574-86. Available: <http://www.ncbi.nlm.nih.gov/pubmed/1783682http://onlinelibrary.wiley.com/doi/10.1002/cne.903130404/abstract>. Citation on page 63.

JAYARAMAN, A. Anatomical evidence for cortical projections from the striatum in the cat. **Brain Res**, v. 195, n. 1, p. 29–36, 1980. ISSN 0006-8993 (Print) 0006-8993 (Linking). Jayaraman, A NETHERLANDS Brain Res. 1980 Aug 11;195(1):29-36. Available: <http://www.ncbi.nlm.nih.gov/pubmed/7397497http://ac.els-cdn.com/000689938090863X/1-s2.0-000689938090863X-main.pdf?_tid=74d6f89e-892d-11e2-90b2-00000aab0f6b&acdnat=1362884090_b392fd0b4721e10302749eea8cf20733>. Citation on page 60.

JENTSCHKE, S.; KOELSCH, S.; FRIEDERICI, A. D. Investigating the relationship of music and language in children: influences of musical training and language impairment. **Ann N Y Acad Sci**, v. 1060, p. 231–42, 2005. ISSN 0077-8923 (Print) 0077-8923 (Linking). Jentschke, Sebastian Koelsch, Stefan Friederici, Angela D Ann N Y Acad Sci. 2005 Dec;1060:231-42. Available: <http://www.ncbi.nlm.nih.gov/pubmed/16597770http://onlinelibrary.wiley.com/store/10.1196/annals.1360.016/asset/annals.1360.016.pdf?v=1&t=he3m0icx&s=66dbc8f5fa33f571960837c7b9c9c8d98400eb5b>. Citation on page 61.

JOHANSEN-BERG, H.; GUTMAN, D. A.; BEHRENS, T. E.; MATTHEWS, P. M.; RUSHWORTH, M. F.; KATZ, E.; LOZANO, A. M.; MAYBERG, H. S. Anatomical connectivity of the subgenual cingulate region targeted with deep brain stimulation for treatment-resistant depression. **Cereb Cortex**, v. 18, n. 6, p. 1374–83, 2008. ISSN 1460-2199 (Electronic) 1047-3211 (Linking). Johansen-Berg, H Gutman, D A Behrens, T E J Matthews, P M Rushworth, M F S Katz, E Lozano, A M Mayberg, H S 078204/Wellcome Trust/United Kingdom Medical Research Council/United Kingdom Wellcome Trust/United Kingdom New York, N.Y. : 1991 Cereb Cortex. 2008 Jun;18(6):1374-83. Epub 2007 Oct 10. Available: <http://www.ncbi.nlm.nih.gov/pubmed/17928332http://cercor.oxfordjournals.org/content/18/6/1374.full.pdf>. Citation on page 64.

JOLLIFFE, I. Principal component analysis. **Technometrics**, American Society for Quality, v. 45, n. 3, p. 276, 2003. Citations on pages 129, 130, 131, and 163.

JUN, H. J.; PARK, M. K. Cognitive behavioral therapy for tinnitus: evidence and efficacy. **Korean journal of audiology**, v. 17, n. 3, p. 101, 2013. Citation on page 95.

JURCAK, V.; TSUZUKI, D.; DAN, I. 10/20, 10/10, and 10/5 systems revisited: their validity as relative head-surface-based positioning systems. **Neuroimage**, Elsevier, v. 34, n. 4, p. 1600–1611, 2007. Citation on page 104.

KABLE, J. W.; GLIMCHER, P. W. The neurobiology of decision: consensus and controversy. **Neuron**, v. 63, n. 6, p. 733–45, 2009. ISSN 1097-4199 (Electronic) 0896-6273 (Linking). Kable, Joseph W Glimcher, Paul W R01 EY010536-13A2S1/EY/NEI NIH HHS/ R01 NS054775-03/NS/NINDS NIH HHS/ R01-EY010536/EY/NEI NIH HHS/ R01-NS054775/NS/NINDS NIH HHS/ Neuron. 2009 Sep 24;63(6):733-45. doi: 10.1016/j.neuron.2009.09.003. Available: <http://www.ncbi.nlm.nih.gov/pubmed/19778504http://ac.els-cdn.com/S0896627309006813/1-s2.0-S0896627309006813-main.pdf?_tid=346c947a-892e-11e2-acb3-00000aacb35d&acdnat=1362884411_bad299301ef6e53a29cc63ed5fd0a68d>. Citations on pages 59 and 60.

KALTENBACH, J. A. Neurophysiologic mechanisms of tinnitus. **J Am Acad Audiol**, v. 11, n. 3, p. 125–37, 2000. ISSN 1050-0545 (Print) 1050-0545 (Linking). Kaltenbach, J A R01 DC 03258/DC/NIDCD NIH HHS/ CANADA J Am Acad Audiol. 2000 Mar;11(3):125-37. Available: <http://www.ncbi.nlm.nih.gov/pubmed/10755809>. Citation on page 65.

KALTENBACH, J. A.; GODFREY, D. A. Dorsal cochlear nucleus hyperactivity and tinnitus: are they related? **Am J Audiol**, v. 17, n. 2, p. S148–61, 2008. ISSN 1059-0889 (Print) 1059-0889 (Linking). Kaltenbach, James A Godfrey, Donald A Am J Audiol. 2008 Dec;17(2):S148-61. doi: 10.1044/1059-0889(2008/08-0004). Epub 2008 Oct 31. Available: <http://www.ncbi.nlm.nih.gov/pubmed/18978198http://aja.asha.org/cgi/content/abstract/17/2/S148http://aja.pubs.asha.org/article.aspx?articleid=1757445>. Citations on pages 59, 60, and 65.

KALTENBACH, J. A.; GODFREY, D. A.; NEUMANN, J. B.; MCCASLIN, D. L.; AFMAN, C. E.; ZHANG, J. Changes in spontaneous neural activity in the dorsal cochlear nucleus following exposure to intense sound: relation to threshold shift. **Hear Res**, v. 124, n. 1-2, p. 78–84, 1998. ISSN 0378-5955 (Print) 0378-5955 (Linking). Kaltenbach, J A Godfrey, D A Neumann, J B McCaslin, D L Afman, C E Zhang, J eng DC03258-01/DC/NIDCD NIH HHS/ Research Support, Non-U.S. Gov't Research Support, U.S. Gov't, P.H.S. NETHERLANDS 1998/11/21 Hear Res. 1998 Oct;124(1-2):78-84. Available: <http://www.ncbi.nlm.nih.gov/pubmed/9822904>. Citations on pages 73 and 78.

KALTENBACH, J. A.; MCCASLIN, D. L. Increases in spontaneous activity in the dorsal cochlear nucleus following exposure to high intensity sound: A possible neural correlate of tinnitus. **Auditory neuroscience**, v. 3, n. 1, p. 57–78, 1996. ISSN 1023-618X (Print) 1023-618X (Linking). Kaltenbach, James A McCaslin, Devin L ENG R01 DC003258/DC/NIDCD NIH HHS/ T32 DC000026/DC/NIDCD NIH HHS/ 1996/01/01 00:00 1996;3(1):57-78. Available: <http://www.ncbi.nlm.nih.gov/pubmed/24244077>. Citations on pages 73 and 78.

KALTENBACH, J. A.; ZACHAREK, M. A.; ZHANG, J.; FREDERICK, S. Activity in the dorsal cochlear nucleus of hamsters previously tested for tinnitus following intense tone exposure. **Neurosci Lett**, v. 355, n. 1-2, p. 121–5, 2004. ISSN 0304-3940 (Print) 0304-3940 (Linking). Kaltenbach, James A Zacharek, Mark A Zhang, Jinsheng Frederick, Sarah R01 DC03258/DC/NIDCD NIH HHS/ Ireland Neurosci Lett. 2004 Jan 23;355(1-2):121-5. Available: <http://www.ncbi.nlm.nih.gov/pubmed/14729250http://ac.els-cdn.com/S0304394003012321/1-s2.0-S0304394003012321-main.pdf?_tid=1b6e292a-c86c-11e2-9c74-00000aab0f02&acdnat=1369837921_d7342c4eb397445a4142ea6583fb96d1>. Citation on page 65.

KAMADA, T.; KAWAI, S. An algorithm for drawing general undirected graphs, information processing letters, vol. 31.-pp. 7-15. 1989. Citations on pages 129, 130, 134, and 138.

KAPING, D.; VINCK, M.; HUTCHISON, R. M.; EVERLING, S.; WOMELSDORF, T. Specific contributions of ventromedial, anterior cingulate, and lateral prefrontal cortex for attentional selection and stimulus valuation. **PLoS Biol**, v. 9, n. 12, p. e1001224, 2011. ISSN 1545-7885 (Electronic) 1544-9173 (Linking). Kaping, Daniel Vinck, Martin Hutchison, R Matthew Everling, Stefan Womelsdorf, Thilo Canadian Institutes of Health Research/Canada PLoS Biol. 2011 Dec;9(12):e1001224. doi: 10.1371/journal.pbio.1001224. Epub 2011 Dec 27. Available: <http://www.ncbi.nlm.nih.gov/pubmed/22215982http://www.plosbiology.org/article/fetchObjectAttachment.action?uri=info%3Adoi%2F10.1371%2Fjournal.pbio.1001224&representation=PDF>. Citations on pages 68 and 73.

KATTNER, F. Revisiting the relation between contingency awareness and attention: evaluative conditioning relies on a contingency focus. **Cogn Emot**, v. 26, n. 1, p. 166–75, 2012. ISSN 1464-0600 (Electronic) 0269-9931 (Linking). Kattner, Florian eng England 2011/05/11 06:00 Cogn Emot. 2012;26(1):166-75. doi: 10.1080/02699931.2011.565036. Epub 2011 May 24. Available: <http://www.ncbi.nlm.nih.gov/pubmed/21557120>. Citation on page 70.

KAUFMAN, L.; ROUSSEEUW, P. J. **Finding groups in data: an introduction to cluster analysis**. [S.l.]: John Wiley & Sons, 2009. Citation on page 163.

KERNS, K. A.; ESO, K.; THOMSON, J. Investigation of a direct intervention for improving attention in young children with adhd. **Developmental neuropsychology**, Taylor & Francis, v. 16, n. 2, p. 273–295, 1999. Citation on page 45.

KIANG, N. Y.; MOXON, E. C.; LEVINE, R. A. Auditory-nerve activity in cats with normal and abnormal cochleas. in: Sensorineural hearing loss. **Ciba Found Symp**, p. 241–73, 1970. ISSN 0300-5208 (Print) 0300-5208 (Linking). Kiang, N Y Moxon, E C Levine, R A eng NETHERLANDS 1970/01/01 Ciba Found Symp. 1970:241-73. Available: <http://www.ncbi.nlm.nih.gov/pubmed/5210916>. Citation on page 67.

KIMURA, A.; IMBE, H.; DONISHI, T.; TAMAI, Y. Axonal projections of single auditory neurons in the thalamic reticular nucleus: implications for tonotopy-related gating function and cross-modal modulation. **European Journal of Neuroscience**,

v. 26, n. 12, p. 3524–35, 2007. ISSN 1460-9568 (Electronic) 0953-816X (Linking). Kimura, A Imbe, H Donishi, T Tamai, Y France Eur J Neurosci. 2007 Dec;26(12):3524-35. Epub 2007 Dec 4. Available: <http://www.ncbi.nlm.nih.gov/pubmed/18052989http://onlinelibrary.wiley.com/store/10.1111/j.1460-9568.2007.05925.x/asset/j.1460-9568.2007.05925.x.pdf?v=1&t=he3m1xfc&s=5f16cb5009c3d1c1f2174c96ac04badd73f1316c>. Citation on page 58.

KIMURA, A.; YOKOI, I.; IMBE, H.; DONISHI, T.; KANEOKE, Y. Auditory thalamic reticular nucleus of the rat: anatomical nodes for modulation of auditory and cross-modal sensory processing in the loop connectivity between the cortex and thalamus. **J Comp Neurol**, v. 520, n. 7, p. 1457–80, 2012. ISSN 1096-9861 (Electronic) 0021-9967 (Linking). Kimura, Akihisa Yokoi, Isao Imbe, Hiroki Donishi, Tomohiro Kaneoke, Yoshiki J Comp Neurol. 2012 May 1;520(7):1457-80. Available: <http://www.ncbi.nlm.nih.gov/pubmed/22101990http://onlinelibrary.wiley.com/store/10.1002/cne.22805/asset/22805_ftp.pdf?v=1&t=h9s4c8io&s=9d219a784d4408f1055e5af613754f0d15b364ff>. Citation on page 59.

KIRAN, B. R.; THOMAS, D. M.; PARAKKAL, R. An overview of deep learning based methods for unsupervised and semi-supervised anomaly detection in videos. **Journal of Imaging**, Multidisciplinary Digital Publishing Institute, v. 4, n. 2, p. 36, 2018. Citation on page 213.

KNIGHT, R. T.; SCABINI, D.; WOODS, D. L. Prefrontal cortex gating of auditory transmission in humans. **Brain Res**, v. 504, n. 2, p. 338–42, 1989. ISSN 0006-8993 (Print) 0006-8993 (Linking). Knight, R T Scabini, D Woods, D L NS21135/NS/NINDS NIH HHS/ NETHERLANDS Brain Res. 1989 Dec 18;504(2):338-42. Available: <http://www.ncbi.nlm.nih.gov/pubmed/2598034http://ac.els-cdn.com/0006899389913814/1-s2.0-0006899389913814-main.pdf?_tid=78fa70fe-892d-11e2-b614-00000aab0f26&acdnat=1362884097_25b3f7bbb6d0316d8b8483afc650d50a>. Citation on page 69.

KOLB, B.; FORGIE, M.; GIBB, R.; GORNY, G.; ROWNTREE, S. Age, experience and the changing brain. **Neurosci Biobehav Rev**, v. 22, n. 2, p. 143–59, 1998. ISSN 0149-7634 (Print) 0149-7634 (Linking). Kolb, B Forgie, M Gibb, R Gorny, G Rowntree, S Neurosci Biobehav Rev. 1998 Mar;22(2):143-59. Available: <http://www.ncbi.nlm.nih.gov/pubmed/9579307http://ac.els-cdn.com/S0149763497000080/1-s2.0-S0149763497000080-main.pdf?_tid=98a36406-892d-11e2-84b3-00000aab0f6b&acdnat=1362884150_8db1fddc599734bfa08e25058f140c8e>. Citation on page 63.

KOSTER, E. H. W.; FOX, E.; MACLEOD, C. Introduction to the special section on cognitive bias modification in emotional disorders. **Journal of abnormal psychology**, American Psychological Association, v. 118, n. 1, p. 1, 2009. Citation on page 45.

KRAUS, K. S.; CANLON, B. Neuronal connectivity and interactions between the auditory and limbic systems. effects of noise and tinnitus. **Hear Res**, v. 288, n. 1-2, p. 34–46, 2012. ISSN 1878-5891 (Electronic) 0378-5955 (Linking). Kraus, Kari Suzanne Canlon, Barbara Netherlands Hear Res. 2012 Jun;288(1-2):34-46. doi: 10.1016/j.heares.2012.02.009. Epub 2012 Mar 7. Available: <http://www.ncbi.nlm.nih.gov/pubmed/22440225http://ac.els-cdn.com/S0378595512000457/1-s2.0-S0378595512000457-main.pdf?_tid=62d53dee-892e-11e2-b8e4-00000aacb35f&acdnat=1362884489_a3a30550f45417d9b9d6971431d7c6fa>. Citations on pages 60, 65, and 74.

KRAUSE, M.; HOFFMANN, W. E.; HAJOS, M. Auditory sensory gating in hippocampus and reticular thalamic neurons in anesthetized rats. **Biol Psychi-**

atry, v. 53, n. 3, p. 244–53, 2003. ISSN 0006-3223 (Print) 0006-3223 (Linking). Krause, Michael Hoffmann, William E Hajos, Mihaly Biol Psychiatry. 2003 Feb 1;53(3):244-53. Available: <http://www.ncbi.nlm.nih.gov/pubmed/12559658http://ac.els-cdn.com/S0006322302014634/1-s2.0-S0006322302014634-main.pdf?_tid=b74d047c-52ee-11e2-a9df-00000aacb362&acdnat=1356919780_94484b44985e0b01813ccedbbf7296bfhttp://ac.els-cdn.com/S0006322302014634/1-s2.0-S0006322302014634-main.pdf?_tid=bb6e65d2-52ee-11e2-9c64-00000aab0f26&acdnat=1356919787_c7e628e2825e9392c93da4e3675d83bf>. Citation on page 58.

KUCHINKE, L.; FRITSCH, N.; MULLER, C. J. Evaluative conditioning of positive and negative valence affects p1 and n1 in verbal processing. **Brain Res**, v. 1624, p. 405–13, 2015. ISSN 1872-6240 (Electronic) 0006-8993 (Linking). Kuchinke, Lars Fritsch, Nathalie Muller, Christina J eng Research Support, Non-U.S. Gov't Netherlands 2015/08/16 06:00 Brain Res. 2015 Oct 22;1624:405-13. doi: 10.1016/j.brainres.2015.07.059. Epub 2015 Aug 12. Available: <http://www.ncbi.nlm.nih.gov/pubmed/26275918>. Citations on pages 70 and 73.

KUELZ, A. K.; RIEMANN, D.; HALSBAND, U.; VIELHABER, K.; UNTERRAINER, J.; KORDON, A.; VODERHOLZER, U. Neuropsychological impairment in obsessive-compulsive disorder—improvement over the course of cognitive behavioral treatment. **Journal of clinical and experimental Neuropsychology**, Taylor & Francis, v. 28, n. 8, p. 1273–1287, 2006. Citation on page 45.

KUSNER, M. J.; LOFTUS, J.; RUSSELL, C.; SILVA, R. Counterfactual fairness. **Advances in neural information processing systems**, v. 30, 2017. Citation on page 50.

LAMME, V. A. Why visual attention and awareness are different. **Trends Cogn Sci**, v. 7, n. 1, p. 12–18, 2003. ISSN 1879-307X (Electronic) 1364-6613 (Linking). Lamme, Victor A.F. ENG 2003/01/09 04:00 Trends Cogn Sci. 2003 Jan;7(1):12-18. Available: <http://www.ncbi.nlm.nih.gov/pubmed/12517353>. Citation on page 68.

LANDGREBE, M.; LANGGUTH, B.; ROSENGARTH, K.; BRAUN, S.; KOCH, A.; KLEINJUNG, T.; MAY, A.; RIDDER, D. de; HAJAK, G. Structural brain changes in tinnitus: grey matter decrease in auditory and non-auditory brain areas. **NeuroImage**, v. 46, n. 1, p. 213–8, 2009. ISSN 1095-9572 (Electronic) 1053-8119 (Linking). Landgrebe, Michael Langguth, Berthold Rosengarth, Katharina Braun, Susanne Koch, Amelie Kleinjung, Tobias May, Arne de Ridder, Dirk Hajak, Goeran Neuroimage. 2009 May 15;46(1):213-8. Epub 2009 Feb 12. Available: <http://www.ncbi.nlm.nih.gov/pubmed/19413945http://ac.els-cdn.com/S1053811909001414/1-s2.0-S1053811909001414-main.pdf?_tid=fbc2f87e73bbf4fbf56323251b08f545&acdnat=1343139467_22118ba496d9f7cb5a2bf9ba8646b236>. Citations on pages 59, 60, 64, 65, and 78.

LANDRY, E. C.; SANDOVAL, X. C. R.; SIMEONE, C. N.; TIDBALL, G.; LEA, J.; WESTERBERG, B. D. Systematic review and network meta-analysis of cognitive and/or behavioral therapies (cbt) for tinnitus. **Otology & Neurotology**, v. 41, n. 2, p. 153–166, 2020. ISSN 1531-7129. Citation on page 95.

LANG, N.; SIEBNER, H. R.; WARD, N. S.; LEE, L.; NITSCHE, M. A.; PAULUS, W.; ROTHWELL, J. C.; LEMON, R. N.; FRACKOWIAK, R. S. How does transcranial dc stimulation of the primary motor cortex alter regional neuronal activity in the human brain? **European Journal of Neuroscience**, Wiley Online Library, v. 22, n. 2, p. 495–504, 2005. Citation on page 102.

LANGE, S.; GABEL, T.; RIEDMILLER, M. Batch reinforcement learning. In: **Reinforcement learning**. [S.l.]: Springer, 2012. p. 45–73. Citation on page 208.

LANGGUTH, B. A review of tinnitus symptoms beyond 'ringing in the ears': a call to action. **Curr Med Res Opin**, v. 27, n. 8, p. 1635–43, 2011. ISSN 1473-4877 (Electronic) 0300-7995 (Linking). Langguth, Berthold England Curr Med Res Opin. 2011 Aug;27(8):1635-43. Epub 2011 Jun 23. Available: <http://www.ncbi.nlm.nih.gov/pubmed/21699365http://informahealthcare.com/doi/abs/10.1185/03007995.2011.595781http://informahealthcare.com/doi/pdfplus/10.1185/03007995.2011.595781>. Citations on pages 59, 60, 65, and 77.

LANGGUTH, B.; EICHHAMMER, P.; KREUTZER, A.; MAENNER, P.; MARIENHAGEN, J.; KLEINJUNG, T.; SAND, P.; HAJAK, G. The impact of auditory cortex activity on characterizing and treating patients with chronic tinnitus–first results from a pet study. **Acta Otolaryngol Suppl**, n. 556, p. 84–8, 2006. ISSN 0365-5237 (Print) 0365-5237 (Linking). Langguth, Berthold Eichhammer, Peter Kreutzer, Antje Maenner, Peter Marienhagen, Joerg Kleinjung, Tobias Sand, Philipp Hajak, Goran Norway Acta Otolaryngol Suppl. 2006 Dec;(556):84-8. Available: <http://www.ncbi.nlm.nih.gov/pubmed/17114149http://informahealthcare.com/doi/abs/10.1080/03655230600895317http://informahealthcare.com/doi/pdfplus/10.1080/03655230600895317>. Citation on page 78.

LANGGUTH, B.; KLEINJUNG, T.; FISCHER, B.; HAJAK, G.; EICHHAMMER, P.; SAND, P. G. Tinnitus severity, depression, and the big five personality traits. **Prog Brain Res**, v. 166, p. 221–5, 2007. ISSN 0079-6123 (Print) 0079-6123 (Linking). Langguth, B Kleinjung, T Fischer, B Hajak, G Eichhammer, P Sand, P G Netherlands Prog Brain Res. 2007;166:221-5. Available: <http://www.ncbi.nlm.nih.gov/pubmed/17956786http://www.sciencedirect.com/science?_ob=MiamiImageURL&_cid=273019&_user=501045&_pii=S0079612307660208&_check=y&_origin=article&_zone=toolbar&_coverDate=31-Dec-2007&view=c&originContentFamily=serial&wchp=dGLbVlk-zSkzS&md5=932527ebc19389a8bc69826298a4644a/1-s2.0-S0079612307660208-main.pdf>. Citation on page 78.

LANGGUTH, B.; KLEINJUNG, T.; LANDGREBE, M. Tinnitus: the complexity of standardization. **Eval Health Prof**, v. 34, n. 4, p. 429–33, 2011. ISSN 1552-3918 (Electronic) 0163-2787 (Linking). Langguth, Berthold Kleinjung, Tobias Landgrebe, Michael Eval Health Prof. 2011 Dec;34(4):429-33. Epub 2011 Jan 10. Available: <http://www.ncbi.nlm.nih.gov/pubmed/21224265http://ehp.sagepub.com/content/34/4/429.full.pdf>. Citations on pages 59 and 60.

LANGGUTH, B.; LANDGREBE, M.; KLEINJUNG, T.; SAND, G. P.; HAJAK, G. Tinnitus and depression. **World J Biol Psychiatry**, v. 12, n. 7, p. 489–500, 2011. ISSN 1814-1412 (Electronic) 1562-2975 (Linking). Langguth, Berthold Landgrebe, Michael Kleinjung, Tobias Sand, G Philipp Hajak, Goran England World J Biol Psychiatry. 2011 Oct;12(7):489-500. Epub 2011 May 13. Available: <http://www.ncbi.nlm.nih.gov/pubmed/21568629http://informahealthcare.com/doi/abs/10.3109/15622975.2011.575178>. Citation on page 65.

LANTING, C. P.; KLEINE, E. D.; BARTELS, H.; DIJK, P. V. Functional imaging of unilateral tinnitus using fmri. **Acta Otolaryngol**, v. 128, n. 4, p. 415–21, 2008. ISSN 0001-6489 (Print) 0001-6489 (Linking). Lanting, C P De Kleine, E Bartels, H Van Dijk, P Norway Acta Otolaryngol. 2008 Apr;128(4):415-21. Available: <http://www.ncbi.nlm.nih.gov/pubmed/18368576http://informahealthcare.com/doi/abs/10.1080/00016480701793743http://informahealthcare.com/doi/pdfplus/10.1080/00016480701793743>. Citation on page 78.

LANTING, C. P.; KLEINE, E. de; DIJK, P. van. Neural activity underlying tinnitus generation: results from pet and fmri. **Hear Res**, v. 255, n. 1-2, p. 1–13, 2009. ISSN 1878-5891 (Electronic) 0378-5955 (Linking). Lanting, C P de Kleine, E van

Dijk, P Netherlands Hear Res. 2009 Sep;255(1-2):1-13. Epub 2009 Jun 21. Available: <http://www.ncbi.nlm.nih.gov/pubmed/19545617http://www.sciencedirect.com/science?_ob=MImg&_imagekey=B6T73-4WK4896-1-3&_cdi=5047&_user=5674931&_pii=S0378595509001531&_origin=&_coverDate=09%2F30%2F2009&_sk=997449998&view=c&wchp=dGLzVzb-zSkWb&md5=e7fe7bc32014b97ec256eb6b2f1a9672&ie=/sdarticle.pdf>. Citations on pages 59, 60, and 65.

LAPARRA, V.; MALO, J.; CAMPS-VALLS, G. Dimensionality reduction via regression in hyperspectral imagery. **IEEE journal of selected topics in signal processing**, IEEE, v. 9, n. 6, p. 1026–1036, 2015. Citations on pages 129 and 130.

LAROSE, D. T. **Data mining and predictive analytics**. [S.l.]: John Wiley & Sons, 2015. Citation on page 163.

LAZAR, J. N.; PEARLMAN-AVNION, S. Effect of affect induction method on emotional valence and arousal. **Psychology**, v. 5, n. 07, p. 595, 2014. Citation on page 96.

LEAVER, A. M.; RENIER, L.; CHEVILLET, M. A.; MORGAN, S.; KIM, H. J.; RAUSCHECKER, J. P. Dysregulation of limbic and auditory networks in tinnitus. **Neuron**, v. 69, n. 1, p. 33–43, 2011. ISSN 1097-4199 (Electronic) 0896-6273 (Linking). Leaver, Amber M Renier, Laurent Chevillet, Mark A Morgan, Susan Kim, Hung J Rauschecker, Josef P eng F31 DC008921/DC/NIDCD NIH HHS/ RC1 DC010720/DC/NIDCD NIH HHS/ F31 DC008921-03/DC/NIDCD NIH HHS/ RC1 DC010720-01/DC/NIDCD NIH HHS/ F31-DC008921/DC/NIDCD NIH HHS/ RC1 DC010720-02/DC/NIDCD NIH HHS/ RC1-DC010720/DC/NIDCD NIH HHS/ Research Support, N.I.H., Extramural Research Support, Non-U.S. Gov't Neuron. 2011 Jan 13;69(1):33-43. doi: 10.1016/j.neuron.2010.12.002. Available: <https://www.ncbi.nlm.nih.gov/pubmed/21220097>. Citations on pages 63 and 64.

LEAVER, A. M.; SEYDELL-GREENWALD, A.; TURESKY, T. K.; MORGAN, S.; KIM, H. J.; RAUSCHECKER, J. P. Cortico-limbic morphology separates tinnitus from tinnitus distress. **Front Syst Neurosci**, v. 6, p. 21, 2012. ISSN 1662-5137 (Electronic) 1662-5137 (Linking). Leaver, Amber M Seydell-Greenwald, Anna Turesky, Ted K Morgan, Susan Kim, Hung J Rauschecker, Josef P eng RC1 DC010720/DC/NIDCD NIH HHS/ Switzerland Front Syst Neurosci. 2012 Apr 5;6:21. doi: 10.3389/fnsys.2012.00021. eCollection 2012. Available: <https://www.ncbi.nlm.nih.gov/pubmed/22493571>. Citation on page 63.

LEDOUX, J. The amygdala. **Curr Biol**, v. 17, n. 20, p. R868–74, 2007. ISSN 0960-9822 (Print) 0960-9822 (Linking). LeDoux, Joseph England Curr Biol. 2007 Oct 23;17(20):R868-74. Available: <http://www.ncbi.nlm.nih.gov/pubmed/17956742http://ac.els-cdn.com/S0960982207017794/1-s2.0-S0960982207017794-main.pdf?_tid=1cad638c-892e-11e2-b730-00000aab0f6c&acdnat=1362884371_e3f7265c29bb9e4ebd1183268333f7e4>. Citation on page 60.

LEE, J.; SEO, W.; KIM, D.-W. Efficient information-theoretic unsupervised feature selection. **Electronics Letters**, Wiley Online Library, v. 54, n. 2, p. 76–77, 2018. Citation on page 129.

LEGERSTEE, J. S.; TULEN, J. H. M.; DIERCKX, B.; TREFFERS, P. D. A.; VERHULST, F. C.; UTENS, E. M. W. J. Cbt for childhood anxiety disorders: differential changes in selective attention between treatment responders and non-responders. **Journal of Child Psychology and Psychiatry**, Wiley Online Library, v. 51, n. 2, p. 162–172, 2010. Citation on page 45.

LENHARDT, M. L.; SHULMAN, A.; GOLDSTEIN, B. A. The role of the insula cortex in the final common pathway for tinnitus: experience using ultra-high-frequency therapy. **Int Tinnitus J**, v. 14, n. 1, p. 13–6, 2008. ISSN 0946-5448 (Print) 0946-5448 (Linking). Lenhardt, Martin L Shulman, Abraham Goldstein, Barbara A Int Tinnitus J. 2008;14(1):13-6. Available: <http://www.ncbi.nlm.nih.gov/pubmed/18616081>. Citation on page 65.

LEVER, J.; KRZYWINSKI, M.; ALTMAN, N. **Points of significance: Principal component analysis**. [S.l.]: Nature Publishing Group, 2017. Citations on pages 129, 130, 131, and 137.

LEVESQUE, J.; EUGENE, F.; JOANETTE, Y.; PAQUETTE, V.; MENSOUR, B.; BEAUDOIN, G.; LEROUX, J. M.; BOURGOUIN, P.; BEAUREGARD, M. Neural circuitry underlying voluntary suppression of sadness. **Biol Psychiatry**, v. 53, n. 6, p. 502–10, 2003. ISSN 0006-3223 (Print) 0006-3223 (Linking). Levesque, Johanne Eugene, Fanny Joanette, Yves Paquette, Vincent Mensour, Boualem Beaudoin, Gilles Leroux, Jean-Maxime Bourgouin, Pierre Beauregard, Mario Biol Psychiatry. 2003 Mar 15;53(6):502-10. Available: <http://www.ncbi.nlm.nih.gov/pubmed/12644355http://ac.els-cdn.com/S0006322302018176/1-s2.0-S0006322302018176-main.pdf?_tid=ed3314c6-892d-11e2-acb3-00000aacb35d&acdnat=1362884292_c2ca2899cd29566535fde8c79dcc7781>. Citation on page 63.

LEVINE, R. A.; ABEL, M.; CHENG, H. Cns somatosensory-auditory interactions elicit or modulate tinnitus. **Exp Brain Res**, v. 153, n. 4, p. 643–8, 2003. ISSN 0014-4819 (Print) 0014-4819 (Linking). Levine, R A Abel, M Cheng, H G8/Action on Hearing Loss/United Kingdom Germany Exp Brain Res. 2003 Dec;153(4):643-8. Epub 2003 Nov 5. Available: <http://www.ncbi.nlm.nih.gov/pubmed/14600798http://www.springerlink.com/content/q5tgdxqvm2a9k5tu/fulltext.pdf>. Citation on page 64.

LEVINE, S.; KUMAR, A.; TUCKER, G.; FU, J. Offline reinforcement learning: Tutorial, review, and perspectives on open problems. **arXiv preprint arXiv:2005.01643**, 2020. Citation on page 208.

LEWIS, D. A.; ANDERSON, S. A. The functional architecture of the prefrontal cortex and schizophrenia. **Psychol Med**, v. 25, n. 5, p. 887–94, 1995. ISSN 0033-2917 (Print) 0033-2917 (Linking). Lewis, D A Anderson, S A MH00519/MH/NIMH NIH HHS/ MH43784/MH/NIMH NIH HHS/ MH45156/MH/NIMH NIH HHS/ ENGLAND Psychol Med. 1995 Sep;25(5):887-94. Available: <http://www.ncbi.nlm.nih.gov/pubmed/8588007http://journals.cambridge.org/download.php?file=%2F21619_DEDA3EAC460763A80C12E5A20688BEA2_journals__PSM_PSM25_05_S0033291700037375a.pdf&cover=Y&code=a3cc273d5037ff59d4063bbf512011e1>. Citation on page 63.

LI, Y. Deep reinforcement learning: An overview. **arXiv preprint arXiv:1701.07274**, 2017. Citation on page 213.

LI, Z.; GU, R.; ZENG, X. *et al.* The social-neurophysiological model of tinnitus: theory and practice. **J. Formos. Med. Assoc**, v. 114, p. 201–203, 2015. Citations on pages 87 and 101.

LI, Z.; YANG, Y.; LIU, J.; ZHOU, X.; LU, H. Unsupervised feature selection using nonnegative spectral analysis. In: **Proceedings of the AAAI conference on artificial intelligence**. [S.l.: s.n.], 2012. v. 26, n. 1. Citations on pages 129 and 130.

LIANG, X.; DU, X.; WANG, G.; HAN, Z. A deep reinforcement learning network for traffic light cycle control. **IEEE Transactions on Vehicular Technology**, IEEE, v. 68, n. 2, p. 1243–1253, 2019. Citations on pages 211 and 214.

LIMB, C. J. Structural and functional neural correlates of music perception. **Anat Rec A Discov Mol Cell Evol Biol**, v. 288, n. 4, p. 435–46, 2006. ISSN 1552-4884 (Print) 1552-4884 (Linking). Limb, Charles J Anat Rec A Discov Mol Cell Evol Biol. 2006 Apr;288(4):435-46. Available: <http://www.ncbi.nlm.nih.gov/pubmed/16550543http://onlinelibrary.wiley.com/store/10.1002/ar.a.20316/asset/20316_ftp.pdf?v=1&t=hham5pl6&s=5e4c44f70155cee8d56d722434e52bf1cff487a0>. Citation on page 61.

LIN, Y.; DAI, X.; LI, L.; WANG, F.-Y. An efficient deep reinforcement learning model for urban traffic control. **arXiv preprint arXiv:1808.01876**, 2018. Citation on page 213.

LINDBERG, P.; SCOTT, B.; MELIN, L.; LYTTKENS, L. The psychological treatment of tinnitus: An experimental evaluation. **Behaviour Research and Therapy**, v. 27, n. 6, p. 593–603, 1989. ISSN 0005-7967. Citation on page 94.

LLINAS, R.; JAHNSEN, H. Electrophysiology of mammalian thalamic neurones in vitro. **Nature**, v. 297, n. 5865, p. 406–8, 1982. ISSN 0028-0836 (Print) 0028-0836 (Linking). Llinas, R Jahnsen, H NS13742/NS/NINDS NIH HHS/ ENGLAND Nature. 1982 Jun 3;297(5865):406-8. Available: <http://www.ncbi.nlm.nih.gov/pubmed/7078650http://www.nature.com/nature/journal/v297/n5865/abs/297406a0.htmlhttp://www.nature.com/nature/journal/v297/n5865/pdf/297406a0.pdf>. Citation on page 64.

LOCKWOOD, A. H.; SALVI, R. J.; COAD, M. L.; TOWSLEY, M. L.; WACK, D. S.; MURPHY, B. W. The functional neuroanatomy of tinnitus: evidence for limbic system links and neural plasticity. **Neurology**, v. 50, n. 1, p. 114–20, 1998. ISSN 0028-3878 (Print) 0028-3878 (Linking). Lockwood, A H Salvi, R J Coad, M L Towsley, M L Wack, D S Murphy, B W DC 3306/DC/NIDCD NIH HHS/ Neurology. 1998 Jan;50(1):114-20. Available: <http://www.ncbi.nlm.nih.gov/pubmed/9443467http://graphics.tx.ovid.com/ovftpdfs/FPDDNCMCOFBCJD00/fs047/ovft/live/gv031/00006114/00006114-199801000-00025.pdf>. Citation on page 78.

LOGOTHETIS, N. K. What we can do and what we cannot do with fmri. **Nature**, v. 453, n. 7197, p. 869–78, 2008. ISSN 1476-4687 (Electronic) 0028-0836 (Linking). Logothetis, Nikos K England Nature. 2008 Jun 12;453(7197):869-78. doi: 10.1038/nature06976. Available: <http://www.ncbi.nlm.nih.gov/pubmed/18548064http://www.nature.com/nature/journal/v453/n7197/pdf/nature06976.pdf>. Citation on page 59.

LORENZ, I.; MüLLER, N.; SCHLEE, W.; HARTMANN, T.; WEISZ, N. Loss of alpha power is related to increased gamma synchronization—a marker of reduced inhibition in tinnitus? **Neuroscience letters**, v. 453, n. 3, p. 225–228, 2009. ISSN 0304-3940. Citation on page 78.

LUDWIG, D. S.; KABAT-ZINN, J. Mindfulness in medicine. **Jama**, American Medical Association, v. 300, n. 11, p. 1350–1352, 2008. Citation on page 95.

LUXBURG, U. V. A tutorial on spectral clustering, statistics and computing17 (4)(2007), 395-416. **Google Scholar Google Scholar Digital Library Digital Library**. Citations on pages 129, 130, and 133.

MAATEN, L. Van der; HINTON, G. Visualizing data using t-sne. **Journal of machine learning research**, v. 9, n. 11, 2008. Citations on pages 129, 130, and 134.

MACDONALD A. W., r.; COHEN, J. D.; STENGER, V. A.; CARTER, C. S. Dissociating the role of the dorsolateral prefrontal and anterior cingulate cortex in cognitive control. **Science**,

v. 288, n. 5472, p. 1835–8, 2000. ISSN 0036-8075 (Print) 0036-8075 (Linking). MacDonald, A W 3rd Cohen, J D Stenger, V A Carter, C S New York, N.Y. Science. 2000 Jun 9;288(5472):1835-8. Available: <http://www.ncbi.nlm.nih.gov/pubmed/10846167http://www.sciencemag.org/content/288/5472/1835http://www.sciencemag.org/content/288/5472/1835.full.pdf>. Citation on page 69.

MACKINNON, D. P.; LOCKWOOD, C. M.; HOFFMAN, J. M.; WEST, S. G.; SHEETS, V. A comparison of methods to test the significance of the mediated effect. **Psychological Methods**, v. 7, n. 1, p. 83–104, 2002. Citation on page 195.

MADDALENA, H. de; PFRANG, H. [improvement of communication behavior of laryngectomized and voice-rehabilitated patients by a psychological training program]. **HNO**, v. 41, n. 6, p. 289–95, 1993. ISSN 0017-6192 (Print) 0017-6192 (Linking). De Maddalena, H Pfrang, H GERMANY HNO. 1993 Jun;41(6):289-95. Available: <http://www.ncbi.nlm.nih.gov/pubmed/8365915>. Citation on page 70.

____. [subjective attitudes of laryngectomized patients of the cause of the tumor disease. correlation with psychosocial adjustment and pre- and postoperative alcohol and tobacco consumption]. **HNO**, v. 41, n. 4, p. 198–205, 1993. ISSN 0017-6192 (Print) 0017-6192 (Linking). De Maddalena, H Pfrang, H GERMANY HNO. 1993 Apr;41(4):198-205. Available: <http://www.ncbi.nlm.nih.gov/pubmed/8514526>. Citation on page 70.

MAHLKE, C.; WALLHAUSSER-FRANKE, E. Evidence for tinnitus-related plasticity in the auditory and limbic system, demonstrated by arg3.1 and c-fos immunocytochemistry. **Hear Res**, v. 195, n. 1-2, p. 17–34, 2004. ISSN 0378-5955 (Print) 0378-5955 (Linking). Mahlke, C Wallhausser-Franke, E Netherlands Hear Res. 2004 Sep;195(1-2):17-34. Available: <http://www.ncbi.nlm.nih.gov/pubmed/15350276http://ac.els-cdn.com/S0378595504000991/1-s2.0-S0378595504000991-main.pdf?_tid=7b6d8073785bead1c7a0e4a8f3ad2c5b&acdnat=1345695847_872a2548516017646edcffed1e4aa612>. Citations on pages 59, 60, and 65.

MARCHEWKA, A.; ŻURAWSKI, Ł.; JEDNORÓG, K.; GRABOWSKA, A. The nencki affective picture system (naps): Introduction to a novel, standardized, wide-range, high-quality, realistic picture database. **Behavior research methods**, Springer, v. 46, n. 2, p. 596–610, 2014. Citation on page 105.

MARCIANO, E.; CARRABBA, L.; GIANNINI, P.; SEMENTINA, C.; VERDE, P.; BRUNO, C.; PIETRO, G. D.; PONSILLO, N. G. Psychiatric comorbidity in a population of outpatients affected by tinnitus. **Int J Audiol**, v. 42, n. 1, p. 4–9, 2003. ISSN 1499-2027 (Print) 1499-2027 (Linking). Marciano, E Carrabba, L Giannini, P Sementina, C Verde, P Bruno, C Di Pietro, G Ponsillo, N G Canada Int J Audiol. 2003 Jan;42(1):4-9. Available: <http://www.ncbi.nlm.nih.gov/pubmed/12564510>. Citations on pages 70 and 77.

MARCONDES, R.; FREGNI, F.; PASCUAL-LEONE, A. Tinnitus and brain activation: insights from transcranial magnetic stimulation. **Ear Nose Throat J**, v. 85, n. 4, p. 233–4, 236–8, 2006. ISSN 0145-5613 (Print) 0145-5613 (Linking). Marcondes, Renata Fregni, Felipe Pascual-Leone, Alvaro K30HL04095/HL/NHLBI NIH HHS/ Ear Nose Throat J. 2006 Apr;85(4):233-4, 236-8. Available: <http://www.ncbi.nlm.nih.gov/pubmed/16696357>. Citation on page 78.

MAREN, S. What the amygdala does and doesn't do in aversive learning. **Learn Mem**, v. 10, n. 5, p. 306–8, 2003. ISSN 1072-0502 (Print) 1072-0502 (Linking). Maren, Stephen

R01 MH65961/MH/NIMH NIH HHS/ Cold Spring Harbor, N.Y. Learn Mem. 2003 Sep-Oct;10(5):306-8. Available: <http://www.ncbi.nlm.nih.gov/pubmed/14557601http://learnmem.cshlp.org/content/10/5/306.full.pdf>. Citation on page 61.

____. Synaptic mechanisms of associative memory in the amygdala. **Neuron**, v. 47, n. 6, p. 783–6, 2005. ISSN 0896-6273 (Print) 0896-6273 (Linking). Maren, Stephen R01MH050093/MH/NIMH NIH HHS/ R01MH065961/MH/NIMH NIH HHS/ Neuron. 2005 Sep 15;47(6):783-6. Available: <http://www.ncbi.nlm.nih.gov/pubmed/16157273http://ac.els-cdn.com/S0896627305006859/1-s2.0-S0896627305006859-main.pdf?_tid=f54f4dfa-892d-11e2-8479-00000aacb35e&acdnat=1362884305_884d1d9edcb526d4a4cf9b747243aa85>. Citation on page 61.

MARKS, E.; SMITH, P.; MCKENNA, L. I wasn't at war with the noise: How mindfulness based cognitive therapy changes patients' experiences of tinnitus. **Frontiers in Psychology**, v. 11, p. 483, 2020. ISSN 1664-1078. Citation on page 95.

MARSH, R. A.; FUZESSERY, Z. M.; GROSE, C. D.; WENSTRUP, J. J. Projection to the inferior colliculus from the basal nucleus of the amygdala. **J Neurosci**, v. 22, n. 23, p. 10449–60, 2002. ISSN 1529-2401 (Electronic) 0270-6474 (Linking). Marsh, Robert A Fuzessery, Zoltan M Grose, Carol D Wenstrup, Jeffrey J R01 DC 00054/DC/NIDCD NIH HHS/ R01 DC 00937/DC/NIDCD NIH HHS/ J Neurosci. 2002 Dec 1;22(23):10449-60. Available: <http://www.ncbi.nlm.nih.gov/pubmed/12451144http://www.jneurosci.org/content/22/23/10449.full.pdf>. Citation on page 61.

MARTINEZ-DEVESA, P.; WADDELL, A.; PERERA, R.; THEODOULOU, M. Cognitive behavioural therapy for tinnitus. **Cochrane database of systematic reviews**, John Wiley Sons, Ltd, n. 1, 2007. Citations on pages 93 and 95.

MATHEWS, A.; MOGG, K.; KENTISH, J.; EYSENCK, M. Effect of psychological treatment on cognitive bias in generalized anxiety disorder. **Behaviour research and therapy**, Elsevier, v. 33, n. 3, p. 293–303, 1995. Citation on page 45.

MAUDOUX, A.; LEFEBVRE, P.; CABAY, J. E.; DEMERTZI, A.; VANHAUDENHUYSE, A.; LAUREYS, S.; SODDU, A. Connectivity graph analysis of the auditory resting state network in tinnitus. **Brain Res**, 2012. ISSN 1872-6240 (Electronic) 0006-8993 (Linking). Maudoux, A Lefebvre, Ph Cabay, J-E Demertzi, A Vanhaudenhuyse, A Laureys, S Soddu, A Brain Res. 2012 May 10. Available: <http://www.ncbi.nlm.nih.gov/pubmed/22579727http://ac.els-cdn.com/S0006899312008438/1-s2.0-S0006899312008438-main.pdf?_tid=7fe323b259b28e605b90b0cd10964b7b&acdnat=1343845128_7cb78038746157e283f9719bc24b4d70>. Citation on page 70.

MAYBERG, H. S. Defining neurocircuits in depression: Strategies toward treatment selection based on neuroimaging phenotypes. **Psychiatric Annals**, SLACK, 2006. Citation on page 45.

MAYBERG, H. S.; LOZANO, A. M.; VOON, V.; MCNEELY, H. E.; SEMINOWICZ, D.; HAMANI, C.; SCHWALB, J. M.; KENNEDY, S. H. Deep brain stimulation for treatment-resistant depression. **Neuron**, v. 45, n. 5, p. 651–60, 2005. ISSN 0896-6273 (Print) 0896-6273 (Linking). Mayberg, Helen S Lozano, Andres M Voon, Valerie McNeely, Heather E Seminowicz, David Hamani, Clement Schwalb, Jason M Kennedy, Sidney H Neuron. 2005 Mar 3;45(5):651-60. Available: <http://www.ncbi.nlm.nih.gov/pubmed/15748841http://ac.els-cdn.com/S089662730500156X/1-s2.0-S089662730500156X-main.pdf?_tid=1136edc0-892e-11e2-855b-00000aacb361&acdnat=1362884352_05e12178c329b02ca504f675070e114d>. Citation on page 64.

MAYO, J. P. Intrathalamic mechanisms of visual attention. **J Neurophysiol**, v. 101, n. 3, p. 1123–5, 2009. ISSN 0022-3077 (Print) 0022-3077 (Linking). Mayo, J Patrick R01 EY-017592/EY/NEI NIH HHS/ J Neurophysiol. 2009 Mar;101(3):1123-5. doi: 10.1152/jn.91369.2008. Epub 2009 Jan 14. Available: <http://www.ncbi.nlm.nih.gov/pubmed/19144737http://jn.physiology.org/content/101/3/1123.full.pdf>. Citation on page 58.

MCCLELLAND, J. L.; RALPH, M. A. Cognitive neuroscience. Elsevier, 2015. Citation on page 47.

MCCORMICK, D. A.; WANG, Z. Serotonin and noradrenaline excite gabaergic neurones of the guinea-pig and cat nucleus reticularis thalami. **J Physiol**, v. 442, p. 235–55, 1991. ISSN 0022-3751 (Print) 0022-3751 (Linking). McCormick, D A Wang, Z ENGLAND J Physiol. 1991 Oct;442:235-55. Available: <http://www.ncbi.nlm.nih.gov/pubmed/1665858http://jp.physoc.org/content/442/1/235.full.pdf>. Citation on page 64.

MCCULLOUGH, L. D.; SOKOLOWSKI, J. D.; SALAMONE, J. D. A neurochemical and behavioral investigation of the involvement of nucleus accumbens dopamine in instrumental avoidance. **Neuroscience**, v. 52, n. 4, p. 919–25, 1993. ISSN 0306-4522 (Print) 0306-4522 (Linking). McCullough, L D Sokolowski, J D Salamone, J D ENGLAND Neuroscience. 1993 Feb;52(4):919-25. Available: <http://www.ncbi.nlm.nih.gov/pubmed/8450978http://ac.els-cdn.com/030645229390538Q/1-s2.0-030645229390538Q-main.pdf?_tid=89f47ee0-892d-11e2-acb3-00000aacb35d&acdnat=1362884125_fe4ce549ef3788b4ac2009f2e0ac1f75>. Citation on page 64.

MCKENNA, L.; HANDSCOMB, L.; HOARE, D. J.; HALL, D. A. A scientific cognitive-behavioral model of tinnitus: novel conceptualizations of tinnitus distress. **Frontiers in Neurology**, Frontiers, v. 5, p. 196, 2014. Citation on page 87.

_____. A scientific cognitive-behavioral model of tinnitus: novel conceptualizations of tinnitus distress. **Front Neurol**, v. 5, p. 196, 2014. ISSN 1664-2295 (Print) 1664-2295. Citations on pages 93, 100, and 101.

MIDDLETON, J. W.; KIRITANI, T.; PEDERSEN, C.; TURNER, J. G.; SHEPHERD, G. M.; TZOUNOPOULOS, T. Mice with behavioral evidence of tinnitus exhibit dorsal cochlear nucleus hyperactivity because of decreased gabaergic inhibition. **Proc Natl Acad Sci U S A**, v. 108, n. 18, p. 7601–6, 2011. ISSN 1091-6490 (Electronic) 0027-8424 (Linking). Middleton, Jason W Kiritani, Taro Pedersen, Courtney Turner, Jeremy G Shepherd, Gordon M G Tzounopoulos, Thanos eng DC007905/DC/NIDCD NIH HHS/ NS061963/NS/NINDS NIH HHS/ PR093405/PR/OCPHP CDC HHS/ R01 DC007905/DC/NIDCD NIH HHS/ R01 NS061963/NS/NINDS NIH HHS/ Research Support, N.I.H., Extramural Research Support, Non-U.S. Gov't 2011/04/20 06:00 Proc Natl Acad Sci U S A. 2011 May 3;108(18):7601-6. doi: 10.1073/pnas.1100223108. Epub 2011 Apr 18. Available: <http://www.ncbi.nlm.nih.gov/pubmed/21502491>. Citation on page 78.

MILLS, R.; ALBERT, D.; BRAIN, C. Tinnitus in childhood. **Clinical Otolaryngology & Allied Sciences**, Wiley Online Library, v. 11, n. 6, p. 431–434, 1986. Citation on page 57.

MITTERSCHIFFTHALER, M. T.; FU, C. H.; DALTON, J. A.; ANDREW, C. M.; WILLIAMS, S. C. A functional mri study of happy and sad affective states induced by classical music. **Hum Brain Mapp**, v. 28, n. 11, p. 1150–62, 2007. ISSN 1065-9471 (Print) 1065-9471 (Linking). Mitterschiffthaler, Martina T Fu, Cynthia H Y Dalton, Jeffrey A Andrew, Christopher M Williams, Steven C R Hum Brain Mapp. 2007

Nov;28(11):1150-62. Available: <http://www.ncbi.nlm.nih.gov/pubmed/17290372http://onlinelibrary.wiley.com/store/10.1002/hbm.20337/asset/20337_ftp.pdf?v=1&t=he3m230p&s=a77fb5520c10998411295ed14b1b92baade02f49>. Citation on page 62.

MNIH, V.; BADIA, A. P.; MIRZA, M.; GRAVES, A.; LILLICRAP, T.; HARLEY, T.; SILVER, D.; KAVUKCUOGLU, K. Asynchronous methods for deep reinforcement learning. In: PMLR. **International conference on machine learning**. [S.l.], 2016. p. 1928–1937. Citations on pages 216, 217, and 221.

MOHEDANO-MORIANO, A.; PRO-SISTIAGA, P.; ARROYO-JIMENEZ, M. M.; ARTACHO-PERULA, E.; INSAUSTI, A. M.; MARCOS, P.; CEBADA-SANCHEZ, S.; MARTINEZ-RUIZ, J.; MUNOZ, M.; BLAIZOT, X.; MARTINEZ-MARCOS, A.; AMARAL, D. G.; INSAUSTI, R. Topographical and laminar distribution of cortical input to the monkey entorhinal cortex. **J Anat**, v. 211, n. 2, p. 250–60, 2007. ISSN 0021-8782 (Print) 0021-8782 (Linking). Mohedano-Moriano, A Pro-Sistiaga, P Arroyo-Jimenez, M M Artacho-Perula, E Insausti, A M Marcos, P Cebada-Sanchez, S Martinez-Ruiz, J Munoz, M Blaizot, X Martinez-Marcos, A Amaral, D G Insausti, R England J Anat. 2007 Aug;211(2):250-60. Epub 2007 Jun 15. Available: <http://www.ncbi.nlm.nih.gov/pubmed/17573826http://onlinelibrary.wiley.com/store/10.1111/j.1469-7580.2007.00764.x/asset/j.1469-7580.2007.00764.x.pdf?v=1&t=he3m2mrz&s=3d9d61c6ca19627e9b74d3f4d4ed226ff5c22ed7>. Citation on page 61.

MOHLMAN, J.; GORMAN, J. M. The role of executive functioning in cbt: a pilot study with anxious older adults. **Behaviour research and therapy**, Elsevier, v. 43, n. 4, p. 447–465, 2005. Citation on page 45.

MOLLER, A. R. Pathophysiology of tinnitus. **Otolaryngol Clin North Am**, v. 36, n. 2, p. 249–66, v–vi, 2003. ISSN 0030-6665 (Print) 0030-6665 (Linking). Moller, Aage R Otolaryngol Clin North Am. 2003 Apr;36(2):249-66, v-vi. Available: <http://www.ncbi.nlm.nih.gov/pubmed/12856295>. Citations on pages 59 and 60.

____. Neural plasticity in tinnitus. **Prog Brain Res**, v. 157, p. 365–72, 2006. ISSN 0079-6123 (Print) 0079-6123 (Linking). Moller, Aage R Netherlands Prog Brain Res. 2006;157:365-72. Available: <http://www.ncbi.nlm.nih.gov/pubmed/17046676http://www.sciencedirect.com/science?_ob=MiamiImageURL&_cid=273019&_user=501045&_pii=S0079612306570220&_check=y&_origin=article&_zone=toolbar&_coverDate=31-Dec-2006&view=c&originContentFamily=serial&wchp=dGLbVlV-zSkzk&md5=731dcbff669dea2547779a00d348bf0f/1-s2.0-S0079612306570220-main.pdf>. Citations on pages 59 and 60.

MONTE-SILVA, K.; KUO, M.-F.; HESSENTHALER, S.; FRESNOZA, S.; LIEBETANZ, D.; PAULUS, W.; NITSCHE, M. A. Induction of late ltp-like plasticity in the human motor cortex by repeated non-invasive brain stimulation. **Brain stimulation**, Elsevier, v. 6, n. 3, p. 424–432, 2013. Citation on page 102.

MORABIA, A. Epidemiological causality. **History and philosophy of the life sciences**, JSTOR, p. 365–379, 2005. Citation on page 49.

MORRIS, J. S.; FRISTON, K. J.; DOLAN, R. J. Experience-dependent modulation of tonotopic neural responses in human auditory cortex. **Proc Biol Sci**, v. 265, n. 1397, p. 649–57,

1998. ISSN 0962-8452 (Print) 0962-8452 (Linking). Morris, J S Friston, K J Dolan, R J Wellcome Trust/United Kingdom ENGLAND Proc Biol Sci. 1998 Apr 22;265(1397):649-57. Available: <http://www.ncbi.nlm.nih.gov/pubmed/9608726http://rspb.royalsocietypublishing.org/content/265/1397/649http://rspb.royalsocietypublishing.org/content/265/1397/649.full.pdf>. Citation on page 61.

MOUSAVI, S. S.; SCHUKAT, M.; HOWLEY, E. Traffic light control using deep policy-gradient and value-function-based reinforcement learning. **IET Intelligent Transport Systems**, IET, v. 11, n. 7, p. 417–423, 2017. Citations on pages 210 and 211.

MUHLAU, M.; RAUSCHECKER, J. P.; OESTREICHER, E.; GASER, C.; ROTTINGER, M.; WOHLSCHLAGER, A. M.; SIMON, F.; ETGEN, T.; CONRAD, B.; SANDER, D. Structural brain changes in tinnitus. **Cereb Cortex**, v. 16, n. 9, p. 1283–8, 2006. ISSN 1047-3211 (Print) 1047-3211 (Linking). Muhlau, M Rauschecker, J P Oestreicher, E Gaser, C Rottinger, M Wohlschlager, A M Simon, F Etgen, T Conrad, B Sander, D eng Controlled Clinical Trial Research Support, Non-U.S. Gov't Cereb Cortex. 2006 Sep;16(9):1283-8. doi: 10.1093/cercor/bhj070. Epub 2005 Nov 9. Available: <https://www.ncbi.nlm.nih.gov/pubmed/16280464>. Citations on pages 59, 60, 63, 64, and 65.

MUHLNICKEL, W.; ELBERT, T.; TAUB, E.; FLOR, H. Reorganization of auditory cortex in tinnitus. **Proc Natl Acad Sci U S A**, v. 95, n. 17, p. 10340–3, 1998. ISSN 0027-8424 (Print) 0027-8424 (Linking). Muhlnickel, W Elbert, T Taub, E Flor, H Proc Natl Acad Sci U S A. 1998 Aug 18;95(17):10340-3. Available: <http://www.ncbi.nlm.nih.gov/pubmed/9707649http://www.pnas.org/content/95/17/10340.full.pdf>. Citations on pages 65 and 78.

MUNOZ-LOPEZ, M. M.; MOHEDANO-MORIANO, A.; INSAUSTI, R. Anatomical pathways for auditory memory in primates. **Front Neuroanat**, v. 4, p. 129, 2010. ISSN 1662-5129 (Electronic) 1662-5129 (Linking). Munoz-Lopez, Monica M Mohedano-Moriano, Alicia Insausti, Ricardo Switzerland Front Neuroanat. 2010 Oct 8;4:129. doi: 10.3389/fnana.2010.00129. Available: <http://www.ncbi.nlm.nih.gov/pubmed/20976037http://www.frontiersin.org/Journal/DownloadFile/1/8224/1725/1/21/fnana-04-00129_pdf>. Citation on page 61.

MURRAY, E. A. The amygdala, reward and emotion. **Trends Cogn Sci**, v. 11, n. 11, p. 489–97, 2007. ISSN 1364-6613 (Print) 1364-6613 (Linking). Murray, Elisabeth A England Trends Cogn Sci. 2007 Nov;11(11):489-97. Epub 2007 Nov 7. Available: <http://www.ncbi.nlm.nih.gov/pubmed/17988930http://ac.els-cdn.com/S1364661307002458/1-s2.0-S1364661307002458-main.pdf?_tid=1f49a826-892e-11e2-ad87-00000aab0f26&acdnat=1362884376_36798739c464f3b302ffac14f9b3c264>. Citation on page 60.

MURRAY, E. A.; WISE, S. P. What, if anything, can monkeys tell us about human amnesia when they can't say anything at all? **Neuropsychologia**, v. 48, n. 8, p. 2385–405, 2010. ISSN 1873-3514 (Electronic) 0028-3932 (Linking). Murray, Elisabeth A Wise, Steven P ZIA MH002736-14/MH/NIMH NIH HHS/ England Neuropsychologia. 2010 Jul;48(8):2385-405. doi: 10.1016/j.neuropsychologia.2010.01.011. Epub 2010 Jan 25. Available: <http://www.ncbi.nlm.nih.gov/pubmed/20097215http://ac.els-cdn.com/S0028393210000266/1-s2.0-S0028393210000266-main.pdf?_tid=4777fc6c-892e-11e2-ac44-00000aab0f6b&acdnat=1362884443_c4adb31be1279cc721b0306340892701>. Citation on page 60.

NEWELL, A. **Unified theories of cognition**. [S.l.]: Harvard University Press, 1994. Citation on page 45.

NITSCHE, M. A.; DOEMKES, S.; KARAKOSE, T.; ANTAL, A.; LIEBETANZ, D.; LANG, N.; TERGAU, F.; PAULUS, W. Shaping the effects of transcranial direct current stimulation of the human motor cortex. **Journal of neurophysiology**, American Physiological Society, v. 97, n. 4, p. 3109–3117, 2007. Citation on page 104.

NITSCHE, M. A.; PAULUS, W. Excitability changes induced in the human motor cortex by weak transcranial direct current stimulation. **The Journal of physiology**, Wiley Online Library, v. 527, n. 3, p. 633–639, 2000. Citation on page 102.

NORENA, A. J.; EGGERMONT, J. J. Changes in spontaneous neural activity immediately after an acoustic trauma: implications for neural correlates of tinnitus. **Hear Res**, v. 183, n. 1-2, p. 137–53, 2003. ISSN 0378-5955 (Print) 0378-5955 (Linking). Norena, A J Eggermont, J J eng Research Support, Non-U.S. Gov't Netherlands 2003/09/19 05:00 Hear Res. 2003 Sep;183(1-2):137-53. Available: <http://www.ncbi.nlm.nih.gov/pubmed/13679145>. Citations on pages 65, 73, and 78.

O'DONNELL, P.; GRACE, A. A. Synaptic interactions among excitatory afferents to nucleus accumbens neurons: hippocampal gating of prefrontal cortical input. **J Neurosci**, v. 15, n. 5 Pt 1, p. 3622–39, 1995. ISSN 0270-6474 (Print) 0270-6474 (Linking). O'Donnell, P Grace, A A MH42217/MH/NIMH NIH HHS/ MH45156/MH/NIMH NIH HHS/ NS19608/NS/NINDS NIH HHS/ J Neurosci. 1995 May;15(5 Pt 1):3622-39. Available: <http://www.ncbi.nlm.nih.gov/pubmed/7751934http://www.jneurosci.org/content/15/5/3622.full.pdf>. Citation on page 63.

O'DONNELL, P.; LAVIN, A.; ENQUIST, L. W.; GRACE, A. A.; CARD, J. P. Interconnected parallel circuits between rat nucleus accumbens and thalamus revealed by retrograde transynaptic transport of pseudorabies virus. **J Neurosci**, v. 17, n. 6, p. 2143–67, 1997. ISSN 0270-6474 (Print) 0270-6474 (Linking). O'Donnell, P Lavin, A Enquist, L W Grace, A A Card, J P MH45156/MH/NIMH NIH HHS/ MH53574/MH/NIMH NIH HHS/ NINDS33506/DS/DS NIH HHS/ etc. J Neurosci. 1997 Mar 15;17(6):2143-67. Available: <http://www.ncbi.nlm.nih.gov/pubmed/9045740http://www.jneurosci.org/content/17/6/2143.full.pdf>. Citations on pages 58 and 64.

O'MARA, S. The subiculum: what it does, what it might do, and what neuroanatomy has yet to tell us. **J Anat**, v. 207, n. 3, p. 271–82, 2005. ISSN 0021-8782 (Print) 0021-8782 (Linking). O'Mara, Shane Wellcome Trust/United Kingdom England J Anat. 2005 Sep;207(3):271-82. Available: <http://www.ncbi.nlm.nih.gov/pubmed/16185252http://onlinelibrary.wiley.com/store/10.1111/j.1469-7580.2005.00446.x/asset/j.1469-7580.2005.00446.x.pdf?v=1&t=he3m0tcu&s=7c8cc11bb51f61da9cea605e1f2a3c5a49687917>. Citation on page 61.

ONGUR, D.; PRICE, J. L. The organization of networks within the orbital and medial prefrontal cortex of rats, monkeys and humans. **Cereb Cortex**, v. 10, n. 3, p. 206–19, 2000. ISSN 1047-3211 (Print) 1047-3211 (Linking). Ongur, D Price, J L DC00093/DC/NIDCD NIH HHS/ New York, N.Y. : 1991 Cereb Cortex. 2000 Mar;10(3):206-19. Available: <http://www.ncbi.nlm.nih.gov/pubmed/10731217http://cercor.oxfordjournals.org/content/10/3/206.full.pdf>. Citation on page 64.

OPGEN-RHEIN, R.; STRIMMER, K. From correlation to causation networks: a simple approximate learning algorithm and its application to high-dimensional plant gene expression data. **BMC systems biology**, BioMed Central, v. 1, n. 1, p. 1–10, 2007. Citation on page 208.

PAPE, H. C.; MCCORMICK, D. A. Noradrenaline and serotonin selectively modulate thalamic burst firing by enhancing a hyperpolarization-activated cation current. **Nature**, v. 340, n. 6236, p. 715–8, 1989. ISSN 0028-0836 (Print) 0028-0836 (Linking). Pape, H C McCormick, D A ENGLAND Nature. 1989 Aug 31;340(6236):715-8. Available: <http://www.ncbi.nlm.nih.gov/pubmed/2475782http://www.nature.com/nature/journal/v340/n6236/abs/340715a0.htmlhttp://www.nature.com/nature/journal/v340/n6236/pdf/340715a0.pdf>. Citation on page 64.

PAPE, J.; PARASKEVOPOULOS, E.; BRUCHMANN, M.; WOLLBRINK, A.; RUDACK, C.; PANTEV, C. Playing and listening to tailor-made notched music: cortical plasticity induced by unimodal and multimodal training in tinnitus patients. **Neural plasticity**, Hindawi, v. 2014, 2014. Citation on page 94.

PARASCANDOLA, M. Causes, risks, and probabilities: probabilistic concepts of causation in chronic disease epidemiology. **Preventive Medicine**, Elsevier, v. 53, n. 4-5, p. 232–234, 2011. Citation on page 49.

PEARL, J. **Causality**. [S.l.]: Cambridge university press, 2009. Citations on pages 208 and 217.

____. The do-calculus revisited. **arXiv preprint arXiv:1210.4852**, 2012. Citations on pages 217 and 218.

PEDEMONTE, M.; PENA, J. L.; VELLUTI, R. A. Firing of inferior colliculus auditory neurons is phase-locked to the hippocampus theta rhythm during paradoxical sleep and waking. **Exp Brain Res**, v. 112, n. 1, p. 41–6, 1996. ISSN 0014-4819 (Print) 0014-4819 (Linking). Pedemonte, M Pena, J L Velluti, R A GERMANY Exp Brain Res. 1996 Nov;112(1):41-6. Available: <http://www.ncbi.nlm.nih.gov/pubmed/8951405>. Citation on page 61.

PEDERSEN, S. S.; DENOLLET, J. Type d personality, cardiac events, and impaired quality of life: a review. **European journal of cardiovascular prevention & rehabilitation**, v. 10, n. 4, p. 241–248, 2003. ISSN 1741-8267. Citation on page 97.

PESSOA, L. Emotion and cognition and the amygdala: from "what is it?" to "what's to be done?". **Neuropsychologia**, v. 48, n. 12, p. 3416–29, 2010. ISSN 1873-3514 (Electronic) 0028-3932 (Linking). Pessoa, Luiz R01 MH071589/MH/NIMH NIH HHS/ R01 MH071589-08/MH/NIMH NIH HHS/ England Neuropsychologia. 2010 Oct;48(12):3416-29. doi: 10.1016/j.neuropsychologia.2010.06.038. Epub 2010 Jul 7. Available: <http://www.ncbi.nlm.nih.gov/pubmed/20619280http://ac.els-cdn.com/S0028393210002897/1-s2.0-S0028393210002897-main.pdf?_tid=49fbfae2-892e-11e2-b492-00000aab0f6c&acdnat=1362884447_44114aa189679c1c48bc95a577263253>. Citation on page 61.

____. Reprint of: Emotion and cognition and the amygdala: from "what is it?" to "what's to be done?". **Neuropsychologia**, v. 49, n. 4, p. 681–94, 2011. ISSN 1873-3514 (Electronic) 0028-3932 (Linking). Pessoa, Luiz England Neuropsychologia. 2011 Mar;49(4):681-94. doi: 10.1016/j.neuropsychologia.2011.02.030. Available: <http://www.ncbi.nlm.nih.gov/pubmed/21414465http://ac.els-cdn.com/S0028393211000923/1-s2.0-S0028393211000923-main.pdf?_tid=6023f64e-892e-11e2-ac44-00000aab0f6b&acdnat=1362884484_4d7d5ab146f4eb5e836097edf06ec6a8>. Citations on pages 60 and 61.

PETERCHEV, A. V.; WAGNER, T. A.; MIRANDA, P. C.; NITSCHE, M. A.; PAULUS, W.; LISANBY, S. H.; PASCUAL-LEONE, A.; BIKSON, M. Fundamentals of transcranial electric and magnetic stimulation dose: definition, selection, and reporting practices. **Brain stimulation**, Elsevier, v. 5, n. 4, p. 435–453, 2012. Citation on page 102.

PETERS, J.; JANZING, D.; SCHÖLKOPF, B. **Elements of causal inference: foundations and learning algorithms**. [S.l.]: The MIT Press, 2017. Citation on page 208.

PHELPS, E. A. Human emotion and memory: interactions of the amygdala and hippocampal complex. **Curr Opin Neurobiol**, v. 14, n. 2, p. 198–202, 2004. ISSN 0959-4388 (Print) 0959-4388 (Linking). Phelps, Elizabeth A England Curr Opin Neurobiol. 2004 Apr;14(2):198-202. Available: <http://www.ncbi.nlm.nih.gov/pubmed/15082325http://ac.els-cdn.com/S0959438804000479/1-s2.0-S0959438804000479-main.pdf?_tid=eacb6c60-892d-11e2-8f0e-00000aacb360&acdnat=1362884288_8e6923ab2ec3d24388a07cf1d36b923a>. Citation on page 62.

PHELPS, E. A.; LEDOUX, J. E. Contributions of the amygdala to emotion processing: from animal models to human behavior. **Neuron**, v. 48, n. 2, p. 175–87, 2005. ISSN 0896-6273 (Print) 0896-6273 (Linking). Phelps, Elizabeth A LeDoux, Joseph E MH067048/MH/NIMH NIH HHS/ MH38774/MH/NIMH NIH HHS/ MH46516/MH/NIMH NIH HHS/ MH58911/MH/NIMH NIH HHS/ MH62104/MH/NIMH NIH HHS/ Neuron. 2005 Oct 20;48(2):175-87. Available: <http://www.ncbi.nlm.nih.gov/pubmed/16242399http://ac.els-cdn.com/S0896627305008238/1-s2.0-S0896627305008238-main.pdf?_tid=ff4e3050-892d-11e2-b80f-00000aacb360&acdnat=1362884322_3d022185af7a9524278c61b3c97619f0>. Citations on pages 60 and 61.

PINAULT, D. The thalamic reticular nucleus: structure, function and concept. **Brain Res Brain Res Rev**, v. 46, n. 1, p. 1–31, 2004. Pinault, Didier Netherlands Brain Res Brain Res Rev. 2004 Aug;46(1):1-31. Available: <http://www.ncbi.nlm.nih.gov/pubmed/15297152http://ac.els-cdn.com/S0165017304000414/1-s2.0-S0165017304000414-main.pdf?_tid=e795a3d0-892d-11e2-95da-00000aab0f6c&acdnat=1362884283_5d09745b3be9badafb5d25f99f186612>. Citation on page 58.

PINAULT, D.; DESCHENES, M. Anatomical evidence for a mechanism of lateral inhibition in the rat thalamus. **European Journal of Neuroscience**, v. 10, n. 11, p. 3462–9, 1998. ISSN 0953-816X (Print) 0953-816X (Linking). Pinault, D Deschenes, M FRANCE Eur J Neurosci. 1998 Nov;10(11):3462-9. Available: <http://www.ncbi.nlm.nih.gov/pubmed/9824459http://onlinelibrary.wiley.com/store/10.1046/j.1460-9568.1998.00362.x/asset/j.1460-9568.1998.00362.x.pdf?v=1&t=he3lxi0y&s=71d222f1fc3ea675a4b829f5b268b9da2ca83c17>. Citation on page 67.

PLEWNIA, C.; REIMOLD, M.; NAJIB, A.; BREHM, B.; REISCHL, G.; PLONTKE, S. K.; GERLOFF, C. Dose-dependent attenuation of auditory phantom perception (tinnitus) by pet-guided repetitive transcranial magnetic stimulation. **Hum Brain Mapp**, v. 28, n. 3, p. 238–46, 2007. ISSN 1065-9471 (Print) 1065-9471 (Linking). Plewnia, Christian Reimold, Matthias Najib, Arif Brehm, Bernhard Reischl, Gerald Plontke, Stefan K Gerloff, Christian Hum Brain Mapp. 2007 Mar;28(3):238-46. Available: <http://www.ncbi.nlm.nih.gov/pubmed/16773635http://onlinelibrary.wiley.com/store/10.1002/hbm.20270/asset/20270_ftp.pdf?v=1&t=h512ia0h&s=705a2fd53a6af3aa05dd4bd808f7cefa30c66519>. Citation on page 78.

PLOGHAUS, A.; BECERRA, L.; BORRAS, C.; BORSOOK, D. Neural circuitry underlying pain modulation: expectation, hypnosis, placebo. **Trends Cogn Sci**, v. 7, n. 5, p. 197–200, 2003. ISSN 1879-307X (Electronic) 1364-6613 (Linking). Ploghaus, Alexander Becerra, Lino Borras, Cristina Borsook, David Trends Cogn Sci. 2003 May;7(5):197-200. Available: <http://www.ncbi.nlm.nih.gov/pubmed/12757820>. Citation on page 64.

PLONER, C. J.; GAYMARD, B. M.; RIVAUD-PECHOUX, S.; PIERROT-DESEILLIGNY, C. The prefrontal substrate of reflexive saccade inhibition in humans. **Biol Psychi-**

atry, v. 57, n. 10, p. 1159–65, 2005. ISSN 0006-3223 (Print) 0006-3223 (Linking). Ploner, Christoph J Gaymard, Bertrand M Rivaud-Pechoux, Sophie Pierrot-Deseilligny, Charles Biol Psychiatry. 2005 May 15;57(10):1159-65. Available: <http://www.ncbi.nlm.nih.gov/pubmed/15866556http://ac.els-cdn.com/S0006322305001824/1-s2.0-S0006322305001824-main.pdf?_tid=0a6d3c4c-892e-11e2-8d50-00000aacb35e&acdnat=1362884341_00c1090ff5b4a0b7a06cd7db78853cf9>. Citation on page 69.

PREACHER, K. J.; HAYES, A. F. Spss and sas procedures for estimating indirect effects in simple mediation models. **Behavior research methods, instruments, & computers**, Springer, v. 36, n. 4, p. 717–731, 2004. Citation on page 195.

____. Asymptotic and resampling strategies for assessing and comparing indirect effects in multiple mediator models. **Behavior research methods**, Springer, v. 40, n. 3, p. 879–891, 2008. Citation on page 195.

PRICE, J. L. Prefrontal cortical networks related to visceral function and mood. **Ann N Y Acad Sci**, v. 877, p. 383–96, 1999. ISSN 0077-8923 (Print) 0077-8923 (Linking). Price, J L Ann N Y Acad Sci. 1999 Jun 29;877:383-96. Available: <http://www.ncbi.nlm.nih.gov/pubmed/10415660http://onlinelibrary.wiley.com/store/10.1111/j.1749-6632.1999.tb09278.x/asset/j.1749-6632.1999.tb09278.x.pdf?v=1&t=hza055vo&s=d7a031f4155eb87ae4794fe0d9f5f77f61b0ab6e>. Citation on page 63.

PROBST, T.; PRYSS, R.; LANGGUTH, B.; SCHLEE, W. Emotional states as mediators between tinnitus loudness and tinnitus distress in daily life: Results from the "trackyourtinnitus" application. **Sci Rep**, v. 6, p. 20382, 2016. ISSN 2045-2322 (Electronic) 2045-2322 (Linking). Probst, Thomas Pryss, Rudiger Langguth, Berthold Schlee, Winfried eng Research Support, Non-U.S. Gov't England 2016/02/09 06:00 Sci Rep. 2016 Feb 8;6:20382. doi: 10.1038/srep20382. Available: <https://www.ncbi.nlm.nih.gov/pubmed/26853815>. Citations on pages 85 and 96.

PROBST, T.; PRYSS, R. C.; LANGGUTH, B.; RAUSCHECKER, J. P.; SCHOBEL, J.; REICHERT, M.; SPILIOPOULOU, M.; SCHLEE, W.; ZIMMERMANN, J. Does tinnitus depend on time-of-day? an ecological momentary assessment study with the "trackyourtinnitus" application. **Frontiers in Aging Neuroscience**, v. 9, n. 253, 2017. ISSN 1663-4365. Available: <https://www.frontiersin.org/article/10.3389/fnagi.2017.00253>. Citation on page 90.

RADEMAKER, M.; STEGEMAN, I.; HO-KANG-YOU, K.; STOKROOS, R.; SMIT, D. The effect of mindfulness-based interventions on tinnitus burden. a systematic review. **Frontiers in neurology**, v. 10, p. 1135, 2019. ISSN 1664-2295. Citation on page 95.

RAHMAN, A.; REATO, D.; ARLOTTI, M.; GASCA, F.; DATTA, A.; PARRA, L. C.; BIKSON, M. Cellular effects of acute direct current stimulation: somatic and synaptic terminal effects. **The Journal of physiology**, Wiley Online Library, v. 591, n. 10, p. 2563–2578, 2013. Citation on page 102.

RAJAN, R.; IRVINE, D. R. Neuronal responses across cortical field a1 in plasticity induced by peripheral auditory organ damage. **Audiol Neurootol**, v. 3, n. 2-3, p. 123–44, 1998. ISSN 1420-3030 (Print) 1420-3030 (Linking). Rajan, R Irvine, D R SWITZERLAND Audiol Neurootol. 1998 Mar-Jun;3(2-3):123-44. Available: <http://www.ncbi.nlm.nih.gov/pubmed/9575381http://content.karger.com/ProdukteDB/produkte.asp?Aktion=ShowPDF&ArtikelNr=000013786&Ausgabe=225245&ProduktNr=224213&filename=000013786.pdf>. Citation on page 65.

RASIA-FILHO, A. A.; LONDERO, R. G.; ACHAVAL, M. Functional activities of the amygdala: an overview. **J Psychiatry Neurosci**, v. 25, n. 1, p. 14–23, 2000. ISSN 1180-4882 (Print) 1180-4882 (Linking). Rasia-Filho, A A Londero, R G Achaval, M CANADA J Psychiatry Neurosci. 2000 Jan;25(1):14-23. Available: <http://www.ncbi.nlm.nih.gov/pubmed/10721680http://www.ncbi.nlm.nih.gov/pmc/articles/PMC1407702/pdf/jpn00084-0020.pdf>. Citation on page 60.

RAUSCHECKER, J. P.; LEAVER, A. M.; MUHLAU, M. Tuning out the noise: limbic-auditory interactions in tinnitus. **Neuron**, v. 66, n. 6, p. 819–26, 2010. ISSN 1097-4199 (Electronic) 0896-6273 (Linking). Rauschecker, Josef P Leaver, Amber M Muhlau, Mark eng R01 NS052494/NS/NINDS NIH HHS/ RC1 DC010720/DC/NIDCD NIH HHS/ RC1 DC010720-01/DC/NIDCD NIH HHS/ RC1 DC010720-02/DC/NIDCD NIH HHS/ Research Support, N.I.H., Extramural Neuron. 2010 Jun 24;66(6):819-26. doi: 10.1016/j.neuron.2010.04.032. Available: <https://www.ncbi.nlm.nih.gov/pubmed/20620868>. Citations on pages 15, 57, 59, 60, 64, 66, 67, 77, 78, 80, 81, and 84.

RESSLER, K. J.; MAYBERG, H. S. Targeting abnormal neural circuits in mood and anxiety disorders: from the laboratory to the clinic. **Nat Neurosci**, v. 10, n. 9, p. 1116–24, 2007. ISSN 1097-6256 (Print) 1097-6256 (Linking). Ressler, Kerry J Mayberg, Helen S 1R01MH073719/MH/NIMH NIH HHS/ DA-019624/DA/NIDA NIH HHS/ MH069884/MH/NIMH NIH HHS/ MH071537/MH/NIMH NIH HHS/ P50 MH077083/MH/NIMH NIH HHS/ P50 MH58922/MH/NIMH NIH HHS/ R01 DA019624-01A2/DA/NIDA NIH HHS/ R01 DA019624-02/DA/NIDA NIH HHS/ Nat Neurosci. 2007 Sep;10(9):1116-24. Available: <http://www.ncbi.nlm.nih.gov/pubmed/17726478http://www.nature.com/neuro/journal/v10/n9/pdf/nn1944.pdf>. Citations on pages 59 and 60.

RICHTER-LEVIN, G. The amygdala, the hippocampus, and emotional modulation of memory. **Neuroscientist**, v. 10, n. 1, p. 31–9, 2004. ISSN 1073-8584 (Print) 1073-8584 (Linking). Richter-Levin, Gal Neuroscientist. 2004 Feb;10(1):31-9. Available: <http://www.ncbi.nlm.nih.gov/pubmed/14987446http://nro.sagepub.com/content/10/1/31http://nro.sagepub.com/content/10/1/31.full.pdf>. Citation on page 62.

RICHTER-LEVIN, G.; AKIRAV, I. Amygdala-hippocampus dynamic interaction in relation to memory. **Mol Neurobiol**, v. 22, n. 1-3, p. 11–20, 2000. ISSN 0893-7648 (Print) 0893-7648 (Linking). Richter-Levin, G Akirav, I Mol Neurobiol. 2000 Aug-Dec;22(1-3):11-20. Available: <http://www.ncbi.nlm.nih.gov/pubmed/11414274http://download.springer.com/static/pdf/589/art%253A10.1385%252FMN%253A22%253A1-3%253A011.pdf?auth66=1364180008_f713032e843470bf0d1e22b41eccc2dd&ext=.pdf>. Citation on page 62.

RIDDER, D. D.; VANNESTE, S. Eeg driven tdcs versus bifrontal tdcs for tinnitus. **Frontiers in psychiatry**, Frontiers, v. 3, p. 84, 2012. Citation on page 96.

RIDDER, D. D.; VANNESTE, S.; CONGEDO, M. The distressed brain: a group blind source separation analysis on tinnitus. **PLoS One**, v. 6, n. 10, p. e24273, 2011. ISSN 1932-6203 (Electronic) 1932-6203 (Linking). De Ridder, Dirk Vanneste, Sven Congedo, Marco PLoS One. 2011;6(10):e24273. Epub 2011 Oct 6. Available: <http://www.ncbi.nlm.nih.gov/pubmed/21998628http://www.plosone.org/article/fetchObjectAttachment.action?uri=info%3Adoi%2F10.1371%2Fjournal.pone.0024273&representation=PDF>. Citations on pages 59, 60, and 65.

RIDDER, D. D.; VANNESTE, S.; WEISZ, N.; LONDERO, A.; SCHLEE, W.; ELGOYHEN, A. B.; LANGGUTH, B. An integrative model of auditory phantom perception: tinnitus as a

unified percept of interacting separable subnetworks. **Neurosci Biobehav Rev**, v. 44, p. 16–32, 2014. ISSN 1873-7528 (Electronic) 0149-7634 (Linking). De Ridder, Dirk Vanneste, Sven Weisz, Nathan Londero, Alain Schlee, Winnie Elgoyhen, Ana Belen Langguth, Berthold eng Research Support, Non-U.S. Gov't 2013/04/20 06:00 Neurosci Biobehav Rev. 2014 Jul;44:16-32. doi: 10.1016/j.neubiorev.2013.03.021. Epub 2013 Apr 15. Available: <http://www.ncbi.nlm.nih.gov/pubmed/23597755>. Citations on pages 15, 69, 82, and 83.

RIEGEL, M.; MOSLEHI, A.; MICHAŁOWSKI, J. M.; ŻURAWSKI, Ł.; HORVAT, M.; WYPYCH, M.; JEDNORÓG, K.; MARCHEWKA, A. Nencki affective picture system: Cross-cultural study in europe and iran. **Frontiers in psychology**, Frontiers, v. 8, p. 274, 2017. Citation on page 105.

RIEGEL, M.; ŻURAWSKI, Ł.; WIERZBA, M.; MOSLEHI, A.; KLOCEK, Ł.; HORVAT, M.; GRABOWSKA, A.; MICHAŁOWSKI, J.; JEDNORÓG, K.; MARCHEWKA, A. Characterization of the nencki affective picture system by discrete emotional categories (naps be). **Behavior research methods**, Springer, v. 48, n. 2, p. 600–612, 2016. Citation on page 105.

ROBERTS, L. E.; EGGERMONT, J. J.; CASPARY, D. M.; SHORE, S. E.; MELCHER, J. R.; KALTENBACH, J. A. Ringing ears: the neuroscience of tinnitus. **J Neurosci**, v. 30, n. 45, p. 14972–9, 2010. ISSN 1529-2401 (Electronic) 0270-6474 (Linking). Roberts, Larry E Eggermont, Jos J Caspary, Donald M Shore, Susan E Melcher, Jennifer R Kaltenbach, James A DC000151-28/DC/NIDCD NIH HHS/ DC008532-03/DC/NIDCD NIH HHS/ P3005188/PHS HHS/ R01 DC000151-28A2/DC/NIDCD NIH HHS/ R01 DC004825-01/DC/NIDCD NIH HHS/ R01 DC008532-03/DC/NIDCD NIH HHS/ R01 DC009097/DC/NIDCD NIH HHS/ R01 DC009097-01A1/DC/NIDCD NIH HHS/ R01DC004825/DC/NIDCD NIH HHS/ RC1 DC010645-01/DC/NIDCD NIH HHS/ RC1DC010645/DC/NIDCD NIH HHS/ J Neurosci. 2010 Nov 10;30(45):14972-9. Available: <http://www.ncbi.nlm.nih.gov/pubmed/21068300http://www.jneurosci.org/content/30/45/14972.full.pdf>. Citations on pages 56 and 59.

ROBERTS, L. E.; HUSAIN, F. T.; EGGERMONT, J. J. Role of attention in the generation and modulation of tinnitus. **Neurosci Biobehav Rev**, v. 37, n. 8, p. 1754–73, 2013. ISSN 1873-7528 (Electronic) 0149-7634 (Linking). Roberts, Larry E Husain, Fatima T Eggermont, Jos J eng Research Support, Non-U.S. Gov't Review Neurosci Biobehav Rev. 2013 Sep;37(8):1754-73. doi: 10.1016/j.neubiorev.2013.07.007. Epub 2013 Jul 19. Available: <https://www.ncbi.nlm.nih.gov/pubmed/23876286>. Citations on pages 84, 87, 90, and 101.

ROBINSON, S. Antidepressants for treatment of tinnitus. **Prog Brain Res**, v. 166, p. 263–71, 2007. ISSN 0079-6123 (Print) 0079-6123 (Linking). Robinson, Shannon Netherlands Prog Brain Res. 2007;166:263-71. Available: <http://www.ncbi.nlm.nih.gov/pubmed/17956790http://www.sciencedirect.com/science?_ob=MiamiImageURL&_cid=273019&_user=501045&_pii=S0079612307660245&_check=y&_origin=article&_zone=toolbar&_coverDate=31-Dec-2007&view=c&originContentFamily=serial&wchp=dGLbVlS-zSkWz&md5=2550e1a654b479113cbb22f330fe435d/1-s2.0-S0079612307660245-main.pdf>. Citations on pages 59, 60, and 77.

ROBINSON, S. K.; VIIRRE, E. S.; STEIN, M. B. Antidepressant therapy in tinnitus. **Hear Res**, v. 226, n. 1-2, p. 221–31, 2007. ISSN 0378-5955 (Print) 0378-5955 (Linking). Robinson, Shannon K Viirre, Erik S Stein, Murray B Netherlands Hear Res. 2007 Apr;226(1-2):221-31. Epub 2006 Sep 14. Available: <http://www.ncbi.nlm.nih.gov/pubmed/16973315http://ac.els-cdn.com/S037859550600219X/

1-s2.0-S037859550600219X-main.pdf?_tid=21dd94ee-892e-11e2-9e13-00000aab0f01&acdnat=1362884380_437861d4e072318e9115730ba76ce9e7>. Citations on pages 66 and 77.

ROWEIS, S. T.; SAUL, L. K. Nonlinear dimensionality reduction by locally linear embedding. **science**, American Association for the Advancement of Science, v. 290, n. 5500, p. 2323–2326, 2000. Citations on pages 129, 130, and 132.

SAH, P.; ARMENTIA, M. L. D. Excitatory synaptic transmission in the lateral and central amygdala. **Ann N Y Acad Sci**, v. 985, p. 67–77, 2003. ISSN 0077-8923 (Print) 0077-8923 (Linking). Sah, P Lopez De Armentia, Mikel Ann N Y Acad Sci. 2003 Apr;985:67-77. Available: <http://www.ncbi.nlm.nih.gov/pubmed/12724149http://onlinelibrary.wiley.com/store/10.1111/j.1749-6632.2003.tb07072.x/asset/j.1749-6632.2003.tb07072.x.pdf?v=1&t=hza05weu&s=dbfbe70deea782936293894fd401857101e8a605>. Citation on page 60.

SALZMAN, C. D.; FUSI, S. Emotion, cognition, and mental state representation in amygdala and prefrontal cortex. **Annu Rev Neurosci**, v. 33, p. 173–202, 2010. ISSN 1545-4126 (Electronic) 0147-006X (Linking). Salzman, C Daniel Fusi, Stefano R01 DA020656/DA/NIDA NIH HHS/ R01 DA020656-03/DA/NIDA NIH HHS/ R01 DA020656-05/DA/NIDA NIH HHS/ R01 MH082017/MH/NIMH NIH HHS/ R01 MH082017-03/MH/NIMH NIH HHS/ R01 MH082017-04/MH/NIMH NIH HHS/ R01 MH082017-05/MH/NIMH NIH HHS/ R01 MH088458/MH/NIMH NIH HHS/ RC1 MH088458-01/MH/NIMH NIH HHS/ RC1 MH088458-02/MH/NIMH NIH HHS/ Annu Rev Neurosci. 2010;33:173-202. doi: 10.1146/annurev.neuro.051508.135256. Available: <http://www.ncbi.nlm.nih.gov/pubmed/20331363http://www.ncbi.nlm.nih.gov/pmc/articles/PMC3108339/pdf/nihms294181.pdf>. Citation on page 61.

SANDER, D.; GRAFMAN, J.; ZALLA, T. The human amygdala: an evolved system for relevance detection. **Rev Neurosci**, v. 14, n. 4, p. 303–16, 2003. ISSN 0334-1763 (Print) 0334-1763 (Linking). Sander, David Grafman, Jordan Zalla, Tiziana England Rev Neurosci. 2003;14(4):303-16. Available: <http://www.ncbi.nlm.nih.gov/pubmed/14640318>. Citation on page 60.

SASAKI, K.; GEMBA, H.; TSUJIMOTO, T. Suppression of visually initiated hand movement by stimulation of the prefrontal cortex in the monkey. **Brain Res**, v. 495, n. 1, p. 100–7, 1989. ISSN 0006-8993 (Print) 0006-8993 (Linking). Sasaki, K Gemba, H Tsujimoto, T NETHERLANDS Brain Res. 1989 Aug 21;495(1):100-7. Available: <http://www.ncbi.nlm.nih.gov/pubmed/2776028http://ac.els-cdn.com/0006899389912225/1-s2.0-0006899389912225-main.pdf?_tid=7f3b55d2-892d-11e2-8e07-00000aab0f27&acdnat=1362884107_da2e47dae198d0881daf95b1ddc6ace3>. Citation on page 69.

SAVASTANO, M. Characteristics of tinnitus in childhood. **Eur J Pediatr**, v. 166, n. 8, p. 797–801, 2007. ISSN 0340-6199 (Print) 0340-6199 (Linking). Savastano, M Germany Eur J Pediatr. 2007 Aug;166(8):797-801. Epub 2006 Nov 16. Available: <http://www.ncbi.nlm.nih.gov/pubmed/17109163http://www.springerlink.com/content/nm2k835435853q73/http://www.springerlink.com/content/nm2k835435853q73/fulltext.pdf>. Citation on page 57.

SCHAUL, T.; QUAN, J.; ANTONOGLOU, I.; SILVER, D. Prioritized experience replay. **arXiv preprint arXiv:1511.05952**, 2015. Citation on page 214.

SCHERER, K. R.; SCHORR, A.; JOHNSTONE, T. Book. **Appraisal processes in emotion: Theory, methods, research**. [S.l.]: Oxford University Press, 2001. ISBN 0195351541. Citation on page 92.

SCHLEE, W.; MUELLER, N.; HARTMANN, T.; KEIL, J.; LORENZ, I.; WEISZ, N. Mapping cortical hubs in tinnitus. **BMC Biol**, v. 7, p. 80, 2009. ISSN 1741-7007 (Electronic) 1741-7007 (Linking). Schlee, Winfried Mueller, Nadia Hartmann, Thomas Keil, Julian Lorenz, Isabel Weisz, Nathan England BMC Biol. 2009 Nov 23;7:80. Available: <http://www.ncbi.nlm.nih.gov/pubmed/19930625http://www.biomedcentral.com/1741-7007/7/80http://www.ncbi.nlm.nih.gov/pmc/articles/PMC2787501/pdf/1741-7007-7-80.pdf>. Citations on pages 60, 63, and 67.

SCHMIDHUBER, J. Deep learning in neural networks: An overview. **Neural networks**, Elsevier, v. 61, p. 85–117, 2015. Citation on page 212.

SCHNABEL, T.; SWAMINATHAN, A.; SINGH, A.; CHANDAK, N.; JOACHIMS, T. Recommendations as treatments: Debiasing learning and evaluation. In: PMLR. **international conference on machine learning**. [S.l.], 2016. p. 1670–1679. Citation on page 50.

SCHNEIDER, P.; ANDERMANN, M.; WENGENROTH, M.; GOEBEL, R.; FLOR, H.; RUPP, A.; DIESCH, E. Reduced volume of heschl's gyrus in tinnitus. **NeuroImage**, v. 45, n. 3, p. 927–39, 2009. ISSN 1095-9572 (Electronic) 1053-8119 (Linking). Schneider, Peter Andermann, Martin Wengenroth, Martina Goebel, Rainer Flor, Herta Rupp, Andre Diesch, Eugen Neuroimage. 2009 Apr 15;45(3):927-39. Epub 2009 Jan 6. Available: <http://www.ncbi.nlm.nih.gov/pubmed/19168138http://ac.els-cdn.com/S1053811908013049/1-s2.0-S1053811908013049-main.pdf?_tid=e5010e843aa23e2b397acbaf43c5e985&acdnat=1345695836_59dd752647ce7741a436daf8ca686530>. Citation on page 78.

SCHÖLKOPF, B.; MIKA, S.; SMOLA, A.; RÄTSCH, G.; MÜLLER, K.-R. Kernel pca pattern reconstruction via approximate pre-images. In: SPRINGER. **International Conference on Artificial Neural Networks**. [S.l.], 1998. p. 147–152. Citations on pages 129, 130, and 131.

SCHULMAN, J.; MORITZ, P.; LEVINE, S.; JORDAN, M.; ABBEEL, P. High-dimensional continuous control using generalized advantage estimation. **arXiv preprint arXiv:1506.02438**, 2015. Citation on page 212.

SEARCHFIELD, G. D.; MORRISON-LOW, J.; WISE, K. Object identification and attention training for treating tinnitus. **Tinnitus: Pathophysiology and Treatment**, v. 166, p. 441–460, 2007. ISSN 0079-6123. Bqc09 Times Cited:18 Cited References Count:75 Progress in Brain Research. Available: <<GotoISI>://WOS:000280613600045>. Citation on page 84.

SEARCHFIELD K. WISE, K. K. G. Conference Paper, **Game training of tinnitus**. 2012. Citation on page 84.

SEITZ, A. R.; KIM, D.; WATANABE, T. Rewards evoke learning of unconsciously processed visual stimuli in adult humans. **Neuron**, v. 61, n. 5, p. 700–7, 2009. ISSN 1097-4199 (Electronic) 0896-6273 (Linking). Seitz, Aaron R Kim, Dongho Watanabe, Takeo R01 EY 015980/EY/NEI NIH HHS/ R01 EY015980-03/EY/NEI NIH HHS/ R21 EY 017737/EY/NEI NIH HHS/ R21 EY017737-02/EY/NEI NIH HHS/ Neuron. 2009 Mar 12;61(5):700-7. doi: 10.1016/j.neuron.2009.01.016. Available: <http://www.ncbi.nlm.nih.gov/pubmed/19285467http://ac.els-cdn.com/S089662730900083X/1-s2.0-S089662730900083X-main.pdf?_tid=860d269e-2c72-11e4-83c5-00000aab0f27&acdnat=1408983291_5a1e639970ca8b6e48b069e54b6d35db>. Citation on page 68.

SEKI, S.; EGGERMONT, J. J. Changes in spontaneous firing rate and neural synchrony in cat primary auditory cortex after localized tone-induced hearing loss. **Hear Res**, v. 180, n. 1-2, p. 28–38, 2003. ISSN 0378-5955 (Print) 0378-5955 (Linking). Seki, Satoshi Eggermont, Jos J eng Research Support, Non-U.S. Gov't Netherlands 2003/06/05 05:00 Hear Res. 2003 Jun;180(1-2):28-38. Available: <http://www.ncbi.nlm.nih.gov/pubmed/12782350>. Citations on pages 65, 73, and 78.

SESACK, S. R.; PICKEL, V. M. Prefrontal cortical efferents in the rat synapse on unlabeled neuronal targets of catecholamine terminals in the nucleus accumbens septi and on dopamine neurons in the ventral tegmental area. **J Comp Neurol**, v. 320, n. 2, p. 145–60, 1992. ISSN 0021-9967 (Print) 0021-9967 (Linking). Sesack, S R Pickel, V M MH40342/MH/NIMH NIH HHS/ NS08193/NS/NINDS NIH HHS/ J Comp Neurol. 1992 Jun 8;320(2):145-60. Available: <http://www.ncbi.nlm.nih.gov/pubmed/1377716http://onlinelibrary.wiley.com/doi/10.1002/cne.903200202/abstract>. Citation on page 63.

SEYDELL-GREENWALD, A.; LEAVER, A. M.; TURESKY, T. K.; MORGAN, S.; KIM, H. J.; RAUSCHECKER, J. P. Functional mri evidence for a role of ventral prefrontal cortex in tinnitus. **Brain Res**, v. 1485, p. 22–39, 2012. ISSN 1872-6240 (Electronic) 0006-8993 (Linking). Seydell-Greenwald, Anna Leaver, Amber M Turesky, Ted K Morgan, Susan Kim, Hung J Rauschecker, Josef P eng RC1 DC010720/DC/NIDCD NIH HHS/ RC1-DC010720/DC/NIDCD NIH HHS/ Research Support, N.I.H., Extramural Research Support, Non-U.S. Gov't Netherlands Brain Res. 2012 Nov 16;1485:22-39. doi: 10.1016/j.brainres.2012.08.052. Epub 2012 Sep 6. Available: <https://www.ncbi.nlm.nih.gov/pubmed/22982009>. Citations on pages 57, 59, and 63.

SHARMIN, S.; SHOYAIB, M.; ALI, A. A.; KHAN, M. A. H.; CHAE, O. Simultaneous feature selection and discretization based on mutual information. **Pattern Recognition**, Elsevier, v. 91, p. 162–174, 2019. Citation on page 129.

SHEIKHPOUR, R.; SARRAM, M. A.; GHARAGHANI, S.; CHAHOOKI, M. A. Z. A survey on semi-supervised feature selection methods. **Pattern Recognition**, Elsevier, v. 64, p. 141–158, 2017. Citation on page 129.

SHEKHAWAT, G. S.; VANNESTE, S. High-definition transcranial direct current stimulation of the dorsolateral prefrontal cortex for tinnitus modulation: a preliminary trial. **Journal of Neural Transmission**, v. 125, n. 2, p. 163–171, 2018. ISSN 0300-9564. Citation on page 96.

SHERMAN, S. M. A wake-up call from the thalamus. **Nat Neurosci**, v. 4, n. 4, p. 344–6, 2001. ISSN 1097-6256 (Print) 1097-6256 (Linking). Sherman, S M Nat Neurosci. 2001 Apr;4(4):344-6. Available: <http://www.ncbi.nlm.nih.gov/pubmed/11276218>. Citation on page 64.

SHOSAKU, A.; SUMITOMO, I. Auditory neurons in the rat thalamic reticular nucleus. **Exp Brain Res**, v. 49, n. 3, p. 432–42, 1983. ISSN 0014-4819 (Print) 0014-4819 (Linking). Shosaku, A Sumitomo, I GERMANY, WEST Exp Brain Res. 1983;49(3):432-42. Available: <http://www.ncbi.nlm.nih.gov/pubmed/6641840>. Citation on page 58.

SHULER, M. G.; BEAR, M. F. Reward timing in the primary visual cortex. **Science**, v. 311, n. 5767, p. 1606–9, 2006. ISSN 1095-9203 (Electronic) 0036-8075 (Linking). Shuler, Marshall G Bear, Mark F New York, N.Y. Science. 2006 Mar 17;311(5767):1606-9. Available: <http://www.ncbi.nlm.nih.gov/pubmed/16543459http://www.sciencemag.org/content/311/5767/1606.full.pdf>. Citation on page 68.

SHULMAN, A. A final common pathway for tinnitus - the medial temporal lobe system. **Int Tinnitus J**, v. 1, n. 2, p. 115–126, 1995. ISSN 0946-5448 (Print) 0946-5448 (Linking). Shulman Int Tinnitus J. 1995;1(2):115-126. Available: <http://www.ncbi.nlm.nih.gov/pubmed/10753332>. Citations on pages 59, 60, and 65.

SIEDLECKA, E.; DENSON, T. F. Experimental methods for inducing basic emotions: A qualitative review. **Emotion Review**, Sage Publications Sage UK: London, England, v. 11, n. 1, p. 87–97, 2019. Citation on page 96.

SIEGLE, G. J.; CARTER, C. S.; THASE, M. E. Use of fmri to predict recovery from unipolar depression with cognitive behavior therapy. **American Journal of Psychiatry**, Am Psychiatric Assoc, v. 163, n. 4, p. 735–738, 2006. Citation on page 45.

SIEGLE, G. J.; STEINHAUER, S. R.; FRIEDMAN, E. S.; THOMPSON, W. S.; THASE, M. E. Remission prognosis for cognitive therapy for recurrent depression using the pupil: utility and neural correlates. **Biological psychiatry**, Elsevier, v. 69, n. 8, p. 726–733, 2011. Citation on page 45.

SILVA-GOMEZ, A. B.; ROJAS, D.; JUAREZ, I.; FLORES, G. Decreased dendritic spine density on prefrontal cortical and hippocampal pyramidal neurons in postweaning social isolation rats. **Brain Res**, v. 983, n. 1-2, p. 128–36, 2003. ISSN 0006-8993 (Print) 0006-8993 (Linking). Silva-Gomez, Adriana B Rojas, Dario Juarez, Ismael Flores, Gonzalo Netherlands Brain Res. 2003 Sep 5;983(1-2):128-36. Available: <http://www.ncbi.nlm.nih.gov/pubmed/12914973http://ac.els-cdn.com/S0006899303030427/1-s2.0-S0006899303030427-main.pdf?_tid=da94523a-892d-11e2-ac44-00000aab0f6b&acdnat=1362884260_ae16e0a94b3e08d19dd4fbeed2b6b555>. Citation on page 63.

SMITS, M.; KOVACS, S.; RIDDER, D. de; PEETERS, R. R.; HECKE, P. van; SUNAERT, S. Lateralization of functional magnetic resonance imaging (fmri) activation in the auditory pathway of patients with lateralized tinnitus. **Neuroradiology**, v. 49, n. 8, p. 669–79, 2007. ISSN 0028-3940 (Print) 0028-3940 (Linking). Smits, Marion Kovacs, Silvia de Ridder, Dirk Peeters, Ronald R van Hecke, Paul Sunaert, Stefan Germany Neuroradiology. 2007 Aug;49(8):669-79. Epub 2007 Apr 3. Available: <http://www.ncbi.nlm.nih.gov/pubmed/17404721http://www.springerlink.com/content/4l123462615qw122/fulltext.pdf>. Citation on page 78.

SOMORJAI, R. Methods for estimating the intrinsic dimsnionality of high-dimensional point sets. In: **Dimensions and entropies in chaotic systems**. [S.l.]: Springer, 1986. p. 137–147. Citation on page 134.

SONG, L.; SMOLA, A.; GRETTON, A.; BORGWARDT, K. M.; BEDO, J. Supervised feature selection via dependence estimation. In: **Proceedings of the 24th international conference on Machine learning**. [S.l.: s.n.], 2007. p. 823–830. Citation on page 129.

SOTRES-BAYON, F.; QUIRK, G. J. Prefrontal control of fear: more than just extinction. **Curr Opin Neurobiol**, v. 20, n. 2, p. 231–5, 2010. ISSN 1873-6882 (Electronic) 0959-4388 (Linking). Sotres-Bayon, Francisco Quirk, Gregory J P50 MH086400-015561/MH/NIMH NIH HHS/ R01 MH058883-13/MH/NIMH NIH HHS/ R01 MH081975-02/MH/NIMH NIH HHS/ England Curr Opin Neurobiol. 2010 Apr;20(2):231-5. doi: 10.1016/j.conb.2010.02.005. Epub 2010 Mar 18. Available: <http://www.ncbi.nlm.nih.gov/pubmed/20303254http://ac.els-cdn.com/S0959438810000279/1-s2.0-S0959438810000279-main.pdf?_tid=4f570db0-892e-11e2-b0a2-00000aacb361&acdnat=1362884456_044bde73d5418304621764c53db6e4c5>. Citations on pages 59 and 60.

SPENCER, J.; CHOUDHURY, S.; VENKATRAMAN, A.; ZIEBART, B.; BAGNELL, J. A. Feedback in imitation learning: The three regimes of covariate shift. **arXiv preprint arXiv:2102.02872**, 2021. Citation on page 217.

SPIRTES, P.; GLYMOUR, C. N.; SCHEINES, R.; HECKERMAN, D. **Causation, prediction, and search**. [S.l.]: MIT press, 2000. Citation on page 208.

STAHL, C.; UNKELBACH, C.; CORNEILLE, O. On the respective contributions of awareness of unconditioned stimulus valence and unconditioned stimulus identity in attitude formation through evaluative conditioning. **J Pers Soc Psychol**, v. 97, n. 3, p. 404–20, 2009. ISSN 0022-3514 (Print) 0022-3514 (Linking). Stahl, Christoph Unkelbach, Christian Corneille, Olivier eng Research Support, Non-U.S. Gov't 2009/08/19 09:00 J Pers Soc Psychol. 2009 Sep;97(3):404-20. doi: 10.1037/a0016196. Available: <http://www.ncbi.nlm.nih.gov/pubmed/19685998>. Citations on pages 70 and 91.

STEELE, J. D.; LAWRIE, S. M. Segregation of cognitive and emotional function in the prefrontal cortex: a stereotactic meta-analysis. **Neuroimage**, Elsevier, v. 21, n. 3, p. 868–875, 2004. Citation on page 101.

STÖGBAUER, H.; KRASKOV, A.; ASTAKHOV, S. A.; GRASSBERGER, P. Least-dependent-component analysis based on mutual information. **Physical Review E**, APS, v. 70, n. 6, p. 066123, 2004. Citation on page 134.

STOLZBERG, D.; CHEN, G. D.; ALLMAN, B. L.; SALVI, R. J. Salicylate-induced peripheral auditory changes and tonotopic reorganization of auditory cortex. **Neuroscience**, v. 180, p. 157–64, 2011. ISSN 1873-7544 (Electronic) 0306-4522 (Linking). Stolzberg, D Chen, G-D Allman, B L Salvi, R J eng F31 DC010931-01/DC/NIDCD NIH HHS/ F31DC010931-01/DC/NIDCD NIH HHS/ R01 DC009091/DC/NIDCD NIH HHS/ R01 DC009091-05/DC/NIDCD NIH HHS/ R01 DC009219/DC/NIDCD NIH HHS/ R01 DC009219-04/DC/NIDCD NIH HHS/ R01DC0090910/DC/NIDCD NIH HHS/ R01DC009219/DC/NIDCD NIH HHS/ Research Support, N.I.H., Extramural 2011/02/12 06:00 Neuroscience. 2011 Apr 28;180:157-64. doi: 10.1016/j.neuroscience.2011.02.005. Epub 2011 Feb 23. Available: <http://www.ncbi.nlm.nih.gov/pubmed/21310217>. Citation on page 78.

STRAUSS, D. J.; DELB, W.; D'AMELIO, R.; LOW, Y. F.; FALKAI, P. Objective quantification of the tinnitus decompensation by synchronization measures of auditory evoked single sweeps. **IEEE Trans Neural Syst Rehabil Eng**, v. 16, n. 1, p. 74–81, 2008. ISSN 1534-4320 (Print) 1534-4320 (Linking). Strauss, Daniel J Delb, Wolfgang D'Amelio, Roberto Low, Yin Fen Falkai, Peter eng 2008/02/29 09:00 IEEE Trans Neural Syst Rehabil Eng. 2008 Feb;16(1):74-81. doi: 10.1109/TNSRE.2007.911086. Available: <http://www.ncbi.nlm.nih.gov/pubmed/18303808>. Citation on page 78.

SUN, K.; TIAN, P.; QI, H.; MA, F.; YANG, G. An improved normalized mutual information variable selection algorithm for neural network-based soft sensors. **Sensors**, Multidisciplinary Digital Publishing Institute, v. 19, n. 24, p. 5368, 2019. Citation on page 142.

SUN, W.; LU, J.; STOLZBERG, D.; GRAY, L.; DENG, A.; LOBARINAS, E.; SALVI, R. J. Salicylate increases the gain of the central auditory system. **Neuroscience**, v. 159, n. 1, p. 325–34, 2009. ISSN 0306-4522 (Print) 0306-4522 (Linking). Sun, W Lu, J Stolzberg, D Gray, L Deng, A Lobarinas, E Salvi, R J eng G42/Action on Hearing Loss/United Kingdom R01 DC009091/DC/NIDCD NIH HHS/ R01 DC009091-02/DC/NIDCD NIH

HHS/ R01 DC009219/DC/NIDCD NIH HHS/ R01 DC009219-02/DC/NIDCD NIH HHS/ R01DC009091/DC/NIDCD NIH HHS/ R01DC009219/DC/NIDCD NIH HHS/ Research Support, N.I.H., Extramural Research Support, Non-U.S. Gov't 2009/01/22 09:00 Neuroscience. 2009 Mar 3;159(1):325-34. doi: 10.1016/j.neuroscience.2008.12.024. Epub 2008 Dec 24. Available: <http://www.ncbi.nlm.nih.gov/pubmed/19154777>. Citation on page 78.

SUTTON, R. S.; BARTO, A. G. **Reinforcement learning: An introduction**. [S.l.]: MIT press, 2018. Citation on page 210.

SZITA, I.; LÖRINCZ, A. Learning tetris using the noisy cross-entropy method. **Neural computation**, MIT Press, v. 18, n. 12, p. 2936–2941, 2006. Citation on page 212.

TANGKARATT, V.; SASAKI, H.; SUGIYAMA, M. Direct estimation of the derivative of quadratic mutual information with application in supervised dimension reduction. **Neural computation**, MIT Press, v. 29, n. 8, p. 2076–2122, 2017. Citation on page 135.

TENENBAUM, J. B.; SILVA, V. D.; LANGFORD, J. C. A global geometric framework for nonlinear dimensionality reduction. **science**, American Association for the Advancement of Science, v. 290, n. 5500, p. 2319–2323, 2000. Citations on pages 129, 130, and 131.

THOMAS, C.; GHODRATITOOSTANI, I.; DELBEM, A. C.; ALI, A.; DATTA, A. Influence of gender-related differences in transcranial direct current stimulation: A computational study. In: IEEE. **2019 41st Annual International Conference of the IEEE Engineering in Medicine and Biology Society (EMBC)**. [S.l.], 2019. p. 5196–5199. Citations on pages 52, 102, and 103.

TOMASI, D.; CAPARELLI, E. C.; CHANG, L.; ERNST, T. fmri-acoustic noise alters brain activation during working memory tasks. **NeuroImage**, v. 27, n. 2, p. 377–86, 2005. ISSN 1053-8119 (Print) 1053-8119 (Linking). Tomasi, D Caparelli, E C Chang, L Ernst, T GCRC 5-MO1-RR-10710/RC/CCR NIH HHS/ K02 DA16991/DA/NIDA NIH HHS/ K24 DA16170/DA/NIDA NIH HHS/ M01 RR010710-06S1/RR/NCRR NIH HHS/ R03 DA017070-01/DA/NIDA NIH HHS/ Neuroimage. 2005 Aug 15;27(2):377-86. Available: <http://www.ncbi.nlm.nih.gov/pubmed/15893942http://ac.els-cdn.com/S105381190500265X/1-s2.0-S105381190500265X-main.pdf?_tid=0213c73c-892e-11e2-a597-00000aab0f6b&acdnat=1362884327_65617dfbe80dc26b0dfa65ee8087b999>. Citation on page 63.

TOOSTANI, I. G.; NAMI, M.; SANCHEZ, T. G.; DELBEM, A. C. B. The sleep toll in tinnitus: A brief review based on the neurofunctional tinnitus model. **Journal of Advanced Medical Sciences and Applied Technologies**, Shiraz University of Medical Sciences, v. 3, n. 4, p. 189–196, 2017. Citations on pages 45 and 52.

TORGERSON, W. S. Multidimensional scaling: I. theory and method. **Psychometrika**, Springer, v. 17, n. 4, p. 401–419, 1952. Citations on pages 129 and 130.

TORRES-GARCIA, M. E.; SOLIS, O.; PATRICIO, A.; RODRIGUEZ-MORENO, A.; CAMACHO-ABREGO, I.; LIMON, I. D.; FLORES, G. Dendritic morphology changes in neurons from the prefrontal cortex, hippocampus and nucleus accumbens in rats after lesion of the thalamic reticular nucleus. **Neuroscience**, v. 223, p. 429–38, 2012. ISSN 1873-7544 (Electronic) 0306-4522 (Linking). Torres-Garcia, M E Solis, O Patricio, A Rodriguez-Moreno, A Camacho-Abrego, I Limon, I D Flores, G Neuroscience. 2012 Oct 25;223:429-38. doi: 10.1016/j.neuroscience.2012.07.042. Epub 2012 Jul 31. Available: <http://www.ncbi.nlm.nih.gov/pubmed/22858596http://ac.els-cdn.com/S0306452212007671/1-s2.0-S0306452212007671-main.pdf?_tid=58319d16-33ab-11e2-a6c4-00000aab0f02&acdnat=1353482359_69705c934f57fa41aeaff4ad362c0cd0>. Citation on page 58.

TREVIS, K. J.; MCLACHLAN, N. M.; WILSON, S. J. Cognitive mechanisms in chronic tinnitus: psychological markers of a failure to switch attention. **Frontiers in psychology**, Frontiers, v. 7, p. 1262, 2016. Citations on pages 87 and 101.

TSOTSOS, J. K. Book. **A computational perspective on visual attention**. Cambridge, Mass.: MIT Press, 2011. xvi, 308 p. p. 2010036050 101563207 015743417 (OCoLC)664450690 John K. Tsotsos. ill. (some col.) ; 24 cm. Includes bibliographical references and indexes. Attention: we all know what it is – Computational foundations – Theories and models of visual attention – Selective tuning: overview – Selective tuning: formulation – Attention, recognition, and binding – Selective tuning: examples and performance – Explanations and predictions – Wrapping up the loose ends. ISBN 9780262015417 (hardcover alk. paper) 0262015412 (hardcover alk. paper). Available: <http://mitpress-ebooks.mit.edu/product/computational-perspective-on-visual-attention>. Citation on page 67.

TYLER, R.; COELHO, C.; TAO, P.; JI, H.; NOBLE, W.; GEHRINGER, A.; GOGEL, S. Identifying tinnitus subgroups with cluster analysis. **American journal of audiology**, v. 17, n. 2, p. S176–S184, 2008. ISSN 1059-0889. Available: <http://www.ncbi.nlm.nih.gov/pmc/articles/PMC2668860/pdf/nihms-99150.pdf>. Citation on page 78.

TYLER, R. S. Book. **Tinnitus treatment : clinical protocols**. New York: Thieme, 2006. xv, 240 p. p. 2005019828 edited by Richard S. Tyler. ill. ; 26 cm. Includes bibliographical references and index. Neurophysiological models, psychological models, and treatments for tinnitus / Richard S. Tyler – Tinnitus self-treatment / Daiv I. Sizer and Robert R.A. Coles – Internet-based self-help treatment of tinnitus / Gerhard Andersson and Viktor Kaldo – Treating tinnitus in patients with otologic conditions / David M. Baguley, Catriona A. Williamson, and David A. Moffat – Lifestyle changes for tinnitus self-management / Robert L. Folmer ... [et al.] – Tinnitus habituation therapy / Richard S. Hallam and Laurence McKenna – Tinnitus-related insomnia treatment / Laurence McKenna and H. Clare Daniel – Cognitive-behavioral therapy with applied relaxation / Gerhard Andersson and Viktor Kaldo – Tinnitus activities treatment / Richard S. Tyler ... [et al.] – Tinnitus retraining therapy / Grazyna M. Bartnik and Henryk Skarzynski – Music and the acoustic desensitization protocol for tinnitus / Paul B. Davis – Hearing aids and tinnitus / Grant D. Searchfield – Tinnitus sound therapies / Robert L. Folmer ... [et al.] – Incorporating group and individual sessions into a tinnitus management clinic / Craig W. Newman and Sharon A. Sandridge – Tinnitus person-centered therapy / Anne-Mette Mohr and Uno Hedelund – Scary monsters and waterfalls: tinnitus narrative therapy for children / Rosie C. Kentish And Susan R. Crocker. ISBN 1588901815 (TMP hard copy alk. paper) 3131320710 (GTV hard copy alk. paper). Available: <Tableofcontentshttp://www.loc.gov/catdir/toc/ecip0515/2005019828.html>. Citation on page 67.

UHRIG, M. K.; TRAUTMANN, N.; BAUMGÄRTNER, U.; TREEDE, R.-D.; HENRICH, F.; HILLER, W.; MARSCHALL, S. Emotion elicitation: A comparison of pictures and films. **Frontiers in psychology**, Frontiers, v. 7, p. 180, 2016. Citation on page 105.

UHRIG, M. K.; TRAUTMANN, N.; BAUMGäRTNER, U.; TREEDE, R.-D.; HENRICH, F.; HILLER, W.; MARSCHALL, S. Emotion elicitation: A comparison of pictures and films. **Frontiers in Psychology**, v. 7, p. 180, 2016. ISSN 1664-1078. Available: <http://www.ncbi.nlm.nih.gov/pmc/articles/PMC4756121/>. Citation on page 96.

VANNESTE, S.; PLAZIER, M.; OST, J.; LOO, E. van der; HEYNING, P. Van de; RIDDER, D. D. Bilateral dorsolateral prefrontal cortex modulation for tinnitus by transcranial direct current

stimulation: a preliminary clinical study. **Experimental brain research**, Springer, v. 202, n. 4, p. 779–785, 2010. Citation on page 96.

VASSILOPOULOS, S. P.; BANERJEE, R.; PRANTZALOU, C. Experimental modification of interpretation bias in socially anxious children: Changes in interpretation, anticipated interpersonal anxiety, and social anxiety symptoms. **Behaviour Research and Therapy**, Elsevier, v. 47, n. 12, p. 1085–1089, 2009. Citation on page 45.

VAZIRI, Z.; NAMI, M.; LEITE, J. P.; DELBEM, A. C. B.; HYPPOLITO, M. A.; GHODRATI-TOOSTANI, I. Conceptual framework for insomnia: A cognitive model in practice. **Frontiers in Neuroscience**, Frontiers, p. 781, 2021. Citations on pages 45 and 52.

VERNON, P. E. **The structure of human abilities (psychology revivals)**. [S.l.]: Routledge, 2014. Citation on page 45.

VERTES, R. P. Interactions among the medial prefrontal cortex, hippocampus and midline thalamus in emotional and cognitive processing in the rat. **Neuroscience**, v. 142, n. 1, p. 1–20, 2006. ISSN 0306-4522 (Print) 0306-4522 (Linking). Vertes, Robert P MH01476/MH/NIMH NIH HHS/ MH63519/MH/NIMH NIH HHS/ Neuroscience. 2006 Sep 29;142(1):1-20. Epub 2006 Aug 2. Available: <http://www.ncbi.nlm.nih.gov/pubmed/16887277http://ac.els-cdn.com/S030645220600858X/1-s2.0-S030645220600858X-main.pdf?_tid=0df0a7e6-892e-11e2-9e4c-00000aacb35d&acdnat=1362884347_2e43a93a99659b4c09108012653818d1>. Citation on page 63.

WALLHAUSSER-FRANKE, E.; SCHREDL, M.; DELB, W. Tinnitus and insomnia: is hyperarousal the common denominator? **Sleep Med Rev**, v. 17, n. 1, p. 65–74, 2013. ISSN 1087-0792. Citation on page 90.

WANG, S.-F.; HSU, Y.-F.; LIU, Y.-X.; HSIEH, C.-K. Effects of microstructure and cao addition on the magnetic and mechanical properties of nicuzn ferrites. **Journal of Magnetism and Magnetic Materials**, Elsevier, v. 394, p. 470–476, 2015. Citation on page 130.

WANG, Z.; SCHAUL, T.; HESSEL, M.; HASSELT, H.; LANCTOT, M.; FREITAS, N. Dueling network architectures for deep reinforcement learning. In: PMLR. **International conference on machine learning**. [S.l.], 2016. p. 1995–2003. Citation on page 214.

WARDEN, M. R.; SELIMBEYOGLU, A.; MIRZABEKOV, J. J.; LO, M.; THOMPSON, K. R.; KIM, S. Y.; ADHIKARI, A.; TYE, K. M.; FRANK, L. M.; DEISSEROTH, K. A prefrontal cortex-brainstem neuronal projection that controls response to behavioural challenge. **Nature**, v. 492, n. 7429, p. 428–32, 2012. ISSN 1476-4687 (Electronic) 0028-0836 (Linking). Warden, Melissa R Selimbeyoglu, Aslihan Mirzabekov, Julie J Lo, Maisie Thompson, Kimberly R Kim, Sung-Yon Adhikari, Avishek Tye, Kay M Frank, Loren M Deisseroth, Karl 1F32MH088010-01/MH/NIMH NIH HHS/ Howard Hughes Medical Institute/ England Nature. 2012 Dec 20;492(7429):428-32. doi: 10.1038/nature11617. Available: <http://www.ncbi.nlm.nih.gov/pubmed/23160494http://www.nature.com/nature/journal/v492/n7429/pdf/nature11617.pdf>. Citation on page 63.

WATANABE, M.; CHENG, K.; MURAYAMA, Y.; UENO, K.; ASAMIZUYA, T.; TANAKA, K.; LOGOTHETIS, N. Attention but not awareness modulates the bold signal in the human v1 during binocular suppression. **Science**, v. 334, n. 6057, p. 829–31, 2011. ISSN 1095-9203 (Electronic) 0036-8075 (Linking). Watanabe, Masataka Cheng, Kang Murayama, Yusuke Ueno, Kenichi Asamizuya, Takeshi Tanaka, Keiji Logothetis, Nikos eng Research Support, Non-U.S. Gov't 2011/11/15 06:00 Science. 2011 Nov 11;334(6057):829-31. doi: 10.1126/science.1203161. Available: <http://www.ncbi.nlm.nih.gov/pubmed/22076381>. Citation on page 68.

WATANABE, T.; YAGISHITA, S.; KIKYO, H. Memory of music: roles of right hippocampus and left inferior frontal gyrus. **NeuroImage**, v. 39, n. 1, p. 483–91, 2008. ISSN 1053-8119 (Print) 1053-8119 (Linking). Watanabe, Takamitsu Yagishita, Sho Kikyo, Hideyuki Neuroimage. 2008 Jan 1;39(1):483-91. Epub 2007 Aug 25. Available: <http://www.ncbi.nlm.nih.gov/pubmed/17905600http://ac.els-cdn.com/S1053811907007501/1-s2.0-S1053811907007501-main.pdf?_tid=31908d92-892e-11e2-90b2-00000aab0f6b&acdnat=1362884406_2bff675650705e4247e8661fc9654c82>. Citation on page 62.

WATKINS, C. J.; DAYAN, P. Q-learning. **Machine learning**, Springer, v. 8, n. 3-4, p. 279–292, 1992. Citation on page 211.

WEESE, G. D.; PHILLIPS, J. M.; BROWN, V. J. Attentional orienting is impaired by unilateral lesions of the thalamic reticular nucleus in the rat. **J Neurosci**, v. 19, n. 22, p. 10135–9, 1999. ISSN 1529-2401 (Electronic) 0270-6474 (Linking). Weese, G D Phillips, J M Brown, V J Wellcome Trust/United Kingdom J Neurosci. 1999 Nov 15;19(22):10135-9. Available: <http://www.ncbi.nlm.nih.gov/pubmed/10559421http://www.jneurosci.org/content/19/22/10135.full.pdf>. Citation on page 58.

WEINBERGER, N. M. Associative representational plasticity in the auditory cortex: a synthesis of two disciplines. **Learn Mem**, v. 14, n. 1-2, p. 1–16, 2007. ISSN 1549-5485 (Electronic) 1072-0502 (Linking). Weinberger, Norman M DC-02938/DC/NIDCD NIH HHS/ DC-05592/DC/NIDCD NIH HHS/ Cold Spring Harbor, N.Y. Learn Mem. 2007 Jan 3;14(1-2):1-16. Print 2007 Jan-Feb. Available: <http://www.ncbi.nlm.nih.gov/pubmed/17202426http://learnmem.cshlp.org/content/14/1-2/1.full.pdf>. Citation on page 61.

____. The medial geniculate, not the amygdala, as the root of auditory fear conditioning. **Hear Res**, v. 274, n. 1-2, p. 61–74, 2011. ISSN 1878-5891 (Electronic) 0378-5955 (Linking). Weinberger, Norman M eng DC-010013/DC/NIDCD NIH HHS/ DC-02938/DC/NIDCD NIH HHS/ DC-05592/DC/NIDCD NIH HHS/ R01 DC002938/DC/NIDCD NIH HHS/ R01 DC002938-12/DC/NIDCD NIH HHS/ R01 DC005592/DC/NIDCD NIH HHS/ R01 DC005592-04/DC/NIDCD NIH HHS/ R01 DC010013/DC/NIDCD NIH HHS/ R01 DC010013-01A1/DC/NIDCD NIH HHS/ Research Support, N.I.H., Extramural Netherlands 2010/05/15 06:00 Hear Res. 2011 Apr;274(1-2):61-74. doi: 10.1016/j.heares.2010.03.093. Epub 2010 May 11. Available: <http://www.ncbi.nlm.nih.gov/pubmed/20466051>. Citations on pages 61, 71, and 73.

WEISE, C.; HESSER, H.; ANDERSSON, G.; NYENHUIS, N.; ZASTRUTZKI, S.; KRONER-HERWIG, B.; JAGER, B. The role of catastrophizing in recent onset tinnitus: its nature and association with tinnitus distress and medical utilization. **Int J Audiol**, v. 52, n. 3, p. 177–88, 2013. ISSN 1499-2027. Citation on page 93.

WEISSMAN, A. S.; CHU, B. C.; REDDY, L. R.; MOHLMAN, J. Attention problems in anxious and inattentive-impulsive youth: Implications for diagnosis and treatment. **Journal of Clinical Child and Adolescent Psychology**, v. 41, p. 117–127, 2012. Citation on page 45.

WILLIAMS, J. M. G.; WATTS, F. N.; MACLEOD, C.; MATHEWS, A. Book. **Cognitive psychology and emotional disorders**. [S.l.]: John Wiley & Sons, 1988. ISBN 0471918458. Citation on page 91.

WILLIAMS, R. J. Simple statistical gradient-following algorithms for connectionist reinforcement learning. **Machine learning**, Springer, v. 8, n. 3, p. 229–256, 1992. Citation on page 212.

WILLIAMS, R. J.; PENG, J. Function optimization using connectionist reinforcement learning algorithms. **Connection Science**, Taylor & Francis, v. 3, n. 3, p. 241–268, 1991. Citation on page 221.

WILSON, P. H.; HENRY, J. L. Tinnitus cognitions questionnaire: development and psychometric properties of a measure of dysfunctional cognitions associated with tinnitus. **The international tinnitus journal**, v. 4, n. 1, p. 23–30, 1998. Citation on page 92.

WINKLER, I.; DENHAM, S. L.; NELKEN, I. Modeling the auditory scene: predictive regularity representations and perceptual objects. **Trends Cogn Sci**, v. 13, n. 12, p. 532–40, 2009. ISSN 1879-307X (Electronic) 1364-6613 (Linking). Winkler, Istvan Denham, Susan L Nelken, Israel eng Research Support, Non-U.S. Gov't Review England 2009/10/16 06:00 Trends Cogn Sci. 2009 Dec;13(12):532-40. doi: 10.1016/j.tics.2009.09.003. Epub 2009 Oct 12. Available: <http://www.ncbi.nlm.nih.gov/pubmed/19828357http://ac.els-cdn.com/S1364661309002095/1-s2.0-S1364661309002095-main.pdf?_tid=6b65a316-005b-11e6-a664-00000aacb361&acdnat=1460430512_227b7474ccfcf997fda00b2b47ac2e76>. Citations on pages 84 and 90.

WOODS, D. L.; KNIGHT, R. T. Electrophysiologic evidence of increased distractibility after dorsolateral prefrontal lesions. **Neurology**, v. 36, n. 2, p. 212–6, 1986. ISSN 0028-3878 (Print) 0028-3878 (Linking). Woods, D L Knight, R T Neurology. 1986 Feb;36(2):212-6. Available: <http://www.ncbi.nlm.nih.gov/pubmed/3945393>. Citation on page 69.

YAMADA, M.; SUGIYAMA, M.; SESE, J. Least-squares independence regression for non-linear causal inference under non-gaussian noise. **Machine learning**, Springer, v. 96, n. 3, p. 249–267, 2014. Citation on page 135.

YANG, S.; YANG, B.; WONG, H.-S.; KANG, Z. Cooperative traffic signal control using multi-step return and off-policy asynchronous advantage actor-critic graph algorithm. **Knowledge-Based Systems**, Elsevier, v. 183, p. 104855, 2019. Citation on page 215.

YANG, Y.; SHEN, H. T.; MA, Z.; HUANG, Z.; ZHOU, X. l2, 1-norm regularized discriminative feature selection for unsupervised learning. In: **IJCAI international joint conference on artificial intelligence**. [S.l.: s.n.], 2011. Citations on pages 129 and 130.

YOO, J.-Y.; LEE, J.-H. The effects of valence and arousal on time perception in individuals with social anxiety. **Frontiers in Psychology**, v. 6, n. 1208, 2015. ISSN 1664-1078. Available: <https://www.frontiersin.org/article/10.3389/fpsyg.2015.01208>. Citation on page 93.

YU, X. J.; XU, X. X.; CHEN, X.; HE, S.; HE, J. Slow recovery from excitation of thalamic reticular nucleus neurons. **J Neurophysiol**, v. 101, n. 2, p. 980–7, 2009. ISSN 0022-3077 (Print) 0022-3077 (Linking). Yu, Xiong-Jie Xu, Xin-Xiu Chen, Xi He, Shigang He, Jufang J Neurophysiol. 2009 Feb;101(2):980-7. doi: 10.1152/jn.91130.2008. Epub 2008 Dec 10. Available: <http://www.ncbi.nlm.nih.gov/pubmed/19073800http://jn.physiology.org/content/101/2/980.full.pdf>. Citations on pages 58, 67, and 73.

ZAHM, D. S.; WILLIAMS, E.; WOHLTMANN, C. Ventral striatopallidothalamic projection: Iv. relative involvements of neurochemically distinct subterritories in the ventral pallidum and adjacent parts of the rostroventral forebrain. **J Comp Neurol**, v. 364, n. 2, p. 340–62, 1996. ISSN 0021-9967 (Print) 0021-9967 (Linking). Zahm, D S Williams, E Wohltmann, C NS-23805/NS/NINDS NIH HHS/ J Comp Neurol. 1996 Jan 8;364(2):340-62. Available: <http://www.ncbi.nlm.nih.gov/pubmed/8788254http://onlinelibrary.wiley.com/store/10.1002/(SICI)1096-9861(19960108)364:2<340::AID-CNE11>3.0.CO;2-T/asset/11_ftp.pdf?v=1&t=i2kon9ui&s=00ec07e66b3b6022f38abe36aa17eed6dc1750bd>. Citation on page 58.

ZALD, D. H. The human amygdala and the emotional evaluation of sensory stimuli. **Brain Res Brain Res Rev**, v. 41, n. 1, p. 88–123, 2003. Zald, David H 1 F32 MH11641-01A1/MH/NIMH NIH HHS/ T32 DA07097/DA/NIDA NIH HHS/ Netherlands Brain Res Brain Res Rev. 2003 Jan;41(1):88-123. Available: <http://www.ncbi.nlm.nih.gov/pubmed/12505650http://ac.els-cdn.com/S0165017302002485/1-s2.0-S0165017302002485-main.pdf?_tid=9d50538a-2c72-11e4-92d4-00000aab0f02&acdnat=1408983330_bb2c34d936fafc3e4f911dc1741e2abc>. Citation on page 60.

ZENG, F.-G. An active loudness model suggesting tinnitus as increased central noise and hyperacusis as increased nonlinear gain. **Hearing Research**, v. 295, p. 172–179, 2013. ISSN 0378-5955. Citation on page 78.

ZENNER, H. P.; PFISTER, M.; BIRBAUMER, N. Tinnitus sensitization: Sensory and psychophysiological aspects of a new pathway of acquired centralization of chronic tinnitus. **Otology & neurotology : official publication of the American Otological Society, American Neurotology Society [and] European Academy of Otology and Neurotology**, v. 27, p. 1054–63, 2006. Citations on pages 66, 69, 70, 77, 83, and 87.

ZENNER, H.-P.; ZALAMAN, I. M. Cognitive tinnitus sensitization: behavioral and neurophysiological aspects of tinnitus centralization. **Acta oto-laryngologica**, Taylor & Francis, v. 124, n. 4, p. 436–439, 2004. Citation on page 87.

ZHANG, J. S.; KALTENBACH, J. A. Increases in spontaneous activity in the dorsal cochlear nucleus of the rat following exposure to high-intensity sound. **Neurosci Lett**, v. 250, n. 3, p. 197–200, 1998. ISSN 0304-3940 (Print) 0304-3940 (Linking). Zhang, J S Kaltenbach, J A eng Research Support, Non-U.S. Gov't IRELAND 1998/08/26 Neurosci Lett. 1998 Jul 10;250(3):197-200. Available: <http://www.ncbi.nlm.nih.gov/pubmed/9708866>. Citations on pages 73 and 78.

ZHANG, W.; BAO, W.; LIU, X.-Y.; YANG, K.; LIN, Q.; WEN, H.; RAMEZANI, R. Large-scale causal approaches to debiasing post-click conversion rate estimation with multi-task learning. In: **Proceedings of The Web Conference 2020**. [S.l.: s.n.], 2020. p. 2775–2781. Citation on page 50.

ZHANG, X.; YANG, P.; CAO, Y.; QIN, L.; SATO, Y. Salicylate induced neural changes in the primary auditory cortex of awake cats. **Neuroscience**, v. 172, p. 232–45, 2011. ISSN 1873-7544 (Electronic) 0306-4522 (Linking). Zhang, X Yang, P Cao, Y Qin, L Sato, Y eng Research Support, Non-U.S. Gov't 2010/11/04 06:00 Neuroscience. 2011 Jan 13;172:232-45. doi: 10.1016/j.neuroscience.2010.10.073. Epub 2010 Oct 31. Available: <http://www.ncbi.nlm.nih.gov/pubmed/21044658>. Citations on pages 73 and 78.

ZHANG, Y.; ZHANG, Z.; QIN, J.; ZHANG, L.; LI, B.; LI, F. Semi-supervised local multi-manifold isomap by linear embedding for feature extraction. **Pattern Recognition**, Elsevier, v. 76, p. 662–678, 2018. Citation on page 129.

ZHOU, S. K.; LE, H. N.; LUU, K.; NGUYEN, H. V.; AYACHE, N. Deep reinforcement learning in medical imaging: A literature review. **arXiv preprint arXiv:2103.05115**, 2021. Citation on page 218.

ZIKOPOULOS, B.; BARBAS, H. Prefrontal projections to the thalamic reticular nucleus form a unique circuit for attentional mechanisms. **J Neurosci**, v. 26, n. 28, p. 7348–61, 2006. ISSN 1529-2401 (Electronic) 0270-6474 (Linking). Zikopoulos, Basilis Barbas, Helen J Neurosci.

2006 Jul 12;26(28):7348-61. Available: <http://www.ncbi.nlm.nih.gov/pubmed/16837581http://www.jneurosci.org/content/26/28/7348.full.pdf>. Citations on pages 58 and 64.

____. Circuits formultisensory integration and attentional modulation through the prefrontal cortex and the thalamic reticular nucleus in primates. **Rev Neurosci**, v. 18, n. 6, p. 417–38, 2007. ISSN 0334-1763 (Print) 0334-1763 (Linking). Zikopoulos, Basilis Barbas, Helen R01 MH057414-05/MH/NIMH NIH HHS/ R01 NS024760-18/NS/NINDS NIH HHS/ England Rev Neurosci. 2007;18(6):417-38. Available: <http://www.ncbi.nlm.nih.gov/pubmed/18330211http://www.ncbi.nlm.nih.gov/pmc/articles/PMC2855189/pdf/nihms76653.pdf>. Citations on pages 58, 59, 67, and 73.

____. Pathways for emotions and attention converge on the thalamic reticular nucleus in primates. **J Neurosci**, v. 32, n. 15, p. 5338–50, 2012. ISSN 1529-2401 (Electronic) 0270-6474 (Linking). Zikopoulos, Basilis Barbas, Helen R01 MH057414-12/MH/NIMH NIH HHS/ R01 NS024760-18/NS/NINDS NIH HHS/ J Neurosci. 2012 Apr 11;32(15):5338-50. doi: 10.1523/JNEUROSCI.4793-11.2012. Available: <http://www.ncbi.nlm.nih.gov/pubmed/22496579http://www.jneurosci.org/content/32/15/5338.full.pdf>. Citations on pages 59, 63, and 67.

GLOSSARY

"SP" "Sham concurrent with PEI (SP)".

"tP" "tDCS concurrent with PEI (tP)".

δ Minimum Clinical Efficacy.

A2C Advantage Actor-Critic.

A3C Asynchronous Advantage Actor-Critic.

ACC anterior cingulate cortex.

ACC anterior cingulate cortex.

AD Average Distance.

ADM Average Distance between Means.

API Application Programming Interface.

APN Average Proportion of Non-overlap.

Ar arousal-ratio.

ASB Adaptive-Seamless Bayesian.

BA Brodmann areas.

BLA basolateral amygdala.

BN Batch Normalization.

BOLD blood oxygen level-dependent.

CAAP Conscious Attended-Awareness Perception.

CAD computer-aided design.

CBM Cognitive-Behavioral Model.

CBT Cognitive Behavioural Therapy.

CC Cognitive Computing.

CCF Conceptual Cognitive Framework.

CGI Clinical Global Impression.

CNN Convolutional Neural Networks.

CPP conscious perception process.

CRL Causal Reinforcement Learning.

CS Conditional Stimulus.

CST CausalSpace Toolbox.

CV Coefficient of Variance.

DAG Directed acyclic graph.

DCN dorsal cochlear nucleus.

DL Discomfort Level.

dlPFC Dorsolateral Prefrontal Cortex.

DM dorsomedial.

DNN Deep Neural Network.

DQL Deep Q-learning.

DRL Deep Reinforcement Learning.

DrL Distributed Recursive Graph Layout.

DRR Dimensionality Reduction via Regression.

ECL Evaluative Conditional Learning.

EEG Electroencephalogeraphy.

EF electric field.

EGI Electronic Geodesic Incorporation.

ER Experience Replay.

ERP event-related potential.

EST Emotional Stroop Task.

FastICA Independent Component Analysis.

FC Fully Connected.

FDA Food and Drug Administration.

FE Finite element.

fMRI functional Magnetic Resonance Imaging.

FN Fresh noise.

FOM Figure of Merit.

Fruchterman Reingold Fruchterman Reingold Graph Layout.

FS Feature Selection.

FT Feature Transformation.

GABA Gamma-aminobutyric acid.

HAV high-arousal-valence pictures.

HD High Definition.

HL Hearing Level.

HTL Hearing Threshold Level.

HV high-valence Pictures.

IC inferior colliculus.

ICA Independent Component Analysis.

iCRP integrated Cognitive Rehabilitation Platform.

ID-tree information dependency tree.

ITC intercalated cells.

kPCA Kernel Principal Component Analysis.

LDL loudness discomfort level.

LLE Locally Linear Embedding.

LMC Loudness Misperception Correction.

LMT Loudness Match Test.

lPFC Lateral PFC.

LPP Late Positive Potential.

LSTM Long Short-Term Memory.

mA Mili Amper.

MBCT Mindfulness-Based Cognitive Therapy.

MBI Mindfulness-based interventions.

MCC Mathews Correlation Coefficient.

MDI Major Depression Inventory.

MDN mediodorsal nucleus.

MDP Markov Decision Processes.

MEG magnetoencephalography.

MGB medial geniculate body.

MGN medial geniculate nucleus.

MI mutual information.

Min Minutes.

MML Minimal Masking Level.

MSE Minimum Squared Error.

MSQ Mini Sleep Questionnaire.

NAc nucleus accumbens.

NAPS Nencki Affective Picture System.

NBN narrow-band noise.

NcC Neurocognitive Computing.

NfTM Neurofunctional Tinnitus Model.

NIBS Non-invasive Brain Stimulation.

nMDS Non-Metric Dimensional Scaling.

NMI Normalized MI.

NNMF Non-Negative Matrix Factorization.

OLS Ordinary Least Square.

PCA principal component analysis.

PEI positive emotion induction.

PET Positron emission tomography.

PFC pre-frontal cortex.

PMT Pitch Matching test.

pOFC posterior orbitofrontal cortex.

POMDP Partially- Observable Markov Decision Process.

Predictive Modeling: it also called predictive analytics, is a mathematical process that seeks to predict future events or outcomes by analyzing patterns that are likely to forecast future results. The goal of predictive modeling is to answer this question: "Based on known past behavior, what is most likely to happen in the future?.

PTA Pure-tone audiometry.

q quanta.

RL Reinforcement Learning.

RNN Recurrent Neural Network.

ROI Region Of Interest.

rs resting-state.

SARSA State-Action-Reward-State-Action.

SOC superior olivary complex.

SOTA Self-Organized Tree Algorithm.

SPECT Single-photon emission computed tomography.

STAI-S6 State Trait Anxiety Inventroy Small Questions.

t-SNE t-Distributed Stochastic Neighbor Embedding.

TBF-12 Tinnitus Impairment Questionnaire.

tDCS transcranial Direct Current Stimulation.

tES transcranial Electrical Stimulation.

THI Tinnitus Handicap Inventory.

TLQ Tinnitus Loudness Questionnaire.

TRN Thalamic reticular nucleus.

TS Tinnitus Severity.

TSCHQ Tinnitus Sample Case History Questionnaire.

TT Testing Tone.

US Unconditional Stimulus.

vm ventromedial.

VP ventral pallidum.

Vr Valence-ratio.


ICMC
USP
SÃO CARLOS